



Whitelaw, Jamie Adam (2017) The dynamic nature and functions of actin in *Toxoplasma gondii*. PhD thesis.

<http://theses.gla.ac.uk/8072/>

Copyright and moral rights for this work are retained by the author

A copy can be downloaded for personal non-commercial research or study, without prior permission or charge

This work cannot be reproduced or quoted extensively from without first obtaining permission in writing from the author

The content must not be changed in any way or sold commercially in any format or medium without the formal permission of the author

When referring to this work, full bibliographic details including the author, title, awarding institution and date of the thesis must be given

Enlighten:Theses  
<http://theses.gla.ac.uk/>  
theses@gla.ac.uk

# The dynamic nature and functions of actin in *Toxoplasma gondii*

By

Jamie Adam Whitelaw  
B.Sc. (Hons), M.Res.

Submitted in fulfilment of the requirements for the  
Degree of Doctor of Philosophy

School of Life Sciences  
College of Medical, Veterinary & Life Sciences  
Institute of Infection, Immunity & Inflammation  
University of Glasgow

---

## Abstract

*Toxoplasma gondii* is an obligate intracellular pathogen. Due to its experimental tractability it has acted as an excellent model system to understand the fundamental principles of pathogenic mechanisms within the group Apicomplexa, including *Plasmodium spp.* the causative agent of malaria. Work on *T. gondii* has provided the foundation to understanding how apicomplexan parasites power motility and invasion, which centres around the parasites gliding machinery. This movement depends on the parasite's acto-myosin system, which is thought to generate the force during gliding. However, recent evidence questions the exact molecular role of this system. Deletions of core components of the gliding machinery, such as parasite actin or subunits of the glideosome indicate that the parasites remain motile and invasive, albeit at significantly reduced efficiencies. These findings could be explained by different possibilities, such as functional redundancies or compensatory mechanisms for multiple components of the glideosome.

*Toxoplasma* only encodes a single copy of ACT1, therefore redundancies for ACT1 are unlikely. Much of the research into the role(s) of TgACT1 focuses on motility and invasion. Interestingly, while the conditional *act1* KO shows a deficiency in gliding and invasion, severe defects affecting parasite survival were observed during intracellular replication and egress. The amount of actin remaining in the *act1* KO parasites was disputed which led to alternate conclusions about actin's role in the parasites. Therefore, this study provides a much more detailed characterisation of the conditional *act1* KO and when the phenotypes are observed in relation to actin levels within the parasite. Furthermore, the study provides evidence of an alternative model for motility that is independent of the parasites acto-myosin system.

Several studies assert that the polymerisation kinetics of TgACT1 is unusual, allowing the formation of only short, unstable actin filaments. However, to date, it has not been possible to study actin *in vivo*, therefore its physiological role has remained unclear. In order to investigate this, parasites expressing a chromobody that specifically binds to F-actin were generated and characterised. Importantly, TgACT1 forms a vast network during the intracellular life-stages that is important for parasite replication and egress. Moreover, these filaments

---

allow vesicle exchange and produce F-actin connections between parasites in neighbouring vacuoles. This study also demonstrates that the formation of F-actin depends on a critical concentration of G-actin, implying a polymerisation mechanism akin to all other actins.

This work is important for understanding the mechanisms used by *Toxoplasma* to move and invade with regards to the functions of the acto-myosin system. Moreover, it highlights a novel role of actin that is required to control the organisation of the parasitophorous vacuole during division.

The role of actin during the lifecycle may have wider implications to other apicomplexan species, such as *Plasmodium spp.* and also much further in the field of parasitology where F-actin information is scarce.

---

## Table of contents

Abstract .....	ii
List of figures .....	x
List of tables .....	xii
Acknowledgements.....	xiii
Publications arising from this work .....	xv
Conference proceedings.....	xv
Author's declaration .....	xvi
Definitions/abbreviations .....	xvii
Chapter 1 Introduction .....	19
1.1 The phylum Apicomplexa .....	19
1.2 History of <i>Toxoplasma gondii</i> .....	20
1.3 Pathogenesis of <i>Toxoplasma gondii</i> .....	21
1.4 Lifecycle of <i>Toxoplasma gondii</i> .....	22
1.4.1 Lifecycle in the definitive host .....	23
1.4.2 Lifecycle in the intermediate host .....	24
1.4.2.1 The lytic lifecycle .....	24
1.4.2.1.1 Gliding motility .....	25
1.4.2.1.2 Invasion .....	26
1.4.2.1.3 Replication .....	28
1.4.2.1.4 Egress.....	29
1.4.2.2 Bradyzoite cysts.....	30
1.5 Morphology of <i>Toxoplasma gondii</i> .....	30
1.5.1 The ultrastructure of the tachyzoite .....	30
1.5.2 The apical complex and secretory organelles .....	32
1.5.2.1 The conoid and cytoskeleton .....	32
1.5.2.2 Micronemes .....	32
1.5.2.3 Rhoptries.....	33
1.5.2.4 Dense granules .....	34
1.5.3 Inner membrane complex .....	35
1.5.4 The apicoplast.....	35
1.6 Actin .....	36
1.6.1 Overview and structure of actin in eukaryotes.....	36
1.6.2 Actin in apicomplexan parasites.....	40
1.7 Actin binding proteins (ABPs) in Apicomplexa .....	43
1.7.1 Nucleation .....	44
1.7.2 Monomer sequestration .....	45
1.7.3 Severing and filament depolymerisation .....	47

1.7.4	Crosslinking and bundling of F-actin .....	47
1.7.5	Myosin motors .....	48
1.8	Small molecules that bind to actin .....	49
1.8.1	Actin polymerisation drugs .....	50
1.8.1.1	Phalloidins .....	50
1.8.1.2	Jasplakinolide .....	50
1.8.2	Actin depolymerisation drugs .....	52
1.8.2.1	Latrunculins .....	52
1.8.2.2	Cytochalasins .....	52
1.9	Actin-related and actin-like proteins in Apicomplexa .....	53
1.9.1.1	Actin-related proteins .....	53
1.9.1.2	Actin-like proteins .....	54
1.10	The role of actin during cell motility .....	55
1.10.1	The mechanisms behind cell motility .....	55
1.10.2	Crawling motility .....	55
1.10.2.1	Swimming .....	59
1.10.2.2	Osmotic engine model .....	60
1.10.3	Apicomplexan gliding motility .....	61
1.10.3.1	Molecular basis of the MyoA-motor complex .....	62
1.10.3.2	The linear motor model .....	63
1.11	Actin during apicomplexan invasion .....	66
1.12	<i>Toxoplasma gondii</i> as a model organism .....	68
1.13	Reverse genetics in Apicomplexa .....	68
1.13.1	Gene knockdown .....	69
1.13.2	Rapid regulation of protein stability .....	71
1.13.3	Gene knockouts .....	71
1.14	Aim of study .....	73
Chapter 2	Materials and Methods .....	75
2.1	Equipment .....	75
2.2	Computer software .....	76
2.3	Biological and chemical reagents .....	76
2.4	Drugs and antibiotics .....	77
2.5	Nucleic acid extraction kits .....	77
2.6	Buffers, solutions and media .....	77
2.7	Antibodies .....	80
2.8	Oligonucleotides .....	81
2.9	Expression vectors .....	82
2.10	Bacterial strains ( <i>Escherichia coli</i> ) .....	83
2.11	Molecular biology .....	83

2.11.1	Isolation of genomic DNA from <i>Toxoplasma gondii</i> .....	83
2.11.2	Isolation of RNA from <i>Toxoplasma</i> .....	84
2.11.3	Making cDNA (reverse transcription).....	84
2.11.4	Nucleic acid concentration.....	84
2.11.5	Polymerase chain reaction .....	85
2.11.5.1	Molecular cloning .....	85
2.11.5.2	Bacterial colony screening .....	86
2.11.5.3	Integration PCR .....	86
2.11.6	Agarose gel electrophoresis .....	86
2.11.7	Restriction endonuclease digest.....	87
2.11.8	Dephosphorylation of digested DNA fragments.....	87
2.11.9	DNA extraction from agarose gel.....	87
2.11.10	Ligation of DNA fragments .....	88
2.11.11	Plasmid transformation into <i>E. coli</i> .....	88
2.11.12	Isolating plasmid DNA from <i>E. coli</i> .....	89
2.11.12.1	Small scale extraction (MiniPrep) .....	89
2.11.12.2	Medium scale extraction (MidiPrep) .....	89
2.11.13	Site-directed mutagenesis.....	90
2.11.14	Ethanol precipitation.....	90
2.11.15	DNA sequencing .....	90
2.12	Cell biology .....	91
2.12.1	Organisms.....	91
2.12.1.1	Host cell strains.....	91
2.12.1.2	Parasite strains.....	91
2.12.2	Culturing <i>Toxoplasma gondii</i> and host cell lines .....	92
2.12.3	Trypsin treatment of host cells.....	92
2.12.4	Transfection of <i>T. gondii</i> .....	93
2.12.4.1	Bio-Rad® transfections .....	93
2.12.4.2	AMAXA® transfections .....	93
2.12.4.3	Transient transfections .....	94
2.12.4.4	Stable transfections .....	94
2.12.5	Isolation of a clonal parasite line .....	95
2.12.6	Cryopreservation of <i>T. gondii</i> and thawing of stabilates .....	96
2.12.7	Inducing the <i>act1</i> KO .....	96
2.13	Phenotypic analysis .....	97
2.13.1	Immunofluorescence analysis.....	97
2.13.2	Quantitative immunofluorescence analysis.....	97
2.13.3	Fluorescence intensity analysis .....	98
2.13.4	Plaque assay.....	98

2.13.5	Trail deposition assay .....	98
2.13.6	Assessing for tight junction formation.....	99
2.13.7	Inside/outside invasion assay .....	99
2.13.8	Invasion/replication assay.....	100
2.13.9	Replication assay .....	100
2.13.10	Apicoplast loss .....	100
2.13.11	Egress assay.....	100
2.13.12	Time-lapse video microscopy .....	101
2.13.12.1	Penetration time of invading parasites.....	101
2.13.12.2	Gliding kinetics .....	101
2.13.12.3	Egress.....	102
2.13.13	Flow chamber attachment .....	102
2.13.14	Bead translocation assay .....	103
2.13.15	3D motility assay.....	104
2.13.16	Electron microscopy.....	104
2.13.16.1	Scanning electron microscopy (SEM).....	104
2.13.16.2	Correlative-light electron microscopy (CLEM).....	105
2.14	Biochemistry .....	105
2.14.1	Isolation of protein from parasite cell lysate.....	105
2.14.2	Sodium dodecyl sulphate polyacrylamide gel electrophoresis .....	106
2.14.3	Protein transfer from SDS gels to nitrocellulose membrane .....	106
2.14.4	Verification of transfer by Ponceau-S staining .....	106
2.14.5	Immunostaining of the membrane .....	107
2.14.6	Visualisation and quantification .....	107
2.14.7	Stripping .....	107
2.14.8	Co-immunoprecipitation .....	107
2.15	Bioinformatics .....	108
2.15.1	DNA sequencing alignments .....	108
2.15.2	Data and statistical analysis .....	108
Chapter 3	Characterisation of a conditional <i>act1</i> KO .....	110
3.1	Analysis of different actin antibodies.....	111
3.2	Down-regulation of ACT1 .....	117
3.3	Phenotypic analysis of the <i>act1</i> KO in correlation with ACT1 down-regulation.....	120
3.4	Kinetics of gliding motility and invasion.....	125
3.5	ACT1 is involved in regulating attachment sites .....	131
3.6	Ultrastructure and trafficking in the <i>act1</i> KO.....	133
3.6.1	Shape of the <i>act1</i> KO.....	133
3.6.2	Motor complex formation.....	134

3.6.3	Trafficking of specialised secretory proteins in the <i>act1</i> KO.....	136
3.6.4	Dense granule secretion into the PV is an actin-independent process 138	
3.6.5	Actin is essential for apicoplast division but not the mitochondria ..	138
3.7	Summary and conclusion .....	140
Chapter 4	The effects of actin-modulating drugs on <i>Toxoplasma gondii</i> .....	142
4.1	Cytochalasin D has an off-target effect .....	142
4.1.1	Generation of an inducible Cytochalasin D resistant ACT1 knockout line	143
4.1.2	Characterisation of gliding .....	145
4.1.3	Cytochalasin D reduces attachment but not to <i>act1</i> KO levels .....	146
4.2	<i>Toxoplasma</i> ACT1 is naturally resistant to latrunculins .....	147
4.2.1	Gliding motility with latrunculin A .....	147
4.2.2	Gliding in the presence of latrunculin B.....	148
4.2.3	Invasion with latrunculin A .....	149
4.3	Forcing actin polymerisation inhibits motility .....	150
4.4	Summary and conclusions.....	152
Chapter 5	Actin Filaments in <i>Toxoplasma gondii</i> .....	154
5.1	Expression of chromobodies highlights a vast network within the parasitophorous vacuoles.....	155
5.2	Chromobody signal changes with actin-modulating drugs .....	156
5.3	Chromobodies bind specifically to <i>Toxoplasma</i> ACT1 .....	159
5.4	Stabilisation of actin filaments phenocopies the <i>act1</i> KO .....	165
5.5	Stable expression of chromobody-Halo .....	166
5.6	F-actin during gliding and invasion .....	169
5.7	Actin forms a network during intracellular replication.....	172
5.8	<i>Toxoplasma</i> ACT1 interacts with the apicoplast .....	174
5.9	Parasites make F-actin connections with neighbouring vacuoles .....	176
5.10	The actin network breaks in a calcium-dependent manner before egress.....	177
5.11	Summary and conclusions.....	181
Chapter 6	A new outlook on parasite motility .....	182
6.1	Blocking microneme secretion/recycling abolishes motility.....	182
6.2	The ability for parasites to cap their membranes is actin-independent .....	184
6.3	New model for parasite motility .....	189
Chapter 7	General discussion and outlook.....	191
7.1	Establishment of the chromobody technology in <i>Toxoplasma</i> .....	191
7.2	Stabilisation of chromobody-RFP .....	193

---

7.3	The phenotypes indicate a cooperative polymerisation process of TgACT1 .....	194
7.4	Off-target effects of actin-modulating drugs .....	196
7.5	Cell-cell communication .....	197
7.5.1	Vesicular transport between parasites .....	197
7.5.2	Connections between vacuoles .....	198
7.5.3	Formation and functions of the network .....	199
7.6	Localisation of actin filaments at the linear motor complex .....	199
7.6.1	Alternative models of gliding .....	201
7.6.2	The role of the host actin during invasion .....	204
7.7	The role of <i>Toxoplasma</i> ACT1 during the lytic cycle of actin: Summary .....	204
7.8	Outlook and future studies .....	205
Chapter 8	List of References .....	207
Chapter 9	Appendices .....	236
9.1	List of supplementary movies .....	236
9.2	Figure copyright permissions .....	238

## List of figures

Figure 1-1: The complete lifecycle of <i>Toxoplasma gondii</i> .....	23
Figure 1-2: The lytic lifecycle of <i>Toxoplasma gondii</i> .....	25
Figure 1-3: Invasion steps of <i>Toxoplasma gondii</i> .....	27
Figure 1-4: Ultrastructure of the <i>Toxoplasma gondii</i> tachyzoite.....	31
Figure 1-5: The structure an actin monomer bound to ADP.....	37
Figure 1-6: Actin nucleation and treadmilling .....	39
Figure 1-7: Isodesmic polymerisation versus cooperative polymerisation .....	42
Figure 1-8: Actin-binding proteins promote nucleation of F-actin .....	44
Figure 1-9: Actin modulating drugs .....	51
Figure 1-10: Actin control during lamellipodia protrusion and crawling motility	58
Figure 1-11: Osmotic engine model.....	61
Figure 1-12: The MyoA-motor complex in <i>Toxoplasma gondii</i> .....	64
Figure 1-13: Reverse genetic tools in <i>Toxoplasma gondii</i> .....	70
Figure 2-1: Cloning strategy for the LoxPAct1 <sup>CDr</sup> plasmid .....	82
Figure 2-2: Vector maps for chromobody expression plasmids. ....	82
Figure 3-1: Investigating the specificity of various antibodies for <i>Toxoplasma</i> ACT1 .....	113
Figure 3-2: Investigating the specificity of various apicomplexan antibodies against <i>Toxoplasma</i> ACT1 .....	117
Figure 3-3: The down-regulation of TgACT1 in the <i>act1</i> KO.....	120
Figure 3-4: Actin is essential for apicoplast division and egress.....	123
Figure 3-5: Phenotypes for gliding and invasion established 48 hours post induction.....	125
Figure 3-6: 2D gliding kinetics of the <i>act1</i> KO.....	127
Figure 3-7: 3D motility profiles of the <i>act1</i> KO .....	128
Figure 3-8: Penetration kinetics of the <i>act1</i> KO .....	130
Figure 3-9: Attachment of motor complex mutants under shear stress .....	132
Figure 3-10: Ultrastructure of the <i>act1</i> KO .....	134
Figure 3-11: Glideosome components localise normally under the plasma membrane .....	135
Figure 3-12: Localisation of the secretory organelles in the <i>act1</i> KO.....	138
Figure 3-13: Actin is required for apicoplast division but not the mitochondria	139
Figure 4-1: Generation of an inducible cytochalasin D resistant <i>act1</i> KO.....	144
Figure 4-2: The effect of cytochalasin D on both gliding motility and attachment. .....	146
Figure 4-3: The effect of latrunculins on gliding motility .....	149
Figure 4-4: Invasion and replication of RH with latrunculin A .....	150
Figure 4-5: The effect of jasplakinolide on the motility tachyzoites. ....	152
Figure 5-1: Expression systems to visualise actin filaments.....	156
Figure 5-2: The effect of actin-modulating drugs on the chromobody expression .....	158
Figure 5-3: Chromobodies bind specifically to TgACT1 .....	162
Figure 5-4: Correlative-light electron microscopy (CLEM) of the actin network	164
Figure 5-5: Chromobody-RFP phenocopies the <i>act1</i> KO.....	166
Figure 5-6: Expression of chromobody-Halo has no effect on the lytic lifecycle	167
Figure 5-7: Expression of chromobody-Halo has no effect on protein trafficking or organellar division.....	169
Figure 5-8: Actin filaments during gliding and invasion .....	171
Figure 5-9: F-actin is dynamic and controls replication. ....	172
Figure 5-10: F-actin holds parasites during replication from the residual body.	173

---

Figure 5-11: F-actin interacting with apicoplasts.....	175
Figure 5-12: F-actin makes connections between neighbouring vacuoles .....	177
Figure 5-13: The actin network breaks in a calcium-dependent manner before egress .....	179
Figure 5-14: Short filamentous-like structures hold the parasites together even after the vast network has been fragmented. ....	180
Figure 6-1: Inhibition of microneme secretion or recycling blocks motility .....	184
Figure 6-2: The formation of a retrograde membrane flow with secretion/endocytic inhibitors .....	186
Figure 6-3: Actin is not required for bead translocation .....	188
Figure 6-4: Retrograde membrane flow model for motility.....	190
Figure 7-1: Actin throughout the lifecycle of <i>Toxoplasma gondii</i> .....	205

---

## List of tables

Table 2-1: Equipment used in this study .....	75
Table 2-2: Computer software .....	76
Table 2-3: Biological and chemical reagents .....	76
Table 2-4: Drugs and antibiotics .....	77
Table 2-5: Nucleic acid extraction kits.....	77
Table 2-6: Buffers and media for bacterial culture .....	77
Table 2-7: Buffers for DNA analysis .....	78
Table 2-8: Buffers for protein analysis .....	78
Table 2-9: Buffers and media for <i>Toxoplasma gondii</i> and mammalian cell culture .....	79
Table 2-10: Primary antibodies.....	80
Table 2-11: Secondary antibodies.....	81
Table 2-12: Main oligonucleotides used in this study .....	81
Table 2-13: <i>Escherichia coli</i> strains.....	83
Table 2-14: Components of a PCR mix .....	85
Table 2-15: PCR thermocycler program .....	85
Table 2-16: Selection strategies for stable transfection of <i>T. gondii</i> .....	95
Table 2-17: Significance rating from GraphPad Prism 6.0.....	109
Table 3-1: Summary of data presented in this thesis compared to published literature. ....	141
Table 9-1: Copyright permissions obtained for figures reproduced from journal publications .....	238

---

## Acknowledgements

First of all, I would like to thank my supervisor Prof. Markus Meissner for the guidance, support, discussions and advice provided to me over the years. I have been exceptionally lucky to have a supervisor who is extremely passionate about his work, his enthusiasm and knowledge is truly inspiring. Thanks on a professional and personal level for giving me the opportunity to do this PhD.

I would like to acknowledge my PhD assessors Prof. Sylke Muller and Dr. Sonya Taylor, your advice and suggestions have helped my development. Thanks also to Prof. Gary Ward for providing encouragement and words of wisdom during his sabbatical year, they will serve me well as I progress into my academic career.

I would also like to express my gratitude to all current and former members of the Meissner lab. I enjoyed working with the invasion team and exchanging ideas, a thank-you to you all. To my lab supervisors, Dr. Allison Jackson and Dr. Nicole Andenmatten, I appreciate the guidance you gave me from my transition between M.Res and PhD. A special acknowledgement goes to my former flatmate Dr. Saskia Egarter who helped in my understanding and shaping of the project.

I have thoroughly enjoyed my time spent at the University of Glasgow over the years and I would like to acknowledge the people of the GBRC, in particular, level 6 for their friendliness both at work and social events outside of work. The University of Glasgow Judo team has allowed me to 'keep calm and throw someone' and you have provided me with a fun outlet and escape from my studies over the years.

*I get by with a little help from my friends:* Robyn, Fernanda, Mario, Simon and Leandro, I have appreciated your approachability, friendship and laughs you have provided me with throughout this journey. Thank-you to Jenna and Matthew for proofreading parts of my thesis, your comments were appreciated.

My family have been amazingly supportive throughout my academic studies. A special thanks go to my mother, Lorraine whose love and encouragement has been unconditional. To my girlfriend Emma, I will return the love and support when it comes your time to finish, I promise!

---

I would like to dedicate this thesis to my grandad. His support and generosity helped me in so many ways and made this possible.

Tom Whitelaw  
(08.06.1937 - 07.06.2015)

---

## Publications arising from this work

The following published papers contain work presented in the thesis:

Egarter\*, S., Andenmatten\*, N., Jackson, A. J., Whitelaw, J. A., Pall, G., Black, J. A., Ferguson, D. J., Tardieux, I., Mogilner, A. and Meissner, M. (2014). The *Toxoplasma* Acto-MyoA Motor Complex Is Important but Not Essential for Gliding Motility and Host Cell Invasion. *PLoS One*, **9**(3): e91819.

Periz\*, J., Whitelaw\*, J. A., Harding\*, C., Gras, S., Del Rosario Minina, M. I., Latorre-Barragan, M., Lemgruber, L., Reimer, M., Insall, R., Heaslip, A. and Meissner, M. (2016) *Toxoplasma gondii* F-actin forms an extensive filamentous network required for material exchange and parasite maturation. *eLife*, **10.7554/eLife.24119**

Whitelaw\*, J. A., Latorre-Barragan\*, F., Gras, S., Pall, G., Leung, J. M., Heaslip, A., Egarter, S., Andenmatten, N., Nelson, S. R., Warshaw, D. M., Ward, G. and Meissner, M. (2016) Surface attachment, promoted by the Acto-myosin system of *Toxoplasma gondii* is important for efficient gliding motility and invasion. *BMC Biology*, **15**(1). doi:10.1186/s12915-016-0343-5

\* denotes equally contributing authors.

## Conference proceedings

Parts of the following thesis have been presented at the following conferences and various other local and national meetings.

25<sup>th</sup> Annual Molecular Parasitology Meeting in Woods Hole, MA, USA in September 2014.

- I gave an oral presentation on “The essential role of actin during the life cycle of *Toxoplasma gondii*”

Actin Dynamics Meeting Regensburg, Germany, in May 2015.

- I gave a poster presentation on “The importance of actin in the survival of *Toxoplasma gondii*”

27<sup>th</sup> Annual Molecular Parasitology Meeting in Woods Hole, MA, USA in September 2016.

- I gave an oral presentation on “*Toxoplasma* establishes an F-actin network within the PV that is essential for replication”

---

## Author's declaration

I, Jamie Adam Whitelaw hereby declare that I am the sole author of this thesis and performed all of the work presented, with the following exceptions highlighted below. No part of this thesis has been previously submitted for a degree at this or another university.



Jamie Whitelaw

### Chapter 3:

- Live-cell video microscopy of RH KillerRed was performed by Miriam Scarpa under my supervision during her summer internship
- 3D motility analysis of the *act1* KO was performed in collaboration with Prof. Gary Ward and Dr. Jacqueline Leung at the University of Vermont, USA
- Attachment flow chamber analysis of mutant parasite lines; *myoA* KO, *mic2* KO and *act1* KO was performed and analysed in our lab by Dr. Gurman Pall
- Scanning EM of the *act1* KO was performed in collaboration with Dr. Leandro Lemgruber, WTCMP imaging technologist, University of Glasgow, UK

### Chapter 5:

- Dr. Javier Periz had the initial idea and implemented the cloning of both chromobody-Halo and chromobody-RFP plasmids
- Co-IP of chromobody-Halo was performed by Dr. Simon Gras
- Replication movies of the chromobody-Halo and chromobody-Halo with GAPM1a was by Dr. Clare Harding and Madita Reimer
- CLEM and SEM of parasites expressing chromobodies and the *act1* KO was performed in collaboration with Dr. Leandro Lemgruber
- Imaris 3D reconstruction of SIM images was performed by Dr. Leandro Lemgruber (WTCMP imaging technologist)

### Chapter 6:

- Bead translocation of DrpB<sup>DN</sup> ( $\pm$  Shld1), RH in PitStop2 and RH in Endo buffer was performed and counted in our lab by Dr. Simon Gras

## Definitions/abbreviations

°C	Degree Celsius	<i>E. coli</i>	<i>Escherichia coli</i>
6-TX	6-thioxanthine	e.g.	Exempli gratia (for example)
aa	Amino acid	EDTA	Ethylene diamine tetraacetic acid
ACT1	Actin	EGTA	Ethylene glycol tetraacetic acid
ADF	Actin depolymerising factor	ELC	Endosomal like compartment
AGE	Agarose gel electrophoresis	ELC1	Essential light chain 1
ALP	Actin-like protein	EM	Electron microscopy
AMA1	Apical membrane antigen 1	ER	Endoplasmic reticulum
Amp	Ampicillin	EtOH	Ethanol
ADP	Adenosine diphosphate	FBS	Fetal bovine serum
Arp	Actin related protein	fw	Forward
ATP	Adenosine triphosphate	g	Gram or Gravity (context dependent)
BLAST	Basic Local Alignment Search Tool	GAP	Glideosome associated protein
bp	Base pair	gDNA	Genomic deoxyribonucleic acid
BSA	Bovine serum albumin	GFP	Green fluorescent protein
Ca <sup>2+</sup>	Calcium	GOI	Gene of interest
CAT	Chloramphenicol acetyltransferase	GPI	Glycophosphatidylinositol
cDNA	Complementary deoxyribonucleic acid	GSH	Glutathione
CDPK	Calcium-dependent protein kinase	h	Hour
CIP	Calf intestinal phosphatase	H <sub>2</sub> O	Water
CLEM	Correlative light electron microscopy	HEPES	4-(2-Hydroxyethyl)-piperazineethanesulphonic acid
C-terminal	Carboxyl terminal	HFF	Human foreskin fibroblast
CytD or CD	Cytochalasin D	HSP	Heat shock protein
dd	Destabilisation domain	Hx or hxgprt	Hypoxanthine-xanthine-guanine phosphoribosyl transferase
DHFR	Dihydrofolate reductase	IFA	Immunofluorescence analysis
DiCre	Dimerisable Cre	IMC	Inner membrane complex
DMEM	Dulbecco's Modified Eagle's Medium	IPTG	Isopropyl-O-D-thiogalactopyranoside
DMSO	Dimethyl sulfoxide	Jas	Jasplakinolide
DN	Dominant negative	kbp	Kilo base pair
DNA	Deoxyribonucleic acid	KD	Knockdown
dNTP	Deoxynucleotide 5'-triphosphate	kDa	Kilo Dalton
Drp	Dynamin related protein	KO	Knockout

lat	Latrunculin	rpm	Revolutions per min
LB	Luria-Bertani	RT	Room temperature
LoxP	Locus crossover in P1	rv	Reverse
M	Molar	s	Second
MCS	Multiple cloning site	SAG1	Surface antigen 1
mg	Milligram	SD	Standard deviation
MIC	Micronemal protein	SDS-PAGE	Sodium dodecyl sulfate polyacrylamide gel electrophoresis
min	Minute	SEM	Standard error of the mean
ml	Millilitre	SOC	Super optimal broth with catabolite repression
MLC	Myosin light chain	<i>spp.</i>	Species
mM	Milimolar	SSR	Site specific recombination
MPA	Mycophenolic acid	t	Time
mRNA	Messenger ribonucleic acid	<i>T. gondii</i> or <i>Tg</i>	<i>Toxoplasma gondii</i>
MT	Microtubule	TAE	Tris-acetate-EDTA
Myo	Myosin	<i>Taq</i>	<i>Thermos aquaticus</i>
NCBI	National Center for Biotechnology Information	TEMED	N,N,N',N'-tetramethylethylenediamine
ng	Nanogram	TJ	Tight junction
nm	Nanometer	TM	Transmembrane
N-terminal	Amino terminal	Tris	Tris [hydroxymethyl] aminomethane
o/n	Over night	U	Unit
ORF	Open reading frame	UTR	Untranslated region
<i>P. berghei</i> or <i>Pb</i>	<i>Plasmodium berghei</i>	UV	Ultraviolet
<i>P. falciparum</i> or <i>Pf</i>	<i>Plasmodium falciparum</i>	V	Volts
PBS	Phosphate buffered saline	v/v	Volume/volume percentage
PCR	Polymerase chain reaction	w/v	Weight/volume percentage
PFA	Paraformaldehyde	WB	Western blot
P <sub>i</sub>	Inorganic phosphaphte	WHO	World health organisation
PM	Plasma membrane	WT	Wild-type
POI	Protein of interest	Xan	Xanthosine monophosphate
PV	Parasitophorous vacuole	X-Gal	5-bromo-4-chloro-3-indoyl- $\beta$ -D-Galactopyranoside
PVM	Parasitophorous vacuole membrane	YFP	Yellow fluourescent protein
r	Resistant	$\mu$ g	Microgram
RFP	Red fluourescent protein	$\mu$ l	Microliter
RNA	Ribonucleic acid	$\mu$ m	Micrometer
RON	Rhoptry neck protein	$\mu$ M	Micromolar
ROP	Rhoptry protein		

---

# Chapter 1 Introduction

## 1.1 The phylum Apicomplexa

The phylum Apicomplexa consists of a diverse group of protozoa parasites belonging to the families of coccidia, gregarines, hematozoa and cryptosporidia. Apicomplexa has the highest diversity range of species of any protist group, with potential numbers reaching  $1 \times 10^7$  different species estimated from environmental DNA samples (Adl *et al.*, 2007). However, to date, only around 6000 species have been identified (Adl *et al.*, 2007).

Members of Apicomplexa are known to parasitise and cause diseases in both vertebrates and invertebrates. This presents a huge burden on the world's economy as they cause severe and debilitating diseases in both humans and animals (Levine, 1988). The most well-known apicomplexan parasite is *Plasmodium spp.* that causes malaria through the bite of an infected female *Anopheles* mosquito. Although new cases of malaria have dropped by almost 40 % and deaths by 60 % (Figures from 2000-2015), it is still estimated that there are over 200 million cases of malaria, accounting for less than half a million deaths according to the World Health Organisation (WHO), January 2016. Nevertheless, other apicomplexan parasites are just as relevant due to their opportunistic nature and socio-economic impacts. Many apicomplexan parasites are food-borne pathogens and have an enormous global economic burden through the loss of commercial poultry and cattle (Sharman *et al.*, 2010; Trees *et al.*, 1999). Opportunistic parasites like *Neospora spp.* and *Toxoplasma gondii* often causes spontaneous abortions resulting in a negative impact on economic growth. Similarly, *Cryptosporidium spp.* cause the disease cryptosporidiosis which can lead to severe gastrointestinal illnesses and more recently been implicated as a major contributor in morbidity and mortality (Checkley *et al.*, 2015).

While most apicomplexan parasites have limited hosts or cell types, *Toxoplasma gondii* could be regarded as the world's most successful parasite. *Toxoplasma* can infect any warm-blooded animal and all nucleated cells within the host (Carruthers, 2002). The success and prevalence of the parasite is reflected in the statistic that around one-third of the world's human population is thought to

be infected with *T. gondii*, many of which do not show any outward symptoms (Hill *et al.*, 2005; Pappas *et al.*, 2009). Despite it being asymptomatic, it does cause severe, life-threatening complications and sometimes fatality in immunocompromised individuals and can have drastic developmental issues of the foetus during pregnancy (Hill *et al.*, 2005).

## 1.2 History of *Toxoplasma gondii*

*Toxoplasma gondii* was first discovered over 100 years ago by two independent groups; first in a hamster-like rodent, *Ctenodactylus gundi* (Nicolle & Manceaux, 1908) and later in a rabbit (Splendore, 1908). The name refers initially to its shape; *Toxon* (the Greek word for arc) and *plasma* for life (Nicolle & Manceaux, 1909). Moreover, *gondii* appears to come from a misspelling of *gundi*, the organism where it was first isolated (Nicolle & Manceaux, 1908). Its importance in human health emerged years later after it was observed that *T. gondii* could be passed congenitally to the unborn foetus from mothers who were asymptomatic causing foetal under-development and miscarriage (Cowen & Wolf, 1937). A few years later, the first fatal case in an adult due to *T. gondii* was reported (Pinkerton & Weinman, 1940). From then much research proceeded to understand the biology of *Toxoplasma* as it was understood that the parasite can infect all warm-blooded animals and birds (Tenter *et al.*, 2000).

From the 1970s, research began to focus on the molecular biology, genetics and immunology of the parasite (Ferguson, 2009). Pfefferkorn and colleagues characterised parasites that displayed different drug resistance and auxotrophic markers using mutagenic techniques (Pfefferkorn & Borotz, 1994; Pfefferkorn & Pfefferkorn, 1977a; Pfefferkorn & Pfefferkorn, 1977b; Pfefferkorn & Pfefferkorn, 1980). The ability to culture the parasite under *in vitro* conditions within the lab made significant progress in understanding many aspects of its lifecycle (Azab & Beverley, 1974; Hughes *et al.*, 1986). Most studies within the lab have focused on the highly virulent type I strain known as RH (Khan *et al.*, 2009a). This strain has been used extensively to study many functions such as host/parasite interactions, aspects of the parasites asexual lifecycle and also in molecular characterisation (Yang *et al.*, 2013). Furthermore, due to much conservation within Apicomplexa, *Toxoplasma gondii* became a valuable model organism in understanding some aspects of the *Plasmodium spp.* asexual

lifecycle, predominantly the mechanisms of invasion (Meissner *et al.*, 2013) (discussed further in chapter 1.12). Recent studies to characterise invasion mechanisms suggested that type I parasites invade in an active manner. This compares to avirulent strains that are thought to go through an alternative pathway of engulfment by a phagocytic cell and then escape from the phagosome (Zhao *et al.*, 2014). This raises the question to whether the RH type I strain has adapted to *in vitro* culturing over time. Molecular characterisation began with Cesbron-Delauw and colleagues, who described the first cloning of individual genes (Cesbron-Delauw *et al.*, 1989). This led to the development of selectable markers for allelic replacement and the generation of gene regulatory tools in *T. gondii* (Donald & Roos, 1993; Kim *et al.*, 1993; Roos *et al.*, 1994; Soldati & Boothroyd, 1993; Soldati & Boothroyd, 1995). In recent years, the genetic tools to study specific gene functions have evolved greatly allowing the complete characterisation of many gene functions and pathways crucial to the parasite (Jimenez-Ruiz *et al.*, 2014; Wang *et al.*, 2016) (discussed further in chapter 1.13).

### 1.3 Pathogenesis of *Toxoplasma gondii*

Toxoplasmosis is an important clinical disease associated with the infection from *Toxoplasma gondii*. Although *T. gondii* has a high prevalence rate throughout the world (Pappas *et al.*, 2009), clinical manifestations of severe toxoplasmosis is surprisingly low (<20 %) (Flegr *et al.*, 2014; Hill *et al.*, 2005; Remington, 1974). Toxoplasmosis is generally asymptomatic in healthy individuals causing mild, flu-like symptoms. However, in cases where the patient has a compromised immune system (e.g. AIDS, organ transplant or undergone chemotherapy), clinical disease can occur with varying severity. In adults, the severity of illness ranges from ocular toxoplasmosis to myocarditis, encephalitis or hydrocephalus and can be fatal (Maenz *et al.*, 2014). On the other hand, if a female is infected during pregnancy, *Toxoplasma gondii* tachyzoites can traverse the placenta, infecting the developing foetus, causing congenital toxoplasmosis (Figure 1-1). This can have drastic effects during development leading to miscarriage or stillbirth (Dunn *et al.*, 1999). However, if the foetus survives, many will not show symptoms until later in their adult life. The disease for a foetal infection can range from mental retardation, being affected by seizures, hearing or vision problems, low birth weight or spleen or liver enlargement.

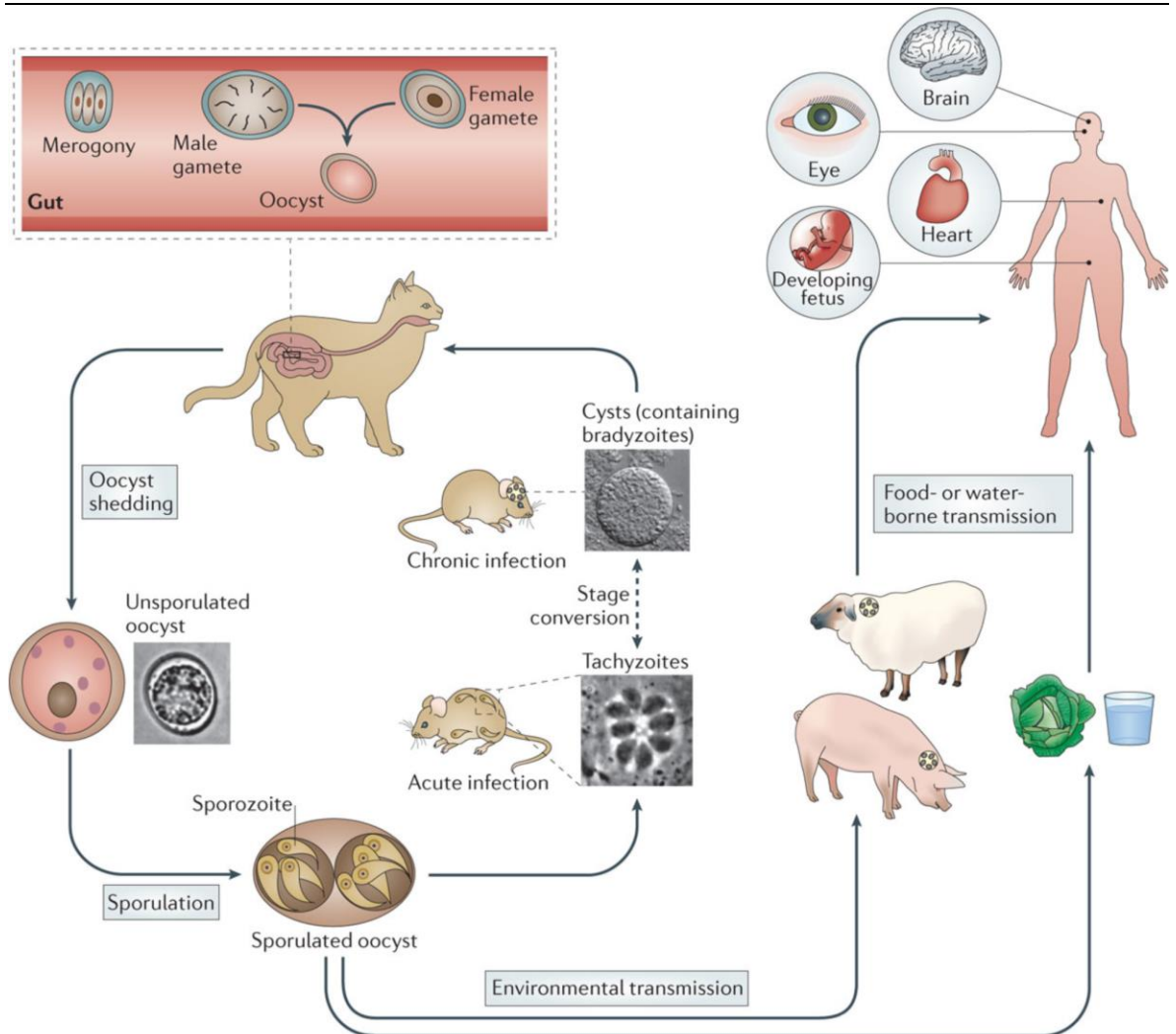
Many of these children will not survive past their teenage years (Moncada & Montoya, 2012).

It is believed that *Toxoplasma* in the brain can manipulate the hosts' behaviour. It has been shown that mice infected with *Toxoplasma* specifically lose their fear of cats leading to the hypothesis, that the parasites manipulate the host to continue their reproductive cycle (Ingram *et al.*, 2013; Vyas, 2015; Webster, 2001). In humans, it has been implied that *Toxoplasma* can cause neurological diseases such as schizophrenia (Kramer, 1966), although a later study showed there is no correlation between incidences of neurological disorders and areas with high prevalence rates of *T. gondii* (Pappas *et al.*, 2009).

Different isolates of *T. gondii* show different virulence levels in their hosts (Khan *et al.*, 2009b). There are three main groups of *Toxoplasma* with various degrees of virulence; Type I is the most virulent while types II and III are less virulent and also have a much slower growth rate than Type I parasites (Fuentes *et al.*, 2001; Grigg *et al.*, 2001). Type I is most commonly found as a clonal isolate across Europe and North America, whereas South America and Asia are largely a mix between both Types II and III and an array of atypical strains (Khan *et al.*, 2009a).

## 1.4 Lifecycle of *Toxoplasma gondii*

As with many Apicomplexa, *Toxoplasma gondii* has a dual host lifecycle first reported in 1970 (Dubey *et al.*, 1970b; Frenkel *et al.*, 1970). The parasite alternates between the sexual reproduction phase which is limited to the intestines of felids, its only definitive host and its asexual lifecycle which can occur in all warm-blooded mammals (Figure 1-1). Unlike most other apicomplexan parasites *T. gondii* does not need to go through its sexual lifecycle before transmission to another host (Su *et al.*, 2003).



Nature Reviews | Microbiology

**Figure 1-1: The complete lifecycle of *Toxoplasma gondii***

Sexual replication occurs in cats, the definitive hosts of *Toxoplasma gondii*. The male and female gametes are formed in cats' guts and unsporulated oocysts are shed into the environment by the cat's faeces. Once in the environment, the oocysts sporulate and are ingested by the intermediate hosts. The fast-replicating tachyzoites are able to invade all nucleated cells and can disseminate throughout the body. These tachyzoites can also traverse the placenta, causing congenital toxoplasmosis. The tachyzoites will infect tissue cells and can differentiate into slow-growing bradyzoites. They will form long-lasting cysts, and if the cat ingests them, the cycle continues. Reprinted by permission from Macmillan Publishers Ltd: [Nature Reviews Microbiology] (Hunter & Sibley, 2012), copyright (2012).

### 1.4.1 Lifecycle in the definitive host

The definitive host for *Toxoplasma gondii* is in all felids and in particular, domesticated cats. It was widely accepted that transmission of bradyzoites to the cat was the predominant route to sexual reproduction (Dubey *et al.*, 1970a). However, ingestion of either the tachyzoite or sporozoite form may also lead to the formation of gametocytes (Figure 1-1). Once inside the cat's stomach, proteolytic enzymes in the stomach digest the bradyzoite cyst wall.

Trophozoites burst out of the cyst and invade the cats intestinal cells. These begin to grow and differentiate to schizonts, some of which form gametes. Micro and macrogametes fuse to form a single oocyst that is shed into the environment through cat faeces (Dubey *et al.*, 1970b) (Figure 1-1).

These oocysts then undergo sporogony where the sporulated oocysts contain two sporoblasts, each containing four sporozoites. To continue infection, another organism ingests these sporulated oocysts. If ingested by a cat, the sexual lifecycle will occur, while ingestion by an intermediate host leads to toxoplasmosis infection. In the intermediate host, excystation of the sporozoites occurs, and these actively cross the epithelial cells of the intestine and enter the lamina propria (Speer & Dubey, 1998). Sporozoites then transform into tachyzoites, which will quickly propagate an infection throughout the body. After this, the tachyzoites go on to complete their asexual lifecycle.

## **1.4.2 Lifecycle in the intermediate host**

*Toxoplasma* is an obligate intracellular parasite with a wide range of hosts. Virtually all warm-blooded vertebrates are susceptible to *Toxoplasma* infection, and within the host, all nucleated cells can be infected (Sibley, 2003). The asexual lifecycle of *T. gondii* has two stages; first, the lytic stage where the parasites undergo multiple rounds of replication within the host's cells (Figure 1-2). The second stage is where the parasites lay dormant within cysts (Blader *et al.*, 2015; Lyons *et al.*, 2002) (Figure 1-1).

### **1.4.2.1 The lytic lifecycle**

The lytic stage of the parasites lifecycle is a stepwise process where the tachyzoites use their gliding machinery to locate a suitable host cell. The parasites then attach, re-orientate and penetrate into the host cell. Once they are inside, the parasites reside within a parasitophorous vacuole and replicate by endodyogeny before egressing out of the cell to re-infect a fresh host cell (Figure 1-2).

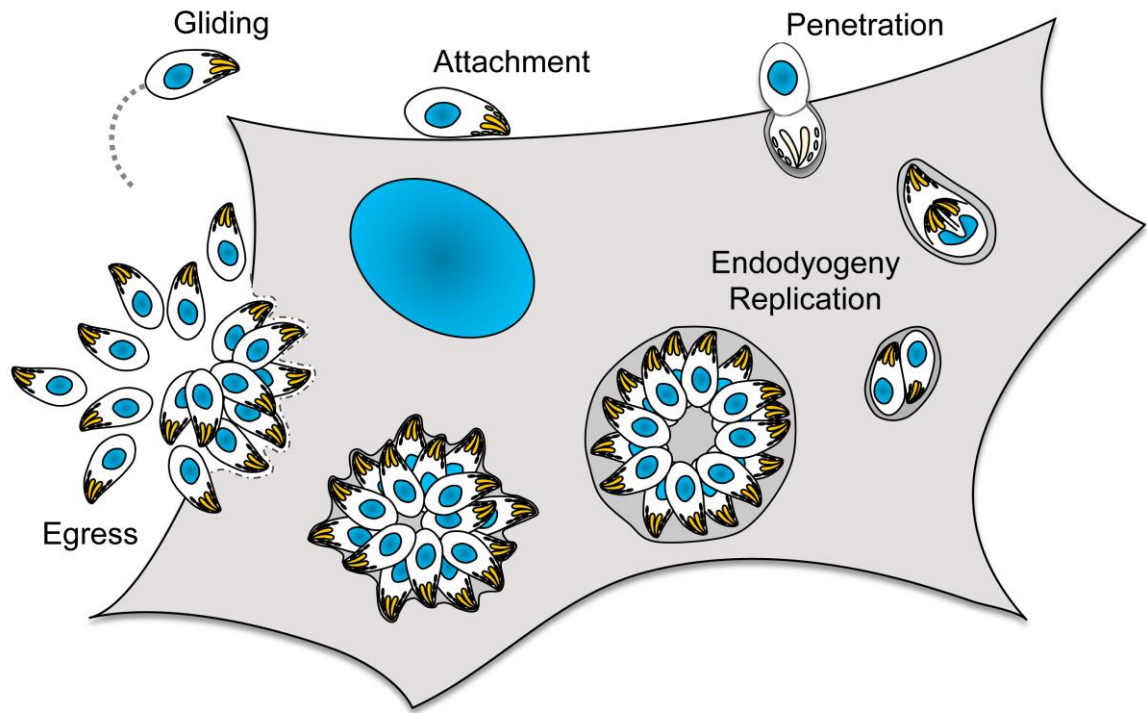


**Figure 1-2: The lytic lifecycle of *Toxoplasma gondii***

*Toxoplasma gondii* use their gliding machinery to locate a host cell. The parasites attach and reorientate to penetrate into the host cell through a tight junction. As the parasites push into the host, they generate a parasitophorous vacuole with which they reside in safety from the host immune system. The parasites then begin to replicate by endodyogeny, where the parasite numbers double after each round of replication. Once the host cell cannot support the infection, the parasites induce their own egress by lysing the parasitophorous vacuole membrane and host. After which, the parasites disseminate to find a new host and continue the cycle. Image inspired from Nicole Andenmatten.

#### 1.4.2.1.1 Gliding motility

*Toxoplasma* tachyzoites are the infective stages to host cells. These cells are highly motile and able to penetrate and migrate through tissue. In most eukaryotes motility is flagella or cilia driven or by crawling over a substrate. While in Apicomplexa, the movement is powered by the parasites own actomyosin motor complex, known as gliding motility (discussed in chapter 1.10.3). This complex allows the parasites to move across a 2D substrate (Hakansson *et al.*, 1999) and through 3D matrices (Leung *et al.*, 2014a). When parasites move over 2D substrates, they display three distinct motions; twirling, circular and helical (Hakansson *et al.*, 1999). The twirling motion is where the parasites appear to spin clockwise while balancing on their basal end. They may also exhibit circular gliding, where they move across the substrate in a circular motion at average speeds of 1.5  $\mu\text{m/s}$  (Hakansson *et al.*, 1999). This motion is comparable with *Plasmodium* sporozoites, which only move in a circular fashion on 2D surfaces (Montagna *et al.*, 2012). Finally, the parasites can move

helically, where they project forward about one body length over the substratum in a biphasic flip along the longitudinal axis of the parasites (Hakansson *et al.*, 1999). To date, the biological relevance of these movements has not been clearly defined. During these three motions, the parasites shed their surface membrane, leaving behind a trail of surface antigens (SAG1) along with a variety of other proteins. However, a more recent study evaluating parasite motility within a 3D matrix highlighted a new distinct motion (Leung *et al.*, 2014a). In 3D, parasites move exclusively in a left-handed corkscrew, leading to the speculation that 2D-motility is somewhat artificial and represents the attempt of the parasite to move in a corkscrew-like manner. During this motion, parasites do not glide at a continuous speed but instead go through fast and slow boosts, which coincides with calcium secretion (Personal communication with Prof Gary Ward, ISAB meeting 2016). This assay is more representative of the *in vivo* situations observed. For example, *Plasmodium* sporozoites are capable of travelling across large distances before invading hepatocytes. The sporozoites move also in a corkscrew-like fashion in 3D, where the movement through dermis is in random patterns caused by obstacles that force the parasite to change direction (Amino *et al.*, 2006), while on 2D coverslip they only move in circular motions (Montagna *et al.*, 2012).

#### 1.4.2.1.2 Invasion

Motility and invasion are both tightly controlled and require the sequential secretion of proteins within the micronemes, rhoptries and dense granules (Carruthers & Boothroyd, 2007). Invasion is a multistep highly conserved process among apicomplexan parasites (Figure 1-3). It involves finding and invading a suitable host cell that is thought to be driven actively by the parasites gliding machinery (Dobrowolski & Sibley, 1996). Once an appropriate cell is located, the parasites discharge their micronemal proteins from their apical end to attach firmly to host cell receptors (Carruthers & Tomley, 2008; Dowse & Soldati, 2004). This firm apical attachment causes the parasites to reorientate at their apical end. The parasites then discharge a second set of specialised secretory organelles, known as rhoptries into the host cytosol. Rhoptry bulb (ROPs) and neck (RONs) proteins are secreted in a regulated manner. Firstly the RONs are discharged from the neck region into the host cytosol and return to the surface to form the scaffold between RON2 and AMA1 termed the tight- or

moving-junction between the parasite and host cell (Bichet *et al.*, 2014; Lamarque *et al.*, 2011). After junction formation, the parasites sequentially secrete their ROPs to begin the formation of the parasitophorous vacuole (PV) made from the invagination of the host plasma membrane (Suss-Toby *et al.*, 1996). Active penetration of the host cell begins at the apical end of the parasite and is thought to be dependent on the parasites gliding machinery. The AMA1-RON2 junction at the apical tip is translocated to the posterior end of the parasite as it pushes further into the host cell (Figure 1-3). The tight-junction acts as a molecular sieve where parasite surface proteins and host cell membrane lipids are cleaved off in a process known as protease mediated shedding (Dowse & Soldati, 2004). The third set of secretory proteins, called dense granules, are constitutively secreted and thought to function in the formation and continual modulation of the PV and host cell environment during replication. At the end of invasion, the tachyzoite resides within the PV and the PVM is closed (Mercier *et al.*, 2005). This whole invasion process from initial tight junction formation to closure takes on average around 30 seconds to complete (Figure 1-3) (Morisaki *et al.*, 1995). The PV is thought to be non-fusogenic with the host endocytic system, allowing it a safe environment to proliferate (Mordue & Sibley, 1997). Promptly after invasion, the PV actively moves towards the host cell nucleus and becomes tightly associated with the mitochondria and endoplasmic reticulum (Sinai *et al.*, 1997).

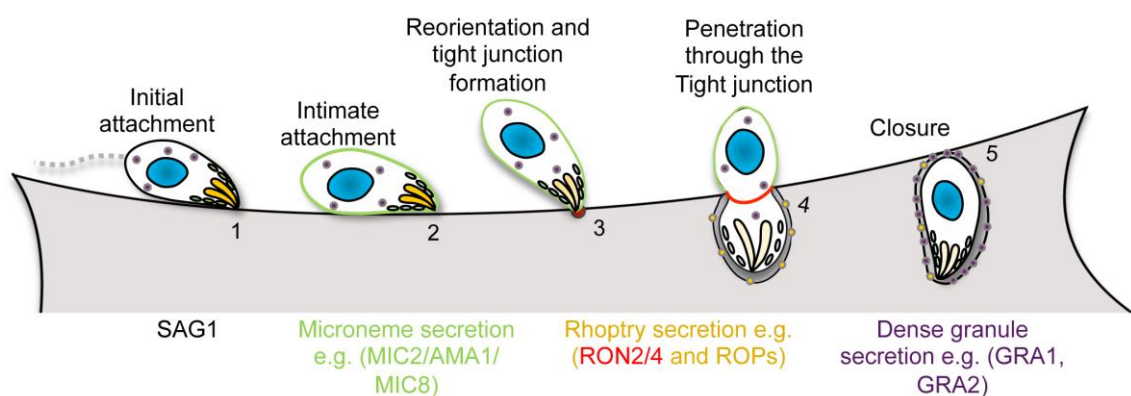


**Figure 1-3: Invasion steps of *Toxoplasma gondii***

The working model of *Toxoplasma* invasion. 1) The parasites locate and attach to the host surface using constitutively secreted surface antigens (SAG1). 2) Micronemal proteins (light green) are secreted to the parasites surface and are involved in intimate attachment to the host, namely through the interactions of MIC2 and host cell receptors. Although not depicted, conoid extension occurs at some point between stages (2-3). Proceeding intimate attachment, the parasite reorientates at the apical end (3), discharging their rhoptry neck proteins (RONs; light yellow) into the cytoplasm of the host. These migrate back to the surface and interact with the micronemal protein AMA1 to stabilise the tight junction (red). This structure is required to provide the

anchorage to the parasites actomyosin system to actively penetrate the host (3-4). Simultaneously or immediately after, the rhoptry bulb proteins (ROPs; orange spheres) are discharged and fuse with the newly forming parasitophorous vacuole (PV) (4). Concurrent with steps 3 and 4 dense granule secretion (purple) to assist in modulating the PV (5). Figure inspired by Carruthers and Boothroyd (2007).

### 1.4.2.1.3 Replication

Once inside, the parasites reside within a parasitophorous vacuole, that resists the fusion with host endosomes and lysosomes (Jones & Hirsch, 1972) and maintains a neutral pH (Sibley *et al.*, 1985). The parasites then begin to replicate by endodyogeny (Figure 1-2) where two daughter cells form within one mother (Hu *et al.*, 2002a). Commitment to replication starts with the division of the centrioles and the interaction of these with the newly forming cytoskeleton ensuring the polarity of the daughter cells. At the same time, DNA replication begins. In early S1 phase, the components of the cytoskeleton are observed as daughter budding begins. This is composed of the conoid followed by the spindle poles and intranuclear microtubules. Following this, the inner membrane complex (IMC) of the daughter cells is initially formed (Agop-Nersesian *et al.*, 2010; Hu *et al.*, 2002b; Nishi *et al.*, 2008). The microtubules drive daughter cell division concurrently with the IMC (Shaw *et al.*, 2000). Next, the organelles are distributed between the newly forming daughter cells in a coordinated manner; firstly the Golgi apparatus, followed by the apicoplast and then nuclear division (He *et al.*, 2001; Hu *et al.*, 2002a). In the latter stages of division, the ER and mitochondrion are divided (Nishi *et al.*, 2008). At the end of division, all the organelles are separated between the two daughter cells and the IMC formation is closed to complete division. Following this, the apical organelles such as micronemes and rhoptries from the mother cell are degraded and recycled by the daughter cells. Finally, these specialised secretory organelles are synthesised *de novo* for each daughter (Nishi *et al.*, 2008). The generation time of *Toxoplasma gondii* tachyzoites will continually replicate with a doubling time averaging 6 hours (Gubbels *et al.*, 2008; Radke *et al.*, 2001).

As the parasites double in number the parasitophorous vacuole (PV) is constantly modified to cope with the increasing numbers. Following invasion, e-vacuoles made up of ROP proteins are secreted into the host cytosol and contribute to the biogenesis of the PV by fusing with the newly forming PVM (Hakansson *et al.*, 2001). Moreover, dense granule proteins such as GRA5, 7 and 8 are secreted

into the PV to maintain the PVM (Mercier & Cesbron-Delauw, 2015; Mercier *et al.*, 2002). The vacuolar space of the PV is modulated soon after invasion through the dense granules including GRA1, 16 and 24. Within an hour of invasion, dense granules, such as GRA2, 4 and 6 begin to make a membranous nanotubular network (MNN) (Sibley *et al.*, 1995). This network is made of tubule structures 40-60 nm that connect the parasites and extend to the PVM. The network is highly dynamic and will persist during the entire development of the parasite. The exact role of the network is still unknown, but it was suggested that it acts as a conduit for nutrient exchange between parasite and host (Mercier *et al.*, 2005; Mercier *et al.*, 2002; Sibley *et al.*, 1995).

#### 1.4.2.1.4 Egress

After several rounds of replication, when the host cell can no longer support the infection, it is important for the parasites to escape and continue the lifecycle (Figure 1-2). To do this, the parasite induces its own egress. A peak in intracellular calcium levels signals the parasites to activate their gliding machinery and lyse both the parasitophorous vacuole and host cell membrane. This increase in calcium levels triggers microneme secretion and causes a disruption to the parasitophorous vacuole membrane (PVM) through the perforin-like protein (PLP1) (Kafsack *et al.*, 2009). Scanning electron microscopy revealed that tachyzoites exit host cells similar to how they invade (Caldas *et al.*, 2010). This indicated that egress is not a result of cell rupture but actively driven by the parasite.

It has been demonstrated that calcium-dependent kinases, in particular, CDPK3, is required for egress. This acts in a calcium-dependent signalling pathway that is induced by changes in environmental potassium levels from either cell damage or permeabilisation. It has also been shown that CDPK3 is involved in triggering microneme secretion and MyoA phosphorylation (Lourido *et al.*, 2012; McCoy *et al.*, 2012). Akin to gliding motility and invasion, it has also been shown that actin is essential for egress. Treating vacuoles with high concentrations of CD blocks egress even after artificial induction with a calcium ionophore (Moudy *et al.*, 2001; Shaw *et al.*, 2000) similar to observations with a conditional *act1* KO (Egarter *et al.*, 2014). Moreover, conditional knockout of the motor complex components severely affects egress (Egarter *et al.*, 2014).

### 1.4.2.2 Bradyzoite cysts

*Toxoplasma gondii* is a member of the cyst-forming coccidia. Therefore, after invasion and replication, some tachyzoites differentiate into the dormant cyst form of bradyzoites (Figure 1-1) (Dubey *et al.*, 1998). This occurs around 10-14 days post infection and is found in tissues throughout the body. The name bradyzoite comes from the Greek term of 'brady=slow' to describe how they replicate (Dubey *et al.*, 1998). Bradyzoites are very similar in their ultrastructure to tachyzoites. The key differences are that bradyzoites are slightly thinner and have many amylopectin containing granules used to store energy (Dubey *et al.*, 1998). These will lay dormant within most tissue cells avoiding the immune system and waiting to be ingested by another organism for transmission. The concern to the health of the host follows the rupture of one of these cysts, where the bradyzoites are released with some transforming back into tachyzoites causing an acute infection (Gross *et al.*, 1997; Lyons *et al.*, 2002).

## 1.5 Morphology of *Toxoplasma gondii*

With the exception of the male gametes during sexual reproduction, members of the phylum Apicomplexa are non-flagellated. Another feature of Apicomplexa is they all have a highly polarised apical complex that is a regulated secretion gateway for invasion (Katris *et al.*, 2014). The morphology of *Toxoplasma gondii* changes depending on the life-stage the parasite is in (Dubey *et al.*, 1998) and for this thesis, I will focus on the tachyzoite stages.

### 1.5.1 The ultrastructure of the tachyzoite

The tachyzoites are often present in a crescent "banana" like shape that measures approximately 2  $\mu\text{m}$  by 10  $\mu\text{m}$  (Figure 1-4). The name "tachyzoite" was first termed by Frenkel in 1973 which was derived from the Greek word *tachos*, meaning speed, in reference to the rapid replicative rate of the parasites within the intermediate host (Frenkel, 1973). For the crescent shape, the parasites are more pointed at the anterior pole and rounded at the posterior end (Dubey *et al.*, 1998). The ultrastructure highlights various organelles, some of which are synonymous to eukaryotic cells but some are highly specific to Apicomplexa. Akin to all eukaryotes, these tachyzoites contain a nucleus, a

single mitochondrion, a single Golgi apparatus and the endoplasmic reticulum (ER) (Pelletier *et al.*, 2002). Apicomplexa characteristics are derived from its apical complex which includes a highly specialised set of secretory organelles termed the micronemes and rhoptries (Morrisette & Sibley, 2002). Including the micronemes and rhoptries, the parasites also have dense granules within their arsenal that are indispensable to the parasites intracellular lifestyle. Many apicomplexan parasites contain a relic-like plastid termed the apicoplast (Waller & McFadden, 2005). The parasite is completely enclosed by the three layered membranous structure composed of the plasma membrane and the inner membrane complex. The IMC acts as an anchor for the motor complex (Mann & Beckers, 2001)

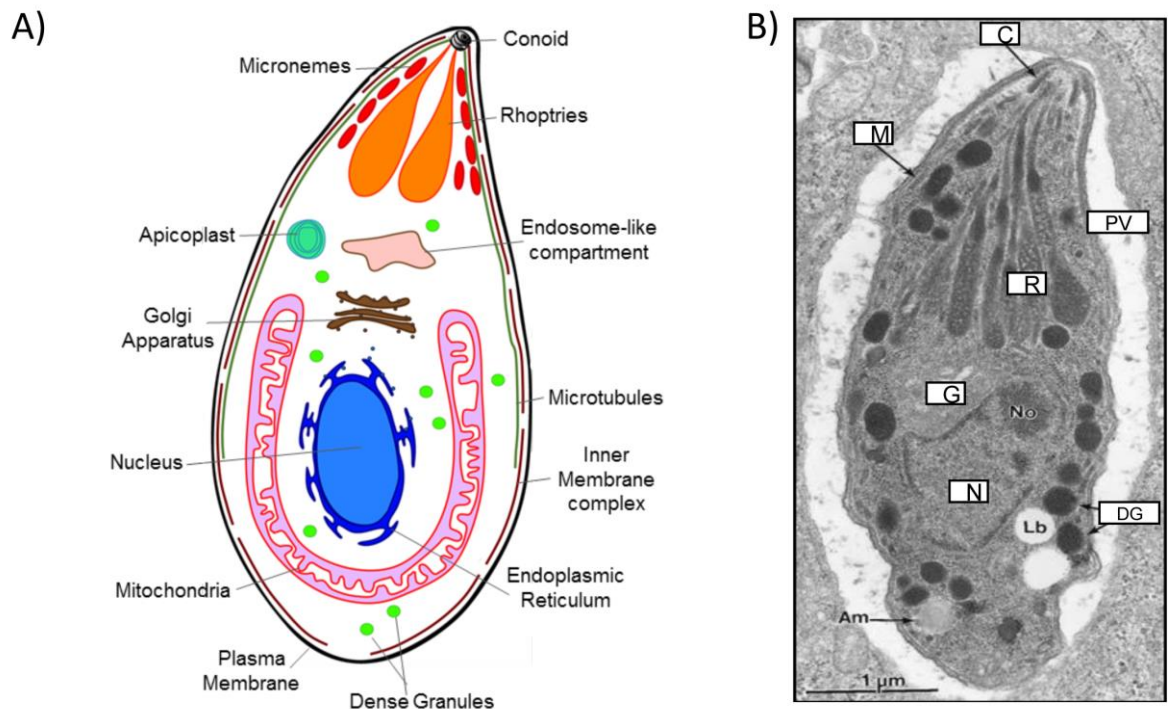


**Figure 1-4: Ultrastructure of the *Toxoplasma gondii* tachyzoite**

**A)** Schematic representation of the *Toxoplasma gondii* tachyzoite highlighting some specific organelles. The tachyzoite is surrounded by a double membranous structure: the plasma membrane (black) and the inner membrane complex (IMC) shown in dark red. Specialised secretory organelles, micronemes (red) and rhoptries (orange) are located at the apical end of the parasites under the conoid. From the conoid, 22 sub-pellicular microtubules (dark green) run 2/3 of the parasites length to maintain the shape. Dense granules (green) are distributed throughout the cytoplasm of the parasites. The centre of the parasites contains a single tubular mitochondrion (pink), an apicoplast (mint green), Golgi stack (brown) and an endosome-like compartment (pink). The nucleus (light blue) is located in the bottom half of the parasites surrounded by the endoplasmic reticulum (dark blue). **B)** An electron micrograph of an intracellular tachyzoite. Highlighted are the micronemes (M), rhoptries (R), dense granules (DG), conoid (C) and nucleus (N). Also highlighted is the parasitophorous vacuole (PV) where the parasites reside. Scale bar: 1 µm. Reprinted with permission from American Society for Microbiology: [*Clinical Reviews Microbiology*] (Dubey *et al.*, 1998), copyright 1998.

## 1.5.2 The apical complex and secretory organelles

### 1.5.2.1 The conoid and cytoskeleton

At the extreme tip of the apical complex of the coccidia members of Apicomplexa lies the conoid and is bound to the cytoskeleton through the interaction of microtubules (Figure 1-4) (Dubey *et al.*, 1998). The conoid is a hollow cone-shaped structure. The cone structure is made of 14 tubulin fibres; spirally wound around two intra-conoid microtubules that are sandwiched between two apical polar ring structures (Hu *et al.*, 2002b). The conoid is suggested to be essential for penetration of the intestinal epithelium (Morrisette & Sibley, 2002). The conoid may also play a major role during tachyzoite invasion. When the parasites are extracellular, the conoid extends beyond this holding centre, appearing to test the environment for a suitable host cell to invade. This extension process is thought to be actin-myosin driven (Del Carmen *et al.*, 2009; Shaw & Tilney, 1999). The polar rings form the microtubule organising centres (MTOC) that the sub-pellicular microtubules emerge from. *Toxoplasma* contains 22 microtubules that emerge from the MTOC and spiral down 2/3 the length of the parasites (Figure 1-4). These microtubules are the key component to *Toxoplasma's* shape and structural stability (Morrisette *et al.*, 1997; Shaw *et al.*, 2000).

### 1.5.2.2 Micronemes

The small ellipsoidal shaped organelles (around 250 x 50 nm) concentrated around the apical end and are known as the micronemes (Figure 1-4). Proteins stored in these organelles are essential for many processes during the lifecycle, most notably gliding motility and invasion (Carruthers & Tomley, 2008). A prerequisite for successful invasion is the correct trafficking of the micronemal proteins to the organelles (Breinich *et al.*, 2009; Kremer *et al.*, 2013). To date, there are over 50 micronemal proteins known, and these condense into two subsets within the micronemes during the trafficking (Kremer *et al.*, 2013). Secretion of micronemal proteins is controlled by the increase of intracellular calcium levels (Lovett *et al.*, 2002). Intracellular  $\text{Ca}^{2+}$  levels peak before egress (Moudy *et al.*, 2001; Withers-Martinez *et al.*, 2014) and during invasion (Arrizabalaga & Boothroyd, 2004), both where microneme secretion is required. A key feature of many micronemal proteins is that they contain adhesive

domains (Sheiner *et al.*, 2011). For example, the thrombospondin-like domains found in MIC2 are implicated in host cell attachment (Carruthers & Tomley, 2008). Previously, MIC2 was thought to be essential (Huynh & Carruthers, 2006) and bridges the interface between the parasites acto-myosin motor complex and host cell receptors through the glycolytic enzyme aldolase (Starnes *et al.*, 2009). This was recently questioned, and while MIC2 and aldolase were found to be non-essential *in vitro*, MIC2 still remains a major adhesive molecule for *Toxoplasma* (Andenmatten *et al.*, 2012; Shen & Sibley, 2014). Similarly, apical membrane antigen 1 (AMA1) bridges the gap during invasion by its intimate interaction with RON2 at the tight junction but is dispensable during *in vitro* culturing (Bargieri *et al.*, 2013; Lamarque *et al.*, 2011; Mital *et al.*, 2005; Srinivasan *et al.*, 2011). Conversely, MIC8 another micronemal protein has adhesive domains but is not involved in attachment but implicated in the release of rhoptry proteins essential for invasion (Kessler *et al.*, 2008). Perforin-like protein 1 (PLP1) is also found in the micronemes but is secreted immediately prior to egress where it disrupts the parasitophorous vacuole membrane facilitating parasites release from the host (Garg *et al.*, 2015; Kafsack *et al.*, 2009).

### 1.5.2.3 Rhoptries

Crucial for invasion are the club-shaped organelles termed rhoptries that appear at the apical end, extending into the conoid (Figure 1-4). Tethering of these rhoptries to the apical end has been suggested to be actin dependent through armadillo repeat only proteins (TgARO) (Mueller *et al.*, 2013). Rhoptry numbers vary, but usually a parasite contains around 8-10, each measuring 1-3  $\mu\text{m}$  in length (Dubremetz, 2007). Rhoptry proteins are located in dual sub-compartments within the organelle. The thin top duct of the rhoptries is termed the neck, which is in direct contact with the conoid and contains the rhoptry neck proteins (RONs) that are the first to be secreted during invasion. After secretion, the RONs form a complex and traverse back to the host surface and provide an adhesive anchor for which AMA1 binds at the ring-like tight-junction during invasion (Figure 1-3) (Beck *et al.*, 2014; Lamarque *et al.*, 2011; Lamarque *et al.*, 2014). The bulbous, sac-like compartment below the neck contains the rhoptry proteins termed ROPs. To date, there have been more than 30 ROPs identified (Bradley *et al.*, 2005). During invasion, ROPs are predominantly

involved in the formation and maintenance of the parasitophorous vacuole where the parasite resides (Figure 1-3) (Carey *et al.*, 2004a; El Hajj *et al.*, 2007). Toxofilin, a rhoptry protein, is secreted into the host and induces F-actin depolymerisation, weakening the host cytoskeleton to facilitate the invasion process (Delorme-Walker *et al.*, 2012; Poupel *et al.*, 2000). Moreover, many ROPs are kinases which are targeted to the host cytoplasm and nucleus and are involved in subversion of the host gene expression (Boothroyd & Dubremetz, 2008). Indeed, it is believed that some ROPs are major virulence factors for *Toxoplasma gondii* (Behnke *et al.*, 2012; Behnke *et al.*, 2015). *Toxoplasma* Type I are the most virulent and contain some rhoptries that are absent from the Type II genome (Yang *et al.*, 2013). In mice, ROP5 and ROP18 have evolved to inactivate IRGs on the PVM and avoid killing of the parasites (Niedelman *et al.*, 2012).

#### 1.5.2.4 Dense granules

Electron dense micro-spherical compartments measuring around 200 nm in diameter are arranged throughout the tachyzoite cytoplasm and are known as the dense granules (Figure 1-4). There are approximately 15 dense granules per parasite that move within the parasite on F-actin tracks (Heaslip *et al.*, 2016). Over the last 20 years, 16 dense granule genes have been characterised. Dense granule (GRA) proteins are secreted during invasion and have been implicated in the formation of the newly formed parasitophorous vacuole (PV) and maintenance of both the PV and the PV membrane (PVM) during replication (Mercier *et al.*, 2005). The PV is constantly adapting during the intracellular stages of the parasites and control of this is essential for continual growth. Moreover, this PVM must be selectively permeable to allow nutrients to pass through (Gold *et al.*, 2015). Some GRA proteins are involved in the biogenesis and stabilisation of the membranous nanotubular network (MNN) otherwise known as the tubo-vesicular network (TVN) in *Plasmodium spp.* (Adjogble *et al.*, 2004; Mercier *et al.*, 2002; Michelin *et al.*, 2009). This network is formed post-invasion and expands throughout as the parasite replicates. A knockout of *gra2* results in the disruption of this network and vacuole disorganisation (Mercier *et al.*, 2002). On the other hand, GRA16 and GRA24 are trafficked to the nucleus of the host and is implicated as major virulence factors for *Toxoplasma* (Bougdour *et al.*, 2014).

### 1.5.3 Inner membrane complex

The inner membrane complex (IMC) is made up of flattened membranous sacs called alveoli and lies just underneath the plasma membrane (Figure 1-4). Supporting the IMC on the cytoplasmic side is the highly organised subpellicular network consisting of a lattice of intramembranous particles (Mann & Beckers, 2001). This subpellicular network connects the IMC to the microtubules (Morrissette *et al.*, 1997). In *Toxoplasma*, the IMC spans almost the whole length of the parasite but is not connected to the conoid or basal body. Measurements of the distance between the IMC and the PM ranges between 22-30 nm in *Plasmodium berghei* sporozoites (Kudryashev *et al.*, 2010) and is similar in *Toxoplasma gondii*. Connecting the two membranous structures by myristoylated and palmitoylated residues is the glideosome-associated protein (GAP) 45. This is thought to be the determining factor to hold the distance between the two membranes, as a conditional knockout of GAP45 causes the PM to detach from the IMC (Egarter *et al.*, 2014). Moreover, the apical and basal ends of the parasites have GAP70 and GAP80 respectively (Frenal *et al.*, 2010). Transmembrane GAPs 40 and 50 are inserted into the alveolar membrane (Bosch *et al.*, 2012) which are essential for IMC biogenesis (Harding *et al.*, 2016). The space between the IMC and PM is thought to harbour the parasites gliding machinery, which will be discussed later in chapter 1.10.3.

### 1.5.4 The apicoplast

Many apicomplexan parasites, with the exception of *Cryptosporidium spp.* contain two endosymbiotic derived organelles, a single mitochondrion and a relic non-photosynthetic plastid known as the apicoplast (Figure 1-4). The apicoplast was discovered around 20 years ago in *Plasmodium* (McFadden *et al.*, 1996). The apicoplast is a relic plastid-like organelle derived from the endosymbiotic engulfment of a cyanobacterium by a red alga (Lim & McFadden, 2010; Waller & McFadden, 2005) and is surrounded by four membranes (Figure 1-4). The outermost membrane is derived from the host phagosome with the second outermost deriving from the plasma membrane of the red algae. The inner two membranes are from the chloroplast of the original organism (Waller & McFadden, 2005). The apicoplast still contains its own 35 Kb circular genome and is essential for parasite survival (Wilson *et al.*, 1996). Many features of the

original plastid have been lost, for example, it's photosynthetic ability. Nevertheless, the apicoplast is still responsible for fatty acid biosynthesis (FASII) (Ramakrishnan *et al.*, 2012; Waller *et al.*, 1998), isoprenoid precursors through the (DOXP) pathway (Nair *et al.*, 2011; Seeber & Soldati-Favre, 2010) and the synthesis of heme and iron clustering (Gisselberg *et al.*, 2013; Lim & McFadden, 2010; van Dooren *et al.*, 2012).

Correct segregation of the apicoplast during replication is actin and Myosin F dependent (Egarter *et al.*, 2014; Jacot *et al.*, 2013) that also depends on dynamin-related protein A (DrpA) (van Dooren *et al.*, 2009). Intriguingly, parasites that have lost their apicoplast can reinvade but succumb to delayed death when they begin to replicate (Fichera & Roos, 1997). Although, it has been shown that for replication the vacuole must contain at least one apicoplast (He *et al.*, 2001). Impressively, *Plasmodium falciparum* blood stage parasites can survive without an apicoplast if the culture is supplemented with isopentenyl phosphate (IPP), however this does not work for *T. gondii* (Yeh & DeRisi, 2011).

## 1.6 Actin

### 1.6.1 Overview and structure of actin in eukaryotes

Actin is one of the most abundant proteins in eukaryotic organisms (Poglazov, 1983). In the cytoskeleton, actin is one of three structural components along with microtubules and intermediate filaments (Alberts *et al.*, 2014). Actin exists in two forms: the monomeric, globular form known as G-actin or filamentous actin (F-actin). It has been well established that actin is a major house-keeping gene, forming the principal component in many processes from motility, cytoskeleton structure, trafficking and cell division to name a few (Olson & Nordheim, 2010; Pollard & Cooper, 2009). This is due to the transduction of mechanical signals and intracellular forces generated by the actin cytoskeleton.

The actin monomer is a 42 kDa protein made up of 375 amino acids that is highly conserved across eukaryotes. The atomic structure of actin was first resolved by complexing actin with DNaseI (Kabsch *et al.*, 1990). This revealed the monomer (also known as globular-actin or G-actin) has four sub-domains (Figure 1-5)

(Kabsch *et al.*, 1990). The comparison of ATP-bound and ADP-bound actin is a marked conformational change in the sub-domain 2 (Otterbein *et al.*, 2001). Sub-domain 1 contains both the N- and C-termini of the protein, while sub-domain 2 contains the highly variable DNase I loop. The cleft between subdomains 2 and 4 is the binding site for adenosine triphosphate (ATP) (Figure 1-5). At this position, the ATP can be hydrolysed to form ADP-bound actin. The changes in nucleotide state modify the confirmation of actin structure (Kabsch *et al.*, 1990; Otterbein *et al.*, 2001).

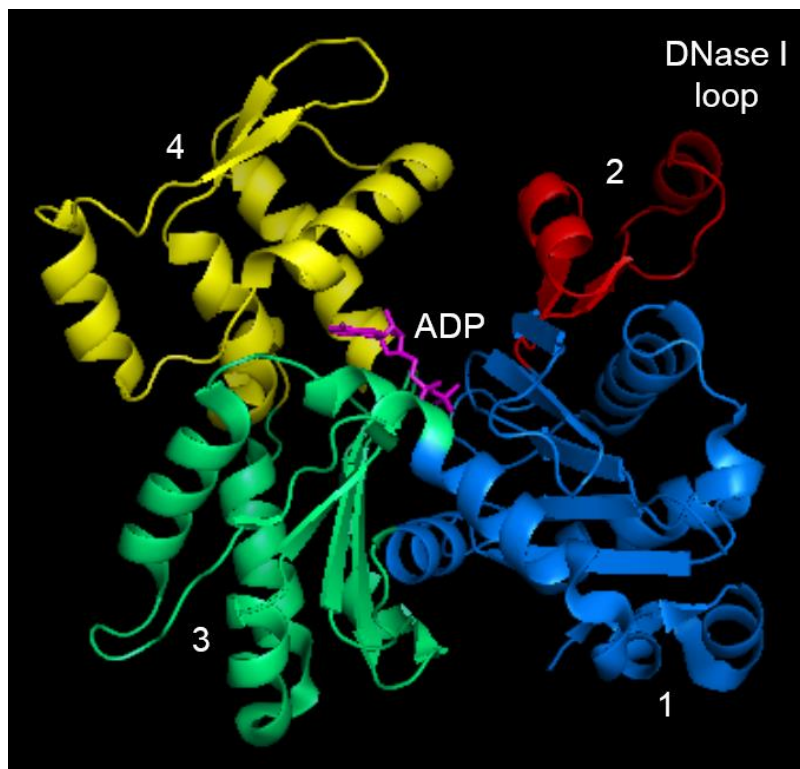


**Figure 1-5: The structure an actin monomer bound to ADP**

The ribbon structure of uncomplexed human  $\alpha$ -actin in the ADP state. The four different sub-domains of actin are shown in various colours. Sub-domain 1 (blue), sub-domain 2 (red) contains the highly variable DNase I loop, sub-domain 3 (green) and sub-domain 4 (yellow). The ADP (magenta) is found in the cleft between subdomains 2 and 4, where nucleotide exchange from ADP to ATP occurs. The structure is based on the actin monomer crystallised by (Otterbein *et al.*, 2001) and solved to 1.54 Å resolution. This image was generated using the PyMOL v1.74 software using the Protein Data Bank (PDB) code 1j6z, which is related to uncomplexed G-actin.

In higher eukaryotes, actin exists in 3 isoforms;  $\alpha$ -,  $\beta$ - and  $\gamma$ -actin, based on their isoelectric points (Garrels & Gibson, 1976). In general, these three isoforms are found in different cell types;  $\alpha$ -actin is restricted to muscle cells, while  $\beta$ -actin and  $\gamma$ -actin are present in all cell types (Herman, 1993). Actin was first discovered in the 1942 (Straub, 1942; Straub, 1943) and together with ATP forms filaments (Straub & Feuer, 1989). Formation of actin filaments proceeds

through a process known as actin nucleation through a cooperative assembly process (Pollard *et al.*, 2000). ATP-bound actin monomers form a nucleus, usually containing three actin monomers (Asakura *et al.*, 1963). Intermediates known as dimers or trimers are thermodynamically unstable and rapidly depolymerise without nucleation factors (Pantaloni *et al.*, 1984). Nucleation factors such as formins, spire or the Arp2/3 complex, function to stabilise the actin nucleus favouring polymerisation (discussed later in chapter 1.7.1). Once nucleation is favoured, the interaction of four actin monomers allows the polymer to become thermodynamically stable. Overcoming nucleation is the first rate-limiting step of actin polymerisation known as the lag phase (Figure 1-6) (Nishida & Sakai, 1983). Interestingly, polymerisation with purified  $\text{Ca}^{2+}$ -ATP-actin has a much longer lag-phase than  $\text{Mg}^{2+}$ -ATP-actin monomers (Carrier *et al.*, 1986). Then the elongation phase occurs, where ATP-bound actin monomers attach to both the barbed (+) end and pointed (-) end, although at different rates (Figure 1-6 A). The actin polymer quickly extends in length (Figure 1-6 B). This is the second rate-limiting step as it is directly proportional to the concentration of available actin monomers. The cytosolic concentration of actin monomers available to polymerise into F-actin is known as the critical concentration ( $C_c$ ) (Pantaloni *et al.*, 1984). If the monomer concentration is below that of the  $C_c$ , no polymerisation can occur. At this state, the existing filament will begin to depolymerise to provide the system with free actin monomers. Conversely, if the monomer concentration exceeds the  $C_c$ , the filament will polymerise and continue to grow until the monomer concentration reaches the  $C_c$ . At this state, G-actin to F-actin will be at a steady state, termed treadmilling (Figure 1-6 B, C). Therefore, the critical concentration determines the monomer to polymer equilibrium. Actin monomers can associate to both the barbed and pointed ends of the filaments (Figure 1-6 A). However, free actin monomers will associate and extend the barbed end with 3-5 times more affinity than the pointed end (Pollard, 1986). Typically, under *in vitro* conditions, the  $C_c$  of ATP-bound G-actin is around  $0.12 \mu\text{M}$  at the barbed end and  $0.6 \mu\text{M}$  for the pointed end (Figure 1-6 A) (Bonder *et al.*, 1983; Sept & McCammon, 2001). ADP-G-actin also has the ability to polymerise, but the  $C_c$  is around 3 times higher than ATP-G-actin (Pollard, 1984).

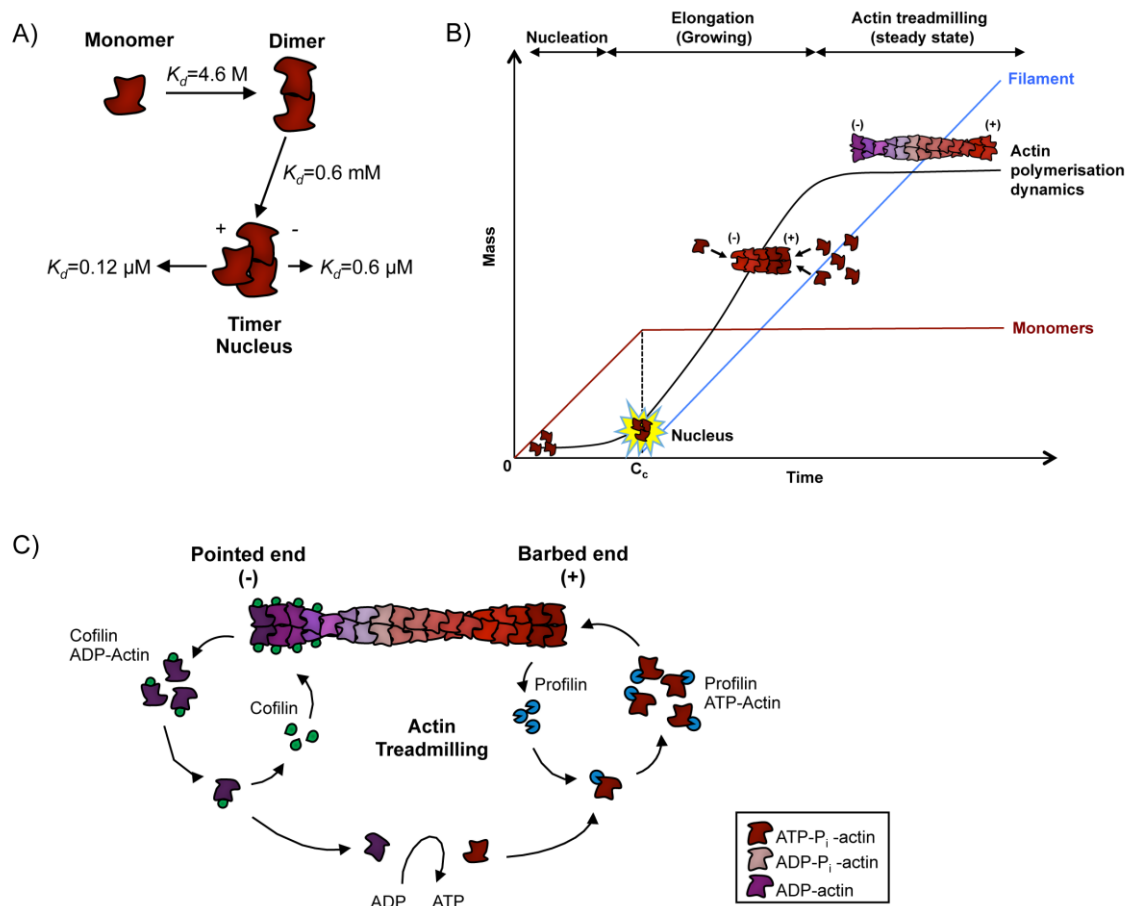


**Figure 1-6: Actin nucleation and treadmilling**

**A)** Spontaneous nucleation of actin filaments is thermodynamically unfavourable with dissociation constant ( $K_d$ ) to form a dimer. Once the nucleation nucleus is formed, filament elongation will occur, with a greater affinity of actin monomers to the (+) end of the filament, depicted by a larger arrow and  $K_d$  of  $0.12 \text{ } \mu\text{M}$  compared to the slow growing end (-) and a  $K_d$  of  $0.6 \text{ } \mu\text{M}$ . Image inspired from Deeks and Hussey (2005). **B)** Graphical representation of actin nucleation and polymerisation. The three phases of actin polymerisation are depicted by the solid black curve. The solid red line shows the total monomer concentration and the blue line represents the filament mass over time. At the start, there is an abundance of actin monomers. Once this reaches the critical concentration (black dashed line), the nucleus is formed and the filament growth now becomes thermodynamically favourable. During the elongation phase, more monomers are attracted to the filament as it grows in length. When the monomer concentration limit is reached, the system remains in a steady state where the assembly and disassembly of actin monomers from the filament is at equilibrium. Figure inspired from mechanobio.info. **C)** Actin filaments grow by addition of ATP-bound actin to the 'barbed' (+) end. The ATP is hydrolysed to ADP-bound actin. Over time, the inorganic phosphate ( $P_i$ ) is slowly released, resulting in the 'pointed' (-) end becoming unstable. The ADP is then exchanged for ATP, and the monomers are ready to integrate that the (+) end again. Actin-binding proteins such as cofilin and profilin act to sequester actin monomers. In particular, cofilin serves to sequester actin monomers from depolymerising filaments. While, profilin-bound ATP-actin is attracted to the FH1 domains of formins for nucleation. Image inspired from Baum *et al.* (2006).

The hydrolysis of ATP-bound actin to ADP-bound actin occurs in a dual process on F-actin: the ATP is cleaved from the actin subunit, and the inorganic phosphate ( $P_i$ ) is slowly released (Korn *et al.*, 1987; Murakami *et al.*, 2010). The cleavage of ATP from the actin subunit increases the stability of the filament with ADP-bound actin subunits. It is this slow release of  $P_i$  that destabilises the filament

for depolymerisation at the pointed or (-) end (Korn *et al.*, 1987). This process is known as actin treadmilling (Figure 1-6 C), where actin subunits are constantly removed from the filament at the (-) end while other subunits are added at the (+) end (Cleveland, 1982; Neuhaus *et al.*, 1983; Wegner, 1976). This process is essential for all functions of actin, in particular, cell motility (Figure 1-10) (Bugyi & Carlier, 2010).

The actin filament is made up of two protofilaments that intertwine to form a right-handed helix with a diameter of around 7-10 nm (Figure 1-6 A) (Dominguez & Holmes, 2011; Egelman, 2004). The length and conformation of these filaments in the cell varies considerably due to the control of actin-binding proteins and concentration of actin monomers (Discussed later in 1.7) (Wear *et al.*, 2000). The arrangements of F-actin can be categorised into three groups: parallel bundles (all the filaments orientate in the same direction), antiparallel bundles (filaments orientate in opposite directions) and dendritic networks (filaments form a lattice) (Chhabra & Higgs, 2007). The lengths of the filaments are controlled by the cells tropomyosins, while the Arp2/3 complex generates dendritic networks and proteins such as coronins and fascin bundle actin filaments (Gandhi & Goode, 2008; Li *et al.*, 2010).

### 1.6.2 Actin in apicomplexan parasites

Protozoan parasites have some of the most diverse actin compositions of eukaryotes (Gupta *et al.*, 2015). *Giardia lamblia* only has 58 % amino acid conservation and is the most divergent actin known to date (Drouin *et al.*, 1995). Recently, actin homologues have also been described for prokaryotes and are involved in morphogenesis and cell polarity (Jones *et al.*, 2001).

The evolution of actin in Apicomplexa shows it to be highly divergent, first reported in 1988 for *Plasmodium falciparum* (Wesseling *et al.*, 1988a; Wesseling *et al.*, 1988b). *Plasmodium spp.* encode two isoforms of actin (ACTI and ACTII), where ACTI is the major isoform, ubiquitously expressed throughout the lifecycle of the parasites. *Plasmodium* ACTII is expressed in gametocytes and mosquito stages, although it appears to only be essential in male gametocyte flagellation (Siden-Kiamos *et al.*, 2012; Vahokoski *et al.*, 2014). Unlike *Plasmodium spp.*, *Toxoplasma gondii* encode a single actin gene, termed ACT1 (Dobrowolski *et al.*,

1997). Comparisons of amino acid sequences indicate that ACT1 from both *Plasmodium spp.* and *T. gondii* are highly conserved (93 %), however, divergent from canonical  $\beta$  and  $\gamma$  actin isoforms (~80 %) (Dobrowolski *et al.*, 1997).

Similar to the differences between  $\alpha$ -,  $\beta$ - and  $\gamma$ -actin isoforms, the differences between apicomplexan actins and canonical actins give rise to some different properties. Both *Plasmodium* actin isoforms can hydrolyse ATP much more efficiently than  $\alpha$ -actin (Vahokoski *et al.*, 2014). In comparison to actin in other eukaryotic cells, *Toxoplasma* actin was reportedly found predominantly in the monomeric state (~97 %), with almost no F-actin detected (Dobrowolski *et al.*, 1997). Actin filaments are expected between the plasma membrane and IMC at the acto-myosin motor complex (discussed further in chapter 1.10.3). Despite this, the detection of actin filaments in the parasites has so far been elusive. Standard immunofluorescence analysis of TgACT1 with actin antibodies has only displayed a cytosolic staining, even after the addition of the F-actin stabilising drug, phalloidin (Schuler *et al.*, 2005b). Moreover, the use of GFP-actin as a reporter could not differentiate between cytosolic GFP-actin and F-actin (Angrisano *et al.*, 2012a). The use of a fluorescent jasplakinolide derivative (SiR-actin) was also unable to label any filaments within the parasites (Unpublished results from Dr. Javier Periz). To date, actin filaments in *Toxoplasma* have only been detected by electron microscopy (Dobrowolski *et al.*, 1997; Schatten *et al.*, 2003; Shaw & Tilney, 1999). Reasons for this could be, that they form very short, unstable filaments (Sahoo *et al.*, 2006). Likewise, phalloidin may be masked by an actin binding protein (Schuler *et al.*, 2005b) or more simply it is unable to bind due to the amino acid divergence of *Toxoplasma* ACT1.

For the past 20 years, much of the work on apicomplexan actin has been through the use of heterologous expression of PfACT1 and TgACT1. This has shown that they are intrinsically unstable and form very short, unbranched filaments of approximately 100 nm in length compared to rabbit actin that polymerises to around 3.5  $\mu\text{m}$  (Sahoo *et al.*, 2006; Schmitz *et al.*, 2005). There is conflicting data regarding the polymerisation kinetics of TgACT1. Under *in vitro* conditions, TgACT1 was shown to polymerise at a 3-4-fold lower concentration than those observed for canonical actins (Sahoo *et al.*, 2006). This would imply that actin

polymerisation in *Toxoplasma gondii* occurs at a much lower concentration of actin monomers than conventional actins. It was noted that the cytoplasmic concentration of TgACT1 is within the range of 8-10  $\mu\text{M}$  (Sahoo *et al.*, 2006). This far exceeds the  $C_c$  required for polymerisation; therefore nucleation should be favourable. However, as the parasite is thought to maintain a ~97 % G-actin state, there must be many actin-binding proteins regulating its dynamics to sequester the monomers so they cannot form filaments. Indeed, *Toxoplasma gondii* contains a strong actin depolymerisation factor (ADF), which may act to sequester the actin monomers (discussed further in Chapter 1.7.3). *Toxoplasma* F-actin is thought to be short and unstable, which is described as an evolutionary adaptation to control processes such as gliding motility. In contrast, a more recent study has suggested that TgACT1 polymerises in an isodesmic manner that does not have a lag-phase or require a critical concentration to polymerise (Skillman *et al.*, 2013). In an isodesmic model, polymerisation of any monomer would occur with equal affinity regardless of the polymer length due to a single equilibrium constant (Figure 1-7 B) (de Greef *et al.*, 2009). In comparison to cooperative polymerisation, there is no lag-phase during filament assembly (Figure 1-7), as dimer formation and filament elongation are both equally energetically favourable. This would make TgACT1 unique when compared to all other known actins and actin homologues (Gupta *et al.*, 2015). In the case of apicomplexan actins, this would suggest that even with minute levels of actin, polymerisation would still be favourable for short unstable filaments.

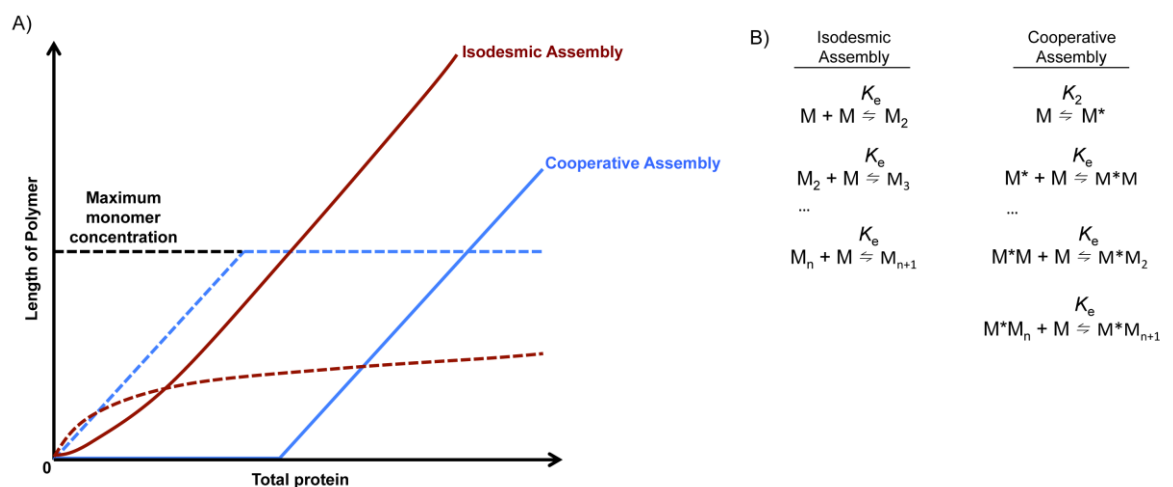


Figure 1-7: Isodesmic polymerisation versus cooperative polymerisation

**A)** In a cooperative polymerisation model (blue), filament growth will occur after the monomer concentration is higher than that of the critical concentration ( $C_c$ ). After which, further elongation of the filament is favourable over dimer formation. In an isodesmic model (red), the monomer association to dimer, trimer and polymers is equally favourable. Isodesmic assembly does not require a  $C_c$ . Solid lines represent the protein in a polymer at equilibrium, while the dashed lines represent the monomer concentrations at this equilibrium for each assembly process. Black dashed line represents the maximum possible monomer concentration. Both monomer concentrations reach the maximum, however, in an isodesmic model, this can be overcome by increasing the total protein concentration. Figure inspired by Miraldi *et al.* (2008). **B)** Isodesmic and cooperative polymerisation equilibrium constants; where M are the monomers,  $K_e$  = elongation equilibrium constant,  $K_2$  = nucleation equilibrium constant. Note that isodesmic polymerization has a single equilibrium constant, while cooperative polymerization has a nucleation constant and an equilibrium constant. Equations taken from Tambara *et al.* (2014).

Although the mechanisms of actin polymerisation and visualisation of actin filaments *in vivo* is elusive in *Toxoplasma gondii*, actin has many roles within the parasites. Treatment of parasites with small molecules that alter the actin dynamics affect many processes throughout the lifecycle, especially gliding motility and invasion. In particular, depolymerisation of F-actin through the use of Cytochalasin D or latrunculin B (discussed in detail in chapter 1.8) affects both gliding motility and invasion (Dobrowolski & Sibley, 1996; Rynning & Remington, 1978; Wetzel *et al.*, 2003). Artificially polymerising actin with jasplakinolide interferes with proper parasite motility and invasion (Poupel & Tardieux, 1999). This lead to the assumption that controlled polymerisation of F-actin is essential for efficient motility and invasion. However, the characterisation of a conditional *act1* KO indicated that ACT1 is important but not essential for motility or invasion. The *act1* KO also highlighted a role for actin in tachyzoite morphology, apicoplast division and egress (Egarter *et al.*, 2014), not observed with actin-modulating drugs.

## 1.7 Actin binding proteins (ABPs) in Apicomplexa

The transition between the monomeric pool and filamentous actin is controlled in spatial time and location within the cell by a vast repertoire of actin binding proteins (Dos Remedios *et al.*, 2003; Welch & Mullins, 2002). These proteins have various functions on actin, such as; nucleation, branching, capping, severing and bundling of actin filaments (Winder & Ayscough, 2005). In addition to providing structural support, actin provides the track for molecular motors such as the myosins to transport cargo along (Hartman & Spudich, 2012). Apicomplexan parasites and protozoan parasites in general, have a greatly reduced repertoire of actin binding proteins and nucleating factors (Gupta *et al.*, 2015).

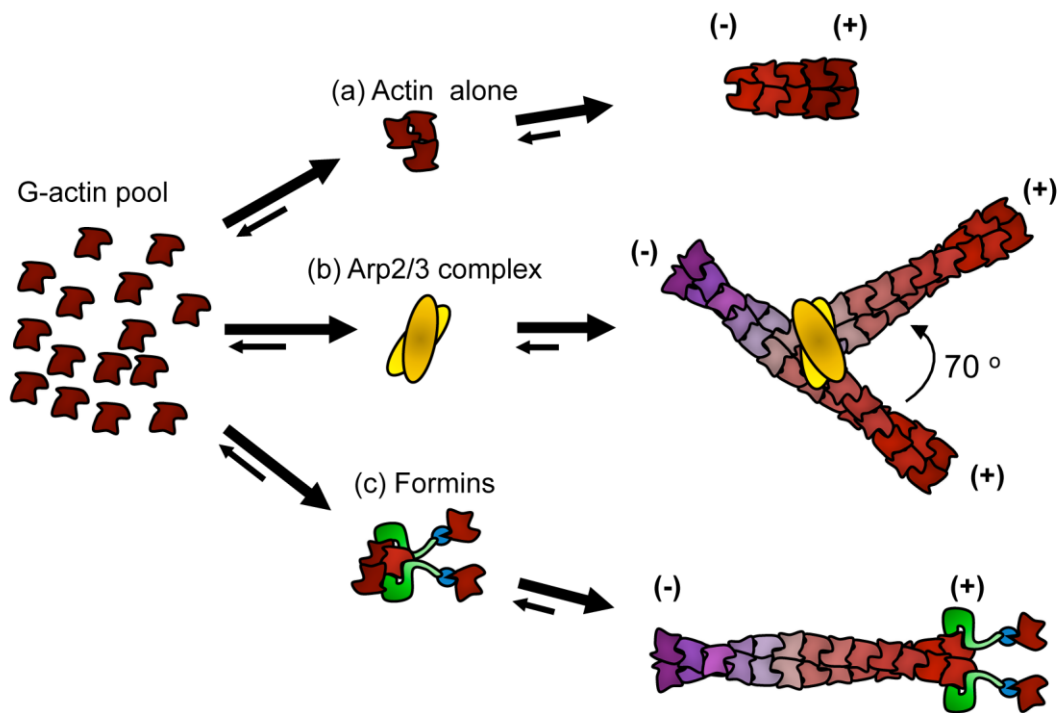


**Figure 1-8: Actin-binding proteins promote nucleation of F-actin**

**A)** On their own, actin monomers are thermodynamically unstable and very slow to self-nucleate but when four monomers interact, the  $C_c$  is overcome and filament growth is thermodynamically favoured. **B-C)** nucleation is favoured through various cofactors. **B)** The Arp2/3 complex is suggested to mimic an actin-trimer. This acts as a stable nucleus and attracts actin monomers for polymerisation. Moreover, the Arp2/3 can branch filaments at a  $70^\circ$  angle. **C)** Formins are thought to stabilise an actin-trimer through the interactions of their FH2-domains (dark green) while the FH1-domain (light green) is an attractant for profilin-bound actin (light blue). Figure inspired from Goley and Welch (2006).

### 1.7.1 Nucleation

Nucleation of actin filaments is an essential function for any cell. Controlled nucleation of F-actin can occur in a variety of ways, mainly through the actin binding proteins such as the actin-related protein (Arp) 2/3 complex (Mullins *et al.*, 1998), formins (Pring *et al.*, 2003) or the Wiskott-Aldrich syndrome protein (WASP) homology 2 (WH2) domain nucleators, such as Spire (Kerkhoff, 2006) (Figure 1-8). These are essential to overcome the rate-limiting step, trimerisation, in actin polymerisation. The Arp2/3 complex is large and consists of seven different subunits. In this complex, Arp2 and Arp3 structurally resemble an actin dimer to attract more actin monomers to serve as a nucleation start point (Figure 1-8). The unique feature of this complex is its ability to bind to an existing actin filament and nucleate a fresh actin filament that is branched at  $70^\circ$  forming an actin network (Figure 1-8) (Beltzner & Pollard, 2008; Machesky & Gould, 1999; Pollard, 2007). Strikingly, Apicomplexa have lost the Arp2/3 complex and its associated WASH/WAVE/WASP complexes

(Gordon & Sibley, 2005), as potent nucleators and branchers of actin filaments (Dominguez, 2009; Gong & Jiang, 2004). Indeed, these parasites only possess formins as actin-nucleating factors (Kuhni-Boghenbor *et al.*, 2012). Formins are large, multi-domain regulatory proteins that associate with the barbed end of actin filaments to promote actin polymerisation and control filament length (Evangelista *et al.*, 2003; Goode & Eck, 2007; Higgs & Peterson, 2005). Nucleation of actin by formins commonly results in F-actin cables rather than branched filaments. Typically, formins would coordinate with profilin for polymerisation, where the profilin provides the ATP-actin monomers to the poly-proline rich, formin-homology 1 (FH1) domain (Figure 1-8). All formins contain a homodimeric formin homology domain (FH2) required for nucleation and barbed-end filament binding for new actin monomers (Figure 1-8) (Pruyne *et al.*, 2002). Once bound to the barbed end, the formin remains associated to prevent capping proteins coupling with the filament (Pring *et al.*, 2003). While there are 15 different formin proteins found in humans to nucleate actin (Schonichen & Geyer, 2010), only three have been identified in *Toxoplasma* (Baum *et al.*, 2006; Daher *et al.*, 2010). While no actin filaments have been detected in *Toxoplasma*, it was shown that controlled polymerisation of actin was essential for parasites motility and invasion (Dobrowolski & Sibley, 1996; Wetzel *et al.*, 2003). *Toxoplasma* formins (FRM) 1 and 2 localise to the pellicle of the parasites, where FRM1 associates with the plasma membrane and FRM2 associated with the IMC. FRM3 localises to the both the anterior and posterior of the parasites. The depletion of FRM1 through the tetracycline regulatable promoter caused smaller plaques to be generated, while each stage of the lifecycle tested was only modestly perturbed (Daher *et al.*, 2010). FRM3 was determined to be dispensable for tachyzoite growth while the overexpression of dominant negative mutants had severe consequences for intracellular growth and replication (Daher *et al.*, 2011). Biochemical experiments show that both FRM1 and FRM2 promote actin polymerisation (Skillman *et al.*, 2012). The interaction with profilin *in vivo* is still not certain as none of the *Toxoplasma* formins have a canonical FH1 domain (Daher *et al.*, 2010).

### 1.7.2 Monomer sequestration

Actin treadmilling occurs by the affinity of actin monomers to the two ends of the filaments and is caused by the continuous hydrolysis of ATP (Bugyi & Carlier,

2010; Neuhaus *et al.*, 1983). Many actin-binding proteins bind to monomers for a variety of functions by sequestering G-actin to either promote polymerisation or depolymerisation (Neuhaus *et al.*, 1983). Again, only a few are present in Apicomplexa; profilin, and an Srv2/cyclase-associated protein (CAP). Moreover, they lack many others including  $\beta$ -thymosin and a conventional gelsolin (Baum *et al.*, 2006).

In mammalian cells, profilin is an actin-binding protein that sequesters actin monomers. Profilin is thought to catalyse the exchange of ADP-actin to ATP-actin by altering the conformation of G-actin, through the opening of the nucleotide-binding site to the cytosol. This increases the ATP-G-actin pool available that can subsequently be used for polymerisation (Kovar *et al.*, 2006; Pantaloni & Carlier, 1993). Working in combination with formins, profilin assists in promoting actin filament assembly (Figure 1-6 CFigure 1-8) (Paul & Pollard, 2008). Apicomplexan parasites are limited to a single profilin gene that is divergent from eukaryotic profilins (Kursula *et al.*, 2008). Biochemical studies have shown that *Toxoplasma* profilin has weak interactions with their formins raising the suggestion that profilin is not facilitating actin polymerisation in *Toxoplasma*, indicating a role in monomer sequestration (Daher *et al.*, 2010; Skillman *et al.*, 2012). Genetic depletion of profilin impairs both gliding motility and invasion but is dispensable for intracellular growth of the parasites (Plattner *et al.*, 2008). The loss of profilin does not alter the detectable actin monomeric pool level, determined with the addition of CD and Jas (Plattner *et al.*, 2008). Many studies have implicated *Toxoplasma* profilin as a potent inducer of IL-12 in mice (Kucera *et al.*, 2010; Plattner *et al.*, 2008; Salazar Gonzalez *et al.*, 2014; Yarovinsky *et al.*, 2005; Yuan *et al.*, 2015). It is thought that the parasites secrete profilin through an unknown mechanism during gliding motility and invasion for the mouse immune system to detect (Yarovinsky, 2014).

The CAP homologue in apicomplexan parasites is much smaller than those identified in higher eukaryotes, where they have lost the N-terminal region and the WH2 domain. This led to the suggestion that their function is solely in monomer sequestration (Hliscs *et al.*, 2010). In *Toxoplasma*, the CAP protein localisation depends on the lifecycle stage of the parasite. During intracellular replication, CAP is isolated to the apical region, while with extracellular parasites it is relocated to the cytoplasm (Lorestani *et al.*, 2012). Moreover, *in*

*vitro* assays of CAP in *Plasmodium berghei* revealed that it is not essential for the asexual stages of the malaria lifecycle (Hliscs *et al.*, 2010).

### 1.7.3 Severing and filament depolymerisation

As well as polymerisation, these filaments are required to be severed or depolymerised. A family of proteins termed actin depolymerisation factor (ADF)/Cofilin or gelsolin regulate these processes. The ADF and Cofilin family influence actin dynamics by sequestering G-actin monomers (Figure 1-8) (Bernstein & Bamburg, 2010; Galkin *et al.*, 2011; Yeoh *et al.*, 2002). ADF is usually more efficient monomer sequestration than Cofilin as it has a much weaker nucleating ability (Bamburg & Bernstein, 2010; Bernstein & Bamburg, 2010). Inhibition of the ADP exchange to ATP by actin bound to ADF/Cofilin prevents re-polymerisation. There are 14 different ADF/Cofilin proteins in humans, while *Toxoplasma* is limited to one and *Plasmodium spp.* have two (Baum *et al.*, 2006). In Apicomplexa, the ADF has a high affinity for ADP-actin and catalyses the conversion to ATP-bound actin (Schuler *et al.*, 2005a), a role normally associated with profilin. Apicomplexan ADF has a limited ability to depolymerise and sever actin filaments, probably due to the loss of PIP<sub>2</sub> (Mehta & Sibley, 2010; Schuler *et al.*, 2005a; Yadav *et al.*, 2011). The loss of ADF in *Toxoplasma* causes an accumulation of F-actin at the apical and basal regions of the parasites and causes a rocking movement of the tachyzoites, comparable with Jas treatment (Mehta & Sibley, 2011).

### 1.7.4 Crosslinking and bundling of F-actin

The reduced repertoire of actin binding proteins in Apicomplexa continues in their ABPs required to crosslink and bundle actin filaments. Apicomplexa only encode a single coronin protein to cross-link or bundle actin filaments while notable absentees are  $\alpha$ -actinin/filamin/spectrin bundling proteins as well as fascin and tropomyosin (Baum *et al.*, 2006). Moreover, they have also lost all cytoskeletal actin structural proteins such as talins and vinculins (Baum *et al.*, 2006). Conventional coronins rapidly remodel cytoskeletal actin for processes including endocytosis (Kimura *et al.*, 2008) and cell motility (Cai *et al.*, 2008). It is thought that coronin has dual functions to accelerate actin polymerisation at the barbed end by recruiting the Arp2/3 complex but also coordinates with

Cofilin to depolymerise ADP-rich actin filaments (Chan *et al.*, 2011; Gandhi & Goode, 2008). Overall, the coronin plasticity is required to increase the actin network by replenishing the monomer pool required for further filament growth (Gandhi & Goode, 2008). In apicomplexan parasites, coronins have the ability to bind F-actin and facilitate the bundling of parallel filaments (Olshina *et al.*, 2015; Tardieux *et al.*, 1998). This protein has been implicated in guiding directional motility and invasion (Olshina *et al.*, 2015; Salamun *et al.*, 2014). In *Toxoplasma* and *Plasmodium spp.*, coronin is involved but not essential for invasion and egress, where the protein relocates from the cytoplasm to the posterior end of moving parasites (Bane *et al.*, 2016; Salamun *et al.*, 2014). Coronin was also shown to localise around the periphery of the invading malaria merozoite (Olshina *et al.*, 2015).

In summary, actin-binding proteins in Apicomplexa are significantly limited and possibly evolved to adapt to the complex lifecycle of these parasites. Furthermore, all known actin-binding proteins in Apicomplexa have been shown to be involved in regulating actin during gliding motility and invasion stages on the parasites.

### **1.7.5 Myosin motors**

Myosins are a large family of motor proteins defined by their ability to displace actin filaments upon ATP hydrolysis (Foth *et al.*, 2006; Szent-Gyorgyi, 2004). They are made up of three domains; the catalytic head domain which contains the ATPase and actin binding site, a neck domain which the regulatory light chains bind and the tail domain which is used to transport cargo. Myosins have been shown to walk along actin filaments and have a strong association with ADP-actin. The affinity of the myosin to actin filaments is drastically lowered when ATP binds to the catalytic head domain. Thus, the affinity of myosins to the actin filament is controlled by the ATPase cycle (Hartman & Spudich, 2012). Conventional myosins have been grouped based on their functions, class I are involved in vesicular trafficking while class II are implicated in muscle contraction. However, there are many 'unconventional' myosins which vary in subcellular location, velocity and force they exert on actin filaments (Sellers, 2000).

Grouped within these ‘unconventional’ myosins are the ones found in Apicomplexa. *Toxoplasma gondii* has the largest repertoire of myosins amongst Apicomplexa, containing 11 different myosins (Foth *et al.*, 2006). Myosin A is the most studied of the apicomplexan myosins and is a core component of the parasites gliding machinery. It is a single-headed myosin with a conserved motor and short neck domains but lacks a tail domain (Heintzelman & Schwartzman, 1997). The myosin light chain 1 (MLC1) binds to the IQ domains of MyoA and targets it to the motor complex to power gliding motility (Hettmann *et al.*, 2000). However, other myosins have important functions. MyoB/C are the product of alternative splicing of the last intron, where MyoB is predominantly expressed in bradyzoite stages but has also been implicated in tachyzoite replication (Delbac *et al.*, 2001). Whereas MyoC localises to the posterior ring along with MORN1 and it thought to be important in daughter cell formation (Gubbels *et al.*, 2006). Myosin H localises to the apical ring and controls conoid protrusion. Myosin F belongs to the class-XXII myosins and has multiple functions within the parasites. MyoF contains WD40 repeats that are thought to interact with ARO, acting as a motor required for rhoptry tethering to the apical complex (Mueller *et al.*, 2013). It is also involved in apicoplast inheritance (Jacot *et al.*, 2013) and more recently has been shown to transport dense granules within the parasites cytoplasm (Heaslip *et al.*, 2016). While many of the myosins are still to be characterised, two uncharacterised myosins, MyoI and MyoJ have recently been implicated in forming vacuole connections (Dominique Soldati, BioMalPar 2016).

## 1.8 Small molecules that bind to actin

Actin-binding drugs are widely used in research for their ability to influence actin filament dynamics. They have been used extensively in biological research, however, their use as pharmacological agents is poor due to uptake problems. Many of these are naturally occurring small molecules derived from fungal and microbial toxins. Overall, their mechanisms are damaging for actin filaments. Some induce polymerisation or stabilisation of filaments in the case of phalloidins and jasplakinolide, while others block further filament assembly resulting in depolymerised filaments such as cytochalasins or latrunculins (Figure 1-9).

## 1.8.1 Actin polymerisation drugs

### 1.8.1.1 Phalloidins

Phalloidin is derived from phallotoxins of poisonous mushrooms, *Amantia phalloides*, and is used extensively as experimental agents for F-actin dynamics. Phalloidin binds to actin filaments and shifts the equilibrium to support further filament formation instead of filament disassembly (Cooper, 1987). Moreover, phalloidin inhibits the ATP hydrolysis of the actin filament, significantly reducing the rate constant for monomer dissociation (Figure 1-9) (Barden *et al.*, 1987). Polymerisation of filaments is a tightly controlled process, balancing monomer association and filament dissociation. By inhibiting the latter, the critical concentration of polymerisation is reduced by 10-30 fold under optimal conditions (Visegrady *et al.*, 2004; Visegrady *et al.*, 2005). Therefore, the lack of free monomers increases filament elongation (Figure 1-9). Due to phalloidins being unable to permeate intact cell membranes, they have predominantly been used solely as biochemical experimental agents with little use *in vivo* (Cooper, 1987). The effect of phalloidins on polymerization is distinctive among actin modulators. Most work, therefore, has been studied on fixed cells *in vitro*. Phalloidin does not bind to or stabilise actin filaments within apicomplexan parasites, possibly due to an actin-binding protein masking its target site (Cintra & De Souza, 1985; Poupel *et al.*, 2000; Schuler *et al.*, 2005b) but may also result from the divergent amino acid composition of apicomplexan actins.

### 1.8.1.2 Jasplakinolide

Jasplakinolide was first isolated from the marine sponge *Jaspis johnstoni* and is used widely to study F-actin dynamics. Its effects include reducing the critical concentration required for filament formations from a tetramer to a trimer (Figure 1-9). This results in almost spontaneous nucleation of monomeric actin into filaments and the continual polymerisation and stabilisation of filaments (Figure 1-9) (Bubb *et al.*, 1994; Bubb *et al.*, 2000).

Treatment of *Toxoplasma gondii* tachyzoites with Jas results in a drastic increase in actin filaments, predominantly seen at both the apical and posterior ends of the parasites (Shaw & Tilney, 1999). Originally it was observed that treatment with Jas causes a block in both gliding motility and invasion,

seemingly affecting motor functions (Poupel & Tardieux, 1999). A later study demonstrated that Jas treated parasites become increasingly motile, although their directional movement was severely affected (Wetzel *et al.*, 2003). Many of these parasites begin to twirl with the direction changing from a clockwise twirling motion to a counter-clockwise motion (Wetzel *et al.*, 2003). Overall, this shows that regular motility requires the tight regulation of filamentous actin. Invasion was completely blocked with Jas treatment in *Plasmodium falciparum* while intracellular development was unaffected (Mizuno *et al.*, 2002).

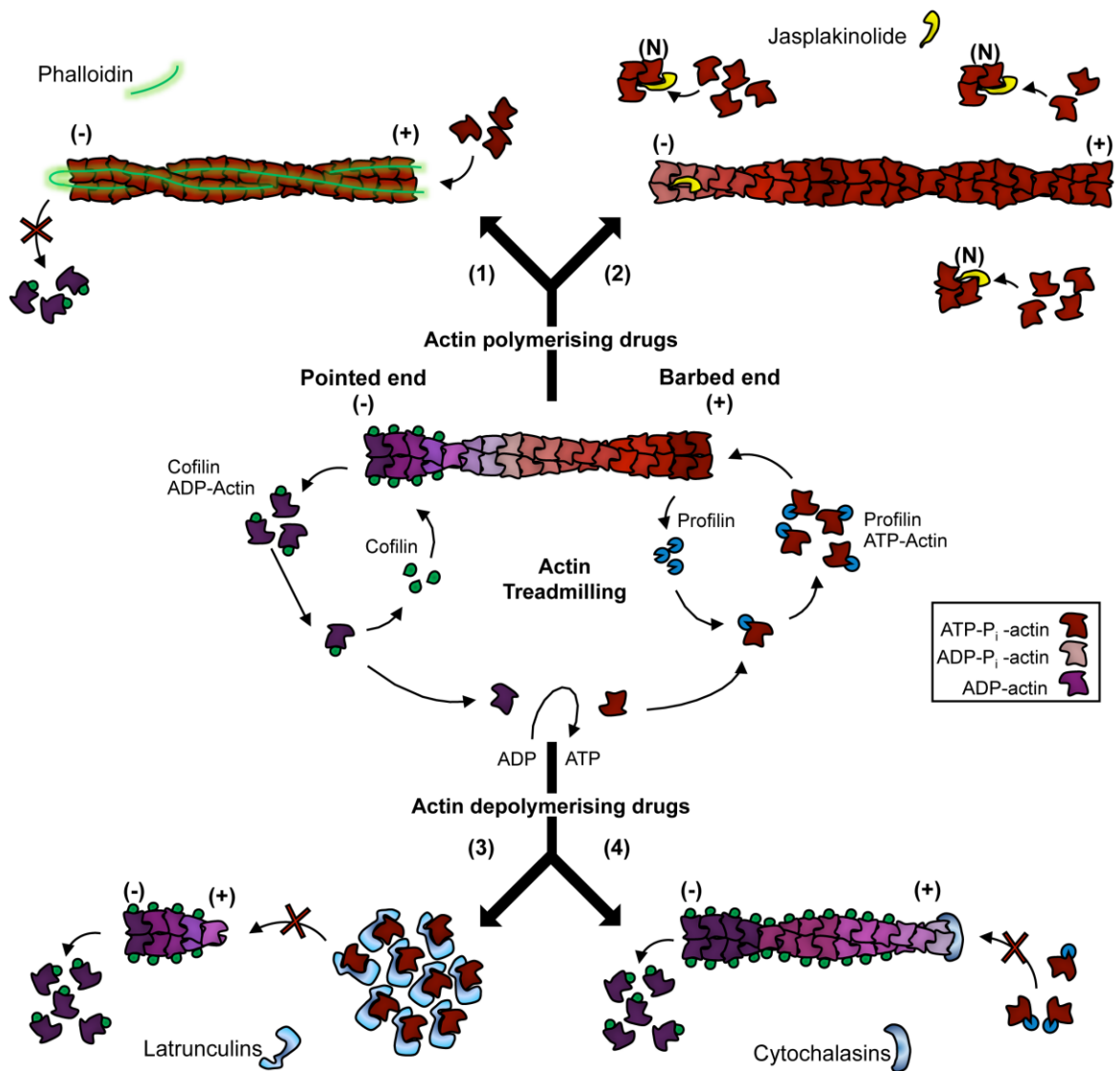


**Figure 1-9: Actin modulating drugs**

Actin modulating drugs function to alter actin dynamics by either promoting polymerisation or depolymerisation of filaments. (1-2) For F-actin stabilisation and polymerisation there are the phallotoxins and jasplakinolide. 1) Phalloidin binds and stabilises the filaments by inhibiting the release of inorganic phosphate. 2) Jasplakinolide functions to lower the critical concentration by promoting nucleation of a trimer nucleus (N). Moreover, jasplakinolide acts to increase filament

length by attracting actin monomers to the barbed end. Other drugs act to depolymerise filaments (3-4). **3)** Latrunculins bind and sequester actin monomers thus inhibiting the filament growth. This causes the filament to depolymerise as all the actin subunits in the filament are hydrolysed. **4)** In the case of cytochalasins, they bind and cap the barbed ends of actin filaments. This blocks further monomers interacting with the filament. In time, these filaments get hydrolysed and begin to depolymerise.

## 1.8.2 Actin depolymerisation drugs

### 1.8.2.1 Latrunculins

Latrunculins are natural toxins purified from the red sea sponge *Latrunculia magnifica*. Initially, these compounds were found to inhibit actin polymerisation and disrupt the arrangement of F-actin by sequestering monomeric actin causing disassembly of actin filaments (Figure 1-9) (Coue *et al.*, 1987). It has been shown that these drugs mimic the activity of actin sequestering proteins, such as profilin (Coue *et al.*, 1987; Spector *et al.*, 1989; Yarmola *et al.*, 2000). Disruption of F-actin by latrunculin A (latA) is both rapid but reversible. With a  $K_d = 200$  nM, latA is more potent than latB and around 10 fold more potent than cytochalasin D (CD) (Spector *et al.*, 1989). This profound efficacy of latA has made it a choice drug to study actin dynamics, and thus supersedes the conventional CD. Latrunculin A and B are highly similar, even down to the binding sites, however, latB differs in the loss of two carbons in the macrocycle ring that form one of its ethyl links. Latrunculin A binds to monomeric actin in a 1:1 ratio between subdomains 2 and 4 (Figure 1-5) near the ATPase binding site, inhibiting ATP exchange (Yarmola *et al.*, 2000). Latrunculin A bridges the gap between subdomains 2 and 4 which rearranges the loop between amino acids Gly55 and Thr66 of sub-domain 2 and movement of the loop between Gly197 and Glu207 (Morton *et al.*, 2000). This conformational change inhibits actin polymerisation. The crystal structure of *Plasmodium* ACT1 highlights a salt bridge between subdomains 2 and 4 suggesting that *Plasmodium* ACT1 may be naturally resistant to latA (Vahokoski *et al.*, 2014). *Cryptosporidium* sporozoite motility can be inhibited in the presence of latB (Wetzel *et al.*, 2005).

### 1.8.2.2 Cytochalasins

Cytochalasins are a group of fungal metabolites that can rapidly permeate cell membranes having fast effects on actin polymerisation. Unlike latA, cytochalasins bind the barbed ends of actin filaments rather than the actin monomers (Figure 1-9). Binding of cytochalasins occurs similarly to capping

proteins at a ratio of one molecule per filament. There are many derivatives of cytochalasins, A-E and H (Scherlach *et al.*, 2010). Interestingly, apart from actin dynamic inhibitors, cytochalasins A and B have unspecific targets (Foissner & Wasteneys, 2007), both inhibiting monosaccharide transport across the plasma membrane (Jung & Rampal, 1977; Lin & Spudich, 1974; Rueckschloss & Isenberg, 2001). Due to their off-target effects in binding glucose transporters, cytochalasins A and B are suggested to be a poor inhibitor for studying actin-based motility. Moreover, cytochalasin A has been shown to indirectly depolymerise microtubules (Foissner & Wasteneys, 2007; Himes & Houston, 1976; Himes *et al.*, 1976). However, the other cytochalasins (C, D, E and H) are deemed to be highly specific for actin capping. Over the years, CD has been the most commonly used drug from the cytochalasin class of small molecules to study actin dynamics. Binding of CD between subdomains 1 and 3 effectively blocks the association of actin monomers to the barbed end and in turn prevents further elongation of filaments (Goddette & Frieden, 1985; Goddette & Frieden, 1986; Nair *et al.*, 2008). A secondary function of cytochalasins is that they also slow the dissociation of the filament at the pointed end by ADF activation (Figure 1-9) (Goddette & Frieden, 1986; Rueckschloss & Isenberg, 2001). In apicomplexan, cytochalasins have been used extensively to study the importance of the acto-myosin system during gliding motility and invasion (Dobrowolski & Sibley, 1996; Drewry & Sibley, 2015; Rynning & Remington, 1978).

## **1.9 Actin-related and actin-like proteins in Apicomplexa**

### **1.9.1.1 Actin-related proteins**

Actin-related proteins, known more commonly as Arps, share a common actin fold and sequence similarity to conventional actins, ranging from 20-60 % (Frankel & Mooseker, 1996; Schafer & Schroer, 1999; Schroer *et al.*, 1994). There are 11 Arps that are highly conserved across eukaryotes (Muller *et al.*, 2005). Actin-related proteins belong to the actin superfamily and act as regulatory proteins involved in modulating the cytoskeleton or regulating chromatin remodelling (Schafer & Schroer, 1999). Location of Arps is restricted to the cytoplasm or nucleus of the cell where they form complexes to fulfil their various functions. The cytoplasmic actin-related proteins; Arp1, Arp10 and Arp11 regulate microtubule motor activity (Schafer *et al.*, 1994), while Arp2 and

Arp3 form a complex to polymerise and branch actin filaments (Gong & Jiang, 2004; Welch *et al.*, 1997a). Nuclear Arps (Arp4-Arp9) are involved in chromatin remodelling (Fenn *et al.*, 2011).

Strikingly, protozoan parasites including *Toxoplasma gondii* have lost many of the actin-related proteins, most notably the Arp2/3 complex and many of the subunits of the complex (Gordon & Sibley, 2005; Gupta *et al.*, 2015). Moreover, *Toxoplasma* only contains two actin-related proteins; Arp1 and an ortholog of Arp4 termed Arp4a (Gordon & Sibley, 2005; Siden-Kiamos *et al.*, 2010; Suvorova *et al.*, 2012). Arp1 is highly conserved and forms part of the dynactin complex required for dynein and kinesin motor movement along microtubules. It is the only known Arp to form a filamentous-like structure (Schafer *et al.*, 1994). As for Arp4a, it is thought to be involved in chromatin remodelling and histone acetyltransferase complexes. A specific mutation Ile162Thr in Arp4a causes a temperature sensitive growth arrest of the tachyzoites. This is caused by the destabilisation and mislocalisation of Arp4a leading to chromosome loss during nuclear division (Suvorova *et al.*, 2012).

### 1.9.1.2 Actin-like proteins

Actin-like proteins, termed ALPs, are similar to Arps but unique to Apicomplexa (Gordon & Sibley, 2005). These ALPs are also not related to the actin-like proteins of bacteria such as MreB or ParM (Carballido-Lopez, 2006). There are several ALPs in the genomes of Apicomplexa, although nomenclature continually changes due to updates to the ToxoDB. and PlasmoDB. For example, Actin-related protein 6 (Arp6) originally published in Gordon and Sibley (2005) recently changed to ALP5 after an update to ToxoDB. The exact location and functions of these ALPs within the parasite are still unclear. To date, only ALP1 has been characterised. This is the closest related protein to actin in Apicomplexa and is thought to have a role in daughter cell formation by transporting contents to the newly forming IMC of these daughter cells (Gordon *et al.*, 2008). The overexpression of ALP1 causes defects in daughter IMC formation along with defects in nuclear and apicoplast segregation (Gordon *et al.*, 2008; Gordon *et al.*, 2010).

Overall, it is suggested that the limited Arps and expression of unique ALPs must be an evolutionary adaptation required for the parasites lifecycle. The limited Arps are thought to be involved in vesicular transport while the ALPs have a more concentrated role unique to the parasites such as actin-based gliding motility (Gordon & Sibley, 2005).

## **1.10 The role of actin during cell motility**

### **1.10.1 The mechanisms behind cell motility**

Cell motility is a highly dynamic phenomenon that is a fundamental process in biology, required not only for general cell locomotion, but also for diverse processes such as embryo development, wound healing and cellular immunity and much more (Lodish *et al.*, 2004). Many eukaryotic cells such as amoebas, protozoan parasites and bacteria are required to move throughout their life (Baum & Frischknecht, 2015). Motility can be driven through a variety of mechanisms. Both eukaryotic cells and bacteria can use flagella based migration. In eukaryotic flagellated cells, motility is driven by dynein movement along microtubules to createing a flagellar-beat to propel the cell forwards. Bacteria use the proton motive forces to power the rotation of their falagellar during motility. In the case of phagocytic immune cells, based on dynamic cytoskeletal shape changes is described as amoeboid crawling. This section highlights examples of well-known motility mechanisms from classical amoeboid movement and also some alternative mechanisms.

### **1.10.2 Crawling motility**

Crawling motility, also known, as amoeboid motility is the best characterised and used by many cells types to move and overcome biological barriers in response to a stimuli. By their nature, metastatic cancerous cells, pathogens such as *Entamoeba histolytica* and phagocytic immune cells are highly motile and use crawling based motility for migration.

Cells move in response to external stimuli from the environment either through physical, chemical, diffusible or non-diffusible signals. Many cells move by a crawling motion over a 2D planar surface. This requires the cell to modulate its cytoskeleton to make plasma membrane protrusions such as lamellipodia,

filopodia and blebs (Bergert *et al.*, 2012; Friedl & Wolf, 2010). The geometry of actin filaments at the membrane dictates the morphology of the membrane protrusions (Bergert *et al.*, 2012). Highly branched actin filaments generate the sheet-like extensions termed lamellipodia while bundled actin filaments generate spike-like filopodia (Pollard & Borisy, 2003; Yang & Svitkina, 2011). Each of these has been observed to facilitate migration under specific circumstances in Zebrafish cells (Diz-Munoz *et al.*, 2010). At this time, I will focus on lamellipodia actin-based motility. This is characterised by cycles of actin polymerisation-driven lamellipodium protrusions (Figure 1-10 A), myosin II-mediated contraction at the rear and continued rounds of adhesion and de-adhesion of integrin-dependent attachment sites (Niculescu *et al.*, 2015; Ryan *et al.*, 2012).

During crawling motility cells characteristically move over a solid substrate in response to an external stimuli. This results in the cells establishing a polarity and activates signals that will in turn cause cytoskeletal reconstruction (Keren, 2011; Ridley *et al.*, 2003). The external stimuli activates Rho-family GTPases and Phosphatidylinositol 4,5-bisphosphate (PIP<sub>2</sub>) and recruits the Wiskott-Aldrich Syndrome Protein (WASP)/SCAR proteins, triggering the Arp2/3 complex to attract ATP-G-actin to the leading edge (Figure 1-10 A) (Hall, 1998; Hall & Nobes, 2000; Ridley, 2006; Tapon & Hall, 1997). The cell then undergoes a series of cytoskeletal changes, firstly by protruding its membrane forward at the leading edge forming a lamellipodium (Bisi *et al.*, 2013; Keren, 2011; Mogilner, 2006; Ridley, 2011). This is caused by rapid polymerisation of F-actin at the leading edge, producing a protrusive force on the cell membrane (Figure 1-10). Moreover, Arp2/3 complexes function with two Rho-family GTPases, Rac1 and Cdc42, to stimulate F-actin branching (Tapon & Hall, 1997). This results in the restructuring of the lamellipodia by the formation of the actin network known as the dendritic network (Svitkina & Borisy, 1999). Formins (mDia1 and mDia2) and Spire have also been implicated in the nucleation of unbranched filaments within the lamellipodia (Kerkhoff, 2006; Vitriol *et al.*, 2015). The filament length is controlled by actin regulatory proteins, Ena/VASP that both assist in actin polymerisation and also controlling the actions of capping proteins (Bear & Gertler, 2009).

Throughout motility, cells regulate the rate of actin assembly at specific regions of the cell allowing cell contact and protrusion in a particular direction (Forscher *et al.*, 1992; Mogilner & Oster, 1996). However, if actin polymerises against the plasma membrane to drive the lamellipodium, there would be little space for the addition of actin monomers. This is where the Brownian motion ratchet theory was originally provided (Guo *et al.*, 2010). It is believed that fluctuations of the plasma membrane and actin at its plus end, provides a gap sufficient for actin monomers to be incorporated into the filament (Guo *et al.*, 2010; Mogilner, 2006). Two main proteins are involved in controlling the actin treadmilling in lamellipodia based motility: profilins and ADF/cofilin. ADF/cofilin acts to sever filaments, and it also recycles old networks by depolymerising ADP-actin near the cell body interface with the lamellum, thus providing an ADP-G-actin pool (Kanellos & Frame, 2016). Subsequently, profilin attracts these ADP-G-actin monomers and catalyses the nucleotide exchange, generating ATP-G-actin (Figure 1-10). This pool of ATP-G-actin is then attracted to the leading edge for further polymerisation. This creates the treadmilling action of actin within the lamellipodia (Blanchoin *et al.*, 2014; Insall & Machesky, 2009).

Simultaneously, as the lamellipodia spread forward, it must form new adhesion sites with the substrate (Figure 1-10 B). These provide both traction for the forward movement and allow the cell to measure the rigidity of the substrate (Borghi *et al.*, 2010; Iwamoto & Calderwood, 2015). The stiffness of the substrate will determine the speed the cell can travel (Mih *et al.*, 2012). For example, a more rigid surface will slow down cell motility. Likewise, softer surfaces also reduce motility speed, indicating an ideal surface lies somewhere in the middle (Dokukina & Gracheva, 2010; Mih *et al.*, 2012).  $\beta$ 1-integrins are positioned periodically along the cell but found to focus at the very front of lamellipodial protrusions (Iwamoto & Calderwood, 2015; Regen & Horwitz, 1992; Zech *et al.*, 2011). These form focal adhesion sites acting as ‘molecular clutches’ (Bard *et al.*, 2008; Elosegui-Artola *et al.*, 2016; Havrylenko *et al.*, 2014). This enables the actin cytoskeleton to interact physically with the extracellular matrix through focal adhesion kinases (FAK) and talins, aiding forward movement and regulating the forces produced by actin dynamics (Calderwood *et al.*, 2013). By engaging the molecular clutch, they resist the

actin retrograde flow, thus indirectly promoting the force produced by the actin polymerisation at the leading edge (Figure 1-10 B) (Case & Waterman, 2015).

After the cell lamellipodia are firmly anchored, myosin II regulates contractility forces from the rear that is translocated throughout the cell (Bondzie *et al.*, 2016; Keren *et al.*, 2009; Wilson *et al.*, 2010). This results in the translocation of the cell body at the lamellipodia-cell-body interface (Figure 1-10 B). It was shown that myosin IIB is required to establish a front to rear polarity. While the contractile forces generated by the acto-myosin network facilitates the retraction at the trailing edge through the interactions of myosin IIA. Together, the cell converts the contractile forces generated by the myosins into traction forces against the extracellular matrix (Oelz *et al.*, 2015). This causes the focal adhesion sites at the rear to disassemble resulting in the cell body retraction from the rear (Figure 1-10 B). Together, the focal adhesion sites and acto-myosin system cooperatively contribute to the forward movement of the cell (Chi *et al.*, 2014). The speed at which these cells move is relatively slow. Primary fibroblasts typically move at speeds of 1-3  $\mu\text{m}/\text{min}$ , whereas amoeboid cells and immune cells can migrate at speeds of 5-15  $\mu\text{m}/\text{min}$  (Bretscher, 2014).

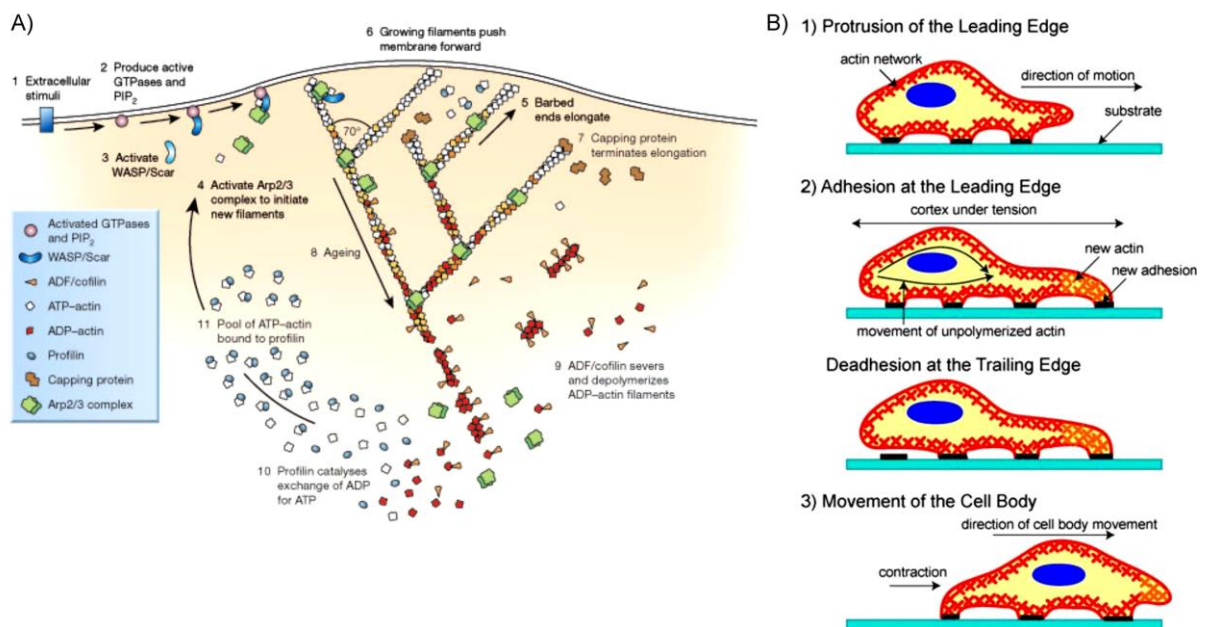


**Figure 1-10: Actin control during lamellipodia protrusion and crawling motility**

**A)** Actin dynamics during lamellipodia protrusion. (1) External stimuli activate Rho GTPases and  $\text{PIP}_2$  (2), which in turn recruit the WASP/SCAR proteins (3) to activate the Arp2/3 complex at the leading edge (4). The Arp2/3 complex promotes actin polymerisation and branching of actin filaments (5). These filaments push against the membrane resulting in lamellipodia protrusion (6). The actin filaments are then capped (7) to terminate the filament length. (8) Ageing filaments are severed or depolymerised through ADF/cofilin interactions (9) and then catalysed from ADP-actin

to ATP-actin through profilin (10). Reprinted with permission from Nature Publishing Group: [Nature], (Pollard, 2003), copyright (2003). **B**) Schematic representation of the three stages of actin-based substrate-dependent motility. 1) The polarised cell polymerises actin at the leading edge causing a lamellipodia extension. 2) The lamellipodia form an attachment site with the surface while the trailing edge depolymerises and detaches from the surface. 3) The cell contracts at the rear, propelling the parasite forwards. Reprinted with permission from Ivyspring International Publisher: [Int. J. Biol. Sci.], (Ananthakrishnan & Ehrlicher, 2007), copyright (2007).

Similarly, *Caenorhabditis elegans* sperm move in an amoeboid fashion, however, lack both actin and myosins. In contrast, the assembly of Major Sperm Protein (MSP1) into filaments forms the lamellipodium. It still requires the formation and release of adhesive sites to transduce the power for motility (Havrylenko *et al.*, 2014). The cell contains internal stores of membranous proteins that are added to the leading edge of the cell and swept back to the rear (Roberts & Ward, 1982). Furthermore, the membrane tension is a master regulator of lamellipodial directionality (Batchelder *et al.*, 2011). Therefore, it was suggested that the *C. elegans* sperm cells move in a polarised endocytic cycle similar to amoeboid without actin or myosins (Bretscher, 2014; Havrylenko *et al.*, 2014).

### 1.10.2.1 Swimming

Recent findings suggest that cells undergo crawling motility and can move even in the absence of adhesive coupling as a response to their microenvironment (Lammermann *et al.*, 2008). In cells such as human leukocytes and *Dictyostelium*, it was effectively shown that these cells can swim when they are suspended in a viscous medium of Ficoll (Barry & Bretscher, 2010; Howe *et al.*, 2013). This demonstrated that adhesion to a solid substrate was not required for movement, and that crawling and swimming are similar processes (Barry & Bretscher, 2010; Bretscher, 2014). In this instance, similar to crawling cells, they throw out large protrusions and change their cytoskeletal shape at the leading edge. The cells surface proteins are then transported from the anterior to posterior of the cell, thought to be similar to a retrograde membrane flow (Bretscher, 1996a). These proteins are then recycled through endocytic pathways, located randomly along the cell. In agreement with this, is the fact that endocytic trafficking factors play a fundamental role in cell motility such as the recycling focal adhesions (Maritzen *et al.*, 2015). Moreover, it is suggested that the membrane transport to the leading edge and retrograde flow during motility are the rate-limiting steps (Fogelson & Mogilner, 2014). Consequently,

these cells swim much slower than they crawl which has been attributed to the viscosity of the medium, resulting in a threefold reduction in speed (Barry & Bretscher, 2010; Bretscher, 2014). While it was originally suggested that a retrograde membrane flow could provide the force for amoeboid swimming (Barry & Bretscher, 2010), it was later shown that this was not the case for *Dictyostelium* (Howe *et al.*, 2013). In fact, the authors suggest that the constant shape changes of the cell drives swimming (Howe *et al.*, 2013). However, for neutrophils, they suspect that the swimming motion could still be due to the retrograde membrane flow, similar to *C. elegans* motility.

### 1.10.2.2 Osmotic engine model

As described for cancer metastasis, the cancerous cells migrate away from the primary tumour site by moving through the surrounding microenvironment and microvessels. They then go on to invade into the blood or lymphatic tissue and circulate the system to colonise a distal site (Joyce & Pollard, 2009). While much work has characterised cancer metastasis in 2D surfaces (Joyce & Pollard, 2009; Machesky, 2008; Stevenson *et al.*, 2012), it gives little evidence of *in vivo* situations. Recent work has shown that unlike 2D planar surfaces, cells can swim and also move through microenvironments by changes in the cells osmotic pressures and shape (Balzer *et al.*, 2012; Barry & Bretscher, 2010; Stroka *et al.*, 2014b). Fluid forces resulting in motility have been studied extensively over the years (Charras *et al.*, 2005; Jaeger *et al.*, 1999; Keren *et al.*, 2009). However, in these systems, the fluid force is coupled with myosin II contractility at the trailing edge (Chi *et al.*, 2014; Keren *et al.*, 2009; Oelz *et al.*, 2015). Moreover, ion channel pumps and aquaporins coordinate with the actin cytoskeleton to drive protrusions at the leading edge of the cells (Chen *et al.*, 2012).

Recently a study by Stroka and colleagues, showed that interfering with actin polymerisation or myosin contractility has no effect on motility through the microenvironment (Stroka *et al.*, 2014b). They convincingly go on to show that cell migration is driven purely by water permeation through the cell membrane (Figure 1-11). This mechanism was termed the ‘osmotic engine model’ (Stroka *et al.*, 2014b). The osmotic engine model requires the coordination of ion channels and aquaporins to control water flux into the cell at the leading edge and water flux out at the trailing edge (Figure 1-11) (Stroka *et al.*, 2014b).

While sodium/hydrogen exchange pumps (NHE1) and aquaporin 5 (AQP5) are randomly localised along the cytoskeleton of migrating cells in 2D, they are highly polarised in cells migrating through 3D microenvironments. This causes different osmolarities at the cells leading edge, and trailing edge through the distribution of the NHE1 and AQP5 (Stroka *et al.*, 2014a). Aquaporins allow the cell to take in water at the leading edge, swell and protrude the forefront. The water is directed to the trailing edge and released causing the cell to retract (Stroka *et al.*, 2014a; Stroka *et al.*, 2014b). Meanwhile, NHE1 is there to regulate the intracellular pH of the cell by exchanging  $\text{Na}^+$  and  $\text{H}^+$  ions (Magalhaes *et al.*, 2011). While this model is of great interest for an actin-myosin independent motility mechanism, it is incompatible for a 2D setting and where the environment cannot generate similar hydrodynamic pressures. This system may provide the link between actin-driven crawling motility in 2D and actin-independent movement in 3D microenvironments.

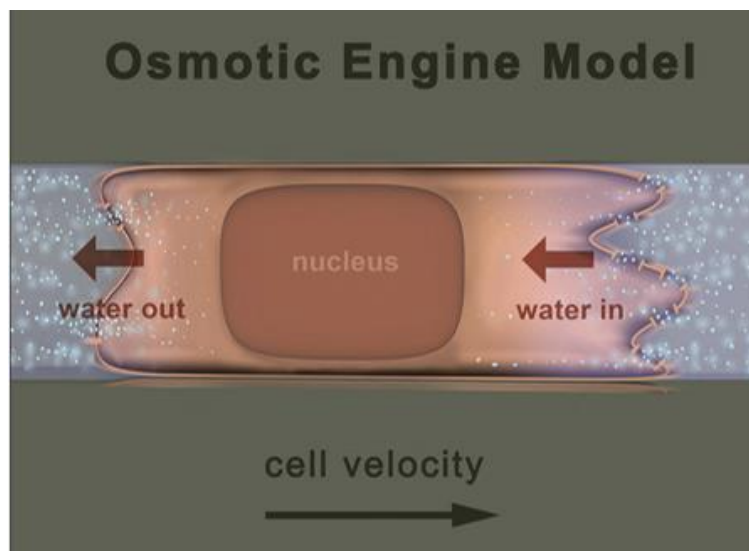


**Figure 1-11: Osmotic engine model**

An osmotic engine model drives cell migration in a confined microenvironment through water permeation across the cell membranes. Water flows in at the leading edge, allowing the cell to extend forwards. While, at the trailing edge, the water is pushed out of the cell causing the back to retract. The translocation is a result of changes in cell volume due to water fluxes. Reprinted with permission from Elsevier Inc: [*Cell*] (Stroka *et al.*, 2014b), copyright (2014).

### 1.10.3 Apicomplexan gliding motility

In the case of Apicomplexa, these parasites employ a unique form of substrate-dependent locomotion that does not require any cytoskeletal shape changes. This motion is known as gliding motility and is powered by the acto-myosin motor system (Figure 1-12) (Heintzelman, 2015). While all apicomplexan

parasites appear to have this complex, some parasite stages are non-motile, such as the merozoites from *Plasmodium spp.* and *Theileria spp.* However, it is thought that this actin-myosin dependent motility also powers invasion into - and egress out of - the host cell (Sibley, 2004).

### 1.10.3.1 Molecular basis of the MyoA-motor complex

It was first reported that actin polymerisation was essential for motility in 1988, where *Eimeria* sporozoites were blocked in movement by the addition of cytochalasin D (CD) (King, 1988). Subsequent actin inhibitor studies revealed that *T. gondii* actin polymerisation was also highly important for the parasites gliding (Dobrowolski & Sibley, 1996; Wetzel *et al.*, 2003). Biochemical studies on parasite actin revealed it to be rather divergent from canonical actins. It was shown that *in vitro*, TgACT1 formed short unstable filaments through an isodesmic polymerisation manner (Sahoo *et al.*, 2006; Skillman *et al.*, 2011; Skillman *et al.*, 2013). This instability and novel polymerisation kinetics was thought to be an evolutionary adaptation to the parasites lifecycle, in particular to function with the linear motor (Skillman *et al.*, 2011).

The myosin A motor was identified as the driving force for motility as a genetic knockdown of *myoA* resulting in a block in motility, invasion and egress (Meissner *et al.*, 2002). Additionally, it was shown that recombinant MyoA can move towards the barbed end of actin filaments at 5  $\mu\text{m/s}$  on an *in vitro* kinetic assay (Herm-Gotz *et al.*, 2002). The motor domain of MyoA only shares <30 % identity with mammalian myosins (Heintzelman & Schwartzman, 1997) and lacks the conserved glycine at the lever arm pivot point. Moreover, they also have a very short C-terminal tail, which is suggested to play a critical role in mechanochemical functions for motor activity (Bosch *et al.*, 2007; Heintzelman & Schwartzman, 1997). Biochemical studies showed that MyoA interacts with a myosin light chain (MLC1) (Figure 1-12) and two essential light chains (ELC1 and ELC2) that are required to promote movement of the MyoA arm (Williams *et al.*, 2015).

In order for the movement to occur through any actin-myosin system, either actin or myosin must be anchored to allow the displacement during the contractile motions. In this instance, it was shown that glideosome associated

proteins termed GAPs provide the anchorage points of the complex (Gaskins *et al.*, 2004). The GAP45 is the connector that holds the IMC to the plasma membrane (Gilk *et al.*, 2009) but also is the anchoring point of MLC1-MyoA complex (Figure 1-12). Further characterisation revealed that GAPs 40 and 50 are integral components of the IMC (Frenal *et al.*, 2010) and are involved in IMC biogenesis (Harding *et al.*, 2016).

Finally, for parasite-substrate dependent movement, the parasites must directly interact and establish transient adhesions with the substrate or the host cell surface. Mainly these interactions are determined by a set of adhesive molecules, which are released by the micronemes, such as the apical membrane antigen-1 (AMA1) and microneme protein-2 (MIC2), a member of the thrombospondin-related anonymous protein (TRAP) family. It is the cytosolic tail domains of these proteins that have been implicated in linking to the acto-myosin motor complex. It was previously thought that the actin filaments bind the transmembrane surface adhesins through the glycolytic enzyme, aldolase (Jewett & Sibley, 2003; Sheiner *et al.*, 2011; Starnes *et al.*, 2009). Subsequent analysis demonstrated that the found interactions have no *in vivo* relevance and aldolase was later ruled out as linker to the acto-myosin system (Shen & Sibley, 2014). Therefore, it is still speculated that an unknown linker protein bridges the adhesions to the acto-myosin motor complex (Shen & Sibley, 2014). These surface adhesins bind to a wide variety of host cell ligands, such as heparin sulphate and other proteoglycan derivatives (Carruthers *et al.*, 2000a; Huynh *et al.*, 2003). Together, this whole complex is better known as the MyoA-motor complex or glideosome (Figure 1-12) (Opitz & Soldati, 2002).

### 1.10.3.2 The linear motor model

This has led to the linear motor model that has dominated the field of Apicomplexa for over a decade. In this model, the MyoA motor is anchored to the IMC of the parasite through the interactions of the MyoA-tail domain to the myosin light chain (MLC1), which in turn is connected to the glideosome associated protein (GAP45) (Frenal *et al.*, 2010; Gilk *et al.*, 2009; Keeley & Soldati, 2004; Leung *et al.*, 2014b). Once anchored to the parasite, MyoA walks short actin filaments that continually polymerise and depolymerise between the parasites IMC and plasma membrane (Heintzelman & Schwartzman, 1997; Herm-

Gotz *et al.*, 2002; Meissner *et al.*, 2002; Wetzel *et al.*, 2003). As the MyoA motor walks along actin filaments, this generates a force that is transmitted through to extracellular adhesive domains. Together, this causes a smooth acto-myosin dependent rearwards translocation of the microneme-substrate complex, which results in the forward gliding movement over the substrate (Soldati & Meissner, 2004).

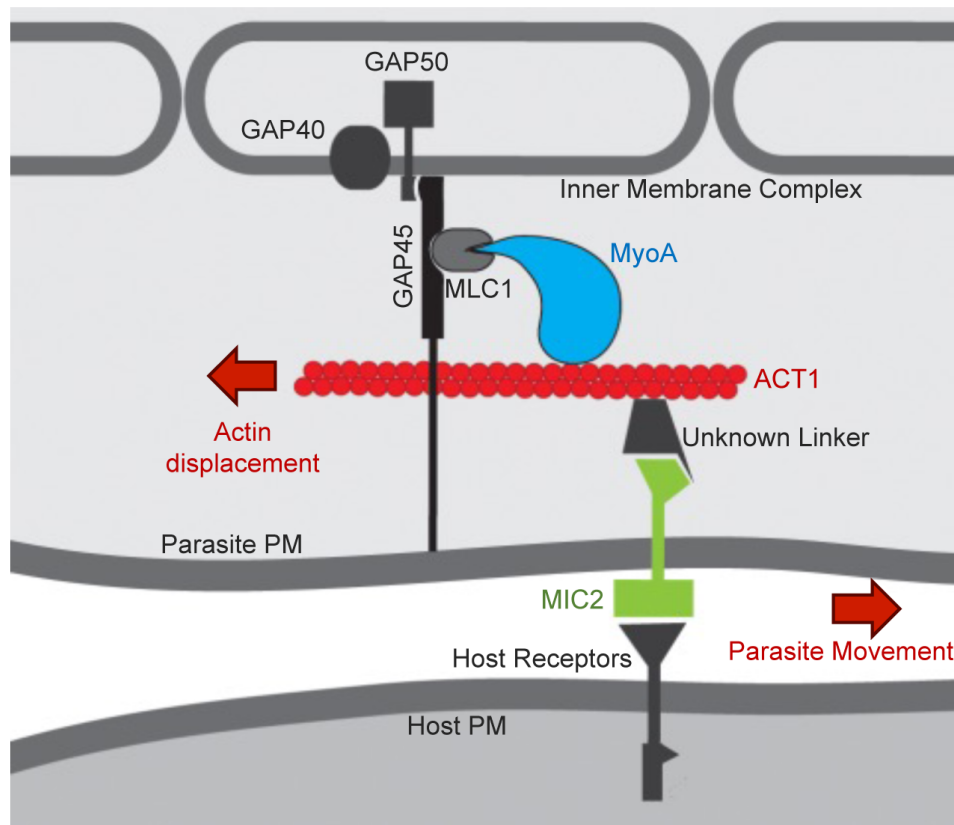


**Figure 1-12: The MyoA-motor complex in *Toxoplasma gondii***

The working model of the motor complex consisting of an unconventional myosin (MyoA) interacts with GAP45 through the myosin light chain MLC1. GAP45 bridges the inner membrane complex (IMC) and plasma membrane. GAP40 and GAP50 provide structural support to the motor complex and IMC. The mechanical forces of MyoA moving along F-actin is transferred to the substrate or host cell plasma membrane via the interactions of adhesive transmembrane proteins such as MIC2. This causes a treadmilling action of the IMC and plasma membrane, resulting in a forward displacement of the parasites. Figure inspired by Nicole Andenmatten.

Recent work using conditional knockout systems (described in chapter 1.13.3) has demonstrated the importance of the motor complex for efficient gliding. However, many components can be functionally removed without complete inhibition of gliding motility (Egarter *et al.*, 2014). Mutants for MyoA, MIC2 and AMA1 can be maintained in an *in vitro* culture indefinitely (Andenmatten *et al.*, 2012; Bargieri *et al.*, 2013; Egarter *et al.*, 2014). While many components of the motor complex could be functionally complemented (Frenal *et al.*, 2014), there is only a single actin gene (Dobrowolski *et al.*, 1997). Nevertheless, it was noted

by Boucher and Bosch (2015) that the parasites have a repertoire of actin-like protein that are still largely uncharacterised (Gordon & Sibley, 2005). Although unlikely, these might provide some functional redundancy for the loss of actin (Boucher & Bosch, 2015).

Over the years there have been different ‘alternative’ models to the linear motor model. The original ‘glideosome’ was described in a reverse topology model by King (1988). This predicts the myosin motor to be anchored to the parasites plasma membrane and displaces actin filaments that are in close proximity to the IMC (King, 1988; Tardieux & Baum, 2016). Although this reverse topology model has never been completely disproved, the above linear motor is most widely accepted model to explain parasite motility to date. In a recent review, a “free” orientation model was also predicted where F-actin is bound to the parasites plasma membrane by F-actin bundling proteins such as coronins (Bane *et al.*, 2016; Olshina *et al.*, 2015; Tardieux & Baum, 2016). This would bypass the necessity for a linker protein and the myosin-GAP complex is not fixed along the anterior-posterior axis. The force generated by the myosin would move a membrane patch that is linked to F-actin through multiple adhesins which would result in forward movement (Tardieux & Baum, 2016). Alternatively, the parasites may employ an entirely different mode of motility that is based on an osmotic gradient, which was proposed by Egarter *et al.* (2014). Indeed, how these parasites can still glide without actin or myosins will greatly enhance the understanding of parasite biology. However, the importance of actin is still clear and it is possible that the motor complex has an alternative function rather than force generation.

Here, I have presented an overview of different concepts that various cell types use for motility. This is by no means a comprehensive view, as there are many other types of motility such as flagellar-based movement and other models that contrast with the models described above. With regards to Apicomplexan motility, it is of great importance to understand how the parasites glide and invade. The continual understanding of the parasites motility could provide novel, targeted therapeutics for the apicomplexan diseases such as toxoplasmosis and malaria.

## 1.11 Actin during apicomplexan invasion

In general, intracellular pathogens invade the target host cell by manipulation of host-dependent signalling pathways, which result in entry through the invagination of the membrane in a process similar to endocytosis. Apicomplexan parasites appear to be unique in their invasion process. While most apicomplexan parasites possess the unique gliding machinery, not all are motile and different species invade through a number of mechanisms. Indeed, the currently accepted linear motor model for gliding motility is described to be essential for *Toxoplasma gondii* and *Plasmodium spp.* invasion (Heintzelman, 2015; Meissner *et al.*, 2013). Emerging data is beginning to shift the focus from the parasites acto-myosin motor being the sole contributor for force production and cell entry (Koch & Baum, 2016; Meissner *et al.*, 2013). The influence of the host cell was thought to be rather passive. However, it is clear that host cell contents such as ATP and magnesium levels are also favoured for invasion (Field *et al.*, 1992; Kimata & Tanabe, 1982; Rangachari *et al.*, 1987). However, the role of the actin cytoskeleton during invasion has been a debated topic for many years.

Alternative gliding and invasion mechanisms exist for other Apicomplexa and may reveal a different outlook. *Cryptosporidium parvum* causes gastrointestinal illnesses, however, unlike *Toxoplasma*, it does not actively invade the gut epithelial cells. While *C. parvum* sporozoites motility is similar to *T. gondii*, they do not appear to use this for invasion (Wetzel *et al.*, 2005). Instead, *C. parvum* attach with their apical end and orientate towards to the host cell. At this point, the parasite remodels the actin cytoskeleton of the host cell and essentially wraps the cell around itself. At the contact site for entry, it has been shown that many actin modulators, such as the Arp2/3 complex, cdc42, VASP and N-WASP, are recruited (Chen *et al.*, 2004; Elliott & Clark, 2000; O'Hara *et al.*, 2008). Furthermore, it was shown that at the attachment site, there is also a range of sodium/glucose co-transporters and aquaporins (Chen *et al.*, 2005). Subsequently, the uptake of glucose causes a water influx that results in the host cell volume increasing to wrap around the parasite. Therefore, *C. parvum* invasion is dependent on modulation of the host cytoskeleton through actin polymerisation. This results in membrane protrusions to encapsulate the parasite (Chen *et al.*, 2005; O'Hara *et al.*, 2008). Interestingly, *Theileria*

sporozoites are non-motile, and their invasion is independent of both parasite and host cell actin (Shaw, 1999; Shaw, 2003). These parasites invade completely different, where their initial attachment to the host cell is strong and non-reversible. Moreover, the parasite can invade at any orientation, which is entirely different from other Apicomplexa such as *Toxoplasma* or *Plasmodium* parasites. After attachment, *Theileria* sporozoites induce a zippering mechanism that involves a firm interaction between the parasite and host cell (Shaw, 2003). Interestingly, while *Theileria* contains rhoptry and microneme proteins, there is little evidence of their role during internalisation (Shaw, 2003). Overall, it appears that *Theileria* parasites can invade without the gliding machinery or host cell actin.

The prevailing view is that invasion by *Toxoplasma* and *Plasmodium spp.* is an active process driven by the parasite, while the host cell is large passive during entry (Dobrowolski & Sibley, 1996; Morisaki *et al.*, 1995). Moreover, different views regarding the role of actin in the process from either the host or parasite is under debate. It was first demonstrated that using cytochalasin D (CD) both phagocytic and non-phagocytic host cells actively participate in *Toxoplasma* invasion (Ryning & Remington, 1978). Later, it was shown using CD resistant parasites, that invasion was purely driven by the actin of the parasite (Dobrowolski & Sibley, 1997; Dobrowolski & Sibley, 1996). However, more recent work has indicated that cellular invasion depends on both the parasite and host cell actin. *Toxoplasma gondii* and *Plasmodium berghei* can modulate the actin cytoskeleton of the host at the point of attachment (Delorme-Walker *et al.*, 2012; Gonzalez *et al.*, 2009). Also, host cell F-actin accumulates around the tight junction to facilitate proper parasite internalisation (Baum *et al.*, 2008b; Gonzalez *et al.*, 2009; Sweeney *et al.*, 2010). Host cell cortactin and actin nucleating factors have also been implicated in host cell entry by *Toxoplasma* (Gaji *et al.*, 2013). Invasion speeds are much slower in *toxofilin* KO parasites, where the parasites are unable to remodel the cortical actin cytoskeleton of the host locally. Moreover, they penetrated half their body length into the cell before stopping and pulling the host cell plasma membrane around the parasite (Bichet *et al.*, 2014; Delorme-Walker *et al.*, 2012). This is similar to the described method for invasion of *C. parvum* (Elliott & Clark, 2000) and the *myoA* KO (Bichet *et al.*, 2016b). *Plasmodium* merozoites may also induce

cytoskeletal re-arrangements of the erythrocyte that greatly enhances invasion (Koch & Baum, 2016).

Overall, it suggests that during host cell entry there are many factors involved. In particular, both actin from parasite and host cell appear to have important functions.

## 1.12 *Toxoplasma gondii* as a model organism

*Toxoplasma gondii* is an ideal model organism to study aspects of apicomplexan biology, in particular cell motility and invasion. As discussed in chapter 1.4, the lifecycle of *T. gondii* is very well understood (Dubey, 2009; Dubey *et al.*, 1998). With the wide variety of cell types that *Toxoplasma* can infect (Kim & Weiss, 2004), it makes it much easier to culture *in vitro* compared with *Plasmodium spp.* that will only infect hepatocytes and erythrocytes (Cowman & Crabb, 2006). The size of *T. gondii* tachyzoites also makes it more appealing in imaging studies etc. rather than *Plasmodium spp.* which are in general much smaller (Baum *et al.*, 2008a). Transfection of exogenous DNA into the parasites is also much simpler in *Toxoplasma* compared to *Plasmodium spp.*

The genome sequence for *T. gondii* was completed around ten years ago (Khan *et al.*, 2005). The parasites are haploid with 14 chromosomes and a 65 Mb genome (Khan *et al.*, 2005; Sibley & Boothroyd, 1992). With the genomes always updated on the databases such as ToxoDB and PlasmoDB, this has significantly enhanced the understanding of the parasites, allowing reverse genetic tools to thrive. In the recent years, the methods to study both classical and reverse genetics have seen a huge leap forward.

## 1.13 Reverse genetics in Apicomplexa

Over the last 20 years, the understanding of gene functions within Apicomplexa has taken a huge step forward, not least with the development of various genetic tools. These tools have allowed the functional analysis of genes by assessing the phenotypic consequences of disruption or removal of the genes. Several strategies have been developed in *Toxoplasma gondii* to control gene expression at different levels. These include the DiCre system (Andenmatten *et*

*al.*, 2012) and newly established CRISPr-Cas9 (Shen *et al.*, 2014; Sidik *et al.*, 2014; Sidik *et al.*, 2016) system that control at the genetic level. A recent study has conducted a full genome-wide characterisation using the CRISPr-Cas9 technology, defining around 200 previous uncharacterised essential genes (Sidik *et al.*, 2016). The tetracycline-inducible system (Meissner *et al.*, 2001; Meissner *et al.*, 2002; van Poppel *et al.*, 2006) and the U1-mediated gene-silencing system (Pieperhoff *et al.*, 2015) function at the transcriptional level. In addition, systems can control expression at the protein level, such as the degradation domain fusion system (Herm-Gotz *et al.*, 2007) and the auxin inducible degradation (AID) system implemented in *Plasmodium* (Kreidenweiss *et al.*, 2013; Philip & Waters, 2015).

### 1.13.1 Gene knockdown

There are various gene knockdown techniques available in *Toxoplasma gondii*. Here, I will focus on the tetracycline-inducible system (Figure 1-13 B). The tetracycline-transactivator system (Tet-TA) (Meissner *et al.*, 2002) is an adapted version of the tetracycline-repressor system (Tet-R) first described in 2001 (Meissner *et al.*, 2001). This system is comprised of two regulatory elements. The tetracycline-responsive promoter (TRE) is placed close to the promoter of the gene of interest (GOI). The other factor is the TetO operator sequences that were placed upstream of a minimal promoter termed the tetracycline-dependent transactivator domain (TATi). Transcription of the gene is activated when the TetO binds to the TRE. However, when the tetracycline homologue, anhydrotetracycline (ATc) is added, this blocks the binding of the TetO to the TRE thereby repressing the gene expression (Meissner *et al.*, 2002) (Figure 1-13 B). This system was also adapted for studies in *Plasmodium* (Meissner *et al.*, 2005).

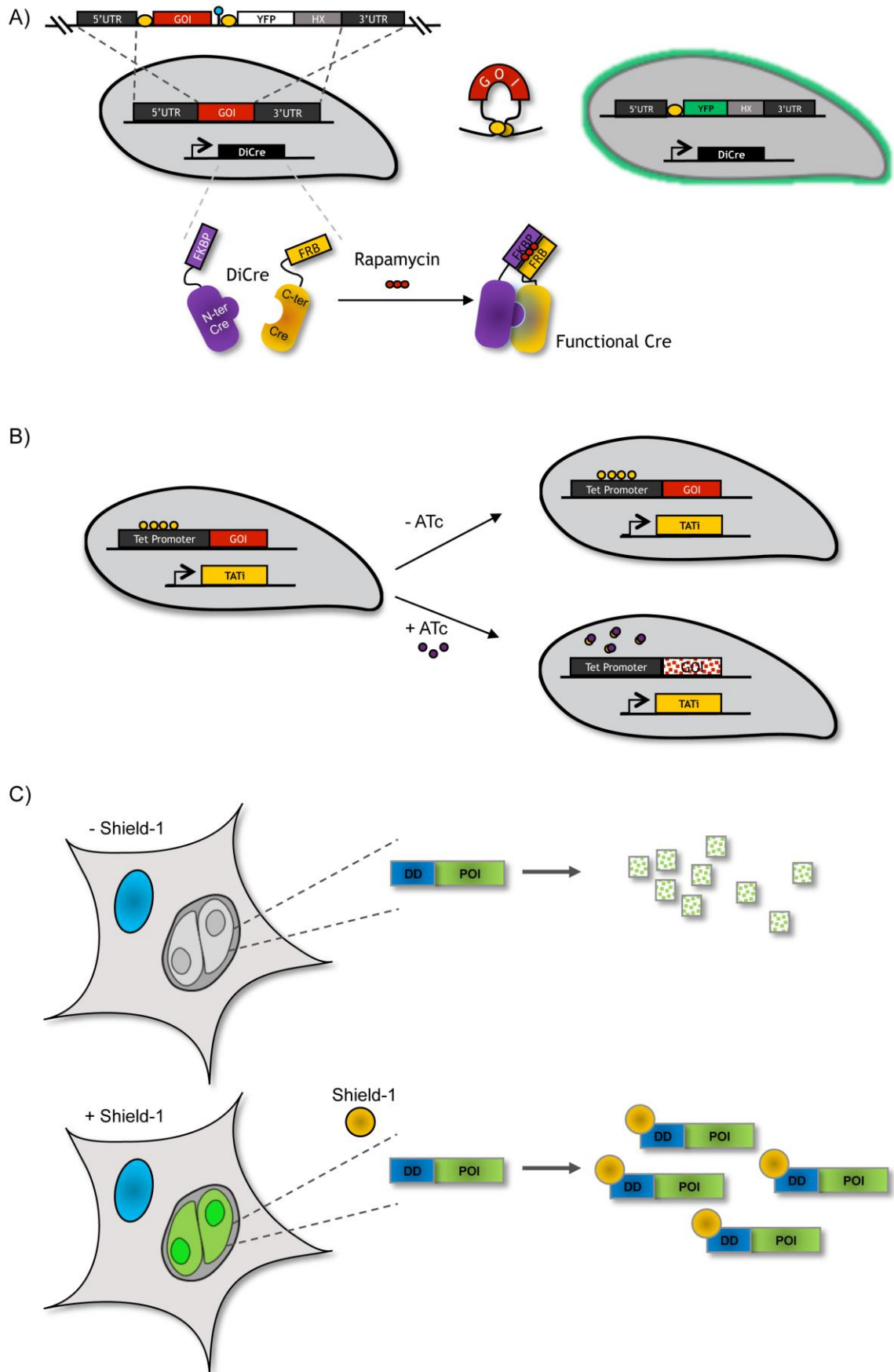


**Figure 1-13: Reverse genetic tools in *Toxoplasma gondii***

Schematic representations of the three most commonly used genetic tools used in *Toxoplasma gondii*. **A)** Control at the genetic level is by the DiCre system. LoxP sites flank the genomic cDNA, which is integrated into the genome via double homologous recombination. The addition of rapamycin reconstitutes the two subunits of DiCre recombinase. The gene of interest is excised

after rapamycin induction and YFP is expressed. **B)** The Tet-inducible system is used to control gene expression at the transcriptional level. Transcription is abolished by the additions of anhydrotetracycline (ATc) by preventing the transactivator binding to the Tet promoter, therefore silencing transcription. **C)** Protein levels are controlled by the ddFKBP destabilisation domain system. Upon addition of Shield-1 the protein of interest is stabilised while in absence of Shield-1 it is targeted to the proteasome for degradation.

### 1.13.2 Rapid regulation of protein stability

In many cases, suppression or deletion at the genetic level is slow, leading to the requirement of a fast inducible system that can rapidly regulate protein stability (Jimenez-Ruiz *et al.*, 2014). The Destabilisation Domain (DD) system works by fusing a protein of interest (POI) to a rapamycin-regulated destabilisation domain, ddFKBP (Herm-Gotz *et al.*, 2007). Once the construct is expressed in the parasites, the protein is trafficked to the proteasome to be rapidly degraded (Figure 1-13 C). Upon addition of the rapamycin analogue Shield-1 (Shld1) the protein is stabilised (Figure 1-13 C) (Herm-Gotz *et al.*, 2007). The system can be used to degrade proteins rapidly but is also suitable for the generation of dominant negative mutants. Degradation of proteins requires the proteasome, which resides in the cytosol, therefore regulation of proteins located in organelles will be ineffective (Wang *et al.*, 2016).

### 1.13.3 Gene knockouts

Complete gene removal is required to overcome the leaky expression that cannot be controlled by the gene or protein knockdown systems described above. With essential genes, a straight knockout strategy would fail therefore the system must be inducible. With this came the development of the DiCre system in Apicomplexa (Figure 1-13 A) (Andenmatten *et al.*, 2012; Collins *et al.*, 2013), based on the Cre-lox system originally described by Sauer and Henderson (1988). The Cre recombinase enzyme is split into two inactive polypeptides, each fused to a different rapamycin binding protein (FKBP12 and FRB) (Jullien *et al.*, 2007; Jullien *et al.*, 2003). The addition of the ligand, rapamycin, brings the FRB and FKBP together and thus reconstituting the function of Cre which results in the LoxP-flanked gene of interest to be excised (Figure 1-13 A) (Jullien *et al.*, 2007). The DiCre cassette was expressed in wild-type *T. gondii* parasites (termed RH DiCre  $\Delta Ku80$ ) and shown to excise a LoxP-flanked *lacZ* to 90 % (Andenmatten *et al.*, 2012).

The system works by generating a geneswap vector consisting of ~2 kb region of both 5' and 3' UTR sequences for homologous recombination. The cDNA of the gene of interest (GOI) is flanked by LoxP sites, and a reporter cassette of YFP is placed downstream of the stop codon of the cDNA (Andenmatten *et al.*, 2012). This geneswap vector is integrated *via* double homologous recombination into a RH DiCre  $\Delta Ku80$  parasite strain (Figure 1-13 A). Once integrated into the genome of the parasite, the addition of rapamycin controls the site-specific recombination. The addition of rapamycin excises the GOI, bringing the YFP under the control of the endogenous promoter (Figure 1-13 A) (Andenmatten *et al.*, 2012). The DiCre system is advantageous since there is no leaky expression of the gene and can be controlled by the endogenous promoter, however, this system is not reversible (Jimenez-Ruiz *et al.*, 2014).

These systems have been used extensively in *Toxoplasma gondii* over the years. However, functional analysis of one gene by all of these techniques is rare. For example, a component of the parasites motor complex, the myosin A motor has been characterised by all techniques described above. Suppression of *myoA* using the Tet-transactivator system (Figure 1-13 B) caused a remarkable reduction in gliding motility and invasion, which led to the conclusion that MyoA is essential for powering these processes (Meissner *et al.*, 2002). Moreover, the parasites that remained motile and invasive were attributed to the residual expression of MyoA, a characteristic of this technology (Meissner *et al.*, 2002). While the over-expression of ddFKBP-*myoA*-tail construct caused a reduction in invasion (Figure 1-13 C), it also highlighted a role of MyoA during intracellular replication (Agop-Nersesian *et al.*, 2009). This raised the possibility that MyoA is important for IMC biogenesis and that the ddFKBP caused a dominant negative phenotype (Agop-Nersesian *et al.*, 2009). Interestingly, analysing the role of MyoA with the DiCre system (Figure 1-13 A) indicated that while MyoA was important for gliding motility and invasion, it was not essential, as a clonal *myoA* KO line could be maintained in culture (Andenmatten *et al.*, 2012; Egarter *et al.*, 2014).

The DiCre system has been successfully employed to characterise many components of the acto-myosin motor complex that were previously deemed essential. Remarkably, re-addressing the question of essentiality demonstrated that null mutants could be generated and maintained in culture for not only

*MyoA* but also *mic2* and *ama1* (Andenmatten *et al.*, 2012; Bargieri *et al.*, 2013). Moreover, other components of the motor complex (ACT1, MLC1, ALD1, GAPs 40, 45, 50 and ROM4 and 5) have been successfully removed and shown to have an important but non-essential role in motility and invasion (Egarter *et al.*, 2014; Harding *et al.*, 2016; Rugarabamu *et al.*, 2015; Shen & Sibley, 2014).

## 1.14 Aim of study

Currently, movement by apicomplexan parasites is thought to be a parasite-driven process that is dependent on its acto-myosin gliding machinery (Keeley & Soldati, 2004). This motor complex, consists of a myosin A motor, the myosin light chain 1 (MLC1) and glideosome associated proteins (GAP40, GAP45 and GAP50), anchored to the inner membrane complex and plasma membrane (Soldati & Meissner, 2004). A core component of the complex is thought to be the *MyoA* motor (Meissner *et al.*, 2002), which functions with short actin filaments (Dobrowolski & Sibley, 1996; Sahoo *et al.*, 2006) to generate the force required for motility. The force is transmitted to key components of the gliding machinery that bridges the interface between the parasites and substrate (Huynh & Carruthers, 2006; Tonkin *et al.*, 2011). Recent data using the newly established DiCre system has revealed that functional knockouts of all the key components of this gliding machinery, including actin, are dispensable for both gliding motility and invasion (Andenmatten *et al.*, 2012; Bargieri *et al.*, 2013; Egarter *et al.*, 2014; Shen & Sibley, 2014). However, the role of actin has come under increased scrutiny due to conflicting results and interpretations (Andenmatten *et al.*, 2012; Drewry & Sibley, 2015; Egarter *et al.*, 2014). Moreover, there is conflicting data regarding the polymerisation kinetics of actin, between an isodesmic or cooperative process (Sahoo *et al.*, 2006; Skillman *et al.*, 2013).

Here, I will use both the conditional *act1* KO and actin-modulating drugs to readdress the role of actin throughout the lytic lifecycle of *Toxoplasma gondii*. Moreover, I also aim to understand when actin is depleted in the conditional *act1* KO and how the levels of actin affect the phenotypes to provide an indication of whether actin is polymerised in an isodesmic process or cooperative manner. As actin filaments have not been detected in the parasites without the use of modulating drugs, I will also attempt to find filaments using novel

---

chromobodies specific to actin. Finally, I will evaluate the role of the acto-myosin system in motility and elucidate an alternative mechanism that could generate a force and drive motility in an actin/myosin-independent manner.

Aims in summary:

- To analyse the functions of actin during the lytic lifecycle of *Toxoplasma gondii*;
- Quantify the level of actin in *Toxoplasma gondii* required during its lytic lifecycle;
- Address how actin polymerises, in either a cooperative or isodesmic manner;
- Visualise actin filaments within *Toxoplasma gondii*;
- Identify a potential new model for *Toxoplasma* motility with relation to the parasites acto-myosin system.

## Chapter 2 Materials and Methods

### 2.1 Equipment

Table 2-1: Equipment used in this study

Applied Precision	DeltaVision Core microscope, DeltaVision RT microscope
BD Biosciences	Syringes, Needles (23 gauge), FACS tubes with cell strainer cap
BioRad	Agarose gel electrophoreses equipment, UV Transilluminator, Gel documentation imaging system, Gene Pulser Xcell, Micropulser, SDS-PAGE system, Blotting apparatus (Transblot SD and Mini transblot electrophoretic transfer cell)
Eppendorf	PCR thermocycler (Mastercycler Epigradient), Thermomixer compact
Fisher Scientific	Ultrasound water bath FB15047
FEI	Tecnai T20 transmission electron microscope
Grant	Water bath
Heraeus Instruments	Incubator
Ibidi	15 $\mu$ -Slide 1 <sup>0.8</sup> Luer collagen IV chambers
Jeol, Japan	Jeol 6400 scanning electron microscope
Kd Scientific	Syringe pump
Kuehner	Shaking incubator (ISF-1-W)
LiCor	Odyssey CLx
Millipore	MilliQ water deionising facility
Photometrics	CoolSNAP HQ <sup>2</sup> CCD camera
Sanyo	CO <sub>2</sub> - incubator tissue culture
Sartorius	Analytical balances
Sciquip	Sigma 6K 15 centrifuge (1150 rotor and 12500 rotor)
StarLab	ErgoOne Single & Multi-Channel pipettes, StarPet Pro pipette controller
Stuart	Heat block, Roller mixer, Orbital Shaker
Thermo Scientific	CO <sub>2</sub> - incubator tissue culture, Nanodrop spectrophotometer, Centrifuge (sorvall legend XFR), Table top centrifuge Heraeus Pico 21, Tabletop cooling centrifuge Heraeus Fresco 21
Toshiba	Terca R804-11E
Zeiss	Axioskop 2 (mot plus) fluorescence microscope with AxioCam MRm CCD camera, Primo Vert (light microscope), Axiovert 40 CFL fluorescence microscope with AxioCam ICc1, Axiovert A1 fluorescence microscope with AxioCam IMc1, ELYRA PS.1 Super-resolution microscope with sCMOS pco SIM camera

## 2.2 Computer software

**Table 2-2: Computer software**

Adobe Systems Inc.	Photoshop CS4 and Illustrator CS4
AcaClone Software	pDraw32
Applied Precision	SoftWoRx Explorer and SoftWoRx suite
BitPlane	Imaris version 8.2.1
Carl Zeiss Microscopy	Zen Black and Zen Blue
CLC Bio	CLC Genomics Workbench 6
CellProfiler Analyst software	Cell Profiler 2.1.1
Fiji	Fiji (is just ImageJ) (Schindelin <i>et al.</i> , 2012)
GraphPad Software Inc.	Prism 6.0
Ibis Biosciences	BioEdit Sequence Alignment tool
LiCor	Image Studio 5.0
Microsoft Corporation	Windows 7, Microsoft Office 2007, 2010
<i>National Center for Biotechnology Information (NCBI)</i>	Basic Local Alignment Search Tool (BLAST)
<i>National Institute of Allergy and Infectious Diseases (NIAID)</i>	ToxoDB, EuPathDB and PlasmoDB
National Institutes of Health	ImageJ 1.34r software
New England Biolabs	NEBaseChanger
OligoCalc	Oligo Analysis tool, Available at: <a href="http://www.basic.northwestern.edu/biotools/oligocalc.html">http://www.basic.northwestern.edu/biotools/oligocalc.html</a>
PerkinElmer	Volocity 3D Image Analysis
Savvy	Plasmid generator tool, Available at: <a href="http://www.rf-cloning.org/savvy.php">http://www.rf-cloning.org/savvy.php</a>
Schrodinger	PyMOL v1.7.4
Thomson Scientific	Endnote X6
Wayne Davis, University of Utah	ApE Plasmid Editor v2.0.46, Available at: <a href="http://biologylabs.utah.edu/jorgensen/wayned/ape/">http://biologylabs.utah.edu/jorgensen/wayned/ape/</a>

## 2.3 Biological and chemical reagents

**Table 2-3: Biological and chemical reagents**

Thermo Fisher Scientific	Bovine serum albumin, ethylene diamine tetraacetic acid, glycerol, glycine, methanol, Tris, Sodium Chloride, PageRuler Prestained Protein Ladder, 40 nM FluoSpheres <sup>®</sup> Carboxylate-Modified Microspheres, Platinum <i>Taq</i> DNA Polymerase High Fidelity
Electron Microscopy Sciences	20 % Paraformaldehyde (PFA)
Formedium	Tryptone, yeast extract
LiCor	Chameleon Duo Pre-stained Protein Ladder
Life Technologies	Phosphate buffered saline (PBS), Trypsin/EDTA (0.05 %), DNaseI, DNA ladder (1 kb plus), NuPage SDS loading buffer and reducing agent, ultrapure agarose
Marvel	Milk powder (skimmed)
Melford	Agar, dithiothreitol, IPTG, X-Gal
New England Biolabs	All restriction endonucleases and associated

Pheonix Research Products	buffers, T4 DNA ligase, <i>Taq</i> polymerase, Phusion® High-Fidelity DNA Polymerase, Calf Intestinal Phosphatase (CIP)
Promega	GelRed nucleic acid stain
Sigma	pGEM®-T Easy Vectors system Ammonium persulfate, bromophenol blue sodium salt, casein hydrolysate, Dulbecco's Modified Eagle Medium (DMEM), ficoll, ethylene glycol tetra-acetic acid, Ponceau S, isopropanol, sodium dodecyl sulfate (SDS), dimethyl sulfoxide (DMSO), N,N,N',N'-tetramethylethylenediamine (TEMED), triton X-100, rapamycin, β-mercaptoethanol, calcium ionophore A23187, Tween20, Giemsa stain, RNase-ZAP, L-glutathione reduced, adenosine 5'-triphosphate disodium salt hydrate, glutamine, 30 % acryl-bisacrylamide mix, sodium deoxycholate, K <sub>2</sub> HPO <sub>4</sub> , magnesium chloride
Southern Biotech	Fluoromount G (with and without DAPI)
VWR	CaCl <sub>2</sub> *2H <sub>2</sub> O, glacial acetic acid, ethanol, methanol, HEPES, potassium chloride, Na <sub>2</sub> HPO <sub>4</sub> , KH <sub>2</sub> PO <sub>4</sub>
Zeiss	Immersion oil

## 2.4 Drugs and antibiotics

Table 2-4: Drugs and antibiotics

Sigma	Ampicillin sodium salt, Gentamicin, Xanthine, Chloramphenicol (CAT), Mycophenolic acid (MPA), 6-Thioxanthine, Pyrimethamine, Cytochalasin D, Latrunculin A, SMIFH2, Ciliobrevin D
Merck Millipore	Jasplakinolide, Latrunculin B
Molecular Probes	

## 2.5 Nucleic acid extraction kits

Table 2-5: Nucleic acid extraction kits

Qiagen	Spin Mini-Prep, Plasmid Midi-Prep, MinElute PCR Purification, MinElute Gel Extraction, DNeasy Blood and Tissue
Roche	High Pure RNA Isolation, High Pure PCR Product Purification

## 2.6 Buffers, solutions and media

Table 2-6: Buffers and media for bacterial culture

LB medium	10 g/l tryptone, 5 g/l yeast extract, 5 g/l NaCl
LB agar	1.5 % (w/v) agar in LB medium
SOB medium	2 % tryptone (w/v), 0.5 % yeast extract (w/v),

SOC medium	0.05 % NaCl (w/v), 2.5 mM KCl, 10 mM MgCl <sub>2</sub>
NYZ broth	20 mM glucose in SOB medium 5 g/l NaCl, 2 g/l MgSO <sub>4</sub> *7H <sub>2</sub> O, 5 g/l yeast extract, 10 g/l casein hydrolysate, pH adjusted to 7.5 with NaOH
Transformation Buffer I (Tfbl)	100 mM RbCl, 50 mM MnCl <sub>2</sub> *4H <sub>2</sub> O, 30 mM Potassium acetate, 10 mM CaCl <sub>2</sub> *2H <sub>2</sub> O, 15 % Glycerol, pH 5.8 with acetic acid
Transformation Buffer II (TfblI)	0.2 M MOPS, 10 mM RbCl, 75 mM CaCl <sub>2</sub> *2H <sub>2</sub> O, 15 % Glycerol, pH 6.5 with NaOH
Ampicillin (1000X)	100 mg/ml in H <sub>2</sub> O
IPTG (100 µl/petri dish)	100 mM IPTG in H <sub>2</sub> O
X-Gal (20 µl/petri dish)	50 mg/ml in N,N-dimethylformamide

**Table 2-7: Buffers for DNA analysis**

50X TAE buffer	2 M Tris, 0.5 M Na <sub>2</sub> EDTA, 5.71 % glacial acetic acid (v/v)
5X Loading dye	15 % Ficoll (v/v), 20 mM EDTA, 0.25 % Bromophenol Blue (w/v) in H <sub>2</sub> O
NEB <sup>®</sup> 1 kb DNA ladder	150 µl 1kb ladder (1 µg/µl), 300 µl 5X DNA loading buffer, 1050 µl H <sub>2</sub> O
Thermo <sup>®</sup> 1 kb+ DNA ladder	150 µl 1kb+ ladder (1 µg/µl), 300 µl 5X DNA loading buffer, 1050 µl H <sub>2</sub> O

**Table 2-8: Buffers for protein analysis**

RIPA buffer	50 mM Tris-HCl (pH 8.0), 150 mM NaCl, 1 mM EDTA, 0.5 % sodium deoxycholate, 0.1 % SDS (w/v), 1 % triton X-100 (v/v)
4X separating gel buffer	1.5 M Tris-HCl (pH 8.8), 0.4 % SDS (w/v)
Separating gel	8-15 % of 30 % acryl-bisacrylamide, 25 % 4X separating gel buffer, 0.1 % APS 10 % (w/v), 0.2 % TEMED (v/v)
4X stacking gel buffer	0.5 M Tris/HCl (pH 6.8), 0.4 % SDS (w/v)
Stacking gel	4 % of 30 % acryl-bisacrylamide, 25 % 4X stacking gel buffer (v/v), 0.1 % APS 10 % (w/v), 0.2 % TEMED (v/v)
SDS PAGE running buffer	25 mM Tris, 192 mM glycine, 0.1 % SDS (w/v)
Transfer buffer for wet blot	48 mM Tris, 39 mM glycine, 20 % methanol (v/v)
Blocking solution	50 % Odyssey blocking buffer in TBS
Washing solution or TBS-T	0.2 % tween (v/v) in TBS
1 M DTT	3.085 g 1,4-dithio-DL-threitol (DTT) in 20 ml 10 mM NaAc (pH 5.2)
10 % APS	1 g ammonium persulfate in 10 ml H <sub>2</sub> O
PageRuler Prestained protein ladder	62.5 mM Tris-H <sub>3</sub> PO <sub>4</sub> (pH 7.5 at 25 °C), 1 mM EDTA, 2 % SDS, 10 mM DTT, 1 mM NaN <sub>3</sub> and 33 % glycerol.
Li-Cor <sup>®</sup> Chameleon <sup>®</sup> Duo protein ladder	Not supplied

**Table 2-9: Buffers and media for *Toxoplasma gondii* and mammalian cell culture**

Dulbecco's modified Eagles medium (DMEM <sub>COMPLETE</sub> )	500 ml DMEM, 10 % FBS (v/v), 2 mM glutamine, 20 µg/ml gentamicin
Dextran Sulfate Media	DMEM <sub>COMPLETE</sub> supplemented with 2.5 % Dextran sulfate (w/v)
10 x PBS	137 mM NaCl, 2.7 mM KCl, 8 mM Na <sub>2</sub> HPO <sub>4</sub> , 1.8 mM KH <sub>2</sub> PO <sub>4</sub> (pH 7.4)
1 x Freezing solution	25 % FBS (v/v), 10 % DMSO (v/v) in DMEM
Electroporation buffer (Cytomix)	10 mM K <sub>2</sub> HPO <sub>4</sub> /KH <sub>2</sub> PO <sub>4</sub> , 25 mM HEPES, 2 mM EGTA pH 7.6, 120 mM KCl, 0.15 mM CaCl <sub>2</sub> , 5 mM MgCl <sub>2</sub> with 5 mM KOH adjusted to pH 7.6, 3 mM ATP, 3 mM GSH
Giemsa staining solution	10 % Giemsa stain (v/v) in H <sub>2</sub> O
Chloramphenicol	10 mg/ml in ethanol (30.9 mM)
MPA (mycophenolic acid)	12.5 mg/ml in methanol (39 mM)
Xanthine	20 mg/ml in 1 M KOH (1.31 mM)
Pyrimethamine	1 mM in ethanol
Rapamycin	50 µM in DMSO
Calcium ionophore A23187	20 µM in DMSO
Sheild-1	1 mM in 70 % EtOH
6-thioxantine	25 mg/ml in 0.3 M NaCl (148.65 mM)
Negative <i>hxgprt</i> selection media	10 mM HEPES, 1 % dialysed FBS, 1.36 % 6-thioxanthine, 1.36 % 0.3 M HCl, 2 mM glutamine, 20 µg/ml gentamicin in DMEM
FACS buffer	1 % FBS, 1 mM EDTA in PBS
PFA fixing solution	4 % PFA (w/v) in PBS
Permeabilisation solution (Harsh)	2 % BSA (w/v), 0.2 % triton X-100 (v/v) in PBS
Permeabilisation solution (Gentle)	2 % BSA (w/v), 0.1 % Saponin (w/v) in PBS
Blocking solution	2 % BSA (w/v) in PBS
Hanks' balanced salt solution (HBSS)	5.33 mM potassium chloride, 0.44 mM KH <sub>2</sub> PO <sub>4</sub> , 4.17 mM sodium bicarbonate, 138 mM sodium chloride, 0.338 mM Na <sub>2</sub> HPO <sub>4</sub> , 1mM EGTA (pH= 7.3), 12.5 mM HEPES
Endo buffer	44.7 mM K <sub>2</sub> SO <sub>4</sub> , 10 mM Mg <sub>2</sub> SO <sub>4</sub> , 106 mM sucrose, 5 mM glucose, 20 mM Tris, 0.3 5 % (w/v) BSA, pH 8.2
Gliding buffer	1 mM EGTA, 100 mM HEPES in HBSS
3D Motility Media	1X Minimum Essential Medium lacking sodium bicarbonate, 1% (v/v) FBS, 10 mM HEPES pH 7.0 and 10 mM GlutaMAX L-alanyl-L-glutamine dipeptide, supplemented with 0.3 mg/ml Hoechst 33342
Phosphate buffer (0.1 M)	10.9 g NA <sub>2</sub> HPO <sub>4</sub> , 3.2 g NaH <sub>2</sub> PO <sub>4</sub> in 500 ml H <sub>2</sub> O, pH 7.4
EM fixation solution	2.5 % Glutaraldehyde (v/v), 4 % Paraformaldehyde (w/v) in 0.1 M Phosphate buffer, pH 7.4

## 2.7 Antibodies

**Table 2-10: Primary antibodies**

Name	Species	Dilution		Source
		IFA	WB	
<i>T. gondii</i> ACT1 <sup>1</sup>	Rabbit	1:1250	1:500	Sibley, L. D.
<i>T. gondii</i> ACT1 <sup>2</sup>	Rabbit	1:250	1:2000	Sibley, L. D.
ACTN05 (C4) ab3280	Mouse	1:500	1:2000	ABCAM
<i>P. falciparum</i> ACT1, Ep1	Rabbit	1:1000	1:1000	Scherf, A.
<i>P. falciparum</i> ACT1, Ep2	Rabbit	1:500	1:1000	Scherf, A.
<i>T. gondii</i> ACT1	Mouse	1:100	1:500	Soldati, D.
<i>T. gondii</i> ACT1 <sup>polyclonal</sup>	Rabbit	1:500	1:500	Baum, J.
<i>T. gondii</i> ACT1 <sup>monoclonal</sup>	Mouse	1:500	1:500	Baum, J.
JLA-20	Mouse	1:100	n.t.	Sigma
β-actin	Rabbit	1:250	1:2000	Sigma
Phalloidin-AlexaFlour <sub>350</sub>		1:1000	n.t.	Molecular Probes
Phalloidin-AlexaFlour <sub>488</sub>		1:1000	n.t.	Molecular Probes
Phalloidin-AlexaFlour <sub>594</sub>		1:1000	n.t.	Molecular Probes
DNase1-AlexaFluor <sub>594</sub>		1:2000	n.t.	Molecular Probes
Aldolase	Rabbit	1:2000	1:3000	Sibley, L. D.
Catalase	Rabbit	(-)	1:3000	Soldati, D.
AMA-1	Mouse	1:500	n.t.	Ward, G.
Mic2 6D10	Mouse	1:500	n.t.	Carruthers, V.
Mic3 T82C10	Rabbit	1:500	n.t.	Lebrun, M.
Rop1	Mouse	1:200	n.t.	Sibley, L. D.
Rop5 T53E2	Mouse	1:1000	n.t.	Dubremetz, J.F.
RON4 TS6H1	Rabbit	1:500	n.t.	Lebrun, M.
GAP40	Rabbit	1:250	n.t.	Soldati, D.
GAP45	Rabbit	1:1000	n.t.	Soldati, D.
Gra1	Mouse	1:500	n.t.	Delauw, M. F.
Gra2	Rabbit	1:500	n.t.	Delauw, M. F.
Gra5	Rabbit	1:500	n.t.	Delauw, M. F.
Gra7	Rabbit	1:500	n.t.	Delauw, M. F.
IMC1	Mouse	1:1000	n.t.	Ward, G.
ISP1	Mouse	1:1000	n.t.	Bradley, P.
MLC1	Rabbit	1:2000	n.t.	Soldati, D.
SAG1 ( <i>Toxoplasma</i> )	Rabbit	1:1000	n.t.	ABCAM
CPN60	Rabbit	1:1000	n.t.	Sheiner, L.
HSP60	Rabbit	1:2000	n.t.	Sheiner, L.
Tom40	Rabbit	1:2000	n.t.	van Dorreen, G.
GFP	Mouse	1:500	1:2000	Roche
HALO <sup>Monoclonal</sup>	Mouse	-	1:1000	Promega
HALO <sup>Polyclonal</sup>	Rabbit	1:500	-	Promega

n.t.=not tested, (-)=does not react

**Table 2-11: Secondary antibodies**

Name	Species	Dilution		Source
		IFA	WB	
Alexa Fluor 350 $\alpha$ -mouse	Goat	1:3000	(-)	Life Technologies
Alexa Fluor 488 $\alpha$ -mouse	Goat	1:3000	(-)	Life Technologies
Alexa Fluor 594 $\alpha$ -mouse	Goat	1:3000	(-)	Life Technologies
Alexa Fluor 633 $\alpha$ -mouse	Goat	1:3000	(-)	Life Technologies
Alexa Fluor 350 $\alpha$ -rabbit	Goat	1:3000	(-)	Life Technologies
Alexa Fluor 488 $\alpha$ -rabbit	Goat	1:3000	(-)	Life Technologies
Alexa Fluor 594 $\alpha$ -rabbit	Goat	1:3000	(-)	Life Technologies
Alexa Fluor 633 $\alpha$ -rabbit	Goat	1:3000	(-)	Life Technologies
Alexa Fluor 350 $\alpha$ -rat	Goat	1:3000	(-)	Life Technologies
Alexa Fluor 488 $\alpha$ -rat	Goat	1:3000	(-)	Life Technologies
Alexa Fluor 594 $\alpha$ -rat	Goat	1:3000	(-)	Life Technologies
IRDye680RD $\alpha$ -Mouse	Goat	(-)	1:5000	Li-Cor
IRDye800CW $\alpha$ -Mouse	Goat	(-)	1:5000	Li-Cor
IRDye680RD $\alpha$ -Rabbit	Goat	(-)	1:5000	Li-Cor
IRDye800CW $\alpha$ -Rabbit	Goat	(-)	1:5000	Li-Cor

(-) = Does not react

## 2.8 Oligonucleotides

Oligonucleotides or primers were used to amplify specific regions of DNA by PCR (See Chapter 2.11.5). The primers were designed carefully with the assistance of OligoCalc analysis tool. Oligonucleotides were planned with a specific criterion; an optimal GC content (40-60 %), a melting temperature between 55 and 65 °C and an overall length between 17 and 24 bases long, avoiding any primer dimers. All oligonucleotides were synthesised and purchased from Eurofins® MWG Operon.

**Table 2-12: Main oligonucleotides used in this study**

Name	Sequence 5' → 3'	Purpose
Act cDNA fw	GGGAATTCGACAAAATGGCGGATGAAGAAGTGCAAGCC	Int PCR 1-1'
Act cDNA rv	CGTTAATTTAAAAGCACTTGC GGTTGGACGATGCTCGGG	Int PCR 1-1'
Act1integ5' fw	CGTCACACCCGCTCAGCCAAAGG	Int PCR 2-2'
YFP int rv	ATGGGCACCACCCCGG	Int PCR 2-2'
HX fw	GCTACGACTTCAACGAGATGTTCCGCG	Int PCR 3-3'
Act1integ3' rv	GGCTCAAACATGACACGTGTGC	Int PCR 3-3'

## 2.9 Expression vectors

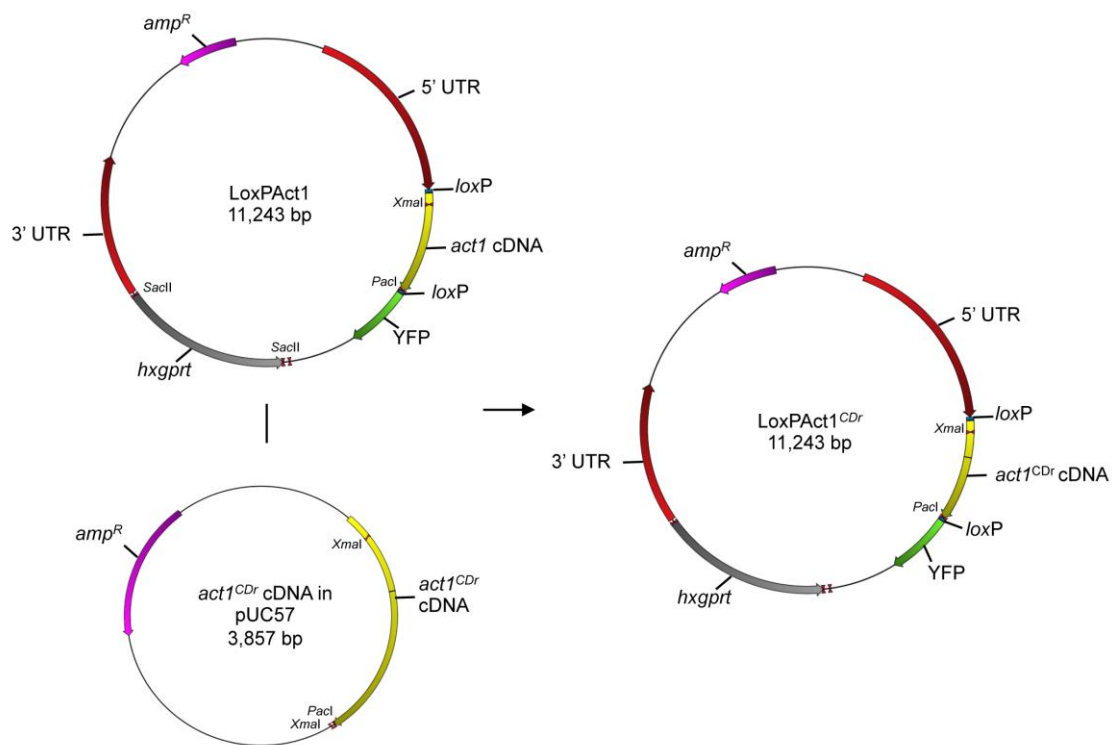


**Figure 2-1: Cloning strategy for the LoXPact1<sup>CDr</sup> plasmid**

The *act1* cDNA containing the nucleic acid mutations Cytosine 407 Guanine (black line in *act1*<sup>CDr</sup> map, yellow block) which confers the resistance to cytochalasin D (CD) was synthesised by CloneTek and provided in a pUC57 vector. The *act1* cDNA from the original LoXPact1 plasmid (Andenmatten *et al.*, 2012) was replaced with the *act1*<sup>CDr</sup> cDNA through a *Pacl* and *XmaI* digestion.

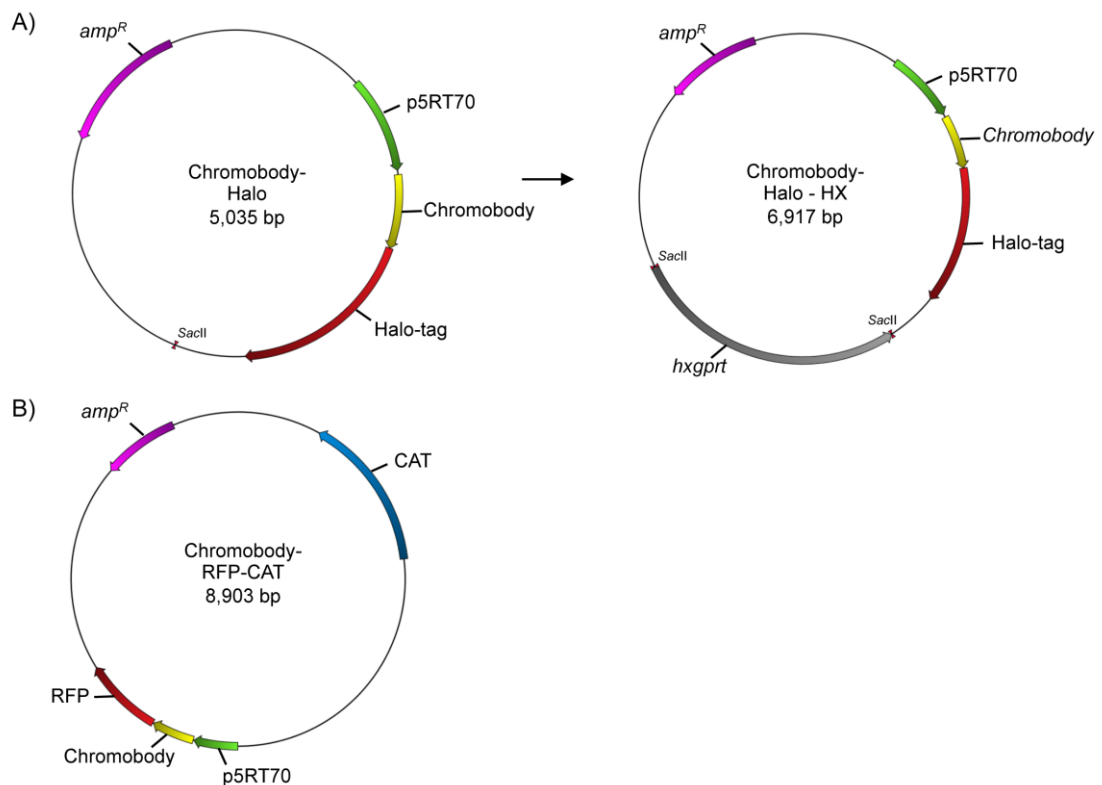


**Figure 2-2: Vector maps for chromobody expression plasmids.**

**A)** Chromobody-Halo plasmid was generated by Dr. Javier Periz and used for transient transfections. For Stable transfections, the *hxgprt* selectable marker was digested from LoxPAct1 plasmid (Figure 2-1) by *Sac*II and inserted into the chromobody-Halo-HX plasmid within the *Sac*II site. **B)** The chromobody-RFP plasmid was generated by Dr. Javier Periz and used to transient transfections. The selectable marker for this plasmid was the chloramphenicol gene (CAT). Expression of all plasmids was under the p5RT70 constitutive promoter (Soldati & Boothroyd, 1995).

## 2.10 Bacterial strains (*Escherichia coli*)

All bacterial strains used in this study were chemically competent, either homemade or commercially bought and stored at -80 °C.

**Table 2-13: *Escherichia coli* strains**

DH5 $\alpha$ <sup>™</sup>	New England BioLabs <sup>®</sup>	<i>fhuA2</i> $\Delta$ ( <i>argF-lacZ</i> )U169 <i>phoA glnV44</i> $\Phi$ 80 $\Delta$ ( <i>lacZ</i> )M15 <i>gyrA96 recA1 relA1 endA1 thi-1 hsdR17</i>
One Shot TOP10 <sup>®</sup>	ThermoFisher Scientific <sup>™</sup>	F- <i>mcrA</i> $\Delta$ ( <i>mrr-hsdRMS-mcrBC</i> ) $\Phi$ 80 <i>lacZ</i> $\Delta$ M15 $\Delta$ <i>lacX74 recA1 araD139</i> $\Delta$ ( <i>araleu</i> )7697 <i>galU galK rpsL</i> (StrR) <i>endA1 nupG</i>
XL10-Gold <sup>®</sup>	Stratagene <sup>™</sup>	TetrD( <i>mcrA</i> )183 D( <i>mcrCB-hsdSMR-mrr</i> )173 <i>endA1 supE44 thi-1 recA1 gyrA96 relA1 lac Hte</i> [F' <i>proAB lacIqZDM15 Tn10</i> (Tetr) Amy Camr].

Home-made chemically competent DH5 $\alpha$ <sup>™</sup> bacteria were produced using the methods described in Green and Rogers (2013). In summary, untransformed DH5 $\alpha$  (NEB) were streaked onto an LB<sub>AGAR</sub> plate without ampicillin and grown overnight. A single colony from this was then cultured in 50 ml LB media without ampicillin at 37 °C, shaking overnight. The culture was then added to 1 L of LB media and grown to a density of 0.5 OD<sub>600</sub> 37 °C, shaking. Cultures were cooled to 4 °C for 15 minutes before pelleting the bacteria (4500 rpm). The pellet was resuspended in TfbI and maintained on ice for 15 minutes before pelleting again at 400 rpm at 4 °C. Finally, the pellet was resuspended in TfbII and aliquoted into sterile Eppendorf tubes on dry ice and transferred to -80 °C for storage.

## 2.11 Molecular biology

### 2.11.1 Isolation of genomic DNA from *Toxoplasma gondii*

Genomic DNA was isolated from extracellular parasites using a Qiagen<sup>®</sup> DNeasy Blood and Tissue kit. As the *act1* KO parasites cannot egress (Egarter *et al.*,

2014), large intracellular vacuoles were scratched and put through a 23 G needle to release the parasites before DNA isolation. In all cases, parasites were centrifuged (5 minutes, 500 g, 4 °C) and re-suspended in 200 µl PBS. The extraction of gDNA was as the manufacturers protocol described with a final elution volume of 100 µl ddH<sub>2</sub>O.

### **2.11.2 Isolation of RNA from *Toxoplasma***

RNA was extracted from extracellular parasites, where each 6 cm culture dish gave approximately  $2 \times 10^7$  tachyzoites/ml. Parasites were centrifuged at 600 g for 5 minutes at 4 °C, after which the samples were kept on ice. Total RNA was isolated from the parasite pellet using the PureLink RNA mini-kit (Roche<sup>®</sup>) following the manufacturer's stated protocol. Throughout the RNA extraction, all equipment and gloves were cleaned with RNaseZAP<sup>™</sup> (Sigma<sup>®</sup>). Isolated RNA was quickly analysed for integrity by running in a standard TAE-based agarose gel (6 ng per lane) for 5 minutes. We were looking for the presence of two distinct bands; 28S and 18S RNA (Aranda *et al.*, 2012). Final pure RNA samples were quantified using the NanoDrop<sup>™</sup> spectrophotometer (Thermo Scientific<sup>®</sup>) (see chapter 2.11.4).

### **2.11.3 Making cDNA (reverse transcription)**

Complementary DNA (cDNA) was prepared with 1 µg of RNA as a template for reverse transcription. cDNA synthesis was carried out using Invitrogen<sup>®</sup> reverse transcriptase (SuperScript<sup>™</sup> III) and random primer sets following steps described in the manufacturer's protocol. For the reverse transcription reaction, an initial incubation step of 25 °C for 10 minutes was followed by 15-minute incubation at 50 °C and final step of 85 °C to terminate the reaction.

### **2.11.4 Nucleic acid concentration**

Nucleic acid concentrations were quantified using a NanoDrop<sup>™</sup> spectrophotometer following the manufacturer's guidelines. The NanoDrop<sup>™</sup> assesses the purity of nucleic acids within the sample by determining if a nucleic acids sample is contaminated with proteins or other chemical contaminants (Desjardins & Conklin, 2010). DNA is considered as 'pure' if the 260/280 nm ratio is approximately 1.8, whereas a ratio is around 2.0 is accepted as 'pure' for RNA samples. Moreover,

nucleic acid samples are also considered as 'pure' if the 260/230 nm ratio is between 2.0-2.2, while ratios out with this range indicate the presence of contaminants usually proteins or phenol.

## 2.11.5 Polymerase chain reaction

The polymerase chain reaction was used for various purposes during this study: the amplification of DNA fragments for molecular cloning, colony screening in transformed bacteria or testing genetically modified *Toxoplasma* strains for the presence of transfected DNA. However, every PCR conducted contained the necessary components at the desired concentration described in (Table 2-14). Once prepared, the PCR reaction was carried out in a thermocycler outlined in (Table 2-15). Unless otherwise stated, the PCR products were run on a 1 % agarose gel (in 1 x TAE buffer) to check for amplification of the correct size.

**Table 2-14: Components of a PCR mix**

Component	Desired concentration
<i>Platinum</i> HiFi Buffer or ThermoPol buffer (10 x)	1 x
dNTPs (10 mM)	200 $\mu$ M
MgSO <sub>4</sub> (50 mM)	2 mM
Forward Oligonucleotide (100 pmol/ $\mu$ l)	0.4 $\mu$ M
Reverse Oligonucleotide (100 pmol/ $\mu$ l)	0.4 $\mu$ M
<i>Platinum</i> HiFi <i>taq</i> Polymerase or <i>taq</i> DNA Polymerase (5 U/ $\mu$ l)	1 Unit
DNA	(~1-50 ng)
H <sub>2</sub> O To a final volume of 25 $\mu$ l	----

**Table 2-15: PCR thermocycler program**

Temperature	Time	Step	Cycles
95 °C	5 minutes	Initial denaturing	1
95 °C	30 seconds	Denaturing	} 25 - 30
55-65 °C*	30 seconds	Annealing	
68 °C	1 minute per 1 kb	Elongation	
68 °C	10 minutes	Final elongation	1
4 °C	----	Storage	Hold

\* The optimal temperature is dependent on the T<sub>m</sub> of the oligonucleotide (I used 5 °C below the stated T<sub>m</sub> for the oligonucleotides from OligoCalc).

### 2.11.5.1 Molecular cloning

For molecular cloning, specific primers were used to amplify DNA fragments from gDNA, cDNA or plasmid DNA. Invitrogen® *Platinum*® HiFi *taq* polymerase

was used to amplify products for molecular cloning due to its high proof-reading capability. The PCR reactions were prepared according to the manufacturer's guidelines as described in Table 2-14 using *Platinum*<sup>®</sup> HiFi *taq* polymerases and respective buffers. For the reaction, the thermocycler was set for 30 cycles with the rest of the set-up as described in Table 2-15.

#### **2.11.5.2 Bacterial colony screening**

Colony PCRs were used to screen a large number of bacteria colonies for the presence of the transformed plasmid. For this, specific primers were designed with around 150 bp upstream and downstream of the target fragment within the plasmid to allow the discrimination between a plasmid that integrated the expected fragment versus a plasmid that had no insert. To test for positive transformations, a PCR master mix was made for a minimum of 24 colonies. This contained the components described in Table 2-14 and NEB<sup>®</sup> Thermopol<sup>®</sup> *taq* polymerase and buffer. Bacteria colonies were picked from an LB<sub>AGAR</sub> plate, spotted onto a fresh LB<sub>AGAR</sub> + ampicillin plate and then re-suspended in 25 µl of PCR master mix. The PCR reaction was carried out as described in Table 2-15 with the only adjustment to reduce the number of cycles to 25.

#### **2.11.5.3 Integration PCR**

To confirm that exogenous DNA was expressed in *T. gondii* or that Cre-mediated excision had occurred, gDNA was extracted from the parasites (see chapter 2.11.1) and used as a template for PCR amplification. The reaction comprised of the components described in Table 2-14 and used both the Thermopol<sup>®</sup> buffer and NEB<sup>®</sup> *taq* polymerase. Note, additional MgSO<sub>4</sub> was not added to the reaction mix as the Thermopol<sup>®</sup> buffer already contains 2 mM MgSO<sub>4</sub>. The thermocycler was set up as stated for 25 cycles in Table 2-15 with no other alterations.

#### **2.11.6 Agarose gel electrophoresis**

Agarose gel electrophoresis separates DNA fragments based on fragment sizes. Agarose gels were made up to a concentration between 0.8 - 2 % agarose (w/v) in 1 x TAE buffer (see chapter 2.6) by boiling in a microwave. The addition of 0.01 % GelRed allowed the visualisation of the DNA fragments later on.

Sample DNA was mixed with 5x loading dye and subsequently loaded into a well along with 5  $\mu$ l of 1 kb DNA ladder (NEB<sup>®</sup>) or 1 kb *plus* DNA ladder (Thermo Scientific<sup>™</sup>).

### 2.11.7 Restriction endonuclease digest

Restriction enzymes are widely used to cut DNA at site-specific palindromic sequences providing blunt or sticky ends. Throughout this study, restriction endonucleases were used extensively for three purposes: molecular cloning, diagnostic purposes or linearising plasmid DNA before transfections. Throughout this study, I used restriction enzymes and their respective buffer supplied by NEB<sup>®</sup>.

For molecular cloning, around 2  $\mu$ g of PCR product and 0.5  $\mu$ g vector were digested with restriction enzymes according to the manufacturer's protocol for 2 hours at the respective temperature.

Plasmid DNA isolated from the bacteria was verified using diagnostic digests. Around 100 ng DNA was digested with the respective enzymes for 2 hours before running on an electrophoresis gel.

For transfections, plasmid DNA (either 60  $\mu$ g for BioRad<sup>®</sup> or 20  $\mu$ g for AMAXA<sup>®</sup> transfections) was linearised with a single cutting enzyme for 3 hours at the respective temperature.

### 2.11.8 Dephosphorylation of digested DNA fragments

Alkaline calf intestinal phosphatase (CIP) from NEB<sup>®</sup> was added to vector at the end endonuclease digestion. This enzyme catalyses the dephosphorylation of the 5' end of DNA. This reaction reduces the likelihood of the vector self-ligating, although still allowing ligation of insert DNA into the CIP treated vector.

### 2.11.9 DNA extraction from agarose gel

Qiagen<sup>®</sup> MinElute DNA extraction kit was used to isolate DNA from within an agarose gel. The desired band was excised from the gel using a sterile scalpel blade over a UV trans-illuminator. The gel fragment was placed in a fresh

Eppendorf tube and weighed. The isolation of the DNA from the gel fragment was conducted as stated in the manufacturer's protocol, eluting finally with 20  $\mu\text{l}$  ddH<sub>2</sub>O.

Following this, 0.5  $\mu\text{l}$  was run on an agarose gel to determine if the purified DNA sample is uncontaminated with other DNA fragments. At this stage, the NEB<sup>®</sup> 1 kb DNA ladder allows a rough estimation of DNA quantity.

### 2.11.10 Ligation of DNA fragments

DNA ligase is used to join two fragments of DNA covalently (insert and plasmid backbone). It catalyses the formation of phosphodiester bonds between the 5' phosphate and 3' hydroxyl ends in dsDNA and requires ATP as the co-factor.

PCR amplified products were occasionally sub-cloned into the bacterial expression vector, pGEM<sup>®</sup> T-easy. pGEM<sup>®</sup>-T easy vectors contain poly-T extensions that allow efficient ligation of poly-A tailed PCR products. For this, 1  $\mu\text{l}$  of PCR product and 1  $\mu\text{l}$  pGEM<sup>®</sup> was mixed with 2X rapid ligation buffer and ligase and incubated for 1 hour at room temperature.

NEB<sup>®</sup> T4 DNA ligase, derived from the bacteriophage T4, was used to ligate inserts into *T. gondii* expression plasmids. For a 10  $\mu\text{l}$  ligation reaction, 1  $\mu\text{l}$  of T4 ligase and 1  $\mu\text{l}$  ligase buffer (10x) was added along with both insert and vector at a molar ratio between 3:1 and 5:1. The total DNA quantity for the reaction did not exceed 120 ng. Ligations were incubated for 1 hour at 22 °C or overnight at 16 °C.

### 2.11.11 Plasmid transformation into *E. coli*

Chemically competent *E. coli* (see chapter 2.9) was used to transform the ligation mix and amplify the desired plasmid. Bacterial cells (50  $\mu\text{l}$ ) were thawed on ice to which 5  $\mu\text{l}$  ligation mixture was added for 20 minutes. After which, the cells were heat-shocked for 30 seconds at 42 °C then returned to the ice for a further 2 minutes. The transformation mix was resuspended in 500  $\mu\text{l}$  pre-heated NZY broth and transferred to a 37 °C shaking incubator for 1 hour before plating on an LB<sub>AGAR</sub> plate containing ampicillin and incubated overnight

at 37 °C. Transformed bacterial colonies were screened by a colony PCR (see chapter 2.11.5.2).

### **2.11.12 Isolating plasmid DNA from *E. coli***

Plasmid DNA was isolated from competent bacteria after transformation through a series of steps. The bacteria are pelleted and lysed under alkaline conditions to release the nucleic acids. The lysis buffer contains SDS, sodium hydroxide and RNase A. The SDS is used to lyse the bacterial cell wall to release the DNA while the sodium hydroxide raises the pH and thus denatures proteins and dissociates DNA to single strands. The RNase A will degrade any RNA contaminants. During this process, plasmid DNA remains supercoiled and can resist these chemicals. Next, the lysis buffer is neutralised using a buffer containing potassium acetate to neutralise the pH and renatures the plasmid DNA. At this pH, the SDS precipitates proteins and also any chromosomal DNA that will be interacting with proteins. By high-speed centrifugation, all unwanted contaminants from the lysis will be pelleted, thus yielding a solution containing the plasmid DNA. The DNA was purified using a silica-gel membrane bound column through a series of stringent washes. Plasmid DNA binds to the silica-gel-membrane where an initial wash step is used to remove any remaining cellular debris followed by two washes with high ethanol solution to remove the salts from the first isolation. The DNA is eluted from the silica gel using molecular grade water.

#### **2.11.12.1 Small scale extraction (MiniPrep)**

Single colonies from LB<sub>AGAR</sub> plates were inoculated in 4 ml LB media overnight at 37 °C. The pelleted bacteria was resuspended and isolated using Qiagen® Spin MiniPrep kit following the manufacturer's protocol. The final elution was with 50 µl ddH<sub>2</sub>O, yielding between 5-20 µg of plasmid DNA.

#### **2.11.12.2 Medium scale extraction (MidiPrep)**

For larger yields of plasmid DNA, 50 ml of bacterial culture was grown overnight. The plasmid DNA was extracted using Qiagen® Spin MidiPrep kit following the manufacturer's protocol eluting with 200 µl of ddH<sub>2</sub>O, typically giving yields between 50 and 300 µg of plasmid DNA.

### **2.11.13 Site-directed mutagenesis**

To make a specific, intentional single or multiple nucleotide changes in a DNA plasmid sequence, a site directed mutagenesis reaction was carried out. Primers were designed using NEBaseChanger software with 5' end annealing back-to-back. Between 1-25 ng/ $\mu$ l of DNA was mixed with NEB<sup>®</sup> Q5<sup>®</sup> Hot Start High-Fidelity 2X Master Mix along with 0.5  $\mu$ M forward and reverse primers and ddH<sub>2</sub>O. The amplification cycling conditions were similar to those described in Table 2-15 for PCR amplification. The changes however are, denaturing step is conducted at 98 °C and extension at 72 °C. After the amplification reaction; phosphates are added to the blunt end of then PCR product; then it is ligated, and the parental plasmid was digested. This all occurs through the KLD reaction as described in the manufacturer's protocol. Finally, this treated plasmid was transformed into chemically competent bacteria as described in chapter 2.11.11.

### **2.11.14 Ethanol precipitation**

For transfections, plasmid DNA was purified through a series of ethanol precipitation steps. Plasmid DNA was mixed with 1/10 volume of 3 M sodium acetate (pH 5.2) and 3 volumes of ice-cold 100 % ethanol and transferred to -80 °C for at least 1 hour. Afterwards, the precipitating DNA was centrifuged for 30 minutes at 13,000 rpm at 4 °C. Next, the DNA was then washed twice with ice-cold 70 % ethanol to remove residual salts. Finally, the supernatant was removed, and the pellet was air dried before the DNA pellet was resuspended in either P3 buffer (AMAXA<sup>®</sup>) or cytomix (Bio-Rad<sup>®</sup>), depending on which transfection machine is to be used.

### **2.11.15 DNA sequencing**

Plasmid DNA was sequenced by GATC<sup>®</sup> Biotech using their LIGHTRUN<sup>™</sup> Sanger sequencing facilities. Sequencing requires a total volume of 10  $\mu$ l with 80-100 ng/ $\mu$ l of purified plasmid DNA and 5  $\mu$ l of 5 pmol/ $\mu$ l of primer.

---

## 2.12 Cell biology

### 2.12.1 Organisms

Various organisms were used throughout this study, from *Toxoplasma gondii* parasites strains to their mammalian host cells used to culture and maintain them.

#### 2.12.1.1 Host cell strains

**Human foreskin fibroblasts (HFFs)** were purchased from ATCC (American Type Culture Collection) at passage 15 and are maintained up to passage 23. These cells grow in a monolayer due to contact inhibition. This makes them ideal for many phenotypic analysis assays for *Toxoplasma*. These were the primary cell line that was used to culture *Toxoplasma* in this study.

**HeLa cells** are an immortalised cell line isolated from cervical cancer cells (Scherer *et al.*, 1953). These also grow in monolayers and were used for phenotypic assays with latrunculin A. These were initially provided by ATCC and maintained indefinitely in the lab.

**RADA2 cells** are latrunculin A resistant HeLa cells first described in Fujita *et al.* (2003). The RADA refers to the two point mutations (R183A and D184A) in the actin gene. These were kindly provided by Dr. Cora-Ann Schoenenberger and were used in latrunculin A invasion assays.

#### 2.12.1.2 Parasite strains

Various parasites strains have been used throughout this study, but all are genetically altered from the highly virulent Type 1 RH  $\Delta$ hxgp $rt$  strain of *Toxoplasma gondii* (Donald & Roos, 1993). This strain was predominantly used as the wild-type control or for random integration of plasmid DNA.

**$\Delta$ Ku80 $\Delta$ HX** is a strain based on RH, which lacks the *Ku80* gene, enhancing homologous recombination (Fox *et al.*, 2009; Huynh & Carruthers, 2009). *Ku80* is part of the *Ku* heterodimer, which is involved in DNA repair and non-homologous DNA end joining (NHEJ). Knockouts of *Ku80* almost eliminate random integration,

in turn favouring the insertion of constructs with homologous sequences into the proper loci.

RH DiCre  $\Delta Ku80\Delta HX$  was adapted from the  $\Delta Ku80::DiCre$  (Andenmatten *et al.*, 2012) and generated in our lab by Dr. Gurman Pall. The strain is of an RH background where the DiCre plasmid was randomly integrated, followed by the deletion of *Ku80*. RH DiCre  $\Delta Ku80\Delta HX$  is the parental strain for inducible knockout constructs containing *LoxP* sites and for this study the parental for the *LoxPAct1* strain. Moreover, an indicator strain for gene removal was also generated for geneswap vectors lacking a fluorescent reporter cassette. For this, *Ku80* was replaced with *Tub8-LoxP-KillerRed-LoxP-YFP* with homologous recombination. Therefore, parasites express KillerRed and upon rapamycin treatment, begin to express YFP indicating the Cre recombinase activity has occurred.

### 2.12.2 Culturing *Toxoplasma gondii* and host cell lines

Host cells used in this study (chapter 2.12.1.1) were grown on TC treated plastics and maintained in Dulbecco's modified Eagle's medium (DMEM) supplemented with 10 % Foetal Bovine serum, 2 mM L-glutamine and 25 mg/ml gentamycin, known as DMEM<sub>COMPLETE</sub>. Host cells were maintained in an incubated humid environment of 37 °C and 5 % CO<sub>2</sub>.

Human foreskin fibroblasts (HFFs) were the primary cell line infected when culturing *Toxoplasma gondii* strains. Extracellular parasites were inoculated onto a confluent layer of HFFs. Alternatively, intracellular parasites could be artificially liberated from within their vacuoles and inoculated onto a fresh monolayer of host cells. To artificially release parasites, these were scratched using a cell scraper followed by syringe lysis of the host through a 23 G needle three times.

### 2.12.3 Trypsin treatment of host cells

HFFs were split 1:4 weekly up to passage 23 by our technician Matthew Gow. Other cell types were also passed weekly but in a 1:20 ratio.

Splitting and maintaining host cells was performed using the trypsin/EDTA to detach the cells gently from the bottom of the culturing flasks. Trypsin is a protease that cleaves distinct peptide bonds. For this, culture media was removed, and the cells were washed with cold PBS to remove traces of FBS, which blocks the enzymatic activity of trypsin. Cells were covered with trypsin and incubated for 3 minutes at 37 °C, 5 % CO<sub>2</sub>. Flasks would be gently tapped to facilitate further detachment of the cells. Finally, fresh DMEM<sub>COMPLETE</sub> was added to stop the trypsin activity, and the cell suspension was transferred to new culturing flasks or dishes.

## **2.12.4 Transfection of *T. gondii***

Transfection is where exogenous DNA is integrated and expressed in *T. gondii*. The most efficient method of introducing linearised DNA into *T. gondii* is through electroporation (Soldati & Boothroyd, 1993). Throughout the study, two different systems were used to transfect parasites; the Bio-Rad<sup>®</sup>, which yields around 30 % efficiency transient or the AMAXA<sup>®</sup> Nucleofactor<sup>™</sup> which gave an impressive >90 % for transient transfections also yielding a very high rate of stable integration.

### **2.12.4.1 Bio-Rad<sup>®</sup> transfections**

Transfections with the Bio-Rad<sup>®</sup> Gene Pulser Xcell<sup>™</sup> were conducted in cytomix, (see chapter 2.6) a buffer which mimics the cytosolic ion composition of the cells, resulting in the greatest survival rate (van den Hoff *et al.*, 1992). 60 µg of DNA was linearised and ethanol precipitated. The pelleted DNA was dissolved in cytomix to a volume of 100 µl; parasites were re-suspended in 640 µl of cytomix to which 30 µl ATP (100 mM) and 30 µl GSH (100 mM) was added. This transfection mix was transferred into an electroporation cuvette (BioRad<sup>®</sup>; 4 mm). Electroporation was conducted using the following settings; mode: square wave, voltage: 1700 V, pulse length: 200 µs, the number of pulses: 2 and interval between pulses: 5 ms.

### **2.12.4.2 AMAXA<sup>®</sup> transfections**

For transfections using the AMAXA<sup>®</sup>, only 20 µg of DNA is required. DNA after ethanol precipitation was mixed with 200 µl of pelleted parasites in 100 µl total

of Lonza® P3 buffer. Lonza® F158 program was used to electroporate, yielding an impressive transfection rate.

#### 2.12.4.3 Transient transfections

Transient transfections of circular DNA into *T. gondii* will be lost over several replication cycles since the DNA will be expressed only as an extra-chromosomal. This approach is useful to analyse the expression of localisation of recombinant proteins without having to go for stable transfections (discussed in chapter 2.12.4.4). Immediately after electroporation, the parasites were inoculated on coverslips containing a confluent monolayer of HFFs and incubated from 24 to 72 hours before fixation.

#### 2.12.4.4 Stable transfections

Similar to eukaryotes, DNA is preferentially integrated randomly into the genome of *T. gondii* and only around 5 % of all transfections integrate by homologous recombination (Donald & Roos, 1993). This was a major obstacle in gene targeting. However, a major development in *T. gondii* genetics was to remove the gene; *Ku80* (Fox *et al.*, 2009; Huynh & Carruthers, 2009). The *Ku* genes are involved in DNA repair of double strand breaks *via* non-homologous end joining machinery (NHEJ) (Manivasakam *et al.*, 2001). Therefore deletion of *Ku80* loses the ability for NHEJ and favours homologous recombination up to around 90 %.

DNA integrated into the genome *via* homologous recombination was linearised using site-specific endonucleases upstream of the expression cassette. Linearised DNA was transfected into approximately  $1 \times 10^7$  freshly egressed parasites as described in chapter 2.12.4.

Linearised DNA integrated into the genome *via* random integration plasmid DNA was transfected as above. One difference from homologous recombination is that the DNA integrates randomly into the genome. This is achieved by the addition of the restriction enzyme *NotI* (10 Units) into the transfection mix, a procedure known as Restriction Enzyme Mediated Insertion or REMI (Black *et al.*, 1995). This activates the DNA repair machinery of the cells and increases the probability of integration of exogenous DNA into the *T. gondii* genome by up to

400 times (Black *et al.*, 1995). However, more often than not with REMI, additional copies of plasmid can integrate into the genome (Gubbels & Striepen, 2004).

To obtain stable integration after transfection, parasites were inoculated onto a fresh monolayer of HFFs with the addition of a selectable drug (See Table 2-16) in the culture media.

**Table 2-16: Selection strategies for stable transfection of *T. gondii***

Selectable marker gene	Drug	Selection procedure
Dihydrofolate reductase-thymidylate synthase allele (DHFR-TS) from <i>T. gondii</i> (Donald & Roos, 1993)	Pyrimethamine (1 $\mu$ M) 1000X	Drug added immediately after electroporation and maintained to until stable resistant pool emerged.
Chloramphenicol acyl transferase (CAT) from <i>E. coli</i> (Kim <i>et al.</i> , 1993)	Chloramphenicol (10 $\mu$ M) 1000X	Drug added immediately after electroporation. The effect is delayed (3-4 lytic cycles); therefore it is important to passage about $5 \times 10^6$ parasites every two days to keep pool heterogeneous until drug treatment leads to parasite death.
HXGPRT from <i>T. gondii</i> (Donald <i>et al.</i> , 1996; Pfefferkorn & Borotz, 1994; Pfefferkorn <i>et al.</i> , 2001)	(+) selection: Mycophenolic acid (25 $\mu$ g/ml) and Xanthine (40 $\mu$ g/ml) 500X  (-) selection: 6-thioxanthine (340 $\mu$ g/ml)	Drugs diluted in DMEM <sub>COMPLETE</sub> to appropriate concentration before adding them to the cells 24 hours post electroporation. Drug treatment maintained until a stable resistant pool emerged.  DMEM <sub>COMPLETE</sub> was replaced by negative <i>hxgp</i> rt selection media (Table 2-9) 24 hours post-electroporation and maintained until stable resistant pool emerged.

## 2.12.5 Isolation of a clonal parasite line

After the pool of transfected parasites recover from the drug selection pressure, it is important to isolate a clonal parasite expressing the desired plasmid DNA. To do this, 50  $\mu$ l of the lysed parasites were incubated in every 2<sup>nd</sup> well down column A of a 96 well plate. Each well was mixed 10 times before transferring 50  $\mu$ l to the well below. Finally, using a multi-channel pipette the wells were mixed 10 times before transferring 50  $\mu$ l to the adjacent column and so on. Parasites were incubated for 5 days undisturbed. After which, the wells were analysed for the formation of plaques which would have been caused by a single

parasite going through its lifecycle multiple times. Single clones were isolated and tested for correct expression of the plasmid by IFA (chapter 2.13.1) and integration PCR (chapter 2.11.5.3).

### **2.12.6 Cryopreservation of *T. gondii* and thawing of stabilates**

To generate parasite stabilates, large intracellular vacuoles were frozen in cryotubes. In detail, HFFs were highly infected with the *T. gondii* strain for around 30 hours. This aimed to have most of the host cells infected with large vacuoles. Cells were gently removed from the dish using a cell scraper and resuspended in 750 µl DMEM only and an equal volume of 2x freezing media (see Table 2-9). This suspension was transferred to a cryo-tube and immediately frozen to -20 °C. One day later, tubes were transferred to -80 °C where they could be stored for up to 6 months. If a longer period was required, cells were deposited in liquid nitrogen tanks indefinitely.

### **2.12.7 Inducing the *act1* KO**

The inducible *act1* KO was obtained by addition of 50 nM rapamycin to the parental LoxPAct1 strain for 4 hours at 37 °C, 5 % CO<sub>2</sub> (Andenmatten *et al.*, 2012). Rapamycin is used to reconstitute the two halves of Cre-recombinase that are fused to rapamycin binding domains. Cre is an enzyme, which recognises LoxP sites and excises the gene of interest between the LoxP sites. Culturing the *act1* KO at a high percentage was rather complicated. With an initial induction rate of around 90 %, the 10 % of uninduced parasites will quickly outgrow the *act1* KO as they can complete the lytic life cycle faster than the *act1* KO (Egarter *et al.*, 2014). Therefore, dextran sulfate 2.5 % in DMEM<sub>COMPLETE</sub> was added to the parasites 24 hours after addition to HFFs. Dextran sulfate was used to isolate egress mutants since it blocks re-invasion of extracellular parasites by binding to glycans thus enhancing the *act1* KO population as they cannot egress (Coleman & Gubbels, 2012). Cells were washed 3 times in DMEM<sub>COMPLETE</sub> before the cells were scratched and syringed to release the *act1* KO parasites. This cycle was sustained every 48 hours.

## 2.13 Phenotypic analysis

Experiments were designed to characterise the phenotypes observed for the mutant parasites.

### 2.13.1 Immunofluorescence analysis

For immunofluorescence analysis (IFA), coverslips were fixed with 4 % paraformaldehyde (PFA) for 20 minutes at room temperature and washed once in PBS. Subsequently, coverslips were either blocked without permeabilising (2 % BSA in PBS) or blocked with permeabilisation (0.2 % Triton X-100, 2 % BSA in PBS) for 20 minutes on an orbital shaker. Primary antibody was diluted in the respective buffer used for blocking. Immunolabelling was conducted in a wet chamber (petri dish containing wet blue roll, parafilm and 20  $\mu$ l of buffer containing the primary antibody) at room temperature for 1 hour. After this, coverslips were replaced back into the well, followed by three washes with PBS for 5 minutes each. To each well, 150  $\mu$ l of secondary antibody (1:3000) was added and placed on the orbital shaker for 45 minutes. Again, coverslips were washed three times in PBS for 5 minutes before mounting on glass microscope slide with either Fluomount-G containing DAPI or without DAPI.

### 2.13.2 Quantitative immunofluorescence analysis

Wild-type (RH) and parental *LoxPAct1* strains were used as controls. For the *act1* KO, parasites were induced with rapamycin as described and cultured for 24 hours on HFFs prior to fixation. An IFA was conducted using  $\alpha$ -ACT1 (Soldati, 1:100) with AlexaFlour 594 (Molecular Probes, 1:3000) as the secondary antibody. Images obtained using an Axioskop 2 (mot plus) fluorescence microscope with AxioCam MRm CCD camera and Velocity software. Images were saved as single red and green channel 16-bit .tif files. CellProfiler 2.1.1 software was used to analyse and quantify fluorescence intensities. RGB images were imported into the program as grey images prior analysis. The pipeline was adjusted to detect objects within the range of 5 to 40 pixels to represent vacuole area. Objects were identified using a global threshold strategy with a three class-Otsu threshold and weighted variances. Under these parameters, the program identified each image YFP-expressing parasites (generated by the DiCre cassette after correct gene removal) and red-coloured region of interest

(corresponding to ACT1 signal). The red signal was quantified on the basis of the total pixel occupied by the YFP expressing objects. The intensity of the red channel was measured for each object and exported to an Excel spreadsheet. The obtained data was filtered manually using area and integrated intensity parameters to include all parasites in a vacuole and exclude any clustered vacuoles, random objects or out of focus vacuoles. Intensities from 60 vacuoles per time point were quantified and processed.

### **2.13.3 Fluorescence intensity analysis**

To analyse the fluorescent intensity of cross-reactive ACT1 antibodies, LoxPAct1 and *act1* KO parasites were cultured on HFF cells for the desired time. The coverslips were fixed with 4 % PFA and stained with the respective ACT1 antibody. Image acquisition was conducted using a 100x oil objective lens on a DeltaVision Core microscope with a CoolSNAP HQ<sup>2</sup>CCD camera. After staining with the ACT1 antibodies, Z-stacked images were processed using the ImageJ software; Plot Profile. A rectangular region of interest was placed over the longest length of each vacuole and the intensity was analysed in both the green and red channels. These were plotted against each other in GraphPad Prism 7.0.

### **2.13.4 Plaque assay**

Plaque assays were used to determine if any stage of the lifecycle is perturbed. From this, 1000 freshly lysed parasites were added to confluent a monolayer of HFF cells within a 6-well plate and incubated for 5 days at 37 °C, 5 % CO<sub>2</sub>. The monolayer was then washed with PBS and fixed with ice cold methanol for 10 minutes. Subsequently, the HFFs were stained with Giemsa (1:10 in H<sub>2</sub>O) for 45 minutes and then washed three times with PBS. Images were acquired using Axiovert 40 CFL fluorescence microscope with AxioCam ICc1. Sizes of ten plaques were measured in three independent experiments using ImageJ 1.34r software and calculated as a percentage value and normalised against RH *Δhxgprt*.

### **2.13.5 Trail deposition assay**

To examine the motility of the parasites over a 2D surface, we assayed for their surface antigen trail deposition. Glass coverslips were coated with 100 % FBS at

room temperature for at least 2 hours. These were washed three times with PBS before use. Parasites were artificially liberated using a 23 G needle, counted and adjusted to  $1 \times 10^6$  parasites in 200  $\mu$ l of pre-warmed gliding buffer (see Table 2-9) and deposited into the coverslips adapted from Hakansson *et al.* (1999). Parasites are incubated at room temperature for 5 minutes and then transferred to a 37 °C incubator for a further 30 minutes. Note, for all deposition assays involving the use of chemical inhibitors, the drugs were added to the parasites and left for 15 minutes before adding to the coverslips. After this, the buffer was exchanged for 4 % PFA carefully. Fixation was for 20 minutes after which the PFA was removed, and the coverslips left to air dry for a further 5 minutes. Immunostaining under non-permeabilising conditions with an antibody against the surface antigen SAG1 allows the visualisation of the trails deposited by the parasites. Assays were performed in triplicate on three independent occasions. For each coverslip, 15 fields of view were counted for the number of trails deposited and normalised to RH *Δhxgprt*.

### **2.13.6 Assessing for tight junction formation**

To assess whether *Toxoplasma* tachyzoites penetrate through a conventional tight junction, we can evaluate this using a pulse invasion assay and staining the tight junction formation with  $\alpha$ -RON4. For this,  $1 \times 10^6$  parasites were artificially released from their vacuole and allowed to invade for 10 minutes. After which, the media was removed and 4 % PFA was added, fixing the parasites mid-penetration. Coverslips were blocked under non-permeabilising conditions and stained for the rhoptry neck protein, RON4, which should form a ring around the parasite.

### **2.13.7 Inside/outside invasion assay**

Here we used an inside/outside invasion assay, based on the “red/green” invasion assay described by Huynh and Carruthers (2006). In detail,  $1 \times 10^6$  parasites were allowed to invade a confluent monolayer of HFF cells for 1 hour and fixed with 4 % PFA. Extracellular parasites were stained with  $\alpha$ -SAG1 under non-permeabilising conditions. Total numbers of parasites within 15 fields of view were counted along with the total number of SAG1 positive parasites within the same 15 fields. By deduction, we were able to determine the number of

invaded parasites. Invasion rates were performed in triplicate and normalised to RH *Δhxgprt*.

### 2.13.8 Invasion/replication assay

The invasion/replication assay was used to analyse the ability of the extracellular parasite to invade the host cells and replicate as described in Kremer *et al.* (2013). In summary,  $1 \times 10^5$  were artificially egressed and inoculated onto a confluent layer of HFFs for 1 hour at 37 °C, 5 % CO<sub>2</sub>. After 1 hour, coverslips are washed by immersion in PBS 10 times using forceps and then incubated in fresh media and left for a further 24 hours under normal culturing conditions. Coverslips were fixed with 4 % PFA for 20 minutes followed by immunostaining with  $\alpha$ -IMC1. Invasion rates were determined by counting the total number of vacuoles from 15 random fields of view. The invasion rates were normalised against RH *Δhxgprt*.

### 2.13.9 Replication assay

For replication, the assay was conducted as described in chapter 2.13.8. After immunostaining with  $\alpha$ -IMC1, 200 vacuoles were counted. Vacuoles were scored for parasites per vacuole at 2, 4, 8, 16 and 16+ and giving as a percentage.

### 2.13.10 Apicoplast loss

Loss of the apicoplast was observed and discussed for the *act1* KO after 96 hours (Egarter *et al.*, 2014). To characterise at which time after gene excision the apicoplasts division defect occurs, LoxPAct1 parasites were induced and incubated for 24-hour intervals before fixing. Vacuoles were stained for with antibodies against both ACT1 ( $\alpha$ -ACT1-Soldati) and an apicoplast marker  $\alpha$ -HSP60 (Sheiner). 200 vacuoles were counted and scored for the correct ratio of apicoplast to parasites within the PV.

### 2.13.11 Egress assay

To determine the parasites ability to egress from the host cell, calcium ionophore (A23187) was used to artificially induce egress (Black *et al.*, 2000).  $5 \times 10^5$  parasites were inoculated onto a monolayer of HFFs and left for 36 hours

to replicate under standard conditions. After which time, pre-warmed serum-free DMEM containing 2  $\mu\text{M}$   $\text{Ca}^{2+}$  ionophore A23187 was added to three coverslips for each strain. As a control, serum-free DMEM<sub>only</sub> was added to one coverslip to indicate that egress is not natural but ionophore-induced. The plate was transferred to 37 °C, 5 % CO<sub>2</sub> incubator for either 5 or 10 minutes and then fixed with 4 % PFA for 20 minutes. Coverslips are immunostained with  $\alpha$ -SAG1 under non-permeabilising conditions, which will only stain extracellular egressed parasites. Egress was quantified where 200 vacuoles were scored as egressed, lysed but unmoved, or intact vacuoles and normalised to RH  $\Delta\text{hxgprt}$ .

### 2.13.12 Time-lapse video microscopy

Time-lapse video microscopy was used to analyse the kinetics of mutant parasites gliding over a 2D surface similar to Hakansson *et al.* (1999) and also penetration time into a confluent monolayer of HFFs using a DeltaVision® Core microscope and SoftWoRx® software or Fiji software. The microscope was equipped with a fitted chamber which allowed the maintenance of standard culturing conditions of 37 °C, 5 % CO<sub>2</sub>.

#### 2.13.12.1 Penetration time of invading parasites

Large intracellular vacuoles were artificially liberated through a 23 G needle, re-suspended in pre-warmed DMEM<sub>COMPLETE</sub> and added a confluent layer of HFFs grown on a glass-bottom live cell dish (Ibidi  $\mu$ -dish<sup>35mm-high</sup>). Time-lapse images were taking at 1 image per second at 40X objective in DIC for both RH  $\Delta\text{hxgprt}$  and LoxPAct1 parasites. As for the *act1* KO parasites, a final image was taking with both DIC and FITC to distinguish knockout parasites from un-induced LoxPAct1 parasites due to the YFP expression of *act1* KO parasites. For penetration times, 15 invasion events were analysed and scored from the initial start point of a tight junction to complete parasite internalisation.

#### 2.13.12.2 Gliding kinetics

Ibidi  $\mu$ -dish<sup>35mm-high</sup> were coated in 100 % FBS for 2 hours at room temperature. Intracellular parasites were put through a 23 G needle, washed once in pre-heated gliding buffer (See Table 2-9) and added to the dish. Time-lapse videos were taking with a 20X objective at 1 frame per second. For the wrMTrck

tracking plugin, images need to be taken with fluorescence. Wild-type parasites expressing *KillerRed* were analysed with images taken in the A<sub>594</sub> channel. As for the *act1* KO, images were taken in the FITC channel.

The motility profiles were analysed using the Fiji software with the wrMTrack plugin. For analysis, 20 parasites were tracked during both helical and circular trails with the corresponding distance travelled, average and maximum speeds determined.

### 2.13.12.3 Egress

To assess if and how the filaments break during egress, RH chromobody-Halo parasites were prepared akin to the egress assay (See Chapter 2.13.11). Briefly,  $1 \times 10^4$  parasites were incubated in an Ibidi  $\mu$ -Dish<sup>35mm, high</sup> and left to replicate to become large intracellular vacuoles. After 36 hours, Halo TMR-ligand (1:5,000) was added to the dish, allowed to bind and washed out after 15 minutes. The dish was then transferred to the DV Core microscope, where a region of interest was found at 40X objective. Ca<sup>2+</sup> ionophore (10  $\mu$ M) was directly above the area of interest. Images were captured at 1 frame per second.

### 2.13.13 Flow chamber attachment

Parasites attachment strengths were assessed under shear stress conditions. Parasites were incubated in Collagen VI Ibidi<sup>®</sup> chambers under increasing flow rates. Parasites were artificially liberated and syringe filtered to remove cell debris. Both the control and parasites of interest were counted and adjusted to  $2 \times 10^5$  each in 250  $\mu$ l DMEM<sub>COMPLETE</sub> and loaded into the Ibidi chamber. Parasites were allowed to attach for 20 minutes at 37 °C, 5 % CO<sub>2</sub>. After which, the chamber was assembled onto the microscope and connected to a syringe pump containing DMEM<sub>COMPLETE</sub>. Care was taken to avoid bubbles in the tube or chamber. An initial flow rate of 0.1 ml/min was transferred through the chamber to remove all non-attached parasites for 10 minutes. An initial image was taken as a starting point under no flow. An increasing flow rate was passed through the chamber for 1 minute at a time. At the end of each minute before the flow rate is increased, an image was taken in both channels at the same

position. In the end, parasites that remained attached were counted. At least seven independent experiments were completed for each condition.

The attachment strength of *T. gondii* was tested in the presence of 0.5  $\mu\text{M}$  cytochalasin D. Parasites were pre- and post- treated with the drug. For the pre-treated parasites; before loading into the Ibidi chamber, the parasites were incubated for 10 minutes in the presence of 0.5  $\mu\text{M}$  CD then allowed to attach. For post-treatment with CD, parasites were allowed to attach the same as the controls. For both conditions, parasites were washed with 0.5  $\mu\text{M}$  CD in the flow media.

The motor complex mutants; *act1* KO, *mlc1* KO, *MyoA* KO and *mic2* KO were analysed by Dr. Gurman Pall.

#### **2.13.14 Bead translocation assay**

Glass-bottom live cell dishes (Ibidi  $\mu$ -dish<sup>35mm-high</sup>) were coated with 0.1 % poly-L-lysine for 30 minutes. After which time, these were washed with MilliQ H<sub>2</sub>O and air dried in a sterile environment. The 40 nM FluoSpheres<sup>®</sup> Carboxylate-Modified Microspheres from Invitrogen<sup>™</sup> were diluted 1:80 in HBSS containing 25 mM HEPES and 1 % BSA. The beads were sonicated twice in an ice bath and pulse centrifuged for 10 seconds to pellet bead clumps.

Parasites were scratched, syringed and filtered prior to counting. Parasites were then adjusted to  $2.5 \times 10^7$  per ml and centrifuged for 5 minutes at 3000 rpm. These were then re-suspended in 250  $\mu\text{l}$  ice-cold HBSS + 25 mM HEPES and transferred to the live cell dish. These were incubated on ice for 20 minutes to allow for attachment. Beads were diluted 1:50 from the stock in HBSS + 25 mM HEPES and added at equal volume to the parasites in the dish. These were transferred to a 37 °C incubator for 15 minutes. After which, 4 % PFA was added to the dish for 15 minutes, then 2 washes were carried out to remove excess beads. Finally, the dishes were incubated with HBSS containing 25 mM HEPES and 0.01 % Hoechst. Non-fluorescent parasites were stained with  $\alpha$ -SAG1 under non-permeablising conditions to highlight their cell structure. Parasites were assessed for their ability to caps the beads. Three situations were quantified;

beads were not bound to the parasites (Un-bound), beads bound but not translocated (Bound) and finally capped (Capped).

### **2.13.15 3D motility assay**

Tachyzoites were prepared and assayed in the Matrigel<sup>®</sup> as previously described in Leung *et al.* (2014a). Briefly, the *act1* KO parasites were released by syringe lysis of infected HFF monolayers using a 27-G needle, filtered through a 3 µm Nucleopore filter, and gently centrifuged at 1,000 x g for 4 minutes. The pellet was washed and resuspended at a final concentration of around 2x10<sup>8</sup> tachyzoites/ml in 3D Motility Media. The tachyzoite suspension was then mixed with 3 volumes of 3D Motility Media and 3 volumes of Matrigel<sup>®</sup> (BD Biosciences<sup>™</sup>) and pre-chilled on ice. Motility through the Matrigel<sup>®</sup> was imaged, tracked and processed using Imaris x64 v. 7.6.1 software (Bitplane AG) as previously described in Leung *et al.* (2014a). Three independent biological replicates, each with three technical replicates, were performed. Our collaborators Dr. Jacqueline Leung and Prof. Gary Ward at the University of Vermont, USA, conducted this assay and all analyses.

### **2.13.16 Electron microscopy**

For this section, after infecting HFFs with the parasites and fixing with EM fixative solution (Table 2-9), the full processing and imaging were conducted by Dr. Leandro Lemgruber, the WTCMP imaging technologist.

#### **2.13.16.1 Scanning electron microscopy (SEM)**

The infected cells were processed as previously described Magno *et al.* (2005). Briefly, the infected cells were fixed in 2.5 % glutaraldehyde and 4 % paraformaldehyde in 0.1 M phosphate buffer. Following several washes with 0.1 M phosphate buffer, the cells were dehydrated in ascending ethanol series and critical point dried. Before metal sputtering, the cell monolayer was scraped with Scotch tape, exposing the cytoplasm of the cells, as well as the parasitophorous vacuoles. These exposed cells were metal coated with gold/palladium and observed in a Jeol 6400 scanning electron microscope (Jeol, Japan). Further image processing was carried out with the Fiji software.

### 2.13.16.2 Correlative-light electron microscopy (CLEM)

For standard correlative-light electron microscopy, host cells were grown in gridded glass bottom petri dishes and infected with chromobody-Halo parasites. The cells were incubated with Halo-TMR ligand for 15 minutes before fixation with EM fixative. Vacuoles presenting an extensive intravacuolar network were imaged with an Elyra super-resolution microscope as in Harding *et al.* (2016). Samples were processed for transmission electron microscopy as described previously in Loussert *et al.* (2012). Thin sections of the same areas imaged in 3D-SIM were imaged in a Tecnai T20 transmission electron microscope (FEI, Netherlands).

For correlative-light/cryo-electron microscopy, cells were fixed in EM fixative, infiltrated in 2.1 M sucrose overnight and rapidly frozen by immersion in liquid nitrogen. Cryo-sections were obtained at -100 °C using an Ultracut cryo-ultramicrotome (Leica, Austria). Cryo-sections were blocked in 3 % BSA in PBS and incubated in the presence of  $\alpha$ -Halo<sup>Mouse</sup>. After several washes in blocking buffer, the cryo-sections were imaged in an Elyra super-resolution microscope (Carl Zeiss, Germany), and then incubated with 10 nm, gold-labelled anti-mouse (Aurion, Netherlands). The same areas observed on the light microscope were imaged in a FEI T20 transmission electron microscope (FEI, Netherlands).

## 2.14 Biochemistry

### 2.14.1 Isolation of protein from parasite cell lysate

For sample preparation, cell lysates from  $1 \times 10^5$  parasites were loaded per lane. Parasites were pelleted and washed once with ice-cold PBS and re-suspended with 8  $\mu$ l RIPA buffer (See Table 2-8) for 5 minutes on ice to prevent protein degradation. This was pelleted to remove the insoluble material by centrifugation at 4 °C for 10 minutes at maximum speed. The supernatant was transferred to a fresh Eppendorf with 1.2  $\mu$ l reducing agent (Invitrogen<sup>®</sup>) and 3  $\mu$ l NuPage<sup>®</sup> 4x loading dye. Samples were boiled for 10 minutes at 95 °C.

### **2.14.2 Sodium dodecyl sulphate polyacrylamide gel electrophoresis**

Proteins can be separated according to their relative size and charge by denaturing sodium dodecyl sulphate polyacrylamide gel electrophoresis (SDS-PAGE) (Laemmli, 1970). SDS-polyacrylamide gels were made in a 1.5 mm thick glass cassette at 10 % as described in Table 2-8. Note, 10 % APS and TEMED were added immediately before the gels were poured. After pouring the resolving gel, isopropanol was added on top to give a level finish to the gel. After the resolving gel had set, the isopropanol can be removed to which the stacking gel was added along with the appropriately sized comb.

Gel cassettes were assembled in the Bio-Rad<sup>®</sup> mini-PROTEAN<sup>®</sup> Tetra Cell with 1 x SDS running buffer (see Table 2-8). Samples were loaded into the wells along with 2.5  $\mu$ l Chameleon<sup>®</sup> Duo ladder. Samples were run at 120 V through the stacking gel then increased to 150 V for the resolving gel.

### **2.14.3 Protein transfer from SDS gels to nitrocellulose membrane**

For western blotting, proteins were transferred from the SDS gel to a nitrocellulose membrane, thereby immobilising them for further study. During this study, a wet transfer technique was used. For this, a membrane sandwich was assembled which consists of sponge, Whatman filter paper, gel, nitrocellulose membrane, Whatman filter paper and sponge (Assembly described from cathode to anode) all presoaked in transfer buffer. This assembly was placed in Bio-Rad<sup>®</sup> mini-PROTEAN<sup>®</sup> Tetra Cell and submerged with transfer buffer (See Table 2-8). The Cell was positioned in a Styrofoam box containing ice to keep the temperature down around 4 °C thus, preventing overheating. The transfer was run at 110 V for 65 minutes.

### **2.14.4 Verification of transfer by Ponceau-S staining**

The membrane was stained with Ponceau-S solution for 2 minutes at room temperature. This is a verification that the protein transferred to the membrane, and that roughly equal concentration of protein was loaded in each well. This was then removed and washed several times with the transfer buffer.

Progressive washing removes background staining highlighting the bands present and finally yielding a clear membrane for immunostaining.

### **2.14.5 Immunostaining of the membrane**

Membranes were blocked in Li-Cor® Odyssey® blocking buffer (TBS) either for 1 hour at room temperature or overnight at 4 °C on an orbital shaker. For staining, the membrane was incubated in a wet chamber with the primary antibody diluted in blocking buffer (Table 2-10) plus 0.1 % Tween-20 for 1 hour. Membranes were then washed three times with TBST for 5 minutes each after which the membrane was incubated with 5 ml of IRDye® (LiCor®) secondary antibody diluted in blocking buffer (Table 2-11) containing 0.1 % Tween-20 for 1 hours shaking. Finally, the membranes were washed three times again with TBST with a final incubation with TBS only.

### **2.14.6 Visualisation and quantification**

Proteins were detected using the Li-Cor® Odyssey® system. This system allows highly accurate quantitative infrared detection of the protein of interest. Quantification of protein abundance was by Image Studio 5.0 software (LiCor®).

### **2.14.7 Stripping**

To re-probe the membrane with more antibodies or optimise antibody concentrations, membranes were incubated with Li-Cor® stripping buffer for 20 minutes at room temperature on an orbital shaker to remove any bound antibodies. After stripping, the membrane is washed three times in TBS before re-imaging to ensure all traces of the antibodies were removed. After which, the membrane would be immunostained as stated previously.

### **2.14.8 Co-immunoprecipitation**

Extracellular RH and chromobody-Halo parasites were harvested, filtered and washed before being resuspended in an actin stabilisation lysis buffer (60 mM PIPES, 25 mM HEPES, 10 mM EDTA, 2 mM MgCl<sub>2</sub>, 125 mM KCl, completed with Pierce™ Protease inhibitor mini-tablets, EDTA Free Thermo Scientific™ and Triton X-100 0.2 %). Lysates were incubated on ice for 1 hour, then incubated

with equilibrated Magne<sup>®</sup> HaloTag<sup>®</sup> Beads (Promega<sup>®</sup>) for 2 hours at 4°C. Beads were washed 5 times with 1 ml of lysis buffer and elution was made using the TEV protease (Promega<sup>®</sup>) as instructed in the manufacturers protocol. For visualisation, a classical western blot was used with antibodies against TgACT1 (Soldati) and processes using Li-Cor<sup>®</sup> Odyssey Clx. Actin intensity ratios between the lysate before purification and the elution were calculated using Li Cor<sup>®</sup> Odyssey Clx for RH and chromobody-Halo. Dr. Simon Gras conducted this study.

## 2.15 Bioinformatics

### 2.15.1 DNA sequencing alignments

DNA plasmid maps were generated using pDRAW, ApE Plasmid Editor or CLC Genomics Workbench 6.5 software. Sequences returned from GATC (chapter 2.11.15) were aligned to the plasmid maps using CLC Genomics Workbench 6.5. The ‘assemble sequences to reference’ tool was used to check the chromatogram of the sequence along with the respective base alignment. If there are queries within the sequence alignment that were present in both forward and reversed sequences, the complementary sequence would be firstly converted to amino acid sequence to determine if it is a synonymous mutation or nonsynonymous mutation. Next, the sequence would be analysed through the Basic Local Alignment Search Tool (BLAST) (Altschul *et al.*, 1990) on NCBI homepage (<http://blast.ncbi.nlm.nih.gov/Blast.cgi>) or ToxoBD (<http://toxodb.org/toxo/>).

### 2.15.2 Data and statistical analysis

Data collected was first analysed in Microsoft Excel to calculate basic analysis such as averages, percentages and means. Data was transferred to GraphPad Prism 6.0 for statistical analysis. When comparing two groups, the *P* value was calculated using an unpaired Student's t-test or a 1-way ANOVA. When comparing multiple groups, the *P* value was determined using a multiple t-test applying the Holm-Sidak method or a two-way ANOVA.

**Table 2-17: Significance rating from GraphPad Prism 6.0**

<i>P</i> Value	Wording	Summary
$\geq 0.05$	Not Significant	ns
$< 0.05$	Significant	*
$< 0.01$	Very significant	**
$< 0.001$	Extremely significant	***
$< 0.0001$	Extremely significant	****

## Chapter 3 Characterisation of a conditional *act1* KO

Actin is involved in many processes in eukaryotes including motility, cell morphology, cell to cell adhesion, protein trafficking and various other functions (Olson & Nordheim, 2010). In Apicomplexa, actin is thought to be essential for parasite motility and invasion (Baum *et al.*, 2008b; Dobrowolski & Sibley, 1996) without playing a major role in intracellular functions, such as replication and organellar biogenesis (Shaw *et al.*, 2000).

Actin is highly dynamic and required for various types of cellular motility (Mitchison & Cramer, 1996; Theriot & Mitchison, 1991). In the case of Apicomplexan parasites, actin is involved in a unique form of substrate dependent movement, termed gliding motility. This type of motility allows the parasites to both locate and invade a host cell. Gliding motility is believed to be centred around an actin-myosin motor complex that is located just beneath the parasites plasma membrane. In this system, the myosin motor moves along short actin filaments and the force generated is transmitted to transmembrane microneme proteins that interact with host cell surface receptors. This results in the rearward translocation of the microneme-substrate complex and the forward motion of the parasites (Keeley & Soldati, 2004; Soldati & Meissner, 2004). Removal of the main components of the motor complex (ACT1, MyoA, MLC1, MIC2, Aldolase, GAP40, 45 and 50) leads to significantly reduced, but not abrogated, motility and host cell invasion. This retained ability to move and invade cannot be explained fully by the current linear motor model (Andenmatten *et al.*, 2012; Egarter *et al.*, 2014). It is possible that the low level of motility and invasion is due to plasticity between genes in the same family, meaning that mutating one gene leads to compensation by another (Frenal & Soldati, 2015). However, unlike the myosins or micronemal proteins, ACT1 is a single copy gene (Dobrowolski *et al.*, 1997), meaning functional complementation by one of the actin-like proteins is highly unlikely. More recently a second study using the *act1* KO suggested that gliding and invasion can still occur due to residual levels of ACT1 remaining in the *act1* KO (Drewry & Sibley, 2015). In addition to the decrease noted in motility and invasion, ACT1

appears to be essential during intracellular replication and egress of the parasite (Egarter *et al.*, 2014).

This project sets out to characterise the *act1* KO in more depth to consolidate the contradicting findings between studies (Drewry & Sibley, 2015; Egarter *et al.*, 2014). Also of interest, the way in which *Toxoplasma* actin polymerises has become a debate with contradicting data defining cooperative (Sahoo *et al.*, 2006) versus isodesmic approaches (Drewry & Sibley, 2015; Skillman *et al.*, 2013). Cooperative assembly of actin predicts that once a critical concentration ( $C_c$ ) is reached, residual amounts of actin are not able to lead to the formation of F-actin meaning once actin drops below this level a complete phenotype would be observed as no F-actin can be formed. In contrast, isodesmic polymerisation does not require a nucleus to initiate polymerisation where all monomer-polymers interact with equal affinity (Smulders *et al.*, 2010). In this instance, no  $C_c$  is needed for polymerisation, and thus even very small levels of actin could fulfil the requirements for the phenotypes. With this contradicting data regarding the polymerisation kinetics of *Toxoplasma* actin, the project aims to demonstrate when actin is undetectable using quantifiable methods and how the down-regulation of ACT1 relates to the phenotypes observed. This genetic approach should provide insight into whether actin polymerises through cooperative or isodesmic assembly.

### 3.1 Analysis of different actin antibodies

Two bodies of work aimed at the study of actin within parasites used similar knockout strategies to remove the *act1* genes (Andenmatten *et al.*, 2012) yet yielded opposing conclusions. Findings focused on the residual concentration of ACT1 at different time points after deletion of the *act1* gene. Each study used different antibodies and techniques to quantify ACT1 levels (Drewry & Sibley, 2015; Egarter *et al.*, 2014). Unfortunately, the Drewry and Sibley study lacked proper controls to exclude cross-reaction of the ACT1 antibody used to quantify actin levels. This appears to be critical, especially since it was previously shown that ACT1 antibodies can cross-react during immunofluorescence analysis (IFA) (Andenmatten *et al.*, 2012).

To test antibody specificity for *Toxoplasma* ACT1, a range of ACT1 antibodies were analysed by both immunoblot and IFA. Using an immunoblot the specificity of the antibodies was tested for *Toxoplasma* versus host cell actin. The actin monomer in both *Toxoplasma* and the mammalian host has an expected size of around 42 kDa. Lysates from both wild-type parasites (RH) and human foreskin fibroblasts (HFFs) were run on an SDS-gel under denaturing conditions. All antibodies that were raised against a particular epitope of apicomplexan ACT1 were specific to the parasite and not host cell actin (Figure 3-1 A). Commercial antibodies tested revealed a band in both the host and parasite actin at the expected size of 42 kDa (Figure 3-1 A).

Next, commercial actin antibodies were tested against *Toxoplasma* ACT1. LoxPAct1 parasites were induced with rapamycin for 4 hours and cultured as described in chapter 2.12.7. Parasite actin was tested for at 4 days post rapamycin treatment. Actin filaments within the parasites were undetectable with phalloidin, supporting previous observations (Poupel *et al.*, 2000). Similarly, antibodies raised against mammalian actin isoforms do not stain TgACT1 within the vacuoles. Similar to the results obtained from our immunoblot, ACTN05(C4) from Abcam was not unique to TgACT1, with a strong signal remaining in the *act1* KO - 4 days post induction - around the periphery of the parasites (Figure 3-1 B). It should be noted that this antibody has been used in previous studies regarding *Toxoplasma* actin on immunoblot and could be detecting both TgACT1 and mammalian actin isoforms (Achanta *et al.*, 2012; Dobrowolski & Sibley, 1996).

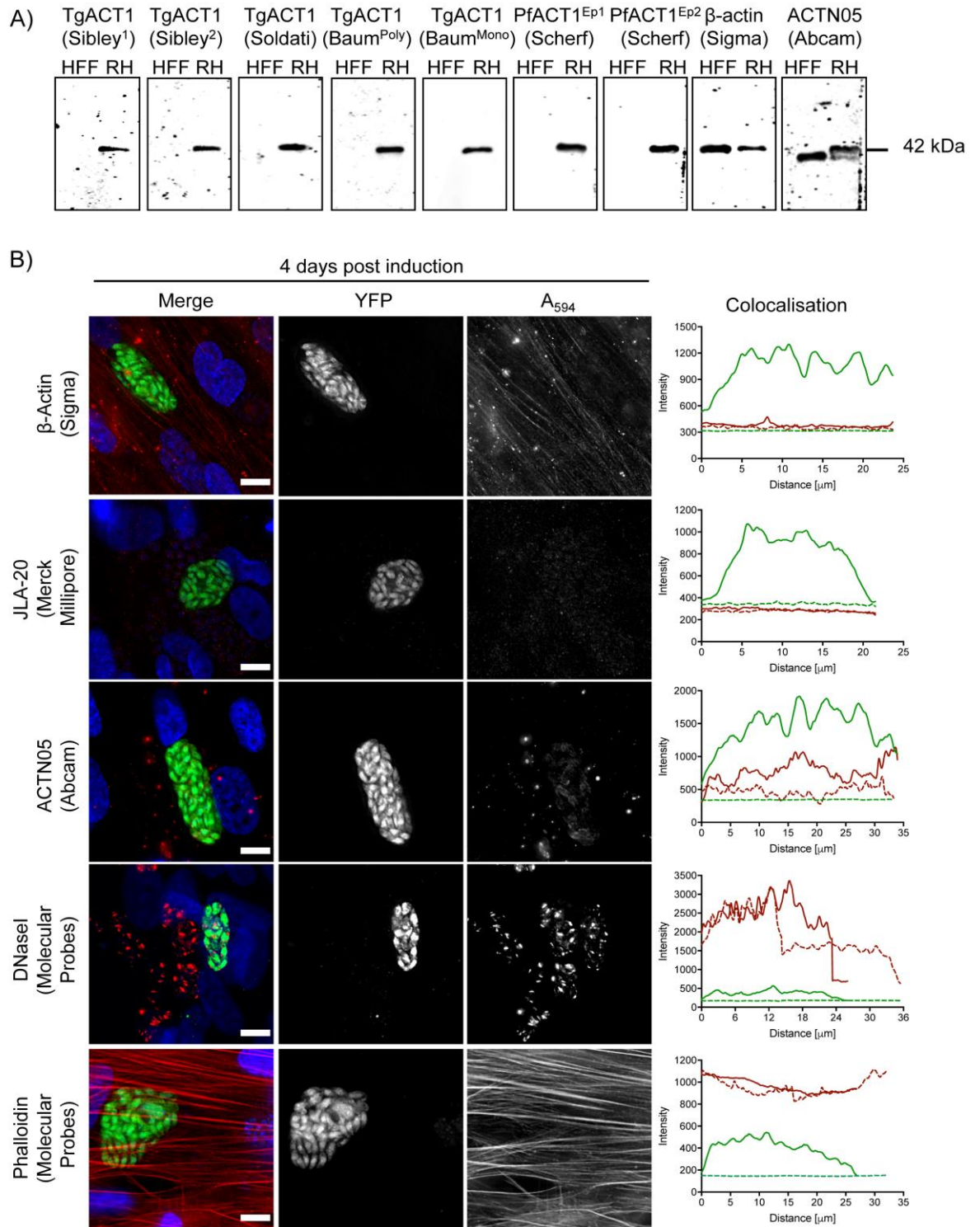


**Figure 3-1: Investigating the specificity of various antibodies for *Toxoplasma* ACT1**

Antibodies raised against actin were analysed for their specificity for either *Toxoplasma gondii* ACT1 via immunofluorescence and immunoblot. Antibodies used were either raised against *Toxoplasma* ACT1, *Plasmodium falciparum* ACT1 or commercially available mammalian actin probes. **A)** Immunoblot to test the ACT1 antibodies for their specificity for TgACT1 compared to host actin. Immunoblots of whole cell lysates from extracellular RH parasites and host cells show all *Toxoplasma* raised antibodies were specific to TgACT1 while the commercially available antibodies bind both human and *Toxoplasma* actin. **B)** Commercially available actin antibodies were tested for their specificity to TgACT1. Most of these antibodies do not react with TgACT1. DNasel appears to cross-react with some apical parasite protein, while the ACTN05 shows a faint signal around the parasites periphery. Scale bars: 10  $\mu$ m. *To the right*, colocalisation of

immunofluorescence signals from an *act1* KO and un-induced LoxPAct1 parasite vacuole. Red lines show the signal detected in the A<sub>594</sub> channel that represents the fluorescence of the ACT1 antibody. Green lines represent the signal detected in the FITC channel, which corresponds to YFP expression of the *act1* KO or background fluorescence of LoxPAct1 parasites. Solid lines represent the *act1* KOs and dashed lines represent the LoxPAct1 vacuoles (found using the DAPI filter).

To analyse the cross-reactivity of the apicomplexan antibodies by IFA, LoxPAct1 parasites were induced for 4 hours with 50 nM rapamycin, washed and continuously cultured (Andenmatten *et al.*, 2012). The *act1* KO was tested at both 4 and 8 days post rapamycin treatment. An assumption was made that no residual actin will be remaining 8 days after *act1* removal when parasites have undergone 4 invasion events and roughly 32 rounds of division (Radke *et al.*, 2001). Parasites were manually lysed and added to coverslips 36 hours prior to fixation and immunostained with various ACT1 antibodies (Figure 3-2 A, B). While all antibodies appear to recognise *Toxoplasma* actin, only 3 showed no cross-reaction at both 4 and 8 days after removal of *act1*. The two antibodies generously supplied by the Sibley lab were not ACT1 specific. Sibley<sup>1</sup> only recognises a protein specific to the apicoplast, while the Sibley<sup>2</sup> antibody used to quantify ACT1 levels in the *act1* KO (Drewry & Sibley, 2015) shows a strong non-specific cross-reaction in the *act1* KO with no difference up to 8 days post excision (Figure 3-2 A, B). However, three antibodies raised against TgACT1 showed a specific signal in wild-type parasites that was absent in the *act1* KO as early as 4 days post rapamycin treatment (Figure 3-2 A, B). This can also be seen in the colocalisation graphs where the red signal in the *act1* KO parasites is similar to the background intensity.





**Figure 3-2: Investigating the specificity of various apicomplexan antibodies against *Toxoplasma* ACT1**

Intracellular *act1* KO parasites were stained using *Toxoplasma* actin antibodies after 4 days (A) and again after 8 days (B). Some “*Toxoplasma* specific” antibodies are highly specific to TgACT1 while others show significant non-specific signal that remains even after 8 days post induction. Scale bars: 10  $\mu$ m. To the right of images, colocalisation of immunofluorescence signals from an *act1* KO and un-induced LoxPAct1 parasite vacuole. This displayed a two-dimensional graph of pixel intensities of a rectangular area of each vacuole. Red lines show the signal detected in the A<sub>594</sub> channel that represents the fluorescence of the ACT1 antibody. Green lines represent the signal detected in the FITC channel, which corresponds to YFP expression of the *act1* KO or background fluorescence of LoxPAct1 parasites. Dashed lines represent the LoxPAct1 vacuoles, while the solid lines represent the *act1* KO vacuoles. The Sibley<sup>1</sup>  $\alpha$ -ACT1 antibody only stains a protein that localises to the apicoplast, also indicated by the sharp peaks in the colocalisation graph. The Sibley<sup>2</sup> antibody significantly cross-reacts even up to 8 days post induction and shows a high intensity signal in the *act1* KO at both time points measured. The two *Plasmodium* ACT1 antibodies are highly cross reactive in *Toxoplasma* and host cells. The epitope1 (Ep1) antibody stains the conoid of the parasites up to 4 days post rapamycin treatment but is absent in the *act1* KO parasites by 8 days post induction. The antibodies provided by the Soldati and Baum labs are specific the most specific for TgACT1 as only a background signal in the A<sub>594</sub> channel is detected in the YFP expressing parasites.

In summary, cross-reactivity occurs with many commercially available actin antibodies when probing for TgACT1 by immunoblot and immunofluorescence. Based on these data, a decision was made to continue with the specific *Toxoplasma* ACT1 antibodies (Figure 3-2) (kindly provided by Dr. Jake Baum and Prof. Dominique Soldati) to quantify ACT1 by immunoblot and IFA.

### 3.2 Down-regulation of ACT1

Recently, the Meissner group published data demonstrating that actin is undetectable after 72 hours post induction in the *act1* KO (Egarter *et al.*, 2014). However, a separate study (using cross-reactive antibodies as described above and Figure 3-2) suggested that residual levels of ACT1 are present in the conditional *act1* KO up to 96 hours post induction (Drewry & Sibley, 2015). To re-address this question, we chose to conduct quantitative immunofluorescence and immunoblot analysis.

For the quantitative immunofluorescence time course analysis, parasites were allowed to invade and replicate for 24 hours in addition to a 12-hour time point, before fixation and staining with the primary TgACT1 antibody provided by Prof. Dominique Soldati (Figure 3-2). The sample was then treated with an AlexaFluor 594 secondary antibody. Images were captured and analysed using CellProfiler software (see chapter 2.13.2), which generates output data based upon the

intensity of the red signal detected, which should correlate to ACT1 expression (Figure 3-3 A).

It was noted that actin levels in wild-type parasites fluctuate over a wide range, but never reach the background (Figure 3-3 A, B). This is likely due to the fact that actin is a major house-keeping gene, with concentrations varying depending on the developmental stage of the parasite (Sebastian *et al.*, 2012). No significant difference was observed in ACT1 levels between RH and the parental LoxPAct1 strains before rapamycin induction. Actin levels within the *act1* KO were measured at 12-hour intervals for 48 hours and then every 24 hours after that (Figure 3-3 A). Actin levels in this parasite line were significantly reduced as early as 12 hours post rapamycin treatment. In the *act1* KO (YFP<sup>+</sup> parasites), a range of ACT1 signal was detected between vacuoles at early time points (up to 36 hours after rapamycin treatment) that overlapped with wild-type ACT1 levels. By 48 hours post induction, the average level of ACT1 detected was close to background (determined with a YFP expressing control strain without the addition of antibodies) (Figure 3-3 A). No significant changes in ACT1 expression were observed after 48 hours, although some vacuoles still had some overlap with wild-type levels, only at the lower expression levels of wild-type cells. In agreement with previous results (Egarter *et al.*, 2014), this method confirmed that ACT1 levels were significantly reduced in YFP<sup>+</sup> parasitophorous vacuoles by 72 hours and by 96 hours post excision actin levels were undetectable (Figure 3-3 A). Importantly, if an ACT1 signal is detected in the *act1* KO after 72 hours, these parasites were then confirmed to be un-induced (as indicated by missing YFP expression) (Figure 3-3 B).

Although not quantified, this clear distinction between the *act1* KO and wild-type parasites was also observed 96 hours post induction using the two other ACT1 antibodies kindly supplied by Dr. Jake Baum (as described above Figure 3-2 B).

As quantitative immunofluorescence analysis can be prone to errors (Waters, 2009), a quantitative immunoblot was conducted to confirm these results. Parasites were induced continually over 4 days. Parasite lysate of all the samples was harvested on the same day. Since contamination with the non-induced population would lead to the detection of ACT1, the *act1* KO parasites

were enriched at 48 and 72-hour time points. Since *act1* KO parasites cannot egress naturally (Egarter *et al.*, 2014), the *act1* KO population could be enriched by incubating the parasites in media containing 2.5 % dextran sulphate. This allows the un-induced (LoxPAct1) parasites to egress and then block their re-invasion. The use of dextran sulfate was used to identify egress mutants by blocking attachment and re-invasion of parasites (Coleman & Gubbels, 2012). However, for the immunoblot, this technique did not work for the 96-hour time point, as there were still significant numbers of un-induced LoxPAct1 parasites in the mix at this time-point leading to ACT1 contamination.

The immunoblot quantification showed that the population of *act1* KOs at 24 and 48 hours post excision has a similar ACT1 expression level to that of wild-type parasites (Figure 3-3 C, D). In line with previous results, there was only a minor signal detectable for ACT1 at 72 hours post-induction. This is significantly reduced from previous time points (Figure 3-3 C) and when quantified, was less than 2 % compared to wild-type (Figure 3-3 D). It could be suggested that this 2 % is from minor contamination of un-induced parasites that weren't eliminated during our enrichment step. These results confirm previous data, and also provide quantification of actin levels throughout the culturing process (Egarter *et al.*, 2014).

In summary, these analyses demonstrate that actin is highly variable within wild-type parasites. More importantly, ACT1 was depleted in the *act1* KO to undetectable levels by both immunofluorescence and immunoblot as early as 72 hours post excision. Based on this quantification, it is proposed that phenotypes obtained at 96 hours post induction reflect the function of actin in the parasite.

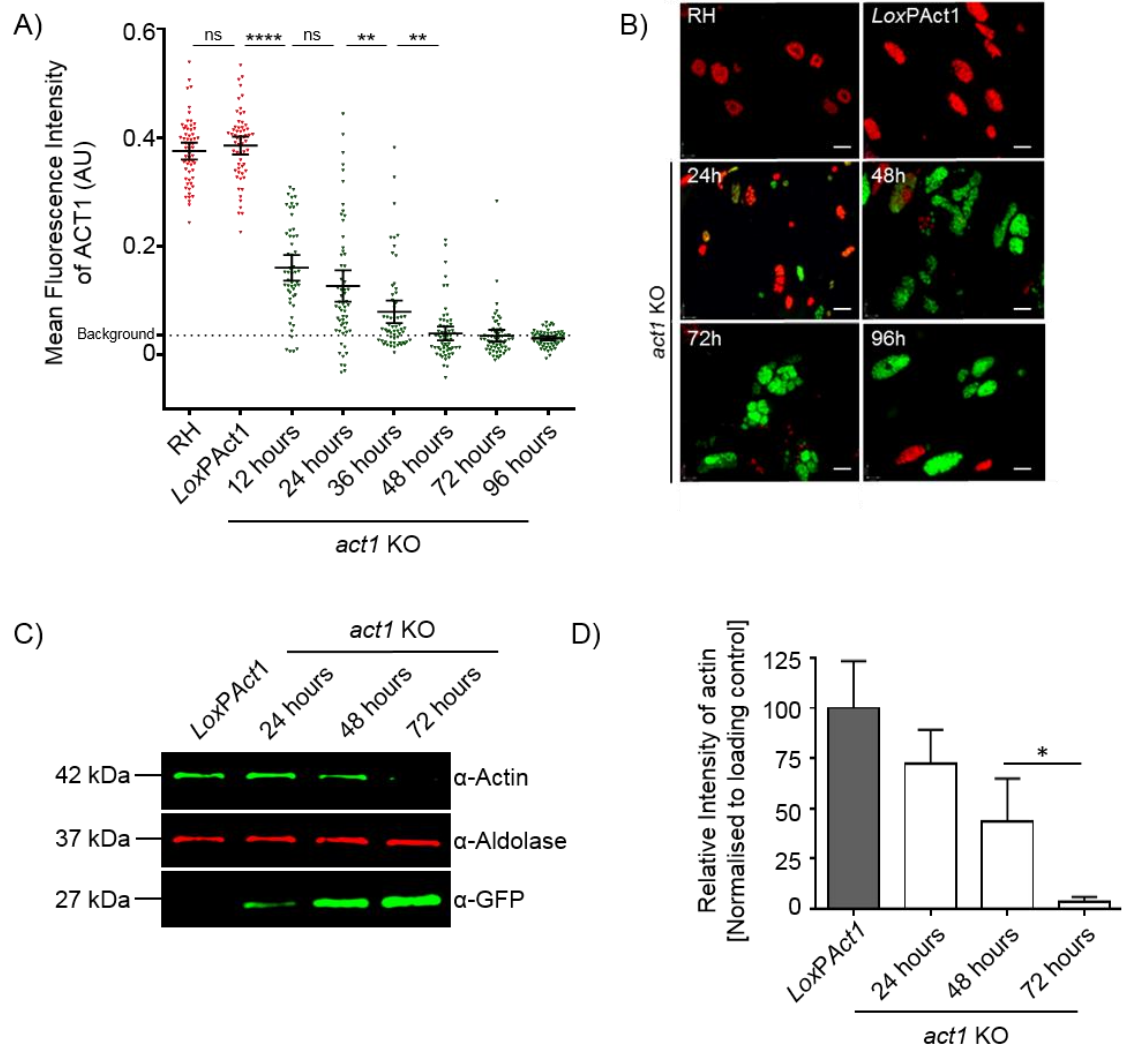


**Figure 3-3: The down-regulation of TgACT1 in the *act1* KO**

Different methods were used to measure the down-regulation of ACT1 after rapamycin induction. **A)** Quantitative immunofluorescence assay (IFA) of actin. Vacuoles were stained with α-ACT1 (Soldati) every 12 hours post induction for 48 hours, and then every 24 hours up to a total of 96. Fluorescence intensity was analysed using CellProfiler software and plotted using the mean. The background was calculated using a YFP<sup>+</sup> parasite strain without antibodies to determine the auto-fluorescence level of host cells. Error bars represent 95 % CI. The dataset was analysed using a two-tailed Student's t-test. \*\*\*\* p < 0.0001, \*\* p < 0.01, non-significant (ns) p > 0.05, n=60 vacuoles. **B)** Representative images of labelled vacuoles used to analyse ACT1 levels over time. After 72 hours, actin was undetectable by IFA in YFP<sup>+</sup> vacuoles. Scale bar: 10 μm. **C)** Western blot analysis of actin protein levels in the *act1* KO over time. Immunoblot was made with parasite lysates taken at 0, 24, 48 and 72 hours post induction. Aldolase was used as a loading control. Expression of YFP upon *act1* excision was checked using α-GFP. **D)** Quantitative measurements of band fluorescence was done using the LiCor Odyssey. The relative levels of ACT1 were normalised using Aldolase (loading control) and then compared against the LoxPAct1 (wild-type control). Error bars represent standard deviation. The datasets were compared using a two-tailed Student's t-test. \* p < 0.05, n=4.

### 3.3 Phenotypic analysis of the *act1* KO in correlation with ACT1 down-regulation

Although significantly hindered, parasites without actin and/or myosin are still capable of moving and invading host cells. Moreover, aspects of the

intracellular replication are completely blocked in the *act1* KO (Egarter *et al.*, 2014). Previous analyses of *act1* KO was conducted at 96 hours post excision when actin was determined to be completely absent (Andenmatten *et al.*, 2012; Egarter *et al.*, 2014). Therefore, we set out to characterise the phenotype(s) of the *act1* KO in more detail at various time points after gene excision. This characterisation will allow the correlation of relative actin levels at specific time points with specific phenotypes. It will also provide an assessment of the critical concentration of actin required to fulfil actins known functions.

During replication, apicoplast instability was one of the severe phenotypes attributed to the *act1* KO (Egarter *et al.*, 2014) resulting in the delayed death of parasites (Fichera & Roos, 1997). We believe this phenotype is one of the main reasons that obtaining a clonal *act1* KO line has proven unsuccessful. Artificial liberation of the *mlc1* KO (with similar characteristics to the *act1* KO but not the apicoplast loss) results in the mixed population culture being maintained for up to 6 weeks (Whitelaw *et al.*, 2017). Of note, at all stages, each wild-type parasite within a vacuole contained an apicoplast. However, as early as 24 hours post induction, apicoplast loss occurs in 50 % of the *act1* KO vacuoles (Figure 3-4 A, C). Moreover, it appears that some of these parasites have undergone up to 3 divisions with many vacuoles not having the correct apicoplast to parasite ratio (1:1) (Figure 3-4 C). This indicates that apicoplast loss had occurred earlier than 24 hours after *act1* loss. Attempts to test this were inconclusive as the majority of the parasites have not begun to express YFP strongly enough to visualise via IFA and the ACT1 signal is still comparable to wild-type. At time points where actin levels are undetectable (72 hours post induction and onwards), no vacuoles had the correct apicoplast to parasite ratio (Figure 3-4 A, C). During this analysis, it was observed that in many *act1* KO vacuoles, the sizes of the apicoplasts appear to be larger than those within wild-type parasites (Figure 3-4 C). Furthermore, it also observed that no vacuoles were completely void of apicoplasts, meaning that at least one apicoplast was detected. Therefore, it is possible that parasites without an apicoplast do not invade or, more likely, do not initiate replication after invasion and die within the host cell.

Parasites egress from the host after a signal to permeabilise both the parasitophorous vacuole membrane and the host cell membrane (Arrizabalaga &

Boothroyd, 2004). In the case of the *act1* KO, parasites are unable to egress, both naturally and after ionophore induction, from the host cell (Egarter *et al.*, 2014). This phenotype was also observed in wild-type parasites upon addition of cytochalasin D (Black *et al.*, 2000). To test egress in the *act1* KO, parasites were incubated for 36 hours in host cells to allow the formation of large vacuoles. Parasites were artificially induced with a calcium ionophore for 5 minutes, and then fixed and stained with  $\alpha$ -SAG1 under non-permeabilising conditions. Therefore, only lysed parasites would be labelled with the SAG1 antibody, allowing the visualisation of vacuoles that have ruptured the membrane and escaped (Figure 3-4 D). Inducing egress for 5 minutes in wild-type parasites caused rupture and completed dissemination of over 95 % of vacuoles. An additional 3 % of vacuoles had permeabilised the vacuole, but had not initiated motility out of the cell (Figure 3-4 B). When testing the *act1* KO, at early points (36 hours post induction) only around 20 % were able to completely egress, while 75 % of the remaining vacuoles had permeabilised the membranes without initiating motility (Figure 3-4 B). At later time points, when actin is not detectable (72-96 hours post induction) full egress was as low as 8 % or completely blocked, respectively (Figure 3-4 B). At these time points the ability to permeabilise the PV membrane is significantly reduced (Figure 3-4 D). Finally, at 96 hours post induction, egress is completely blocked in the *act1* KO, reproducing data from Egarter *et al.* (2014) (Figure 3-4 B).

In summary, both apicoplast maintenance and parasite egress are dependent on ACT1. These phenotypes are observed even when high levels of ACT1 are still detectable (taken from Figure 3-3). One could speculate that a similar effect would be seen for other phenotypes of the *act1* KO. Next, the gliding motility and invasion in the *act1* KO at various time points over the course of 96 hours was analysed. Previously, it was published that the *act1* KO can still glide and invade even when actin is not detectable (Egarter *et al.*, 2014). Interestingly, Drewry and Sibley also observed this finding, but they attributed this lasting motility and invasion to residual actin levels within the *act1* KO parasites (Drewry & Sibley, 2015).

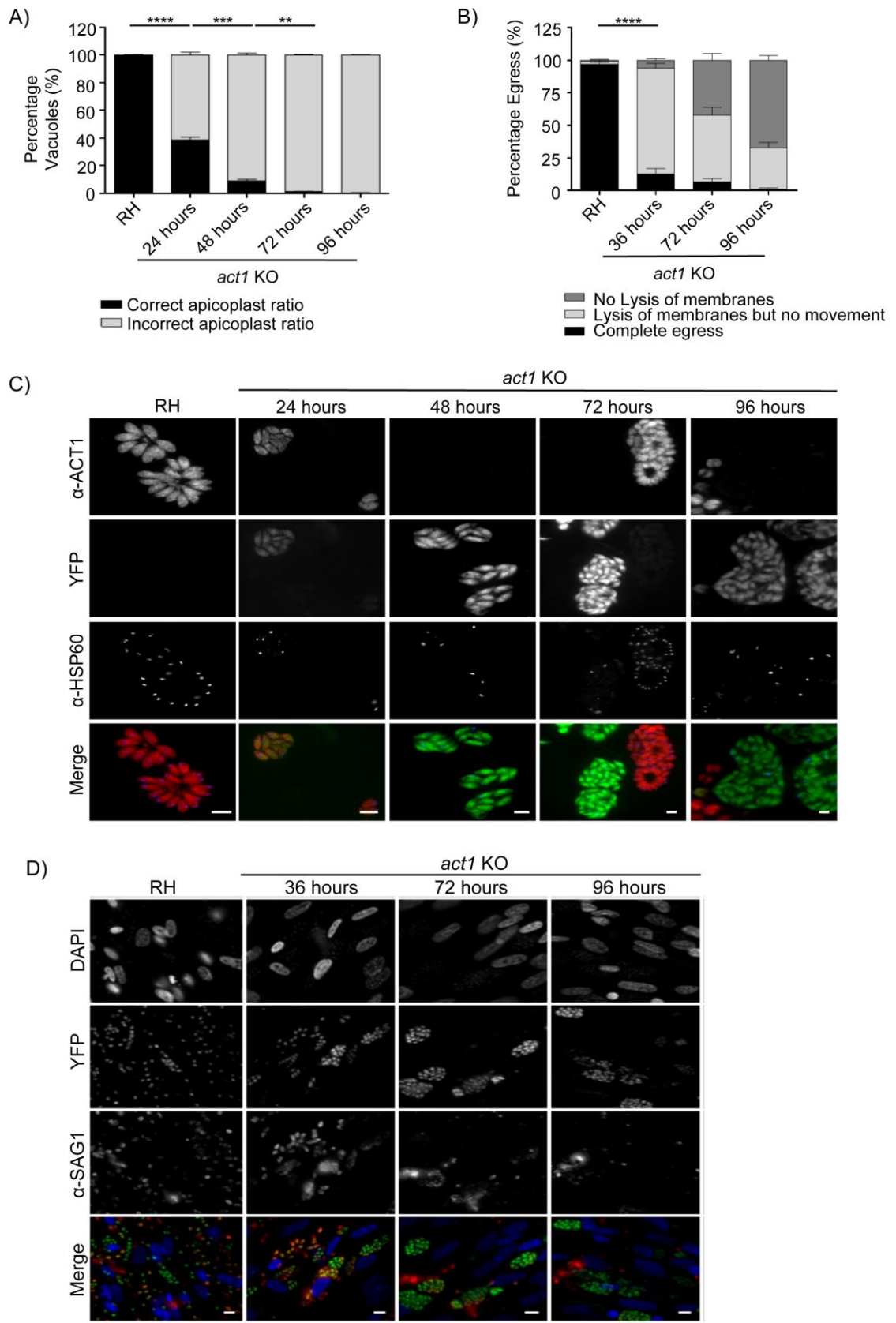


**Figure 3-4: Actin is essential for apicoplast division and egress**

Analysing the phenotypes for apicoplast loss and egress in the *act1* KO post rapamycin treatment. **A)** Quantification of apicoplast loss in the *act1* KO. The ratio of apicoplast to parasites within the vacuoles was quantified at 24-hour intervals after *act1* removal. Vacuoles were stained with  $\alpha$ -ACT1 (Soldati) and  $\alpha$ -HSP60 (Sheiner). Apicoplast loss is observed as early as 24 hours post excision in around 50 % of the vacuoles. Error bars represent  $\pm$  S.E.M. **B)** Artificial egress was induced in the *act1* KO at time points 36, 72, and 96 hours post excision. Three conditions were

considered: lysed and moved away from the vacuole (complete egress), lysis of the membranes without the release of parasites, and no lysis of the PVM or host membranes. Complete egress is mostly blocked by 36 hours and lysis of membranes is mostly blocked by 96 hours. Error bars represent  $\pm$  S.E.M. **C)** Representative images used to score the apicoplast loss assay. Note, at early time points, there are still high levels of ACT1 while some parasites within the vacuole do not contain an apicoplast. Scale bar: 10  $\mu$ m. **D)** Representative images of induced egress in *act1* KO parasites over time. *act1* KO parasites at later time points are unable to lyse the membranes, as determined by the lack of SAG1 staining within the vacuoles. Scale bar: 100  $\mu$ m. All experiments were performed in biological triplicate and compared with a two-tailed Student's t-test, \*\*\*\*  $p < 0.0001$ , \*\*\*  $p < 0.001$ , \*\*  $p < 0.01$ .

When comparing motility and invasion capabilities of the *act1* KO and wild-type parasites, both phenotypes decreased by around 50 % as early as 24 hours post rapamycin treatment (Figure 3-5 A, B). Unexpectedly, the phenotypes for both gliding motility and invasion did not change after 48 hours (though these were only analysed up to 96 hours) post induction (Figure 3-5 A, B). This concludes that ACT1 is still highly important for both gliding motility and invasion. To ensure that the 20 % of parasites were indeed *act1* KO parasites we analysed levels of ACT1 by immunofluorescence. This was important as we assume we have a homogeneous *act1* KO population that is YFP+, however the fact that only 20 % actually form trails and invade is still unknown and intriguing. It was observed that ACT1 antibodies appear to cross-react with  $\alpha$ -SAG1. This cross-reaction meant that trail deposition analysis would be inconclusive. Subsequently, we analysed invasion using  $\alpha$ -GRA7 as a marker for PV formation (Mercier *et al.*, 2005). Parasites were stained for GRA7 one hour after invasion and green fluorescent parasites (indicative of knockouts) with no detectable ACT1 signal (Figure 3-5 C). Therefore, we demonstrate that *act1* KO parasites are capable of invasion without any detectable actin.

Taken together, these results confirm previous findings (Egarter *et al.*, 2014) that ACT1 is essential for apicoplast division and egress, while important (but not essential) for motility and invasion. It may be that trail formation and invasion may have ACT1 independent mechanisms, which will be discussed later in Chapter 6. Whereas, high ACT1 levels appear to be required the maintenance of the apicoplast as slight changes cause drastic perturbations in apicoplast stability during division. In each vacuole, around 10-20 % of *act1* KO parasites still contain an apicoplast. Interestingly, this is the average rate by which the *act1* KO can still glide and invade. Therefore, it could be inferred that retention of the apicoplast is required for effective invasion and thus survival, as each each replicating vacuole always has at least one apicoplast. Moreover, these

data strongly suggest that once actin is below a critical concentration the phenotypes observed for the *act1* KO do not significantly change, even after further depletion of actin, supporting cooperative polymerisation kinetics.

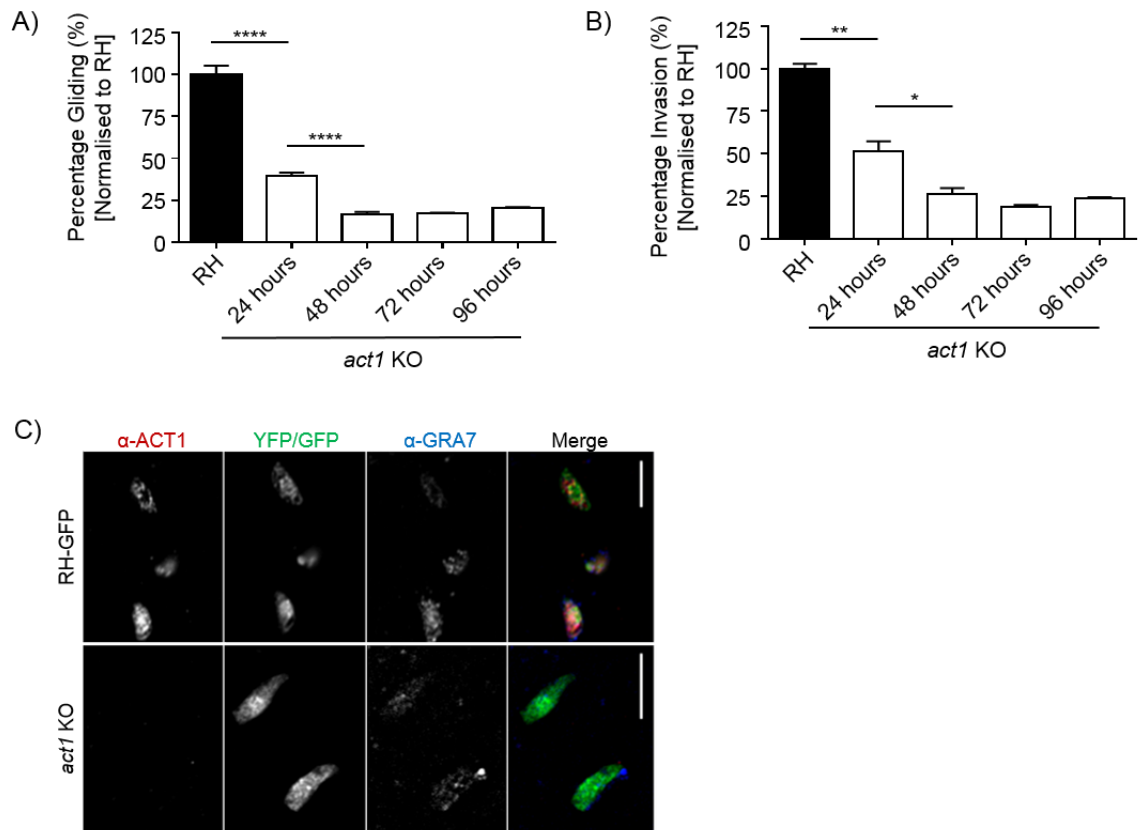


**Figure 3-5: Phenotypes for gliding and invasion established 48 hours post induction**

Characterising the ability of the *act1* KO to deposit trails and invade at various time points after *act1* excision. **A)** Trail deposition assay where the *act1* KO parasites glide across an FBS-coated coverslip and are stained with  $\alpha$ -SAG1. The number of trails observed dropped significantly after *act1* excision (24 hours). The gliding phenotype does not significantly change after 48 hours up to 96 hours. Error bars represent  $\pm$  S.E.M. **B)** Invasion of the *act1* KO at 24 hour time points after *act1* excision. Invasion rates drop significantly by 24 hours, but the phenotype remains constant after 48 hours. Error bars represent  $\pm$  S.E.M. All experiments were performed in biological triplicate and compared with a two-tailed Student's t-test, \*\*\*\*  $p < 0.0001$ , \*\*  $p < 0.01$ , \*  $p < 0.05$ . **C)** Invasion without actin. *act1* KO parasites invade without ACT1 and form a PV with GRA7. Scale bar: 5  $\mu$ m.

### 3.4 Kinetics of gliding motility and invasion

The characterisation of motility and invasion of *Toxoplasma* predominantly relies on end-point trail deposition and invasion assays. These have proved highly valuable, however, they reveal little information about the dynamics of these processes. To analyse the kinetics of motility we exploit the fact that wild-type parasites can move over a 2D-substrate coated with FBS in three distinct types of motility: circular, helical, and twirling (Hakansson *et al.*, 1999). During circular

gliding, the parasite lies on its right side and moves in a counter-clockwise motion at average speeds of 1-1.5  $\mu\text{m/s}$ . Parasites can also be observed twirling, where the parasite uprights itself on its posterior end and begins to spin in a clockwise fashion. During helical motions, parasites propel themselves forward across the substrate in a horizontal twirling movement that results in forward displacement. During this motion, they can move at speeds ranging from 1-3  $\mu\text{m/s}$  (Hakansson *et al.*, 1999). More recently a novel corkscrew-like motility profile was shown in a 3D matrix with speeds ranging from 0.5-2  $\mu\text{m/s}$  (Leung *et al.*, 2014a).

As previously described, static assays for gliding and invasion show that the *act1* KO remains capable of movement across a substrate by gliding motility and also invasion into host cells (Egarter *et al.*, 2014). With this in mind, it should be possible to visualise motility and invasion in real-time. Time-lapse video microscopy was used to understand the kinetics of gliding and invasion for the *act1* KO at 96 hours post induction when there should be no actin remaining in the parasites.

For motile parasites, images were captured at one frame per second under fluorescent conditions ( $A_{594}$  for RH expressing KillerRed or FITC for the *act1* KO). As expected, both RH and the *act1* KO were observed using each of the three motility profiles described above (Supp. Movies appendix 1-4). Using the ImageJ cell tracking software, wrMTrck (Silva *et al.*, 2011), individual parasites that moved in either helical or circular trails were analysed with an aim towards identifying their speed and distance travelled. Twirling parasites were excluded from this analysis as the tracking software cannot distinguish and calculate the tight clockwise movement accurately. Of the *act1* KO parasites that move, the kinetic analysis revealed that overall they were not different in speed or distance travelled compared to wild-type (Figure 3-6). When comparing the movements of wild-type parasites, it was observed that RH could move in helical motions better than circular. This is seen for both speeds ( $1.01 \pm 0.24 \mu\text{m/s}$  for helical and  $0.76 \pm 0.17 \mu\text{m/s}$  for circular) and distance travelled ( $55.08 \pm 10.98 \mu\text{m}$  for helical and  $41.47 \pm 9.92 \mu\text{m}$  and circular) (Figure 3-6 A). This contrasts with the *act1* KO where the knockout parasites travel faster in a circular motion than helical ( $1.19 \pm 0.35 \mu\text{m/s}$  and  $0.86 \pm 0.21 \mu\text{m/s}$  respectively) (Figure 3-6 A). This supports the observations from static trail assays where mutants for the

acto-myosin motor complex were predominantly observed leaving behind circular SAG1 deposits (Egarter *et al.*, 2014). Moreover, *act1* KO parasites were able to move faster than RH in circular motions ( $1.19 \pm 0.35 \mu\text{m/s}$  *act1* KO and  $0.76 \pm 0.17 \mu\text{m/s}$  RH) but travel a shorter distance overall ( $36.82 \pm 14.27 \mu\text{m}$  *act1* KO and  $41.47 \pm 9.92 \mu\text{m}$  RH) (Figure 3-6 A). Intriguingly, live imaging of the *act1* KO highlighted movements and trails comparable to wild-type, while static trail assays of the *act1* KO only form half circles (Egarter *et al.*, 2014). This discrepancy could suggest that the *act1* KO parasites do not shed their membrane as efficiently as wild-type, thus leaving behind fewer trails. This could infer an attachment defect or proteolysis defect in the *act1* KO parasites.

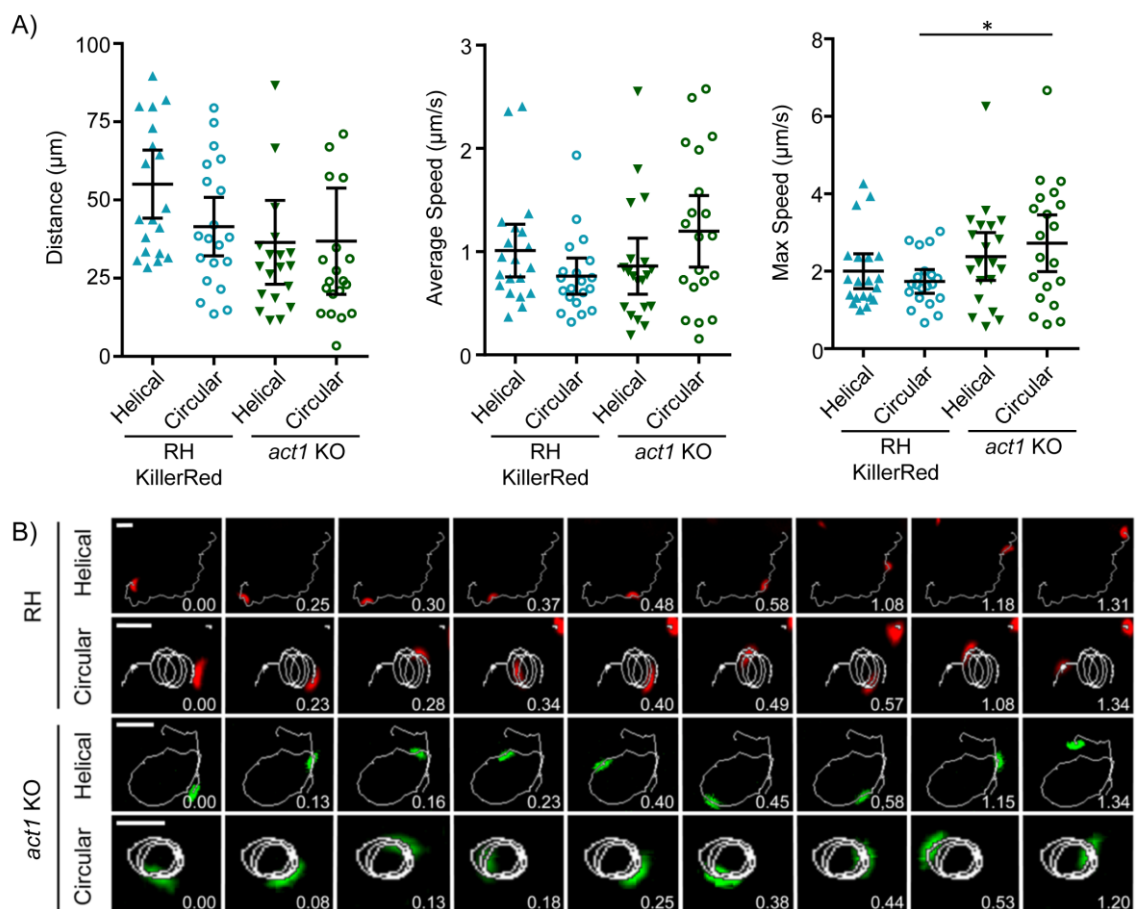


**Figure 3-6: 2D gliding kinetics of the *act1* KO**

Real-time imaging of wild-type and *act1* KO parasites for their ability to glide on an FBS substrate. Parasites were tracked with Fiji wrMTrck software for their distance covered (A), average (B) and maximal speeds (C). RH, on the whole, are more proficient in helical gliding whereas the *act1* KOs can complete much better circular motions. *Act1* KO parasites can glide at similar, even slightly higher speeds than RH. Error bars represent  $\pm 95\%$  CI.  $n=20$  for each movement. The datasets were compared with a One-way ANOVA followed by Tukey's post hoc test, \*  $p<0.05$ . D) Representative images of the parasite and the track analysed by the wrMTrck software (see Supp. Movies appendix 1-4 for movements). Scale bar:  $5 \mu\text{m}$ . Time stamp: m:ss

Next, the *act1* KO motility was assessed in an assay more suited to physiological conditions to determine if this movement could be compared to the 2D results. Our collaborators Prof. Gary Ward and Dr. Jacqueline Leung performed all the 3D motility experiments and analysis. The percentage of *act1* KO parasites moving through a 3D matrix is significantly reduced compared to wild-type (Figure 3-7 A, C) but comparable with the percentage seen in the trail deposition assays (Figure 3-5 A, Figure 3-7 A). Speeds generated by the *act1* KO are similar to wild-type (Figure 3-7 E, F), while the distance covered is significantly reduced (Figure 3-7 D) (Whitelaw *et al.*, 2017). When looking at the instantaneous speed of the *act1* KO and wild-type parasites, it was observed that they show very different profiles (Figure 3-7 B). Wild-type parasites appear to move in a biphasic fast/slow motion, while the *act1* KO moves slower but more continuous over the analysed period. These motility profiles indicate that we were specifically looking at the *act1* KO parasites within the matrix and not the LoxPAct1 uninduced parasites. Therefore, observations seen in 2D and 3D are comparable for the *act1* KO and this demonstrates that the parasites are capable of generating forces for movement in the absence of actin (Whitelaw *et al.*, 2017).

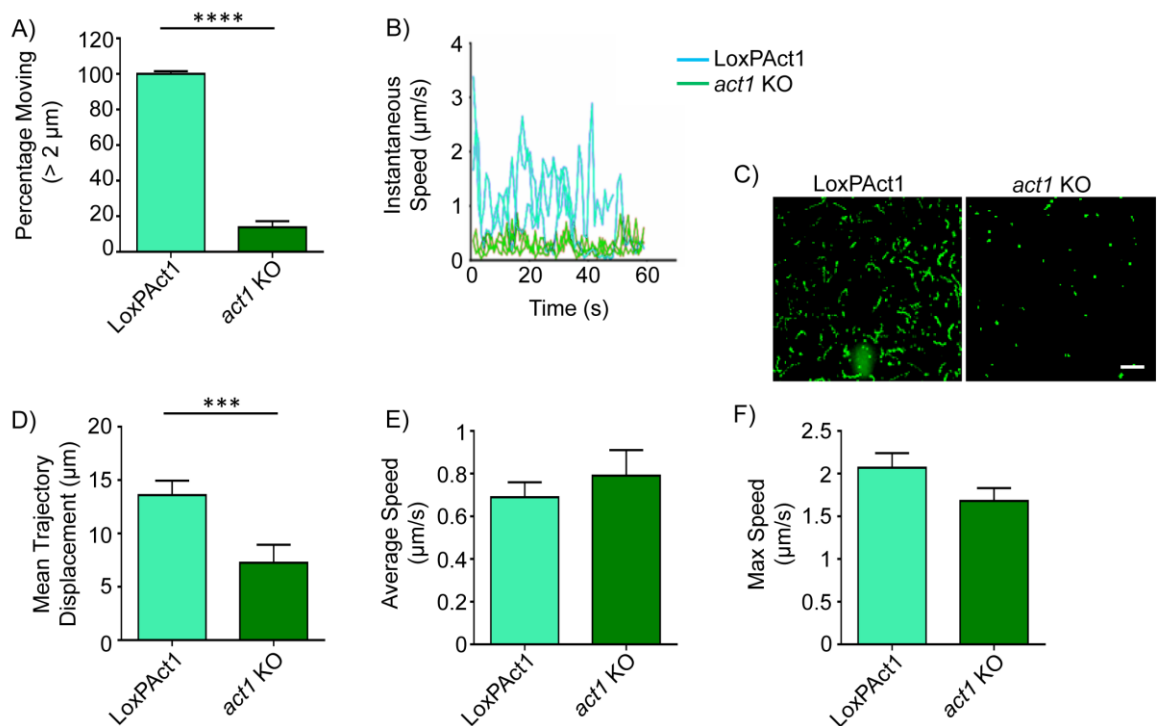


**Figure 3-7: 3D motility profiles of the *act1* KO**

The *act1* KO parasites were analysed for their motility profiles through a 3D matrix by our collaborators Prof. Gary Ward and Dr. Jacqueline Leung. **A)** The percentage of parasites that

move greater than 2  $\mu\text{m}$ . The *act1* KO is significantly reduced in numbers moving. **B)** The instantaneous speed of the parasites shows two different populations. The *act1* KO parasites do not have fast bursts as seen in the parental strains. From this, we can confirm that we analyse the *act1* KOs and not the residual WT parasites. **C)** Representative maximum intensity projection of the matrix. LoxPA*act1* parasites form many corkscrew shaped trails, while the *act1* KO show few. Scale bar: 50  $\mu\text{m}$ . **D)** The mean trajectory displacement shows the *act1* KO to cover significantly less distance than the LoxPA*act1* strain. There is no significant difference in **(E)** average speeds or **(F)** maximal speeds between the two strains. Error bars represent  $\pm$  S.E.M. Datasets were compared by two-way ANOVA with Sidak's multiple comparisons test, \*\*\*\*  $p < 0.0001$ , \*\*\*  $p < 0.001$ , non-significance was determined with  $p > 0.05$ .

During invasion, parasites attach to the host and re-orientate at their apical end before penetrating through a tight junction and residing within the parasitophorous vacuole (Carruthers & Boothroyd, 2007). Wild-type parasites complete this process in 15 to 30 seconds without any membrane ruffling of the host (Suss-Toby *et al.*, 1996).

Similar to gliding motility, once ACT1 is below a critical concentration, the rate of invasion remains constant for the *act1* KO (Figure 3-5 B). To understand the penetration kinetics, images were captured at one frame/second using phase contrast microscopy. For the *act1* KO, a final FITC image was taken to determine if any of the invaded parasites were YFP<sup>+</sup>, which is indicative of *act1* KO population. In line with published data, the controls (RH and LoxPA*act1*) penetrated the cell within 30 seconds (Kafsack *et al.*, 2007) (Figure 3-8 A, B, Supp. Movies appendix 5, 6). Analysis of the *act1* KO highlighted the fact that the penetration speeds of these parasites are highly variable (Figure 3-8 A). As we predicted, some *act1* KO parasites were very slow invaders, taking from 3 to 11 minutes to complete entry. Curiously, the slowest invading *act1* KO parasite appears to penetrate only half of its body length into the host, after which the parasite begins to pull the host cell membrane around itself to complete invasion (Figure 3-8 B, Supp. Movie appendix 7). At this point, it is unclear if this membrane wrapping is parasite or host cell driven. Similar observations were described for the *myoA* KO (Bichet *et al.*, 2016b), where host cell membrane is wrapped around parasites during invasion. This is also similar to the zippering mechanism described for *Cryptosporidium* (Meissner *et al.*, 2013). Then there were the “intermediate invaders”, which take just over one minute to invade (Figure 3-8 A). Unexpectedly, half of *act1* KO parasites analysed invaded at speeds comparable to wild-type (~30 seconds) (Figure 3-8 A, B, Supp. Movie appendix 8). This distribution of invasion speeds is similar to the *mlc1* KO (Whitelaw *et al.*, 2017) but faster than the *myoA* KO (Egarter *et al.*, 2014).

In summary, only around 20 % of *act1* KO parasites are capable of gliding and/or invading. Surprisingly, of the percentage that moved, these parasites can move with a speed similar to wild-type. Moreover, the *act1* KO is significantly impaired in the distance it can travel, suggesting that the force produced is not continuous. Many *act1* KO parasites can penetrate at speeds comparable to wild-type, but overall show an extensive range of penetrating speeds. It would be interesting to see if these fast invading parasites have retained their apicoplast compared to the slower invaders. These results suggest that parasites can produce forces required for motility and invasion in the absence of actin or myosin. However, as most parasites fail to initiate motility, this lead us to believe it is an ‘all-or-nothing’ response. We, therefore, speculate that the molecular function of the acto-myosin-system might be distinct from merely force production.

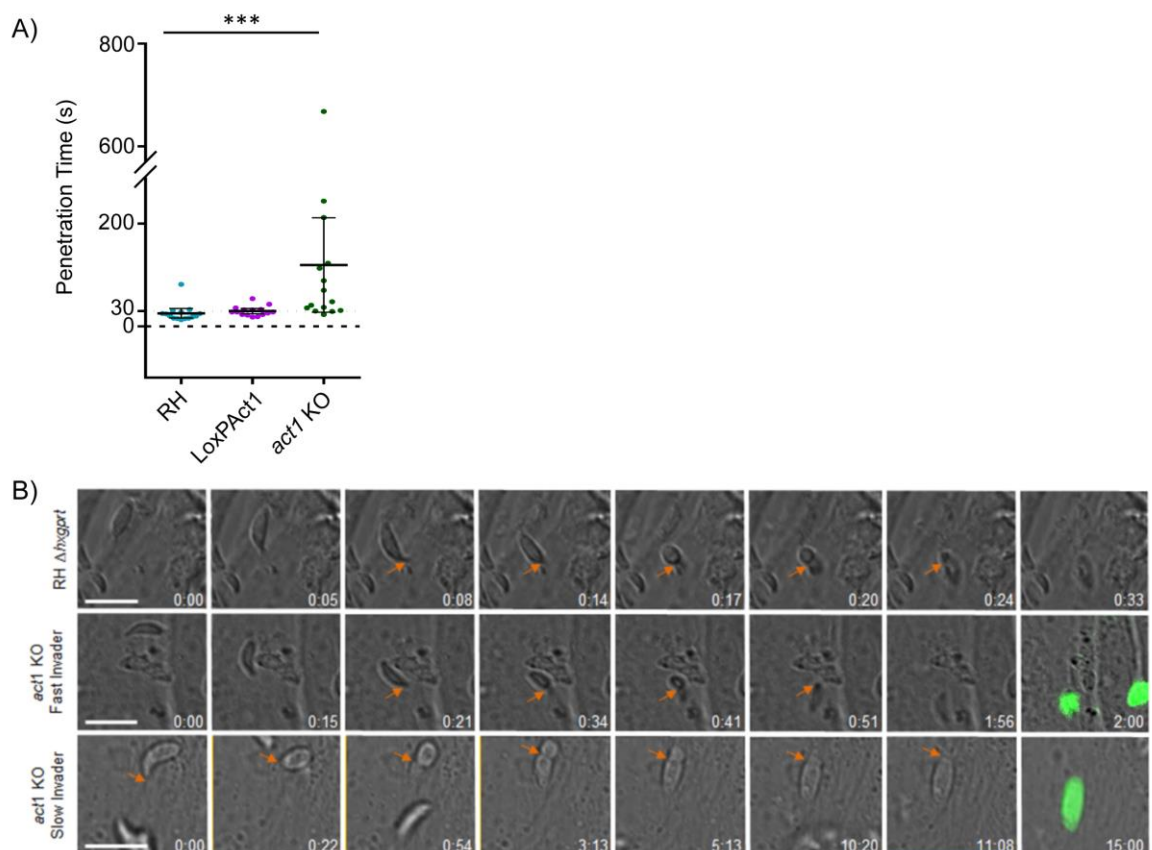


**Figure 3-8: Penetration kinetics of the *act1* KO**

The amount of time needed to invade (from tight junction formation to closure of the vacuole) was analysed for individual parasites. **A)** On average both RH and LoxPAct1 controls invade within 30 seconds as reported in the literature. The *act1* KO parasites penetrate with highly variable speeds. Some can invade at speeds similar to controls while another subset invades much more slowly. Error bars represent  $\pm$  95 % CI.  $n=15$  independent invasion events, compared with a two-tailed Student's t-test, \*\*\*  $p<0.001$ . **B)** Stills of parasite penetration. Orange arrows indicate the tight junction throughout penetration. Final FITC images (indicative of YFP expression) show a fast and slow *act1* KO penetrating a host cell. Scale bars: 10  $\mu$ m. Time stamp, m:ss.

### 3.5 ACT1 is involved in regulating attachment sites

A pre-requisite for both motility and invasion is the ability of the parasite to attach to the surface of a host cell. Surface antigens (SAGs), always present at the parasites surface and allow the parasites to attach to a substrate before being cleaved as the parasites progress forward (Mineo & Kasper, 1994). More intimate attachment is achieved by regulated secretion of micronemal proteins secreted, such as MIC2, which is thought to be the major adhesion for *T. gondii* (Huynh *et al.*, 2003; Rabenau *et al.*, 2001). It is suggested that MIC2 directly links to the acto-myosin motor complex through an unknown linker protein, previously thought to be aldolase (Meissner *et al.*, 2013; Shen & Sibley, 2014; Starnes *et al.*, 2009).

Assays to study the attachment properties of parasites to date are not well defined. The attachment was previously analysed through a red/green invasion assay, where parasites that have not invaded are counted as attached (Huynh *et al.*, 2003). More recently, tachyzoite adhesion was tested through the use of microfluidics creating flow conditions similar to that of physiological shear stress (Harker *et al.*, 2014), allowing a more direct measurement of adhesion strength. To this end, Dr. Gurman Pall adapted a shear stress assay similar to the one described in Harker *et al.* (2014) to study the dynamics of attachment. Parasites were left to attach to a Collagen VI coated Ibidi chamber and subsequently flow was passed through the chamber creating a shear stress. As in Harker (2016), an initial wash step under very low flow conditions was used to wash away weak/unattached parasites. After which, a shear stress was applied to the chamber with increasing flow rates up to 15 dyn/cm<sup>2</sup>. This was in line with the approximate mean arterial shear stress levels (Papaioannou & Stefanadi, 2005). Although this assay reproduces physiological conditions that the parasites experience, it still has a couple of limitations. Most notably in the justification of what is attached and how long they have been attached. As it is a closed microfluidics chamber, parasites that detach from the entry point of liquid may indeed re-attach somewhere down the chamber. In this instance, while parasites are washed away, new parasites may form an attachment and stay firmly bound to the collagen substrate for the duration of the experiment and what is attached is subjective. To overcome this, multiple images can be

analysed from the same chamber and averaged but with this one cannot determine if the parasite has been washed off and again moved into the new field of view. However, at this time, this is the best representation of attachment strengths and has been used throughout this thesis. With this assay, Dr. Gurman Pall analysed the mutants of the motor complex for their respective attachment strengths (Figure 3-9). Results demonstrated that the *act1* KO has a severe attachment phenotype (Whitelaw *et al.*, 2017). When analysing the *mic2* KO, it was found that the *act1* KO was more impaired in attachment than the *mic2* KO (Figure 3-9). On the other hand, the *myoA* KO appears to have similar attachment strengths to wild-type parasites (Figure 3-9) (Whitelaw *et al.*, 2017). As with motility and invasion kinetics, the *act1* KO behaves similarly to the *mlc1* KO in its attachment strengths (Whitelaw *et al.*, 2017).

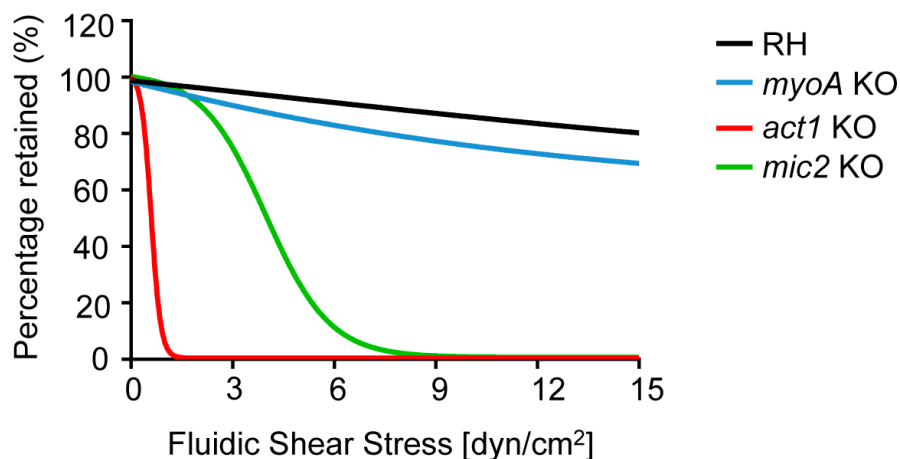


**Figure 3-9: Attachment of motor complex mutants under shear stress**

Trend line graph evaluating the attachment strengths of the *mic2* KO, *myoA* KO and *act1* KO. A shear stress was applied to the chamber with a fluidic pump to wash parasites away. The percentage retained is highlighted in the graph. RH and *myoA* KO have similar strong attachment strengths. The *mic2* KO has a weaker attachment as expected with MIC2 being a major adhesive molecule. *act1* KO parasites have the weakest attachment strength of the tested parasites. Experiments performed by Dr. Gurman Pall.

Together, this demonstrates an important role of the acto-myosin system for efficient attachment to the surface and suggests a function in the regulated turnover of attachment sites, as suggested by Munter *et al.* (2009). It is tempting to speculate that ACT1 and MyoA act as regulators of attachment sites, therefore acting as a molecular clutch to transfer the force generated by ACT1-independent mechanisms to the surface (Case & Waterman, 2015).

## 3.6 Ultrastructure and trafficking in the *act1* KO

In many organisms, actin is involved in the cytoskeletal stability of the cell (Charras & Briehner, 2016). Whereas, in *Toxoplasma*, the structure is maintained by microtubules (Morrisette *et al.*, 1997). In a previous study, extracellular *act1* KO parasites appeared morphologically aberrant at the basal end (Egarter *et al.*, 2014). We, therefore, wished to examine basal complex (Figure 3-10).

### 3.6.1 Shape of the *act1* KO

To analyse the ultrastructure of the *act1* KO, the parasites were processed for scanning electron microscopy (SEM) processing. Immunofluorescence analysis suggested the parasites have a flattened basal end (Figure 3-10 B). The SEM analysis (processed by Dr. Leandro Lemgruber) highlighted that the basal end is not completely flat but more concave (Figure 3-10 A, B, red arrows). It was hypothesised that ACT1 might play a major role during the final stages of endodyogeny, leading to incomplete IMC formation. To test this, *act1* KO parasites were inoculated onto HFFs and allowed to replicate. After fixation, the parasites were stained with  $\alpha$ -IMC1 to find parasites at the end point of division. While early stages of replication appeared relatively normal, at the end of division *act1* KO parasites formed a larger than normal residual body, indicating a defect in the recycling of mother cell material (Figure 3-10 A, white arrows). From this, it is hypothesised that the *act1* KO parasites appear flattened at the basal pole due to an IMC recycling defect (Periz *et al.*, 2017). This flattened appearance of parasites is more pronounced in extracellular parasites (Figure 3-10 B), also observed in a TgUNC1 knockout (Damien Jacot, MPM 2016 abstract). Using the  $\alpha$ -IMC antibody, it was also observed that many *act1* KO parasites replicated asynchronously compared to wild-type cells. This meant that on many occasions the vacuoles had atypical numbers of parasites within it. This also indicates a role for actin for synchronously controlling replication throughout the whole vacuole. Furthermore, it was found that *act1* KO parasites have a highly ruffled membrane, as seen by SEM (Figure 3-10), which might suggest defects of the cortical actin cytoskeleton. Similar observations have also been described for a *Plasmodium falciparum act1* KO (unpublished data from Dr. Sujaan Das).

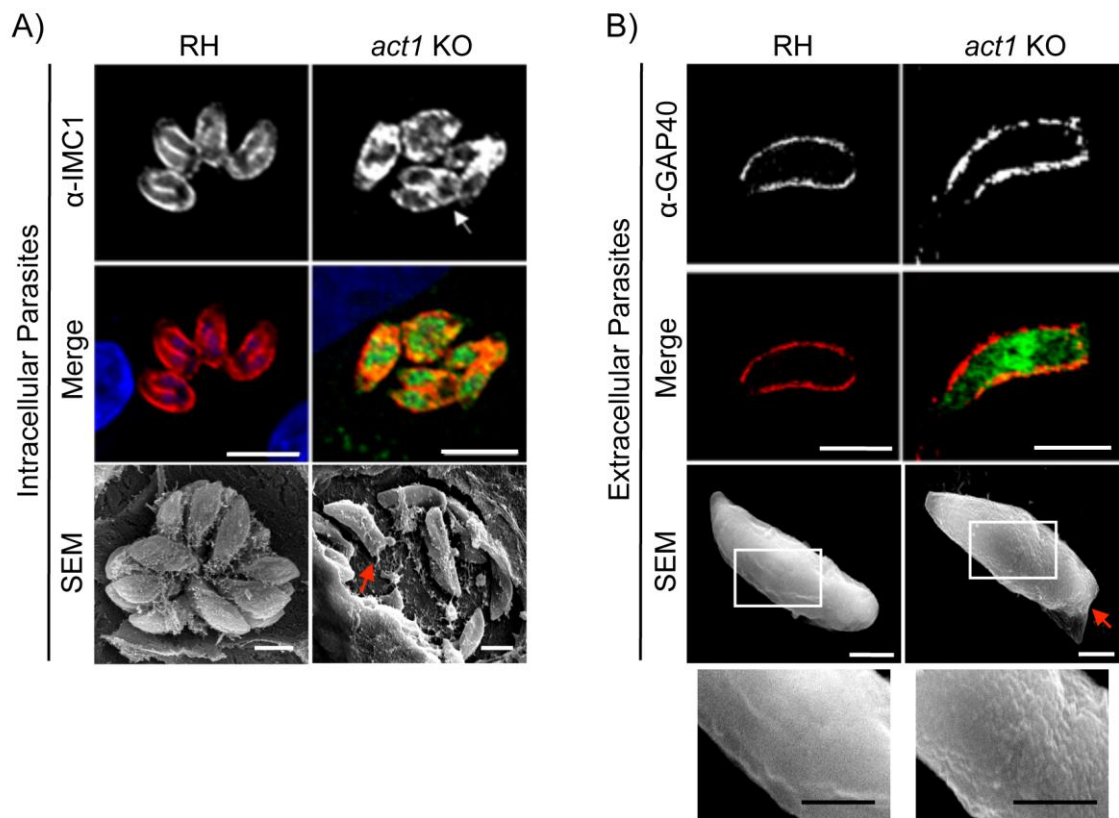


**Figure 3-10: Ultrastructure of the *act1* KO**

Intracellular and extracellular parasites were analysed by both fluorescence imaging and scanning electron microscopy (SEM). **A)** Intracellular parasites were stained with  $\alpha$ -IMC1 to visualise parasites and daughters during cell division. White arrow highlights the residual body and IMC recycling in the *act1* KO. Scale bar: 10  $\mu$ m. The SEM highlighted a disorderly vacuole and a flattened basal end of *act1* KO parasites (red arrows). Scale bar: 2  $\mu$ m. **B)** Extracellular parasites were stained with  $\alpha$ -GAP40, a marker for the IMC. This highlights a similar localisation between RH and the *act1* KO parasites, where the *act1* KO parasites have a flattened posterior end. Scale bar: 5  $\mu$ m. The SEM shows a sort of concave basal complex in the *act1* KO (red arrow). Zoomed area highlights *act1* KO parasites have a much more ruffled membrane compared to RH. Scale bar: 2  $\mu$ m. Electron microscopy images provided by Dr. Leandro Lemgruber.

Transmission electron microscopy of the *act1* KO highlighted the exclusion of the apicoplast while all other organelles appear to be located in their expected location, *i.e.* the rhoptries and micronemes at the apical end (Egarter *et al.*, 2014). However, we wished to find out if the proteins required for gliding and invasion are transported to the appropriate organelles since actin has recently been demonstrated to be involved in dense granule trafficking (Heaslip *et al.*, 2016).

### 3.6.2 Motor complex formation

We wished to determine if the assembly of the ‘glideosome’ complex located just beneath the plasma membrane is affected in the absence of ACT1. Briefly, the ‘glideosome’ consists of the myosin motor connected to the inner membrane

complex (IMC1) through the myosin light chain 1 (MLC1). Embedded within the IMC are the glideosome-associated proteins (GAP), with GAP45 acting as the connector between the IMC and plasma membrane and GAP40 located throughout the IMC. By using a selection of antibodies against different components of the motor complex, we checked for the location of MLC1, IMC1, GAP40 and GAP45 (Figure 3-11). Unfortunately, we do not have a working antibody against MyoA for immunofluorescence so  $\alpha$ -MLC1 was used as a representation. Analysis of the 'glideosome' complex showed that this is positioned correctly in the *act1* KO (Figure 3-11), however the staining pattern of GAP40 appears more uneven compared to the smooth depiction of wild-type parasites. Overall, this suggests that reduced gliding and invasion is not due to the loss of other components of the motor complex. It would appear that the formation of the glideosome is on the whole unaffected by the recycling defect of the IMC during late stages of development. Next, we wished to analyse some other key proteins derived from the micronemes and rhoptries involved in gliding motility and invasion.

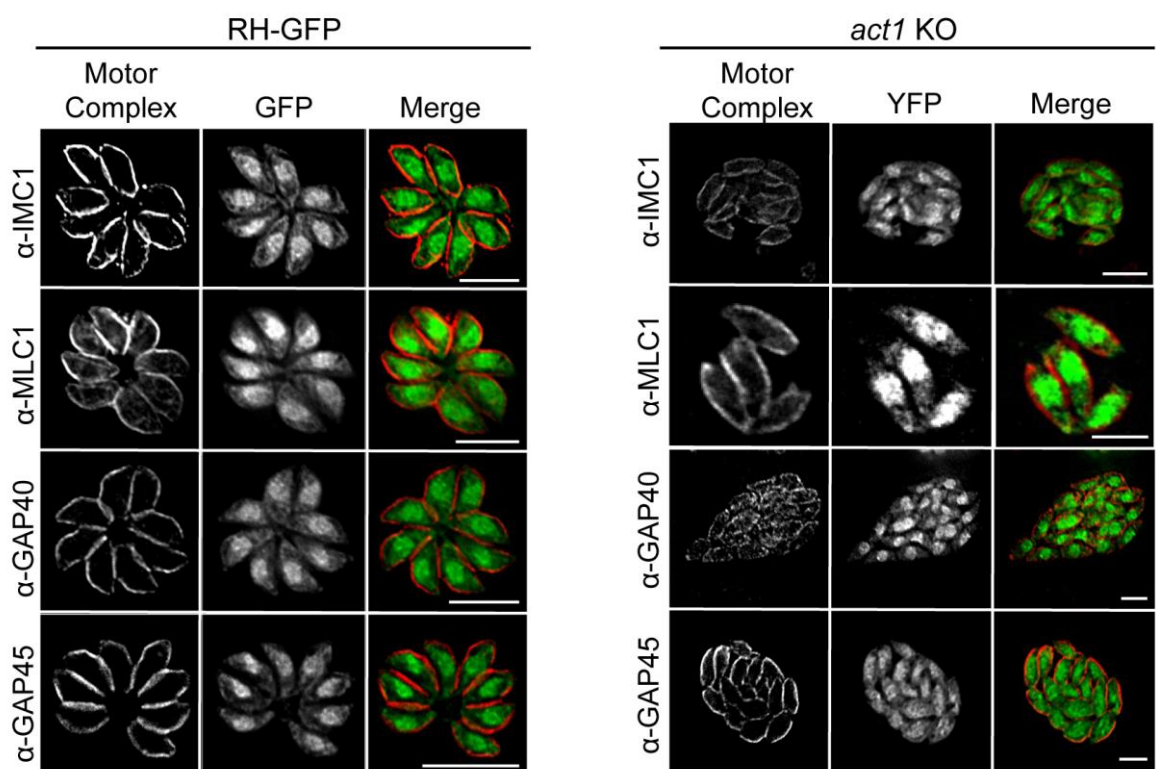


**Figure 3-11: Glideosome components localise normally under the plasma membrane**

*Act1* KO parasites were fixed after 96 hours and stained with antibodies for components of the glideosome. Loss of ACT1 has no impact on the glideosome formation. Glideosome associated proteins (GAP40 and 45) localise to the IMC. As a representation to MyoA, the MLC1 localisation is also unaffected. Scale bar: 10  $\mu$ m.

### 3.6.3 Trafficking of specialised secretory proteins in the *act1* KO

As the *act1* KO is deficient in both gliding and invasion, it is possible that trafficking of the specialised secretory proteins (micronemes and rhoptries), which are key determinants for gliding and invasion, is affected (Carruthers *et al.*, 1999). To test this, different micronemal proteins were analysed using specific antibodies against, AMA1, MIC2, and MIC3. MIC2 binds to a wide variety of surface proteins presented by the host (Brossier *et al.*, 2003; Huynh & Carruthers, 2006) and AMA1 binds the RON complex at the tight junction during invasion (Besteiro *et al.*, 2009; Srinivasan *et al.*, 2011). The IFAs suggest that while both AMA1 and MIC3 localise as expected to the apical region, MIC2 mislocalises in many of the *act1* KO parasites (Figure 3-12 A). MIC2 accumulates at the periphery of the parasite, the basal end (Figure 3-12 A, white arrows), and in some cases close to the nucleus, suggesting trafficking defects for MIC2. This would have to be followed up in more detail. Unfortunately, initial immuno-EM experiments of the *act1* KO with  $\alpha$ -MIC2 were unsuccessful. Overall, ACT1 may have a role in trafficking of MIC2 to the micronemes and as one of the parasites major adhesive components might be a cause of the defect in the attachment.

*Toxoplasma* ARO was shown to interact with MyoF to traffic and tether the rhoptries to the apical end in an acto-myosin dependent manner (Mueller *et al.*, 2013). Therefore, we wished to understand if the rhoptry proteins were targeted properly. Rhoptry proteins (ROPs) 1, 2 and 4 were analysed and found to localised normally at the apical end (Figure 3-12 B). However, a signal was also observed at the basal region/residual body of some parasites (Figure 3-12 B, yellow arrows). This could suggest that while the rhoptry organelles are normally tethered to the apical end, the absence of ACT1 caused some mislocalisation of rhoptry proteins, suggesting a role of ACT1 in directed vesicular transport of ROPs.

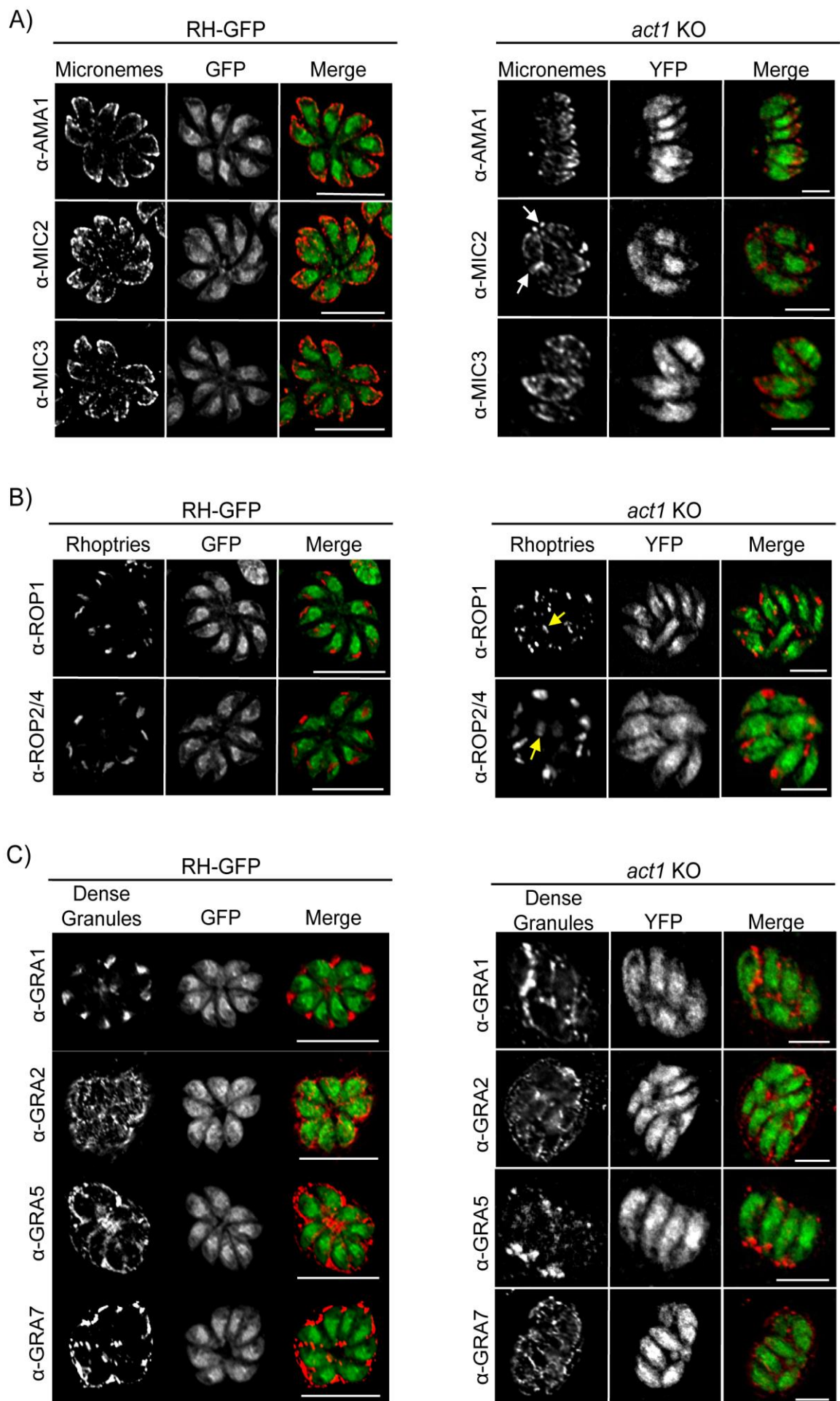


**Figure 3-12: Localisation of the secretory organelles in the *act1* KO**

After 96 hours post rapamycin treatment, *act1* KO parasites were fixed and stained with antibodies against various specialised secretory proteins. **A)** Trafficking of MIC proteins to the micronemes. Loss of ACT1 causes a mislocalisation of MIC2 but has little/no impact on other microneme proteins analysed. White arrows highlight MIC2 at the basal end of the parasites. **B)** Localisation of rhoptry proteins in the *act1* KO. ACT1 is involved in correct apical trafficking of rhoptry proteins, with many seen in the posterior end or residual body of the parasites. Yellow arrows show rhoptry proteins at the basal end/residual body of the parasites. **C)** Dense granules secretion into the PV is not dependent on ACT1. Scale bar: 10  $\mu$ m.

**3.6.4 Dense granule secretion into the PV is an actin-independent process**

A recent study highlighted that other specialised secreted proteins, specifically dense granules, move along actin filaments within the parasites (Heaslip *et al.*, 2016). After invasion, dense granules are secreted into the newly forming PV to assist in building and maintenance of the PV during replication (Mercier *et al.*, 2005). With this recent study in mind, we also wished to see if the dense granules are transported into, and continually modulating the PV during intracellular growth of the *act1* KO. Dense granules are secreted to various locations within the PV. Therefore, the formation of the PV membrane was analysed with  $\alpha$ -GRA5 and 7, the tubulovesicular network (TVN) with  $\alpha$ -Gra2 and the vacuolar space with  $\alpha$ -Gra1 (Mercier & Cesbron-Delauw, 2015) (Figure 3-12 C). Although actin is thought to be essential for dense granule trafficking within the parasites (Heaslip *et al.*, 2016), after secretion, the GRA proteins analysed appear to localise within the vacuole, indicating no secretion defect. This would lead us to believe that ACT1 is important for intra-parasite movement of GRAs only and secretion into the PV is ACT1 independent.

**3.6.5 Actin is essential for apicoplast division but not the mitochondria**

With the exception of *Cryptosporidium spp.*, apicomplexan parasites possess two endosymbiotic organelles, the apicoplast and mitochondria (Lim & McFadden, 2010; Zhu *et al.*, 2000). The apicoplast is a product derived from the secondary endosymbiosis of an alga and an auxotrophic eukaryote (Vaishnava & Striepen, 2006). Through the evolution of the parasite, it has become an essential organelle required for fatty acid biosynthesis, isoprenoid and heme synthesis as well as iron-sulphur clustering (Lim & McFadden, 2010; Waller & McFadden, 2005). Loss of the apicoplast leads to a delayed death of the parasites (Egarter

*et al.*, 2014; Fichera & Roos, 1997; Jacot *et al.*, 2013; Mehta & Sibley, 2011). Due to apicoplast inheritance defects in the *act1* KO (Figure 3-13), we wished to look at the other endosymbiotic organelle, the mitochondria. It was thought that since the mitochondrial organisation is mediated by actin cables in budding yeast (Drubin *et al.*, 1993) it might have an analogous role in *Toxoplasma*. Anti-TOM40 (Sheiner) binds to the mitochondrial outer membrane and was used to check for the presence of the mitochondrion (Figure 3-13). In general, the mitochondrion forms a “lasso-like” structure within the parasite around the nucleus (Nishi *et al.*, 2008). The structures of the mitochondria seen, in general, were open and “lasso-like”. However, some were also observed to have flattened mitochondria (Figure 3-13). Therefore, ACT1 appears to have no essential role in mitochondrial dynamics in *Toxoplasma* and might mainly require the microtubules, similar to *Dictyostelium* (Woods *et al.*, 2016). However, at this point, we cannot exclude a role of ACT1 in tethering of mitochondria to the IMC to keep the ‘lasso’ shape open. Future experiments need to be performed to analyse this in more detail.

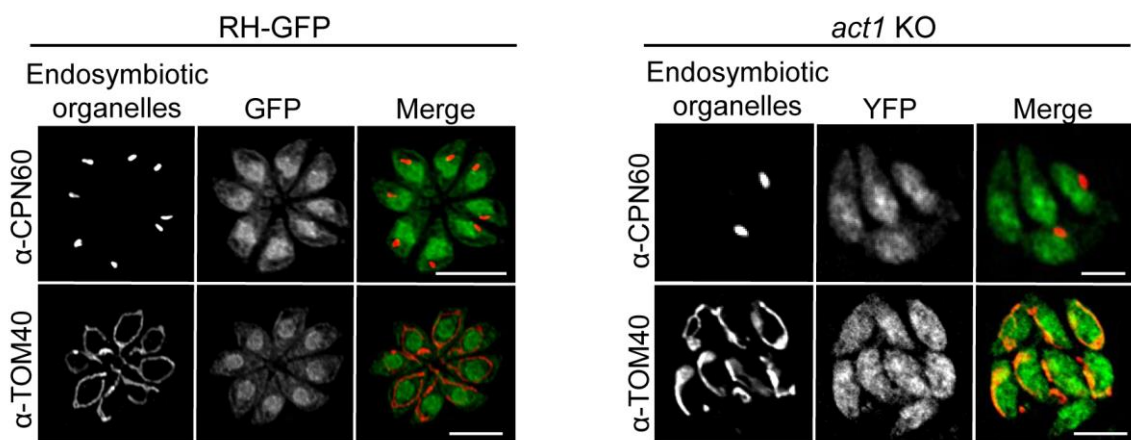


**Figure 3-13: Actin is required for apicoplast division but not the mitochondria**

Division of the endosymbiotic organelles in the absence of ACT1. The loss of ACT1 has no impact on mitochondrial segregation as seen with  $\alpha$ -TOM40. Additionally, the apicoplast phenotype was confirmed with apicoplast marker CPN60. Scale bar: 10  $\mu$ m.

Together these results suggest that ACT1 is essential for apicoplast division and that biogenesis or replication of other organelles is not directly affected by the loss of ACT1. However, it appears that ACT1 may be involved in accurate trafficking of subsets of secretory proteins to their apical organelles. New scanning EM images provide more insights into the loss of the basal complex, which we predict is due to a defect of recycling from the mother cell.

Moreover, the SEM highlights a membrane ruffling on the *act1* KO not observed in wild-type, but the reasons behind this are still unclear.

### 3.7 Summary and conclusion

Recently, many components of the acto-myosin motor complex have been dissected and thoroughly characterised. Many key components have been described as no longer essential for motility and invasion (Andenmatten *et al.*, 2012; Egarter *et al.*, 2014; Shen & Sibley, 2014), while some are more important for structural stability (Harding *et al.*, 2016) rather than motility. One key component of the motor complex is actin, a single copy gene in *Toxoplasma* (Dobrowolski *et al.*, 1997). The conditional *act1* KO was developed to understand the functions of the acto-myosin motor complex. However, recently the exact functions of TgACT1 have come under intense scrutiny and doubt within the field (summarised in Table 3-1).

In summary, this chapter has demonstrated that there is a critical concentration of ACT1 required to fulfil the essential roles for ACT1. As previously stated, actin has a pivotal role in intracellular replication for apicoplast division and priming the parasites for egress (Egarter *et al.*, 2014). Importantly, I show that apicoplast loss and egress is blocked very soon after *act1* removal even when there is still detectable ACT1 protein remaining. Furthermore, ACT1 may have a role in signalling egress as it is unable to lyse the vacuole, a prerequisite step before movement out of the cell. Although the signal may be to initiate motility as perforin alone might not be sufficient for parasite release (Kafsack *et al.*, 2009). Actin was proposed to have essential functions during the extracellular stages of the parasites lytic lifecycle (Dobrowolski & Sibley, 1996). However, as previously shown, actin was important but remarkably not essential for motility or invasion (Egarter *et al.*, 2014). Here, data is provided that there is indeed critical concentrations of actin required for motility and invasion and thus reject the suggested (isodesmic) polymerisation process of apicomplexan actin. This critical concentration occurs even when levels of actin are relatively high within the cell. After which, the phenotypes remain constant. This indicates that even if there is residual actin remaining, once the G-actin level is below the critical concentration, no F-actin can be formed. Therefore, it is predicted that even if there is still minute (undetectable) levels of ACT1 in the *act1* KO at 96 hours

post induction, the phenotypes will not be enhanced. Furthermore, kinematic studies of the *act1* KO reveals these parasites can move and penetrate as well as wild-type, and these processes are more of an ‘all or nothing’ (either normal or completely blocked). A novel role for actin during the parasites attachment to the substrate has been shown. The reduced attachment could be linked with 1) the mislocalisation of MIC2, 2) a highly ruffled membrane or 3) ACT1 is involved in the formation of attachment sites through a ‘molecular clutch’ mechanism. In this instance, we lean towards a role of the acto-myosin system acting as a molecular clutch, allowing the parasite to transmit the force to the surface, which will be later discussed in chapter 6. If parasites can attach, they move normally. However, if the attachment is in any way perturbed they appear completely paralysed in 2D trail deposition but this may also be an effect of inefficient shedding of their surface membranes.

**Table 3-1: Summary of data presented in this thesis compared to published literature.**

<i>act1</i> KO at 96 hours post rapamycin induction	Egarter <i>et al.</i> (2014) <i>PLoS ONE</i>	Drewry and Sibley (2015) <i>MBio</i>	Whitelaw <i>et al.</i> (2017) <i>BMC Biology</i> *
ACT1 level	Non-detectable by IFA & WB	Significant ACT1 still present by qIFA	Non-detectable by qIFA & qWB
Gliding motility (%)	10 †	~ 25 †	22 †
Invasion (%)	10 †	30-fold defect	25 †
Intracellular growth	Slower †	ND	ND
Egress (%)	2 †	5 †	0 †

† - Data normalised to wild-type

\* - Data also presented in this thesis

IFA - immunofluorescence analysis, qIFA - quantitative IFA

WB - Western blot, qWB - quantitative WB

ND - Not defined in this study

## Chapter 4 The effects of actin-modulating drugs on *Toxoplasma gondii*

Actin has a vast range of cellular processes (Olson & Nordheim, 2010). To control these processes, the cell tightly regulates the actin dynamics to respond rapidly to various stimuli (Welch & Mullins, 2002). Actin-modulating drugs have been employed extensively across all species with these drugs controlling the dynamics either by enhancing polymerisation or depolymerisation of actin filaments, through a variety of mechanisms.

Drugs that target actin and affect its polymerisation kinetics are predominantly derived from bacteria, fungi or marine-sponges (Kustermans *et al.*, 2008). All of these compounds share a common structural feature, where the primary hydrophobic core is associated with stereochemically complex side groups. These drug compounds are separated according to their influence on actin. Drugs such as phallotoxins and jasplakinolides can stabilise or induce actin polymerisation (Visegrady *et al.*, 2005). Whereas, there are those that destabilise filaments or inhibit the assembly of filaments, such as cytochalasins or latrunculins (Coue *et al.*, 1987; Goddette & Frieden, 1986).

While there have been no *in vivo* observations of F-actin within the parasites, actin disrupting drugs have been used extensively in Apicomplexa to highlight its importance during the lifecycle. Here we wish to investigate the effect actin disrupting drugs have on the motile and invasive *T. gondii* tachyzoites.

### 4.1 Cytochalasin D has an off-target effect

The fungal metabolite, Cytochalasin D (CD) modulates actin dynamics by capping the barbed ends of actin filaments and has been used for many years studying the dynamics of actin (Peterson & Mitchison, 2002). The addition of CD results in slow depolymerisation of actin filaments by capping the barbed ends of F-actin (Goddette & Frieden, 1986). Cytochalasin D has been used predominantly to study the dynamics of actin in Apicomplexa (Dobrowolski *et al.*, 1997; Drewry & Sibley, 2015; Gonzalez *et al.*, 2009; Rynning & Remington, 1978). Its use during the *Toxoplasma* lytic lifecycle has highlighted that CD affects the parasites in a dose-dependent manner. Cytochalasin D was shown to reduce motility and

invasion rates (Dobrowolski & Sibley, 1996; Drewry & Sibley, 2015; Rynning & Remington, 1978), cause enlarged residual bodies during replication (Shaw *et al.*, 2000) and slow egress (Black *et al.*, 2000). However, unpublished results from the Meissner lab lead us to question the specificity of CD on *Toxoplasma* actin. While it was shown that other cytochalasins have off-target effects, CD is thought to be highly specific (Foissner & Wasteneys, 2007). We noticed that both the *act1* KO and the CytD resistant (CytD<sup>r</sup>) mutant described in Dobrowolski and Sibley (1996) became sensitive to CD at increasing concentrations. Indeed, an off-target effect of CD was inferred in Dobrowolski and Sibley (1996). They succeeded to isolate three clones resistant to CD, however, after sequencing the actin gene in these mutants, only two had the mutation Ala 136 Gly (Figure 4-1 C), while the third had no mutation in the actin gene (Dobrowolski & Sibley, 1996).

#### 4.1.1 Generation of an inducible Cytochalasin D resistant ACT1 knockout line

To evaluate the effect of CD has on parasite actin, an inducible *act1* geneswap vector was generated where the endogenous actin was replaced with a LoxP-flanked copy of *act1* containing the Ala 136 Gly mutation, conferring resistance to CD (Dobrowolski & Sibley, 1996). This allowed the expression of a CD resistant actin that can be excised in a DiCre-dependent manner. Consequently, any protein that remains after *act1* removal is supposed to be resistant to CD.

The *act1* genomic sequence with the mutation GCT → GGT at positions 407 was synthesised by GenScript and provided it in a pUC57 vector. The cDNA of *act1* from the original geneswap vector described in Andenmatten *et al.* (2012) was digested using *Xma*I and *Pac*I and replaced with the resistant cDNA using the same enzymes. The plasmid was then linearised using *Ap*aI and transfected into the RH DiCreΔ*Ku80*Δ*HX* strain (Figure 4-1 A), selecting with Xan and MPA (Donald *et al.*, 1996). Single clones were isolated and tested for *act1* excision and YFP expression after rapamycin treatment (Figure 4-1).

To confirm that the plasmid had integrated correctly, genomic DNA was isolated and analysed for its integration into the expected locus of the genome (Figure 4-1 B). Using site-specific primers for the *act1* gene (1→1'), endogenous *act1* of

the parental strains yielded products of ~1.5 kb whereas both the LoxPAct1 and *act1* KO stains, where the endogenous *act1* had been replaced with *act1* cDNA, yielded products of ~1.1 kb. Thus indicating that the endogenous *act1* was replaced by the geneswap plasmid (Figure 4-1B). Since PCR is highly sensitive, the band present in the *act1* KO lane is most likely due to un-induced contamination in the sample since the rapamycin induction is not 100 % efficient. When we tested for 5' UTR integration and Cre-mediated recombination (2→2'), no signal was detected in the untransfected controls whereas two different sized bands were seen between the LoxPAct1 and *act1* KO parasites (3.3 kb and 2.1 kb respectively) (Figure 4-1 B). This size shift represents that *act1* was excised in the *act1* KO population. A third PCR to check 3' UTR integration (3→3') showed a 2.9 kb band only in the transfected lines. Therefore, double homologous recombination had occurred, replacing the endogenous *act1* with one conferring CD resistance (Figure 4-1 B).

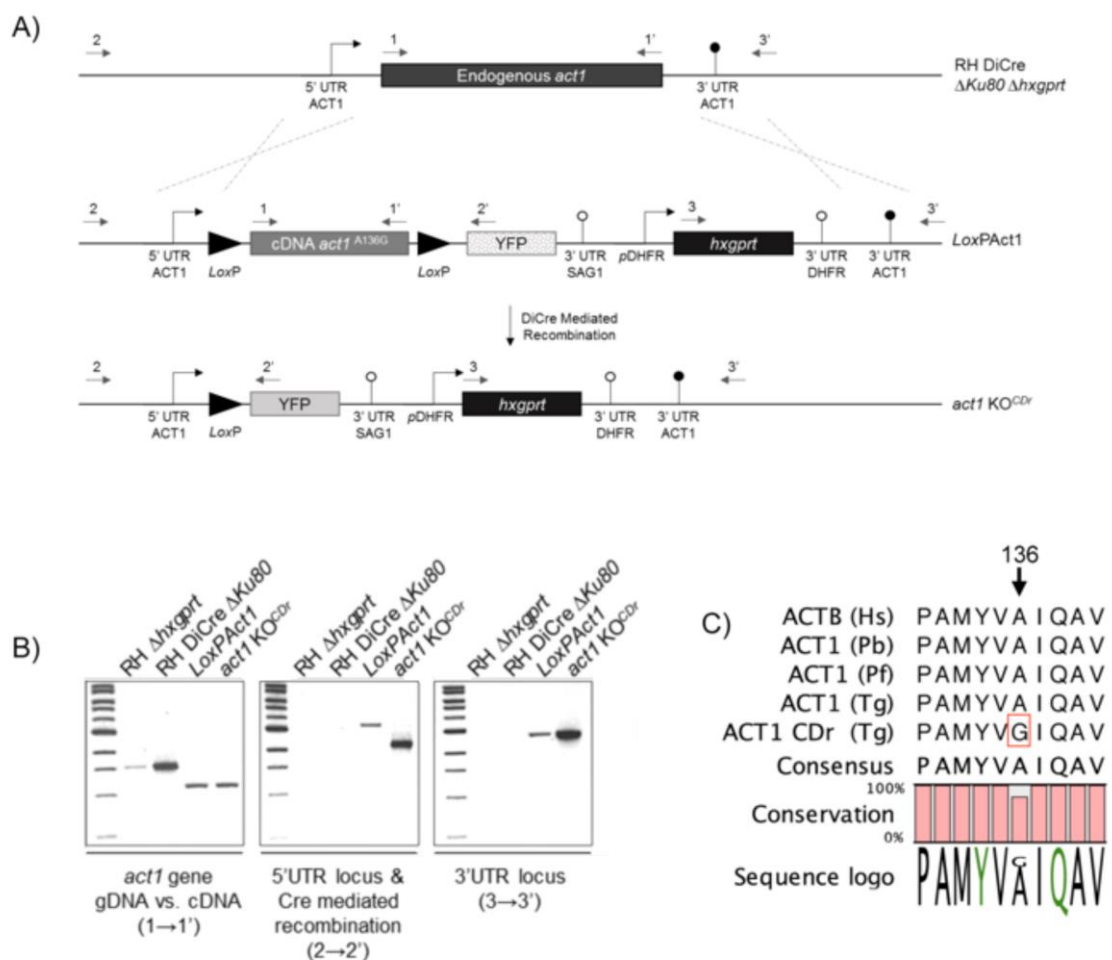


**Figure 4-1: Generation of an inducible cytochalasin D resistant *act1* KO.**

A) Schematic representation of the LoxPAct1CDr geneswap plasmid used to transfect into the RH DiCre  $\Delta$ Ku80 $\Delta$ hvgprt strain. The endogenous *act1* locus was replaced with the cDNA of *act1*

containing the A136G mutation, flanked by LoxP sites via homologous recombination. A reporter cassette of YFP is placed downstream of the cDNA and only expressed once *act1* is excised in a DiCre dependent manner. **B)** An analytical PCR was used to identify correct integration of the LoxPAct1<sup>CDr</sup> plasmid. Primer sets under the gel are highlighted in the schematic (A). **C)** Sequence alignments of different actins highlighting the A136G mutation for CD resistance. ACTB (Hs) is Human  $\beta$ -actin, ACT1 (Tg) from *Toxoplasma gondii*, ACT1 (Pf) from *Plasmodium falciparum* and ACT1 (Pb) from *Plasmodium berghei*.

Induction of the LoxPAct1<sup>CDr</sup> strain led to 95 % excision of *act1* consistent with results described for the *act1* KO in Andenmatten *et al.* (2012). Furthermore, the *act1* KO<sup>CDr</sup> parasites were assessed and had identical phenotypes when compared to *act1* KO, such as: apicoplast loss, morphological defects and reductions in gliding motility and invasion. Therefore, we were able to use this strain confidently knowing that it will behave like the original *act1* KO.

### 4.1.2 Characterisation of gliding

Having both the original LoxPAct1 and LoxPAct1<sup>CDr</sup> strains, we began to elucidate if CD specifically blocks motility through its interaction with actin or through an off-targeted effect. Moreover, could it be distinguished if the *act1* KO is sensitive to CD due to undetectable levels of ACT1 or if there was a secondary target of the drug? The *act1* KO and *act1* KO<sup>CDr</sup> were analysed for their ability to glide over FBS-coated coverslips and compared these to the control RH and CytD<sup>r</sup> parasites kindly provided by Prof. David Sibley (Dobrowolski & Sibley, 1996). As expected, RH was affected by the addition of CD at low concentrations ( $\leq 0.5 \mu\text{M}$ ), while it took much higher concentrations ( $\geq 1 \mu\text{M}$ ) before an effect was observed in the CytD<sup>r</sup> parasites (Figure 4-2 A). Importantly, at all concentrations tested both the *act1* KO and *act1* KO<sup>CDr</sup> resulted in comparable sensitivity to CD (Figure 4-2 A). Since at high concentrations of CD (2-4  $\mu\text{M}$ ) all parasite strains, including CytD<sup>r</sup>, *act1* KO and *act1*<sup>CDr</sup> KO, demonstrated a significant block in gliding motility, it appears that CD affects parasite viability in a more general manner. Furthermore, the effects observed with CD at concentrations higher than 0.5  $\mu\text{M}$  should be interpreted with care.

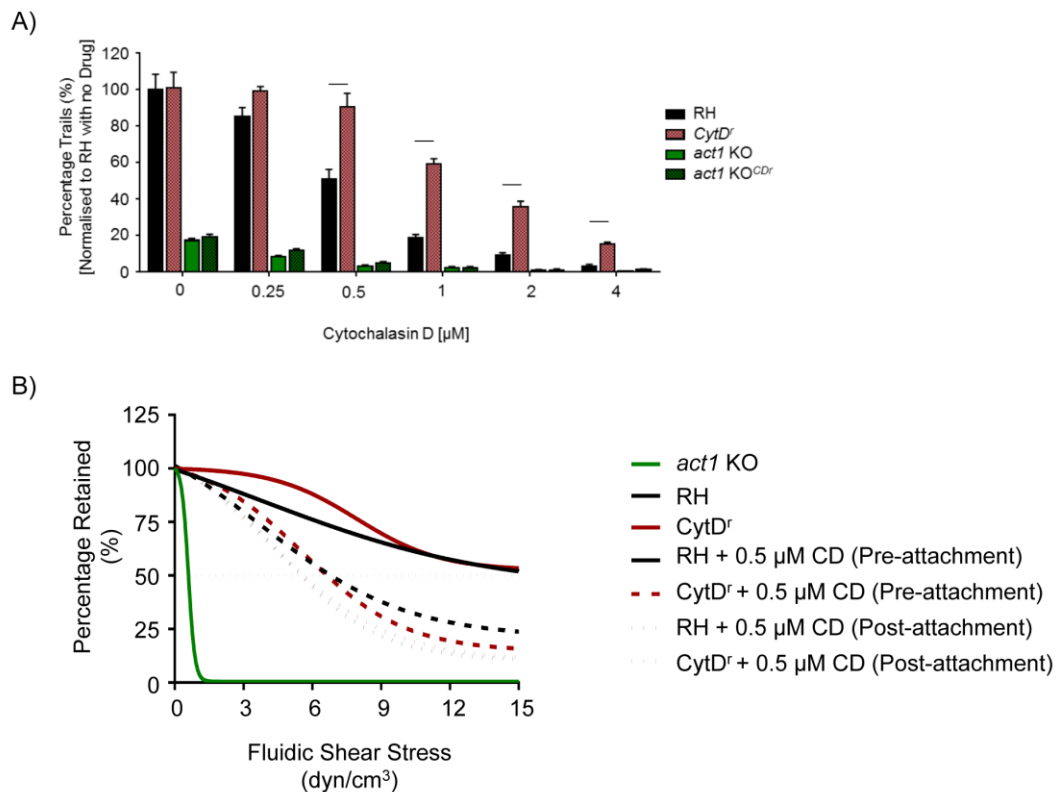


**Figure 4-2: The effect of cytochalasin D on both gliding motility and attachment.**

Evaluating how the addition of CD effects attachment and gliding motility and any potential off-target(s). **A)** Trail deposition assay under increasing concentrations of CD. Parasite strains RH (wild-type control), CytD<sup>r</sup> (a CD resistant strain), *act1* KO and *act1* KO<sup>CD</sup> were tested. The difference between RH and CytD<sup>r</sup> strains is only significant different with concentrations  $\geq 0.5 \mu\text{M}$ . There was no significant difference between the *act1* KO and *act1* KO<sup>CD</sup> strains at all concentrations. Error bars represent  $\pm$  S.E.M. Data sets were compared with multiple t-tests with the Holm-Sidak correction.  $P < 0.05$ . **B)** Trend line to show RH and CytD<sup>r</sup> parasites attachment strength in the presence of  $0.5 \mu\text{M}$  CD. CD containing media was flushed into the chamber as the flow-through. Different conditions were tested for their attachment strengths with CD added pre-attachment or post-attachment. *act1* KO parasites (green line) is shown as a comparison (taken from Figure 3-9). Attachment forces are reduced by around 50 % in the presence of CD compared to the no-drug control. The addition of CD does not diminish the attachment strength to the *act1* KO levels.  $n =$  a minimum of 3 experiments.

### 4.1.3 Cytochalasin D reduces attachment but not to *act1* KO levels

One of the first studies using CD on *Toxoplasma* showed that while it blocked invasion, attachment was unaffected (Ryning & Remington, 1978). Previously we showed that *Toxoplasma* ACT1 has an essential role during attachment (Whitelaw *et al.*, 2017) (chapter 3.5). In malaria sporozoites, the addition of CD or Jasplakinolide (Jas) blocked motility and affected parasite attachment to the substrate (Hegge *et al.*, 2010). Malaria sporozoites pre-incubated with CD are washed off under minimal flow rates. Whereas, if the sporozoites were allowed to attach under normal conditions, the addition of CD had no effect on attachment under shear flow rates (Hegge *et al.*, 2010). From this study, it

appears that depolymerisation of actin filaments before attachment reduced the attachment strengths of the parasites. Indeed, once the attachment site was made, these filaments might be rather stable. Here, we wished to consolidate the effect CD has on the attachment strength of *Toxoplasma* tachyzoites.

Therefore, a flow chamber system was used as described in chapter 3.5 to analyse attachment strengths. Similar to Hegge *et al.* (2010), two experiments were conducted to test the affinity of the parasites to attach to a collagen-coated chamber in the presence of CD (Figure 4-2 B). Parasites were either pre-treated with 0.5  $\mu$ M CD for 15 minutes before allowing them to attach in the chamber or allowed to attach under normal conditions. For both experiments, media containing 0.5  $\mu$ M CD was passed into the chamber at increasing flow rates, creating shear stress conditions. In the two different experiments, parasites were washed off with 50 % slower flow rates than parasites not exposed to the drug (Figure 4-2 B). It appears that the attachment strength is slightly weaker than those pre-incubated with CD (Figure 4-2 B).

Though these data were reproducible, at this point no reliable interpretation is possible since they are hard to reconcile with known functions of F-actin. The effect is most likely secondary due to the off-target effects of CD but could also be a caveat of the experimental design, discussed previously in chapter 3.5.

## 4.2 *Toxoplasma* ACT1 is naturally resistant to latrunculins

The use of CD to study parasite actin dynamics has become questionable due to the unidentified secondary target(s) in the parasites, therefore the actin destabilising Latrunculins (A and B) derived from the sea sponge, *Latrunculia magnificans* were tested. Both latrunculins are more accurate and potent inhibitors than CD (Spector *et al.*, 1989) and bind to free actin monomers, mimicking sequestering proteins to inhibit further polymerisation (Coue *et al.*, 1987; Morton *et al.*, 2000).

### 4.2.1 Gliding motility with latrunculin A

In budding yeast, resistance to latrunculin A comes from two amino acid substitutions R183A D184A (Ayscough *et al.*, 1997; Fujita *et al.*, 2003; Wertman

*et al.*, 1992). The R183 and D184 amino acids are conserved over a range of apicomplexan actins (Figure 4-3 C). However, before mutating these residues in TgACT1, wild-type parasites were analysed for their ability to glide in the presence of latA. Parasites were allowed to glide in increasing concentrations of latA from 0 M to 1  $\mu$ M, where the working concentration in conventional eukaryotic cells is as low as 90 nM (Coue *et al.*, 1987). Surprisingly, even up to 1  $\mu$ M latA, no significant difference was observed in trail deposition (Figure 4-3 A). In agreement, latA also has no effect on *Plasmodium berghei* sporozoite motility (Hegge *et al.*, 2010).

#### 4.2.2 Gliding in the presence of latrunculin B

Motility of *Cryptosporidium* sporozoites (closely related to *Toxoplasma gondii*) can be completely blocked with latrunculin B (latB) (Wetzel *et al.*, 2005). Therefore, we wished to observe the effect latB has on *T. gondii* motility. Latrunculin B binds to free actin monomers in a similar mode of action to latA but appears to be less potent (Spector *et al.*, 1989). A trail deposition assay tested the ability of the parasites to glide in the presence of latB. Results for gliding were comparable between both drugs. Even at high concentrations of latB, trail deposition was not perturbed (Figure 4-3 B).

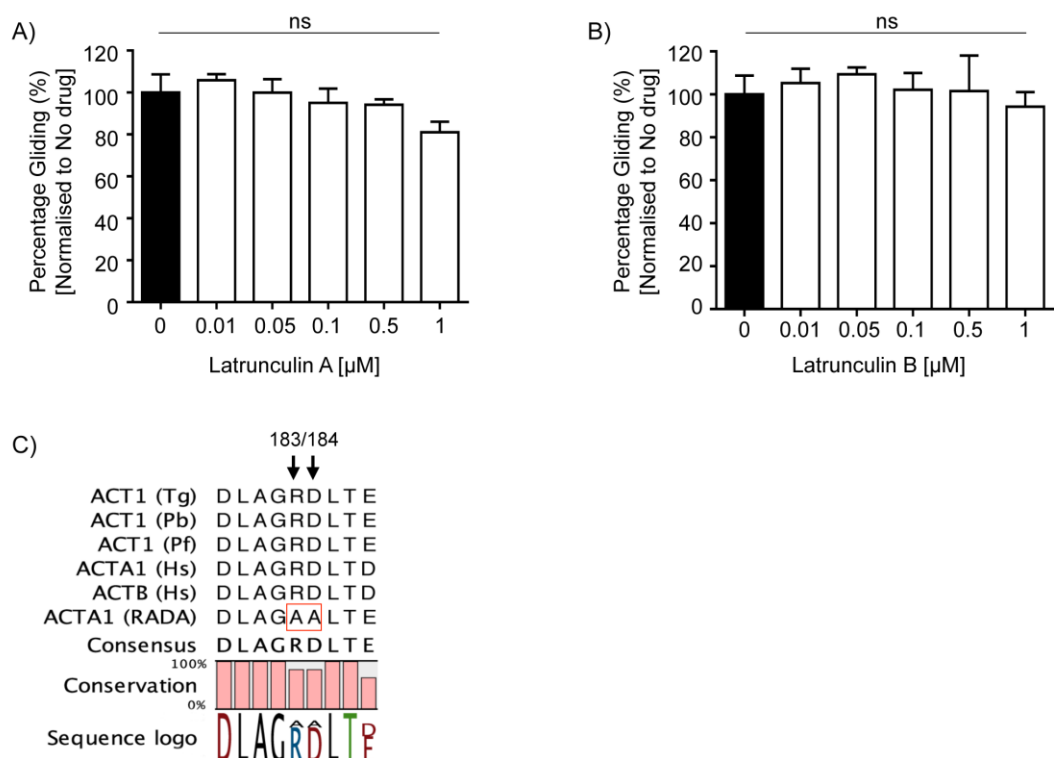


**Figure 4-3: The effect of latrunculins on gliding motility**

A trail deposition assay analysed the ability of the wild-type parasites to glide in the presence of increasing concentrations of latrunculins. No significant difference was observed for trail deposition with either (A) latA or (B) latB. Error bars represent  $\pm$  S.E.M. All experiments were performed in biological triplicate and the dataset were compared with a two-tailed Student's t-test. Non-significance (ns)  $p > 0.05$ . The double mutation of R183A and D184A confers latrunculin A resistance. (C) Sequence alignments of different actins from Humans (Hs), *Toxoplasma gondii* (Tg) and *Plasmodium falciparum* (Pf) and *P. berghei* (Pb).

**4.2.3 Invasion with latrunculin A**

Contradicting studies have highlighted the importance of host actin during invasion. Some studies have shown the host to be rather passive during invasion with the penetrative force solely generated by the acto-myosin system within parasite (Dobrowolski & Sibley, 1997; Dobrowolski & Sibley, 1996). While others studies have described the actin cytoskeleton to be necessary for invasion (Bichet *et al.*, 2016a; Gonzalez *et al.*, 2009; Rynning & Remington, 1978). To readdress this question, we decided to use latA during invasion, since latrunculins had no effect on parasite motility and thus *Toxoplasma* ACT1. Dr. Cora-Ann Schrodenberg kindly provided latA resistant RADA2 HeLa cells first described by Fujita *et al.* (2003). RH parasites and HeLa cells were pre-incubated in 1  $\mu$ M latA for 10 minutes before invasion. Parasites were left to invade for one hour followed by five washes to remove parasites that have yet to invade. These were then left to replicate in the presence of 1  $\mu$ M latA for a further 24 hours. This indicated that the presence of 1  $\mu$ M latA did not inhibit invasion of RH into the RADA2 cells (Figure 4-4 A). Interestingly, 1  $\mu$ M latA also had no effect on parasite replicating inside RADA2 HeLa cells (Figure 4-4 C). Meanwhile, invasion rates in the sensitive HeLa cells were significantly reduced. However, the inhibition observed with latA on the sensitive HeLa cells may be due to cell death. Latrunculin A is a fast acting drug (Coue *et al.*, 1987), therefore, coupled with a high concentration and incubating with latA for 24 hours, it is feasible that we may not have blocked invasion but rather destroyed most of the host cells. To test this, we performed an invasion assay into sensitive HeLa cells where parasites were only allowed to invade for one hour before fixation and staining for extracellular parasites with  $\alpha$ -SAG1. The cells were exposed to increasing concentrations of latA (0-1  $\mu$ M) (Figure 4-4 B). As little as 10 nM latA, significantly reduces the invasion rate. As the concentration of latA increases, invasion rates further decrease, but a full block was never observed within the range tested.

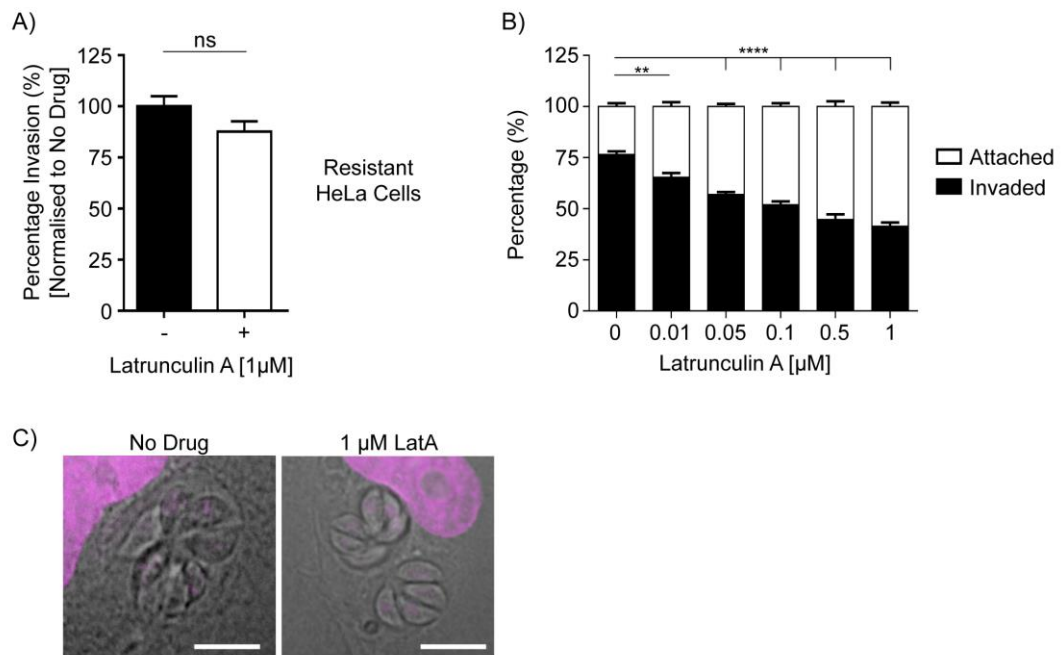


**Figure 4-4: Invasion and replication of RH with latrunculin A**

The role of the actin cytoskeleton of the host during invasion was analysed. **A)** Invasion of wild-type parasites was allowed to invade into RADA2 latrunculin resistant HeLa cells. No significant difference was observed with 1 µM latA. Error bars represent  $\pm$  S.E.M. Dataset were compared with a two-tailed Student's t-test. Non-significance (ns)  $p > 0.05$ . **B)** Invasion of wild-type cells in latA sensitive HeLa cells shows a significant decrease in invasion rates as the concentration of latA increases. Error bars represent  $\pm$  S.E.M. Dataset were compared with a 1-way ANOVA followed by Tukey's post hoc test. \*\*\*\*  $p < 0.0001$  and \*\*  $p < 0.01$ . **C)** Representative images of replicated parasites with and without 1 µM latA. Scale bar: 10 µm.

To conclude, it would seem that parasite ACT1 is naturally resistant to latrunculins. Resistance to latrunculins was alluded to in Vahokoski *et al.* (2014), where they crystallised both ACTI and ACTII proteins from *Plasmodium falciparum* and observed structural evidence of a salt bridge between residues Lys 207 and Glu 188, similar to latrunculin bound  $\alpha$ -actin Vahokoski *et al.* (2014). Nevertheless, latA allowed us to test specifically the role of host cell without affecting the actin dynamics of the parasites (Figure 4-4 B). Our results are in agreement with previous studies, suggesting that while the parasite primarily drives invasion, the actin cytoskeleton of the host is also highly important for this process (Gonzalez *et al.*, 2009; Rynning & Remington, 1978).

### 4.3 Forcing actin polymerisation inhibits motility

Artificially polymerising actin through the use of Jas blocks both gliding motility and attachment in *P. berghei* and *C. parvum* sporozoites (Hegge *et al.*, 2010;

Wetzel *et al.*, 2005). Exposure to Jas causes *T. gondii* tachyzoites to stop gliding in both helical and circular motions, where many parasites begin to exhibit a counter-clockwise twirling rotation (Wetzel *et al.*, 2003). Interestingly, both *T. gondii* sporozoites and tachyzoites display a unique “rolling” movement with Jas treatment. This rolling action is where the parasites move back and forth along the longitudinal axis (Wetzel *et al.*, 2005). In extracellular parasites, the addition of Jas causes the conoid to extend due to extensive actin polymerisation at the apical end (Shaw *et al.*, 2000). While analysing the chromobody effect to actin-modulating drugs (Figure 4-5 B) (discussed later in chapter 5.2), it became apparent that very few trails were seen in the chromobody-Halo parasites after Jas treatment (Periz *et al.*, 2017). Therefore, we wish to understand if artificially forcing the polymerisation of actin has an effect on motility and if the *act1* KO is effected by Jas treatment.

For this, both wild-type and *act1* KO parasites were pre-incubated with 1  $\mu$ M Jas for 10 minutes before the start of the trail deposition assay. Parasites were incubated with the drug on FBS-coated coverslips and allowed to glide for 30 minutes. In agreement with previous findings (Hegge *et al.*, 2010; Wetzel *et al.*, 2003; Wetzel *et al.*, 2005), we found that forcing polymerisation blocked motility of wild-type parasites (Figure 4-5 A). Meanwhile, no significant reduction was observed in the *act1* KO parasites (Figure 4-5 A). Therefore, it was concluded that Jas only has a single target and functions to polymerise actin. Moreover, since there was no decrease in trail formation within the *act1* KO, there must be insignificant or no ACT1 protein remaining in the *act1* KO at 96 hours, supporting results from chapter 3.2 and again opposing the isodesmic process (Skillman *et al.*, 2013). The addition of Jas to the *act1* KO does not cause the conoid to extend as seen for wild-type parasites (Figure 4-5 B). To conclude, forcing actin polymerisation has an adverse effect on parasite motility. However, this does not directly reflect the function of actin, since *act1* KO motility was not blocked. The presented result suggest that the artificial polymerisation of F-actin in the parasite can have more general adverse effects, leading to functional interference with other processes.

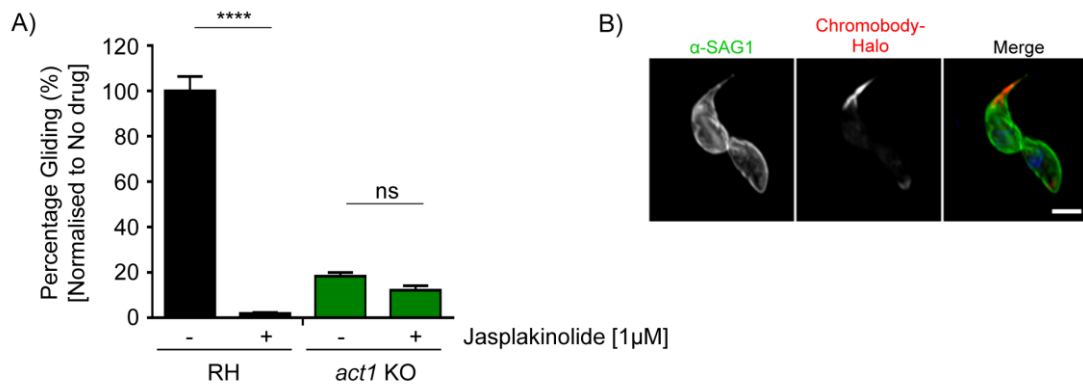


**Figure 4-5: The effect of jasplakinolide on the motility tachyzoites.**

**A)** Trail deposition assay of RH parasites and *act1* KO parasites in the presence of the actin polymerisation drug jasplakinolide. Forcing polymerisation blocks motility in RH but has no effect on an *act1* KO. Error bars represent  $\pm$  S.E.M. Dataset were compared with a two-tailed Student's t-test. \*\*\*\*  $p < 0.0001$ , non-significance (ns)  $p > 0.05$ . **B)** Wild-type parasites treated with 1  $\mu$ M Jas extend their conoid at their apical end (highlighted by chromobody-Halo (red), discussed later in chapter 5.2). Scale bar: 5  $\mu$ m.

## 4.4 Summary and conclusions

In summary, the *act1* KO remains capable of gliding and invasion at around 25 %. This directly conflicted with various studies using the actin-disrupting drugs, CD and latrunculins, where they have been shown to completely block in motility and invasion (Dobrowolski & Sibley, 1996; Rynning & Remington, 1978; Wetzel *et al.*, 2005). Data has been presented to support the argument that conventional actin-modulating drugs are not entirely specific for *Toxoplasma* actin. While CD affects parasite actin similarly to other actins, it has also been shown that the drug has an as-yet-unknown off-target(s) effect within the parasites, also observed in (Dobrowolski & Sibley, 1996; Gonzalez *et al.*, 2009). When actin is depleted to undetectable levels; CD affects both the *act1* KO and *act1* KO<sup>CDr</sup> equally. Moreover, CytD<sup>r</sup> parasites become increasingly sensitive to CD as the concentration exceeds 0.5  $\mu$ M, solidifying the possibility of an off-target effect. To conclude, CD should be used at concentration  $\leq 0.5$   $\mu$ M CD (Figure 4-2 A).

The role of the host cell actin cytoskeleton was thought to be passive during invasion (Dobrowolski & Sibley, 1997; Dobrowolski & Sibley, 1996). Here we have shown that latA specifically inhibits host cell actin but not parasite actin. Therefore, the active block in invasion with latA highlights the importance of the host actin cytoskeleton during invasion. In support of this, the remodelling of the actin cytoskeleton of phagocytic and non-phagocytic cells is critical for

---

parasite invasion (Unpublished results from Mario del Rosario) (Bichet *et al.*, 2014; Zhao *et al.*, 2014). Artificial polymerisation with Jas in wild-type parasites leads to a complete block of motility. *Act1* KO parasites remain motile, and no block occurs after addition of Jas, demonstrating that Jas is specific for ACT1. Moreover, it also indicates that artificial polymerisation of F-actin within the parasite can lead to non-specific phenotypes. Finally, the role of the actin cytoskeleton of the host will need to be re-addressed in future studies.

## Chapter 5 Actin Filaments in *Toxoplasma gondii*

Actin is one of the most abundant proteins in cells and a major house-keeping gene. Actin exists in two forms; the monomeric globular (G-actin) and filamentous actin (F-actin) (Wear *et al.*, 2000). The dynamic transition between the two is tightly regulated in spatial time, location within the cell and as a response to various stimuli (Ballestrem *et al.*, 1998; Mitchison & Cramer, 1996; Welch *et al.*, 1997b). In mammals, the monomeric pool of actin accounts for around 50 % of the total actin (Galdal *et al.*, 1983). To date, no known system has been shown to function on monomeric actin only, although, in many parasitic organisms, the detection of F-actin has been elusive (Dobrowolski *et al.*, 1997; Gupta *et al.*, 2015; Paredez *et al.*, 2011). In comparison to mammalian actins, the pool of G-actin in Apicomplexa is thought to be around 97 % (Dobrowolski *et al.*, 1997; Mehta & Sibley, 2010) and is only properly detected within the cytosol of the parasites. Apicomplexan actin has been characterised as unconventional, highly dynamic and intrinsically unstable (Sahoo *et al.*, 2006; Skillman *et al.*, 2011). Together, this led to the assumption that the parasites must form very short filaments (Sahoo *et al.*, 2006; Schmitz *et al.*, 2005) and have a unique form of actin polymerisation *in vitro*, termed isodesmic (Skillman *et al.*, 2013). However, recent work has shown that apicomplexan actins are not adequately folded when heterologously expressed. This is due to differences in the chaperonin T-complex (Olshina *et al.*, 2016), and therefore previous biochemical studies will have to be readdressed.

Besides its function in gliding motility and host cell invasion, apicomplexan actins have also been shown to be also involved in apicoplast inheritance and egress (Egarter *et al.*, 2014). However the inability to detect filaments within the parasites was a major obstacle in order to perform functional analysis based on its localisation. Filaments in Apicomplexa have only properly been described for malaria gametocytes and *Theileria* sporozoites (Hliscs *et al.*, 2015; Kuhni-Boghenbor *et al.*, 2012). Few reports have visualised filament-like structures in *Toxoplasma*. To date, F-actin has been visualised using scanning electron microscopy (Schatten *et al.*, 2003), an actin antibody that appears to be preferential for filamentous structures (Angrisano *et al.*, 2012b) and by the actin stabilising drug Jasplakinolide (Shaw & Tilney, 1999). Phalloidin, an F-actin binding protein, which has been used extensively to highlight actin filaments in

mammalian systems, is unable to bind to any Apicomplexan actin. Several reasons have been suggested to account for this; 1) a severe lack of filaments. 2) very short unstable filaments as proposed by (Sahoo *et al.*, 2006; Skillman *et al.*, 2011) or 3) a cytosolic protein that may bind to F-actin masking the accessibility of phalloidin or antibodies to the filament (Schuler *et al.*, 2005b).

In a new attempt to visualise F-actin within the parasites, specific nanobodies were expressed that have a strong affinity to actin, known as chromobodies. Chromobodies are minuscule and derived from the heavy chain fragment of antibodies from *Camelidae spp.* specific to actin (Rothbauer *et al.*, 2006) (Figure 5-1 A). The single chain camelid antibody, fused to the fluorescent protein RFP allowed live imaging of actin filaments and has been shown to have no detrimental effect on cell viability or motility (Rothbauer *et al.*, 2006). Several studies have demonstrated the use of chromobodies to be a valuable tool for studying protein functions. The use of actin-chromobodies in plant cells indicated that this was particularly advantageous as it labelled actin without impairing the polymerisation kinetics of F-actin (Rocchetti *et al.*, 2014). More recently, a study using chromobodies, visualised active endogenous proteins expressed in a living Zebrafish, with no deleterious effects (Panza *et al.*, 2015).

## 5.1 Expression of chromobodies highlights a vast network within the parasitophorous vacuoles

This project set out to visualise and begin to understand the dynamics of actin throughout the lifecycle to *Toxoplasma gondii*. Different vectors expressing chromobody-fusions recognising F-actin were generated in order to visualise actin filaments. The chromobody expression was put under the control of a constitutive, strong promoter p5RT70 (Figure 5-1 C). Fused to the C-terminal region of the chromobody was either red fluorescent protein (RFP) or a Halo-tag from Promega<sup>®</sup>. The Halo-tag<sup>®</sup> (a modified haloalkane dehalogenase) is designed to bind covalently to synthetic ligands (Los *et al.*, 2008), allowing visualisation of the chromobody upon addition of a cell permeable, fluorescent TMR-ligand (Figure 5-1 B). Other ligands allow a diverse range of applications; such as bright fluorescence dyes for protein localisation, biotin for protein purification and/or protein-protein interactions (Blackstock & Chen, 2014; Stagge *et al.*, 2013).

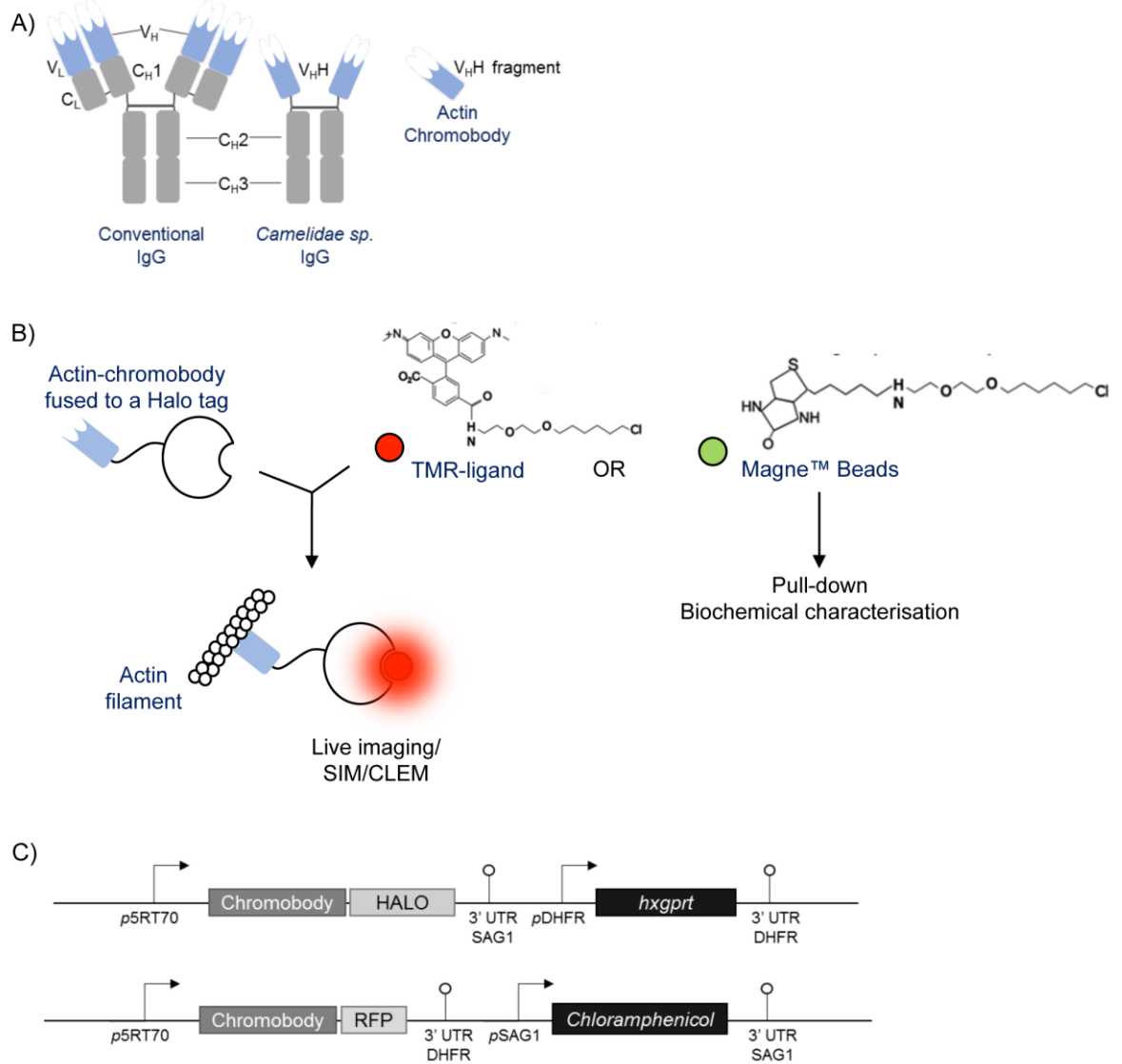


**Figure 5-1: Expression systems to visualise actin filaments**

Chromobody technology used to detect F-actin dynamics in *Toxoplasma gondii*. **A)** Schematic of the actin chromobody development adapted from (Rothbauer *et al.*, 2006). The chromobody is the V<sub>H</sub>H fragment from a Camelidae IgG specific to actin. **B)** The actin-chromobody was C-terminally fused to a Halo-tag (Promega®). The Halo-tag is versatile and can be visualised by incubation with the chloroalkane; TMR-ligand but also functions in pull-down assays for biochemical characterisation using Magne™ beads (Promega®). **C)** Schematic plasmids used to express the chromobodies in *Toxoplasma gondii*. Chromobody is under the control of the constitutive overexpression promoter (p5RT70) and C-terminally fused to either Halo-tag or RFP.

## 5.2 Chromobody signal changes with actin-modulating drugs

Both vectors (Figure 5-1 C) were transiently transfected into the RH  $\Delta$ hvgprt and incubated on HFFs for IFA analysis. While no filaments were readily observed in extracellular parasites (Figure 5-2 A), both chromobodies highlighted an extensive network within the parasitophorous vacuole, seemingly connecting individual parasites (Figure 5-2 B). To confirm that the chromobodies are binding specifically to F-actin in the parasites we used the actin-modulating

drugs; Jasplakinolide (Jas) and cytochalasin D (CD) (Figure 5-2). The addition of Jas to extracellular parasites induces rapid polymerisation of almost all cytosolic G-actin to F-actin at the apical and polar end of the parasite, causing the conoid to extend and formation of a small “bulb” at the basal end (Figure 5-2 A) (Shaw & Tilney, 1999). Moreover, in intracellular parasites, the drug causes the intravacuolar network to appear longer and thicker (Figure 5-2 B). In contrast, the addition of CD caused the filaments to become unstable and depolymerise. Within the vacuole, the chromobody with CD highlighted many punctate dots that were predicted to be possible centres of polymerisation. Indeed, no filaments were observed in extracellular parasites (Figure 5-2 A, B). Intriguingly, there was only a partial colocalisation of chromobody-Halo with an actin antibody (Baum<sup>Polyclonal</sup>), indicating that exogenously added antibody might not gain access to the actin filament, potentially due to sterical hindrance (Periz *et al.*, 2017). However, since F-actin structures were still observed with this antibody, it was concluded that the chromobody specifically binds to F-actin.

To exclude that these filaments were not caused by parasites hi-jacking actin from the host, large intracellular vacuoles were treated with latrunculin A (latA). Since TgACT1 is naturally resistant to this actin-modifying drug (Vahokoski *et al.*, 2014) (see results in chapter 4.2), latA represents a potent inhibitor of host cell actin dynamics without affecting the parasite actin. Parasites expressing chromobody-Halo were allowed to invade and replicate within latA sensitive HeLa cells for 24 hours. After which the cells were incubated with various concentrations of latA for 3 hours before PFA fixation. Phalloidin<sub>488</sub> assessed the integrity of the host cell actin network and the parasite network was visualised with Halo-TMR (Figure 5-2 C). It was observed that at low concentrations latA (<100 nM), both host and parasite filaments appear unaffected. However, at concentrations exceeding 0.5  $\mu$ M LatA, the host F-actin begins to collapse whereas the parasites filaments remain intact, similar to the no drug control. Even up to 5  $\mu$ M, the parasite network appeared normal whereas the HeLa cells were significantly rounded after disruption of the cells cytoskeleton (Figure 5-2 C).

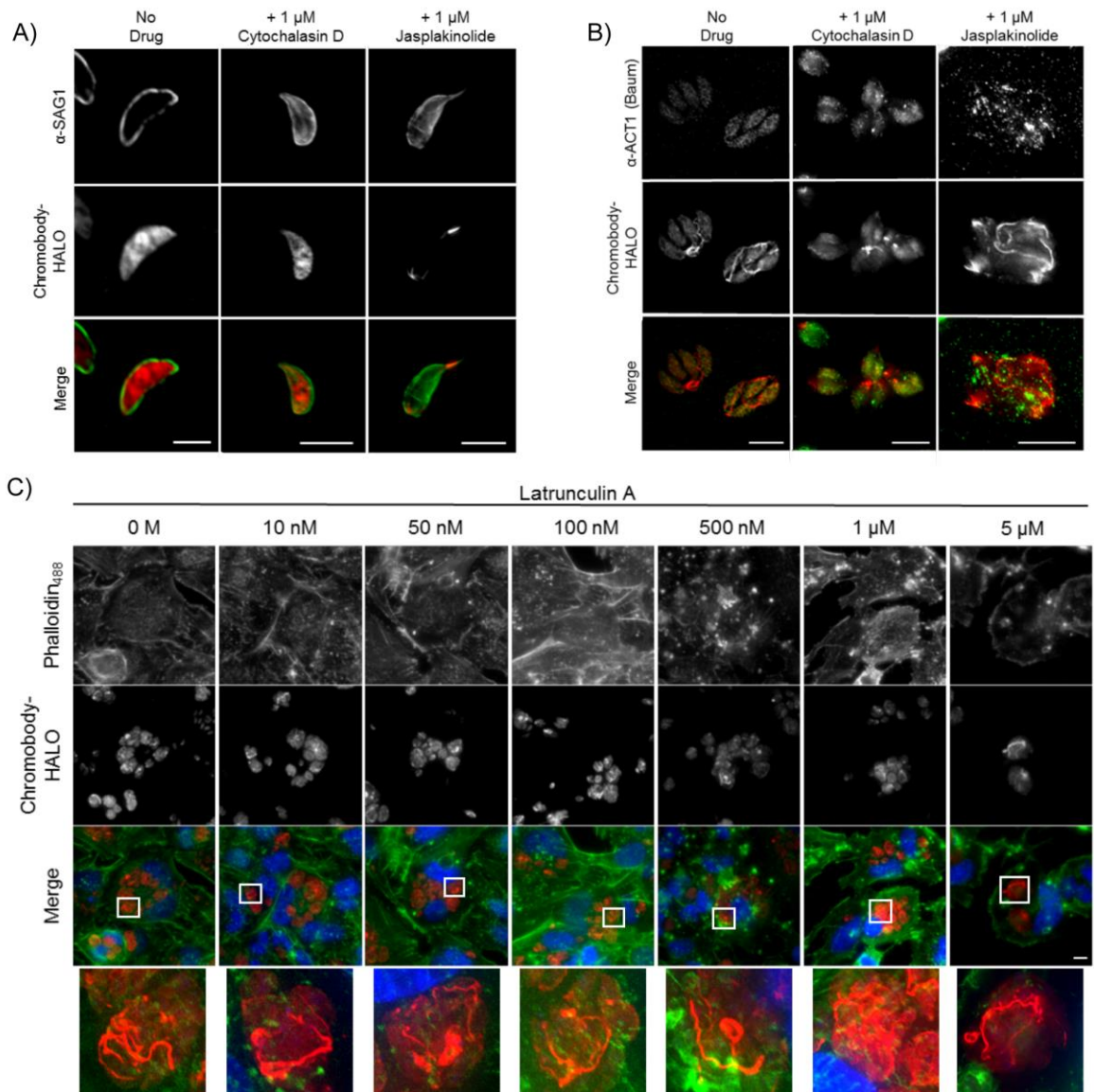


**Figure 5-2: The effect of actin-modulating drugs on the chromobody expression**

Chromobody-Halo parasites were exposed to actin polymerisation and depolymerisation drugs. **A)** Extracellular parasites present a cytosolic staining of chromobody with no apparent filaments. A similar expression is seen with 1  $\mu$ M cytochalasin D (CD) while 1  $\mu$ M jasplakinolide (Jas) causes the extension of the conoid and chromobody signal is only observed at the apical and basal ends of the parasites. Scale bars: 5  $\mu$ m. **B)** Intracellular parasites were exposed to the same concentrations of F-actin modifying drugs. Filaments depolymerise with CD and become much thicker in the presence of Jas. Scale bars: 10  $\mu$ m. **C)** Chromobody-Halo parasites were treated with increasing concentrations of latrunculin A to show that the actin network is solely TgACT1 and not scavenged from the host. Latrunculin A is a potent inhibitor of actin polymerisation of the host but ineffectual for parasite actin. The parasite network remains present even up to 5  $\mu$ M latA while the host actin cytoskeleton is severely affected. Scale bars: 100  $\mu$ m.

Overall, the use of these drugs indicates that the chromobodies expressed by the parasites are indeed binding specifically to *Toxoplasma* F-actin. Chromobodies highlight a novel actin network connecting the parasites that are emphasised in the presence of actin-modifying drug Jas but absent with CD treatment. Moreover, the filaments are unaffected by latA indicating that no actin from the host is being scavenged to make this network.

### 5.3 Chromobodies bind specifically to *Toxoplasma* ACT1

To further verify the specificity of the chromobodies for F-actin, their localisation was tracked in the conditional *act1* KO (Figure 5-3). As stated above, filaments are observed as a network within the parasitophorous vacuole in wild-type cells. After transient expression of the chromobodies into the LoxPAct1 strain, the excision of *act1* was induced with 50 nM rapamycin, and the filaments were tracked over a time course.

In both cases (chromobody-RFP and chromobody-Halo), filaments were non-existent in the *act1* KO at 72 hours (Figure 5-3). In detail, chromobody-RFP expression in wild-type cells only highlights a dense network without any cytosolic staining of RFP (Figure 5-3 A). However, at early time points (24 hours post induction), the signal for chromobody-RFP was often observed within the cytosol of YFP<sup>+</sup> parasites and the filamentous structures became much smaller and disappeared (Figure 5-3 A). This change can be interpreted that the equilibrium shifts to favour G-actin within the cell when the concentration of actin drops and therefore formation of F-actin is reduced or impossible. While at 48 hours post rapamycin treatment, it was observed that the chromobody signal is punctate and often found around the residual body or at either the apical or basal end of the parasites, similar to the observations with CD (Figure 5-3 A). At the latest time point analysed (72 hours post rapamycin treatment), no YFP<sup>+</sup> parasite vacuoles contained a network (Figure 5-3 A). Sometimes punctate spots could still be observed, similar to earlier time points.

Similarly, for the chromobody-Halo in the *act1* KO the dynamics change soon after excision of *act1*. However, unlike the chromobody-RFP, the signal is readily observed in the cytoplasm of wild-type parasites expressing chromobody-Halo (Figure 5-3 B). Filaments in the *act1* KO become shorter after 24 hours, concentrated in the residual body. As the parasites continue to grow, filaments were observed at a much lower frequency, where they appear very short and thin. By 72 hours post induction, the YFP<sup>+</sup> parasites do not have any filaments, and chromobody-Halo appears only cytosolic (Figure 5-3 B).

The Halo-tag offers a variety of functional analysis. Here, the chromobody-Halo parasites were used as bait for a co-immunoprecipitation (Co-IP) experiment to

see if *Toxoplasma* actin could be separated from the other parasites proteins. Dr. Simon Gras extracted whole parasite lysates and incubated with Halo-Magne™ beads from Promega®. Through a series of stringent washes, the sample was eluted from the Magne™ beads using the TEV protease. The input and final elution was run on a SDS-PAGE gel and analysed by western blot. The western blot was probed with a specific actin antibody (TgACT1<sup>Soldati</sup>; see chapter 3.1). Here, a large actin band was present in both input samples (wild-type control and chromobody-Halo parasites) (Figure 5-3 B, C). Indeed, actin was only observed in the chromobody-Halo elution after Co-IP (Figure 5-3 C). This band represents between 1-5 % (n=3) of actin from the initial population. From this, we predict that the chromobody-Halo preferentially binds to F-actin, although this may represent only a fraction of the F-actin that bound to the resin. One way to overcome this is to use CD to depolymerise the filaments before Co-IP to show specificity to F-actin. Moreover, mass spectrometry analysis confirmed that TgACT1 is specifically identified as the top hit in a Co-IP using chromobody-Halo parasites as bait (unpublished work from Dr. Simon Gras).

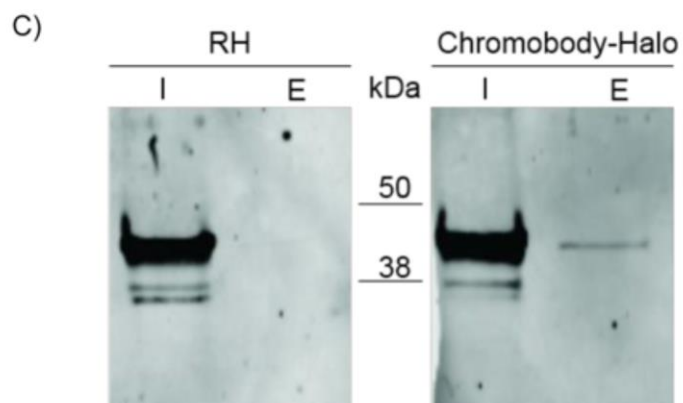
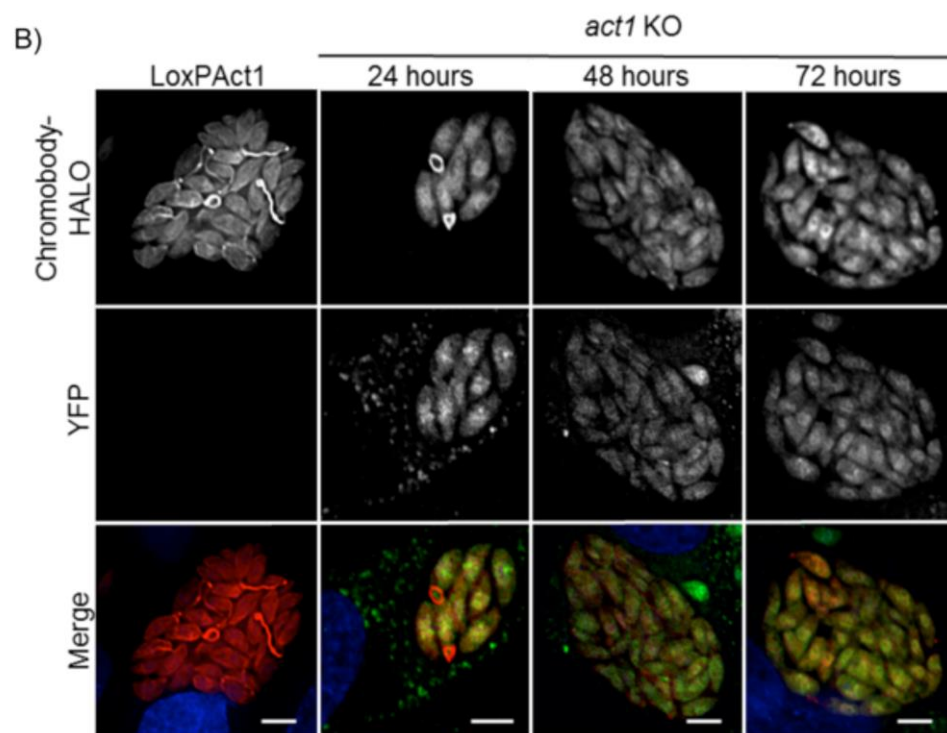
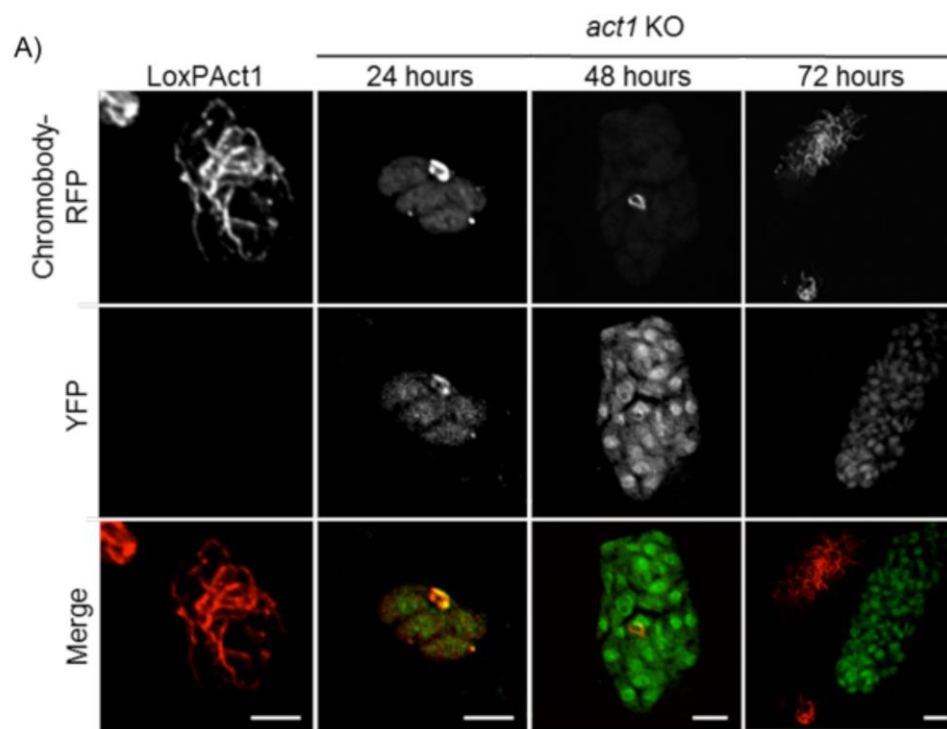


**Figure 5-3: Chromobodies bind specifically to TgACT1**

Chromobodies were transiently expressed into LoxPAct1 then induced with 50 nM rapamycin to excise *act1*. Images were taken at 24-hour intervals. Scale bars: 10  $\mu\text{m}$ . **A)** Chromobody-RFP expression in the *act1* KO. In wild-type cells, the chromobody-RFP is always seen as filamentous. At early time points after excision the chromobody expression becomes cytosolic and by 72 hours no network is visible in the *act1* KO parasites. **B)** Chromobody-Halo expression in the *act1* KO. Similar to the chromobody-RFP, the filaments break up quickly after excision and at 72 hours, no filaments were observed. Scale bars: 10  $\mu\text{m}$ . **C)** Co-immunoprecipitation (Co-IP) of both wild-type (RH) and chromobody-Halo parasites with Halo-Magne™ beads. The western blot was labelled with a specific antibody against actin (TgACT1<sup>Soldati</sup>). Actin labels both inputs with a predominant band at 42 kDa, while only the elution of chromobody-Halo parasites are labelled with actin. Dr. Simon Gras performed this experiment.

To investigate the presence of F-actin within this network, a correlative-light electron microscopy (CLEM) was performed (Figure 5-4). Chromobody-Halo parasites were incubated for around 30 hours to obtain vacuoles with an extensive F-actin network and stained with Halo-TMR for 10 minutes. After which, the live-cell dishes were fixed with EM fixative (4 % glutaraldehyde and 2.5 % PFA). The network was imaged with super-resolution microscopy (3D-SIM) and recorded for its position within a gridded live cell dish. These dishes were then given to Dr. Leandro Lemgruber for processing and transmission electron microscopy (TEM) as described in Loussert *et al.* (2012). From the reconstruction, this network appears to contain multiple actin filaments (shown by arrowheads and false colour pink tracers; Figure 5-4 A). Moreover, vesicle-like structures were also observed along these filaments (full arrows) (Figure 5-4 A). To accompany the standard CLEM, actin filaments in the network were also observed with cryo-immuno CLEM. Chromobody-Halo parasites were incubated in HFFs for around 24 hours and fixed in EM fixative at 4°C. The samples were then processed for TEM as described above by Dr. Leandro Lemgruber. After TEM processing, the samples were placed on a gridded surface for immunofluorescence analysis with Halo specific antibodies. After which, the sample was then processed for immuno-EM by labelling with gold antibodies. Interestingly, actin filaments were observed in an area without the gold particles (white arrows; Figure 5-4 B1). While the area of chromobody-Halo signal on IFA also has a dense gold signal (black arrow; Figure 5-4 B2).

To conclude, the chromobody expression highlights an F-actin network within parasite vacuoles that is sensitive to actin-modulating drugs. Filaments highlighted by the chromobody-RFP are much thicker than what was observed with the chromobody-Halo. Biochemical results from Dr. Simon Gras show that

the chromobodies preferentially bind to F-actin as only around 1-5 % was pulled down in a Co-IP experiment, supporting previous findings that the actin monomer pool is around 95-98 % (Dobrowolski *et al.*, 1997). Overall, from these results, we are confident to use chromobodies as a tool to visualise actin dynamics in the parasites. The formation of filaments is dependent on the presence of G-actin, which has been confirmed. In a time course analysis, it was shown that long filament formation is inhibited as soon as 24 hours after excision of *act1* when a significant amount of actin can still be detected (see chapter 3.2). This strongly indicates that once G-actin is below a critical concentration, no F-actin can be formed, as also reflected by the phenotypic analysis performed in earlier chapters. To conclude, similar mechanisms exist for polymerisation as observed in conventional actin and it is suggested that the isodesmic polymerisation model is dismissed (Skillman *et al.*, 2013). This is the first direct application to study actin dynamics *in vivo* within Apicomplexa.

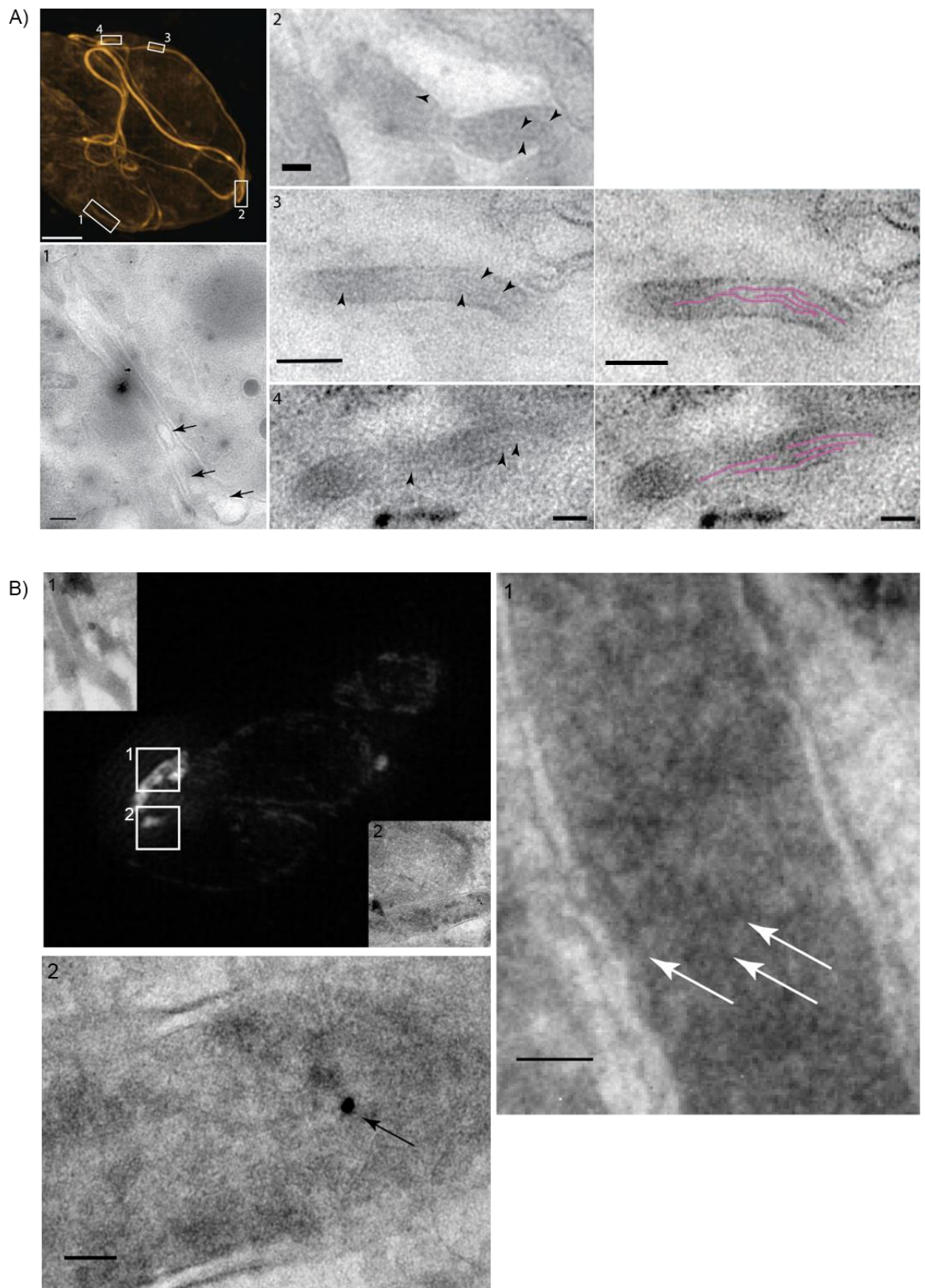


**Figure 5-4: Correlative-light electron microscopy (CLEM) of the actin network**

**A)** The F-actin network was imaged with super-resolution microscopy (3D-SIM), and the same areas were imaged with Transmission Electron Microscopy (TEM). 1) Vesicles were observed within the network tubules (Arrows). Filaments of 5 nm in thickness were present within the network tubules (2-4), extending over 100 nm in length (Arrowheads). The putative actin filaments are indicated in pink for images 3 and 4. Scale bars: 200 nm (3D-SIM); 50 nm (TEM). **B)** Immunolabelled CLEM of a chromobody-Halo vacuole. 1) Actin filaments observed in bundles (white arrows). 2) Immune-labelled Halo is observed in the network, although no distinct filaments are observed. Scale bar: 500 nm. EM images provided by Dr. Leandro Lemgruber.

## 5.4 Stabilisation of actin filaments phenocopies the *act1* KO

Transient expression of chromobody-RFP indicated that these filaments were much thicker than what we observe with chromobody-Halo. It is predicted that this may be due to RFP forming tetramers (Campbell *et al.*, 2002), inhibiting conventional actin kinetics. This filamentous network causes a noticeable defect during the parasites replication. Using an IMC1 antibody as a marker for parasite cytoskeleton, it was observed that vacuoles expressing an extensive network appear to reproduce the division phenotype of the *act1* KO (as discussed in chapter 3.6.1). These parasites divide but do not seem stay in the conformational rosette of wild-type parasites (Figure 5-5). Parasites that control chromobody-RFP expression (seen with a small network organised within a large residual body) replicated relatively normal within the PV. Therefore, an extensive network causes the parasite vacuole to become highly disorganised (Figure 5-5). Vacuole disorganisation occurred in the majority of the vacuoles expressing the chromobody-RFP. From this observation, other markers were checked using various antibodies. As previously shown, the *act1* KO cannot divide its apicoplast during replication (Egarter *et al.*, 2014) (see chapter 3.3). Using  $\alpha$ -CPN60 as an apicoplast marker, it was observed that division of the apicoplast is affected in many vacuoles with a filamentous network, where they do not contain the correct ratio of apicoplast to the parasite (Figure 5-5). We also assessed how the actin antibodies reacted to the filaments. Three different actin antibodies were tested, two that are G-actin specific (from Soldati and Baum<sup>Monoclonal</sup>) and one that is preferential for F-actin (Baum<sup>Polyclonal</sup>) (see chapter 3.1). Instead of the typical cytoplasmic staining, all three co-localise with the filaments (Figure 5-5). This lead us to believe that the pool of monomeric actin is depleted almost entirely to generate the filaments giving rise to defects during replication. Therefore, expression of chromobody-RFP causes a dominant negative effect similar to the *act1* KO during its intracellular stages. This is most likely due to the RFP forming tetramers, although stable expression of the chromobody-RFP would be required to validate this hypothesis.

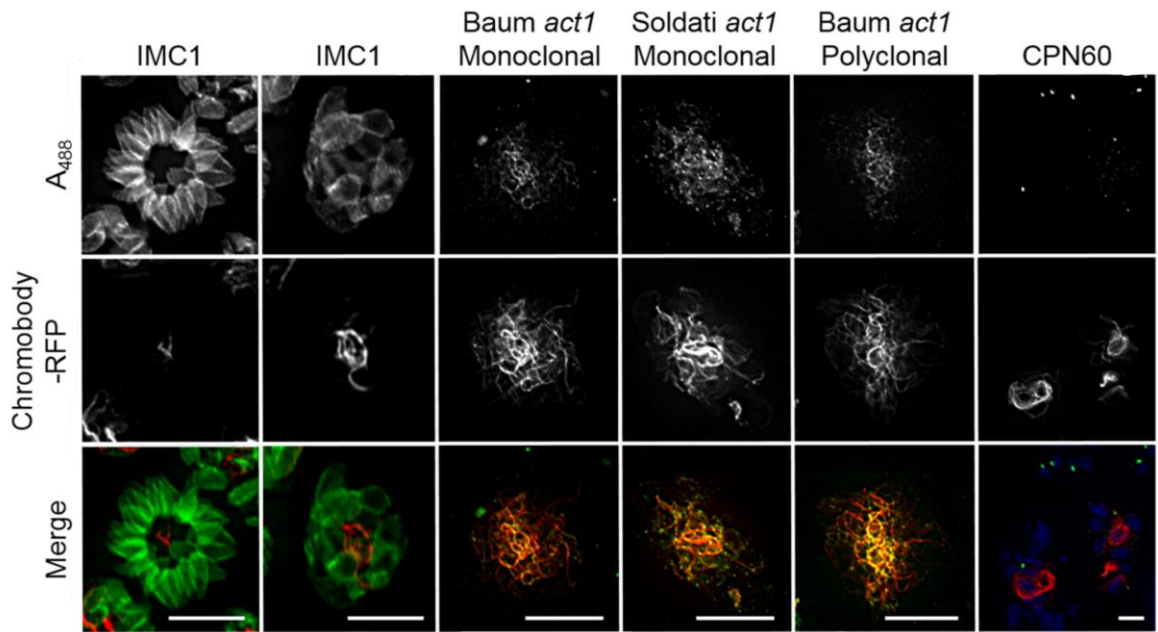


**Figure 5-5: Chromobody-RFP phenocopies the *act1* KO**

The chromobody-RFP expression appears to stabilise the F-actin network during intracellular replication. Antibodies against the IMC highlight that if the cells divide in a normal rosette, the filaments are small and contained within the residual body (left hand image). While large networks cause the vacuoles to become disorganised (see right hand image). Specific antibodies against TgACT1 co-localise with the stabilised F-actin rather than the cytosolic staining normally observed. Apicoplast loss, seen with  $\alpha$ -CPN60 was also observed when the filaments are less dynamic. Scale bars: 10  $\mu$ m.

## 5.5 Stable expression of chromobody-Halo

Next, transgenic parasites stably expressing chromobody-Halo were generated. The chromobody-Halo plasmid was linearised with *Apal*, transfected randomly into RH  $\Delta$ *hxgprt* and selected with the combination of xanthine and MPA (Donald *et al.*, 1996) (Figure 5-1 C). Five clonal lines were isolated and tested for their expression of chromobody-Halo and for their ability to maintain an infection in HFFs over five days (Figure 5-6 A). None of the clones showed significant differences in overall growth, as determined by plaque assays (Figure 5-6 A). Subsequent phenotypic assays showed that expression of chromobody-Halo in clone 1 had no significant effects during the lifecycle. In detail, a trail deposition assay highlighted that parasites expressing the chromobody-Halo have a slightly higher rate of motility than RH (Figure 5-6 B), which might indicate that the chromobody is causing a slight stabilisation of the filaments, in a similar way as low dose treatment with Jas (Wetzel *et al.*, 2003). As for invasion, both RH and clone 1 invade at similar rates through a conventional tight junction (Figure 5-6 C, Figure 5-8 B). Once inside the PV, the parasites begin to replicate. The replication assay highlights that although chromobody-Halo

parasites replicate slightly slower than RH it is not significant. Higher percentages of chromobody-Halo parasites were found to be in early stages ( $\leq 8$ ), while RH had a higher proportion in the 16 parasites per vacuole stage (Figure 5-6 D). Finally, large vacuoles of both RH and chromobody-Halo clone 1 were artificially induced for egress using a calcium ionophore A<sub>23187</sub> for 10 minutes. Vacuoles were counted for their ability to egress using an antibody against the surface antigen SAG1 under non-permeabilising conditions. Both were able to egress at similar rates, indicating that there is no significant difference between parasites (Figure 5-6 E).

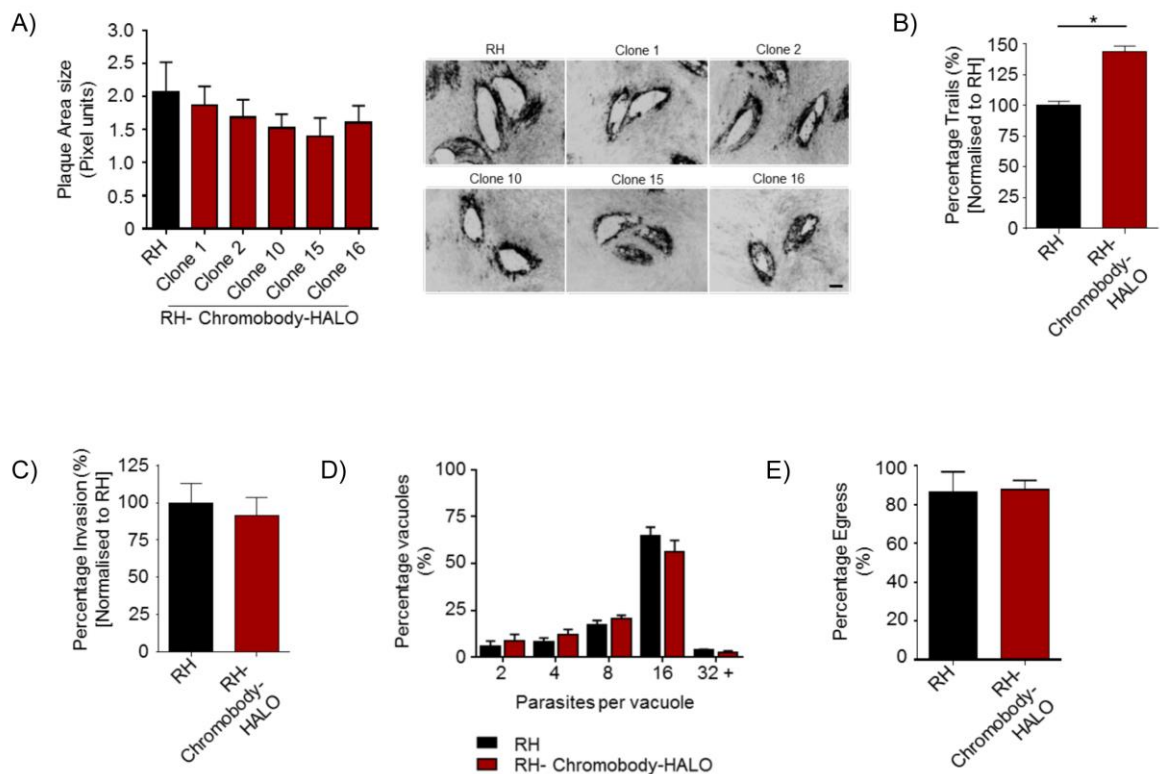


**Figure 5-6: Expression of chromobody-Halo has no effect on the lytic lifecycle**

Parasites stably expressing chromobody-Halo were tested for their lytic lifecycle growth ability compared to wild-type and don't appear to be affected. **A)** A 5-day growth assay between different clones shows no significant difference in plaque area compared to RH. Clone 1 was most similar to wild-type after three independent experiments, so this was used for all other assays. Scale bar, 100  $\mu$ m. **B)** Trail deposition assay where parasites were allowed to glide across FBS-coated coverslips. The number of trails formed was significantly increased in the RH chromobody-Halo parasites, \*  $p < 0.05$ . **C)** No difference is seen in invasion rates of chromobody-Halo parasites compared to wild-type. **D)** Replication is slightly slower but not significantly different. More RH chromobody-Halo parasites are found in the 2, 4 and 8 stages. **E)** No significant difference is seen in egress rates between RH and RH chromobody-Halo parasites. Error bars represent  $\pm$  S.E.M. Datasets were compared with a two-tailed Student's t-test, \*  $p < 0.05$ , non-significant (ns)  $p \geq 0.05$ .

Next, we analysed if vesicular traffic normally occurred, since slight anomalies of vesicular transport could be found in *act1* KO (see chapter 3.6). In the *act1*

KO, it was shown that although the micronemes were tethered to the apical complex, MIC2 seemed to be mis-localised. However, in the chromobody-Halo strain, MIC2 and other micronemal proteins are correctly localised to the apical complex. Moreover, rhoptry proteins 2/4 are tethered to the apical end (Figure 5-7). Dense granule motility is thought to be actin-dependent (Heaslip *et al.*, 2016) and here it is shown that GRA proteins 1 and 2 were indeed secreted into the parasitophorous vacuole as expected. Finally, the apicoplast and mitochondria are normally divided within the chromobody-Halo parasites (Figure 5-7).

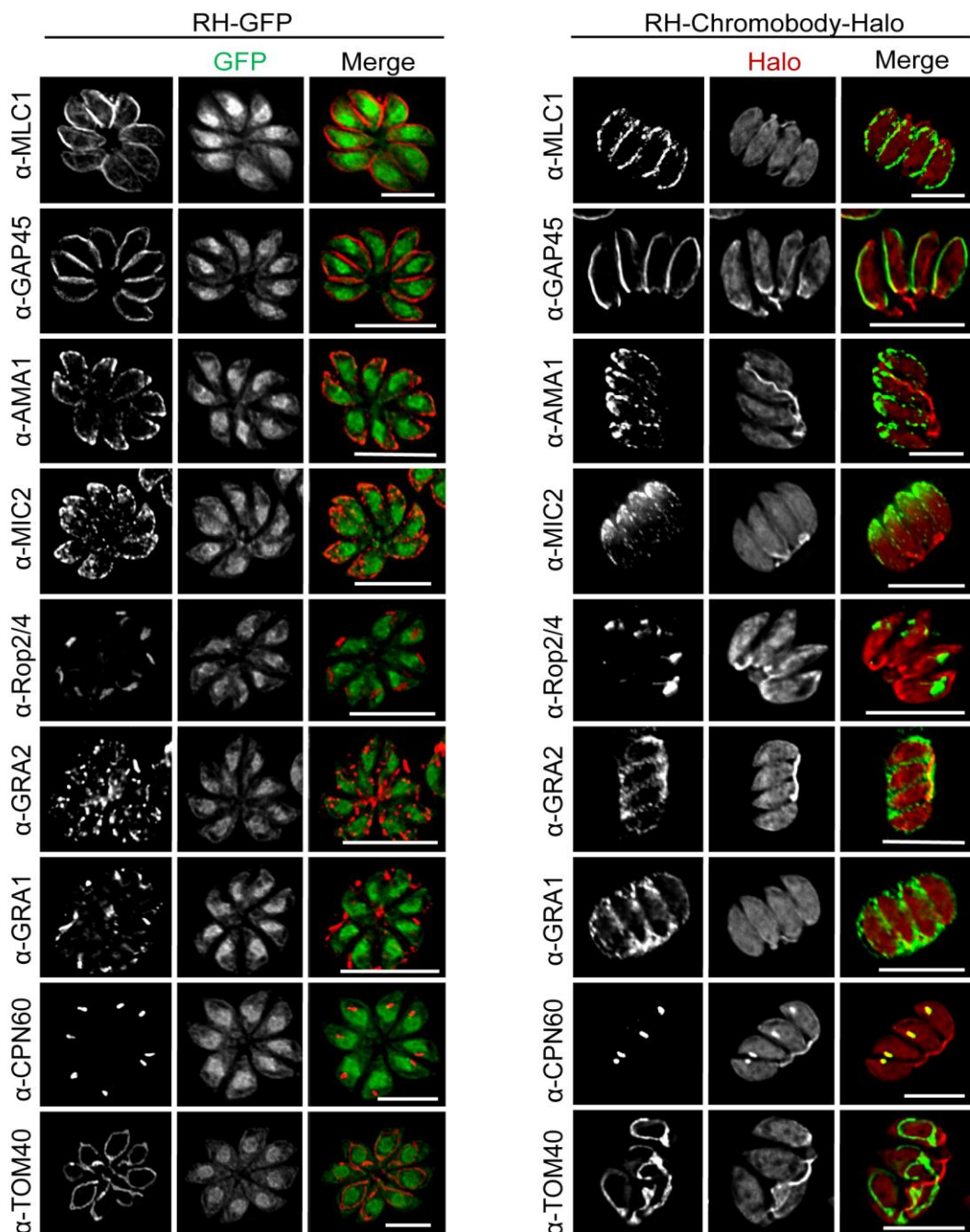


**Figure 5-7: Expression of chromobody-Halo has no effect on protein trafficking or organellar division**

Chromobody-Halo parasites were stained for some protein markers known to be affected by ACT1. Both the micronemes and rhoptries correctly localise to the apical tip. The motor complex appears to be made up normally. Dense granules are also trafficked properly into the PV, and the endosymbiotic organelles (Apicoplast and mitochondria) are divided properly in the chromobody-Halo parasites. Scale bars: 10  $\mu\text{m}$ .

Overall, stable expression of the chromobody-Halo plasmid in RH has no deleterious effects throughout the lytic lifecycle of the parasites. Therefore, we are sure that using the chromobody technology will allow the accurate visualisation of actin filaments without adversely affecting the actin dynamics.

## 5.6 F-actin during gliding and invasion

To further address the question if actin/myosin are producing the force for motility or acting as a molecular clutch (see chapters 3.5 and 6.3), we decided to analyse F-actin dynamics during gliding and invasion. Intriguingly, we failed to detect filaments at the surface of extracellular parasites, where the motor complex is localised. Instead, the chromobody-Halo only shows a cytosolic staining (see also Figure 5-2 A). It was observed that in gliding trails a chromobody-Halo signal was deposited and co-localised with SAG1, indicating that actin must be shed in gliding trails in some fashion during motility (Figure 5-8 A).

During invasion, parasites penetrate through a tight junction consisting of an AMA1-RON2 ring. In *Plasmodium* merozoites, it was observed that actin localises around the RON2 ring during penetration (Angrisano *et al.*, 2012b). Here we wished to check if actin filaments, highlighted by the chromobody-Halo expression, are observed at the tight junction. During penetration, it was observed what could be actin filaments or bundles localise at the basal end of the parasites (Figure 5-8 B). In support of this, a single chromobody-RFP parasite was observed that invaded with a thick actin bundle only at the basal complex (Figure 5-8 E, Supp. Movie appendix 10). Moreover, in the chromobody-Halo parasites, these filament-like structures were only seen in the extracellular part of the invading parasites until the closure of the PV (Figure 5-8 B). During invasion the chromobody signal was almost excluded from the tight junction ring (Figure 5-8 B; white arrows). In contrast, it was shown previously that  $\alpha$ -

ACT1<sup>Polyclonal</sup> from Dr. Jake Baum forms a ring around the parasites that co-localises with the RON2 ring (Angrisano *et al.*, 2012b). Therefore, the  $\alpha$ -ACT1<sup>Polyclonal</sup> was tested on the chromobody-Halo parasites during invasion, however, actin was not observed at the junction with this antibody in our hands (Figure 5-8 C). Although not detected, F-actin may still accumulate at the junction, as the chromobody interaction could be out-competed for the stabilisation by other proteins during invasion. During live invasion events of the chromobody-Halo parasites (one frame per second for both DIC and A<sub>594</sub>), only a cytosolic staining was observed (Figure 5-8 D, Supp. Movie appendix 9). Although an accumulation of signal was observed in the extracellular part of the parasites, this is most likely from the focal point of the sample or that cytosolic chromobody-Halo protein is squeezed to the basal end. The stabilised filaments from the chromobody-RFP were only observed at the basal end of the parasites during invasion (Figure 5-8 E, Supp. Movie appendix 10).

In summary, no obvious F-actin filaments were detected during gliding and invasion that are consistent with a linear motor model or the retrograde membrane flow model (see Chapter 6). While there appears an accumulation of F-actin at the posterior pole of the parasite during invasion, further analysis is required to confirm these data.

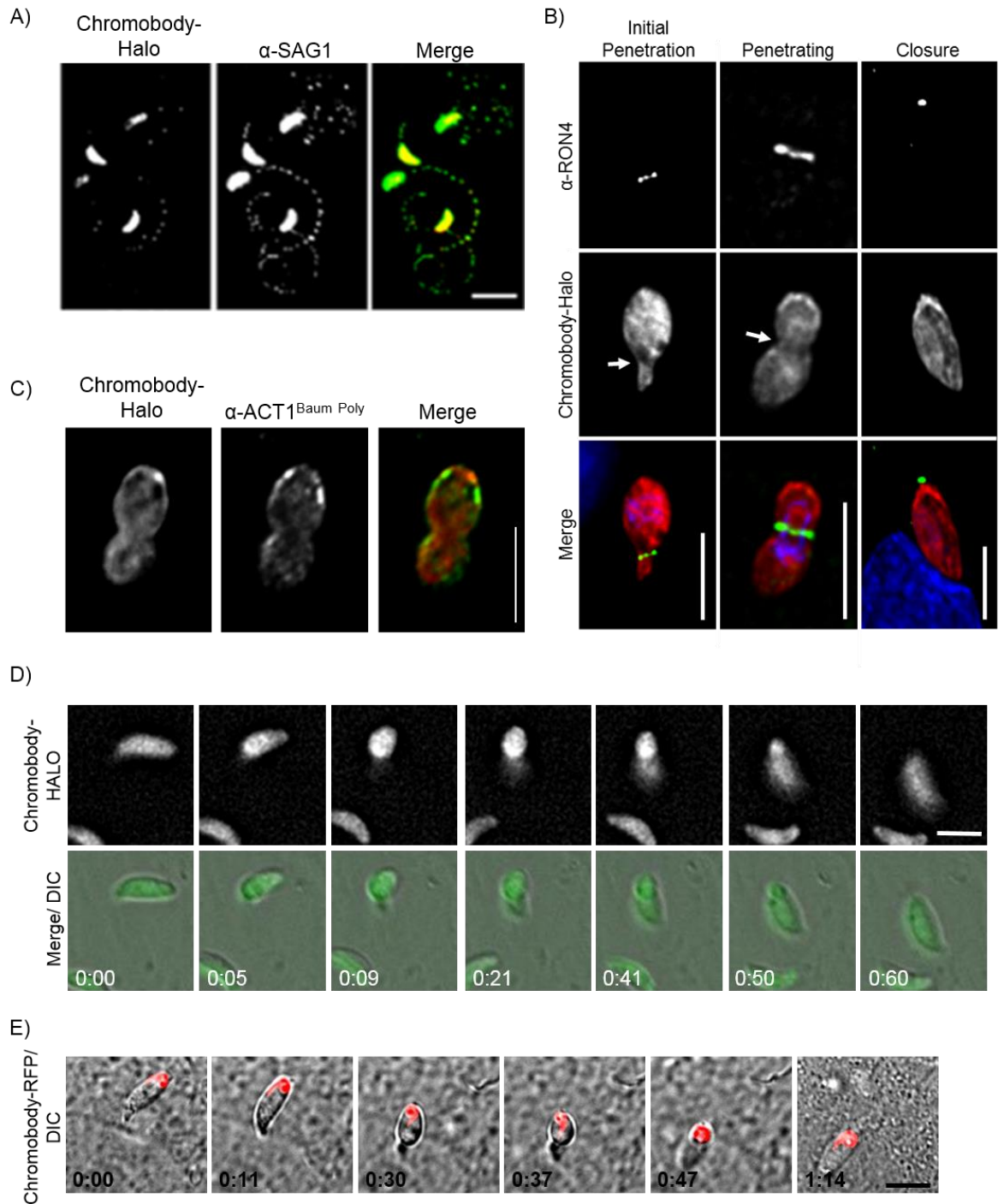


**Figure 5-8: Actin filaments during gliding and invasion**

Actin filaments were expected to be near the IMC during gliding and invasion. **A)** Halo-TMR ligand indicates that actin is secreted into the trails during gliding motility. No such filaments were observed within the parasites. **B)** F-actin appears to be at the basal end of the parasites during while the parasites penetrate through a tight junction. As the parasites penetrate, it appears in many parasites that chromobody-Halo is excluded at the tight junction ring. **C)** F-actin is not seen at the RON2 ring either with chromobody-Halo or the F-actin preferential ACT1 antibody. Live cell video microscopy of invading parasites. **D)** During invasion of chromobody-Halo parasites, no change in signal was observed. **E)** Stabilisation of F-actin with chromobody-RFP parasites indicates that they invade with a large actin network at the basal end of the parasites. Scale bar, : 5  $\mu$ m.

## 5.7 Actin forms a network during intracellular replication

During the intracellular stages of the tachyzoite lifecycle, a vast actin network was observed within the PV connecting to the parasites cytosol similar to filopodia or nanotubes. Here we wished to understand the actin dynamics during replication. This analysis was performed by Dr. Clare Harding using a GAPM3-YFP and GAPM1a-YFP strain as markers for the IMC and chromobody-Halo for F-actin (Figure 5-9). During replication, these filaments are highly dynamic and change continually during the developmental stages. During the early stages of daughter formation, F-actin is seen at the posterior end of the parasites (Figure 5-9). However, in later stages of development, F-actin localises to the developing IMC of the daughter cells (Figure 5-9, Yellow arrows, Supp. Movie appendix 11). Prior to the end of replication, the IMC of the mother collapses and appears to be recycled into the daughter cells suggesting a role of F-actin in recycling at the final stages of endodyogeny (Figure 5-9, White arrows, Supp. Movie appendix 11). During the latter stages of development, GAPM3 vesicles were also observed to be recycled from the mother cell to the daughters and between parasites at the basal complex. This indicates that F-actin might also be required for vesicular trafficking, supported by the CLEM (Periz *et al.*, 2017).

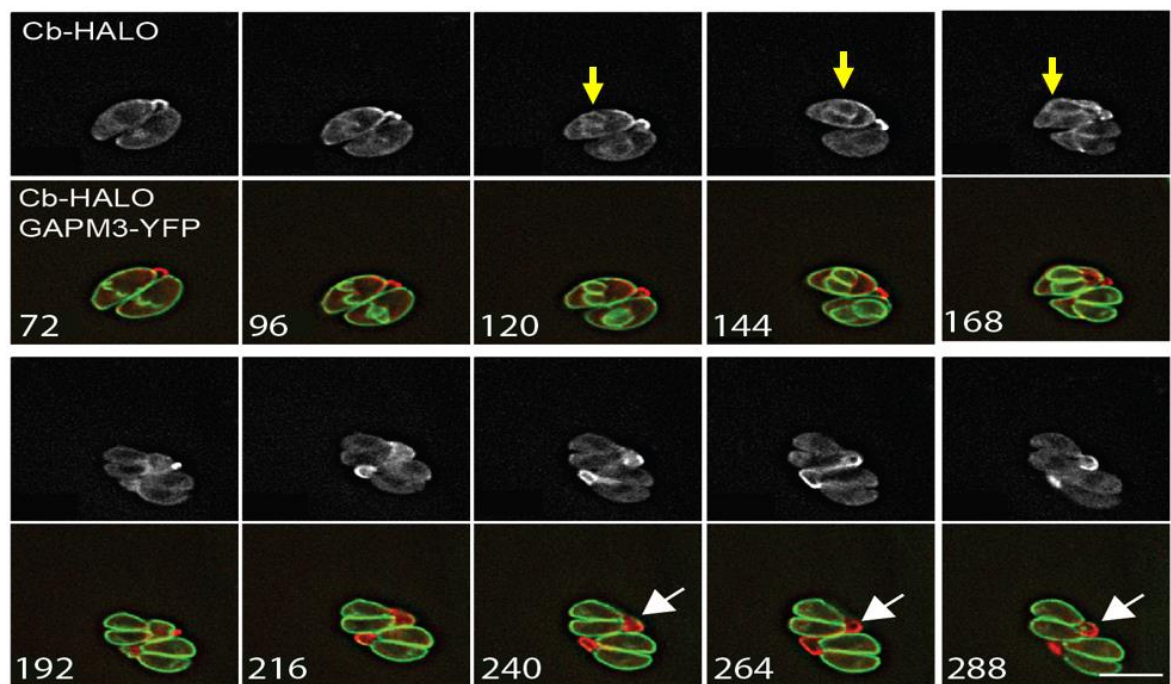


**Figure 5-9: F-actin is dynamic and controls replication.**

F-actin was assessed during parasite replication using GAP-M3 as a marker for the IMC. GAPM3-YFP expressing parasites transiently expressing chromobody-Halo were imaged every 6 mins for 5 hours. F-actin can be seen initially connecting the basal end of the parasites before accumulating

beneath the newly forming daughter cells. At this stage, it concentrates at the rear of the new daughters during emergence and recycles IMC maternal (see, Supp. Movie appendix 11). Scale bar: 5  $\mu$ m, time stamp in minutes. Figure from Dr. Clare Harding and Madita Reimer.

This actin network is highly dynamic during endodyogeny and may be required for organisation of the parasites within the PV. To test this, the network was viewed in scanning electron microscopy. Wild-type (RH), RH chromobody-Halo, RH chromobody-RFP (a transient expression that stabilises the filamentous network) and *act1* KO parasites were analysed. All parasite strains were infected onto HFFs and grown for 24 hours or 30 hours in the case of the *act1* KO. Coverslips were fixed in EM fixative and processed by Dr. Leandro Lemgruber as described in (Magno *et al.*, 2005). Interestingly, structural tubules appear to connect the basal end of the parasites to a central core, probably the residual body (Figure 5-10 A). These connections were also observed in untransfected wild-type parasites. While connections were also observed in the chromobody-RFP parasites, there is a large mass around the residual body and a loss of connections to some parasites causing a minor organisational defect (Figure 5-10 A). Moreover, the *act1* KO shows a complete disorganisation of the parasites within the vacuole and no visible tubule structures were observed between individual parasites (Figure 5-10 A).

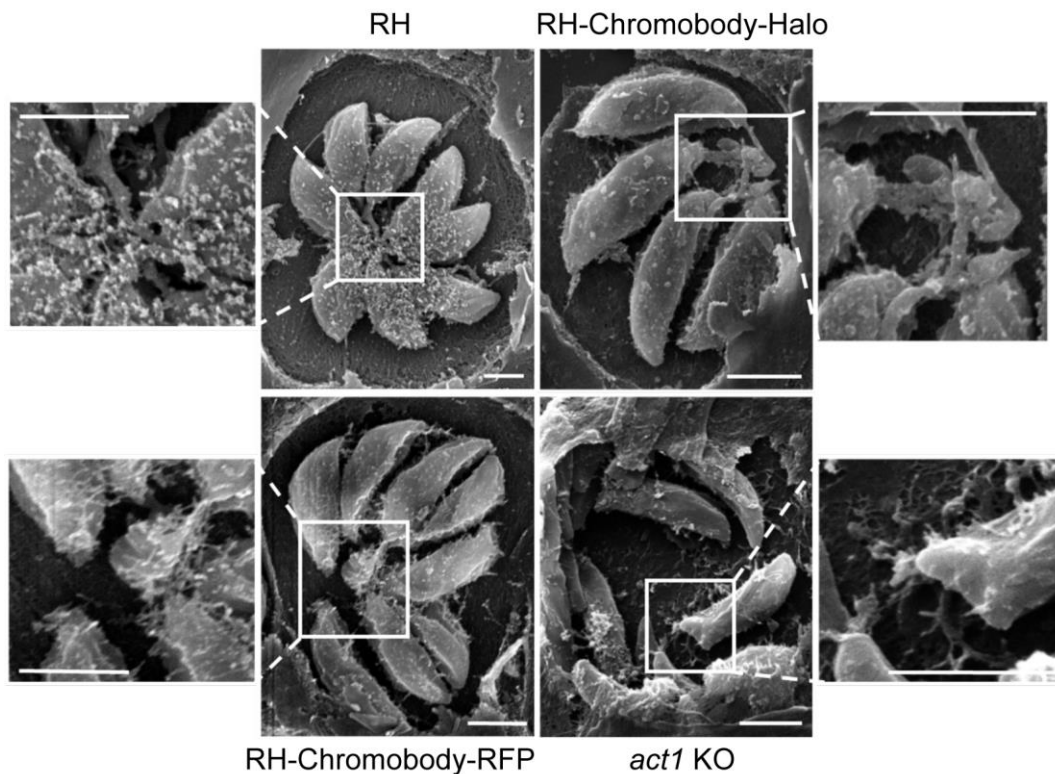


**Figure 5-10: F-actin holds parasites during replication from the residual body.**

Scanning EM of wild type (RH), chromobody-Halo, chromobody-RFP and *act1* KO parasites showing the tubule-like network connecting parasites from the posterior end. The *act1* KO parasites are disorganised within the vacuole and form no connections, while the chromobody-RFP indicates that some parasites have broken their connections to the residual body. Scale bar: 2  $\mu\text{m}$ . Images provided by Dr. Leandro Lemgruber, WTCMP imaging technologist.

To conclude, F-actin is involved in late stages of replication and suggested a role of F-actin during IMC recycling. This supports data from chapter 3.6.1 that the *act1* KO cannot recycle its IMC efficiently causing a flattened basal complex, and that vesicles are transported along filaments seen in Figure 5-4 and Figure 5-9. Actin filaments are required in order to organise daughter parasites within the PV.

## 5.8 *Toxoplasma* ACT1 interacts with the apicoplast

One significant phenotype of the *act1* KO is the inability to replicate the apicoplast in dividing parasites (Andenmatten *et al.*, 2012; Egarter *et al.*, 2014). Changes in expression of actin binding proteins; profilin (Plattner *et al.*, 2008), actin depolymerising factor (ADF) (Haase *et al.*, 2015; Mehta & Sibley, 2011) or the FH2 domain of formin 2 (Daher *et al.*, 2010) also affects the ability of the apicoplast to divide. These proteins are known to control F-actin dynamics. It has also been implicated that the class-XXII myosin F is necessary during the separation of the apicoplast during replication (Jacot *et al.*, 2013). Taking together, apicoplast inheritance is tightly regulated in an actin-myosin dependent fashion. The lack of visualised filaments has so far inhibited the understanding of the dynamics of actin during this process.

With the chromobodies, we wished to understand the dynamics during apicoplast division. Super-resolution microscopy and 3D reconstruction of the filaments highlighted a direct interaction between the apicoplast and the filaments (Figure 5-11). In both the chromobody-RFP (Figure 5-11 A) and chromobody-Halo (Figure 5-11 B) parasite lines, it appears that some apicoplasts are in contact with the filaments. However, it is still unknown how these large filaments that appear outside of the parasite but inside the PV actually come in contact with the apicoplast. More work will have to be conducted to determine.

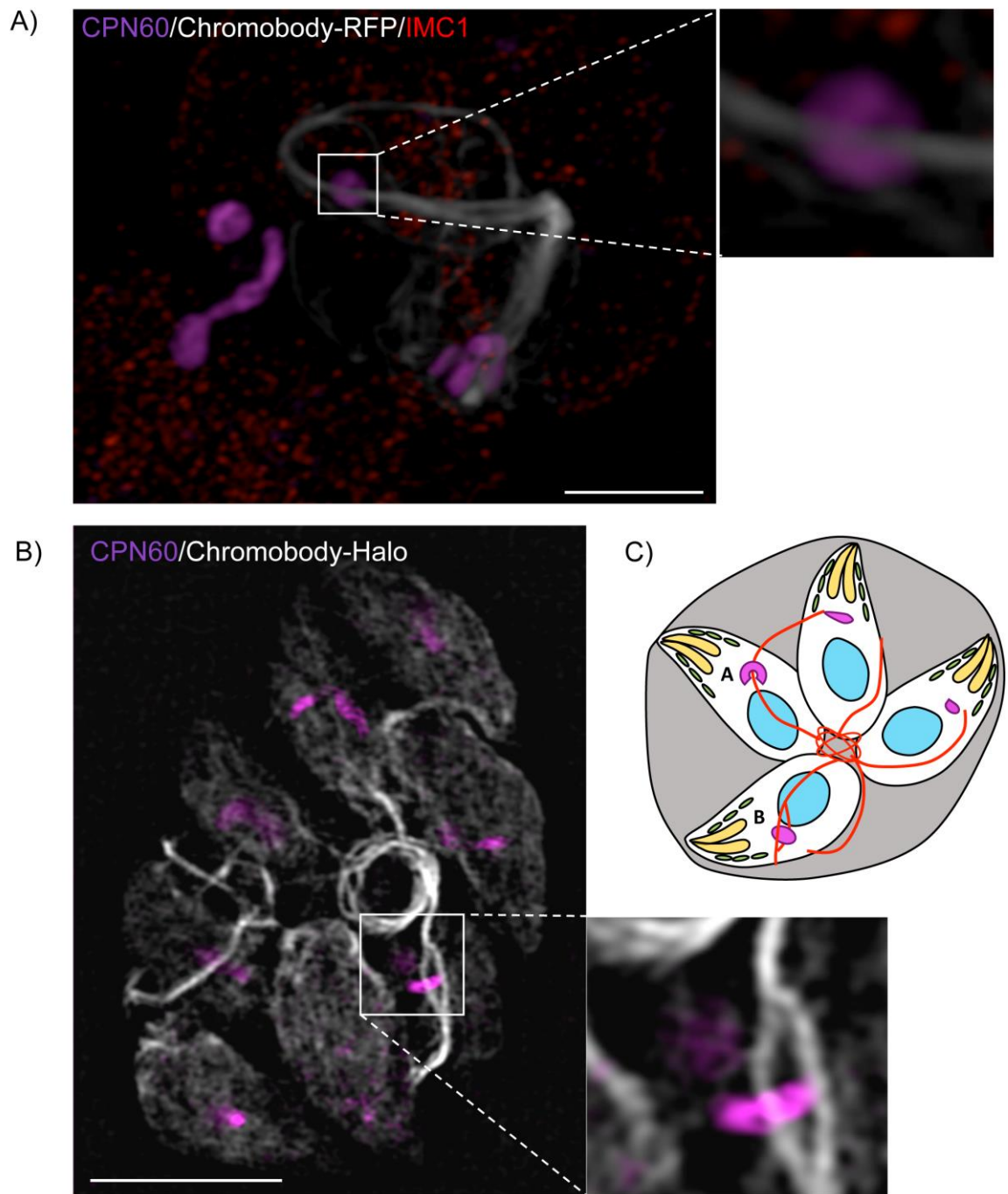


**Figure 5-11: F-actin interacting with apicoplasts**

Filamentous actin appears to interact with the apicoplast within *T. gondii* tachyzoites. **A)** A super-resolution 3D-SIM of chromobody-RFP actin filaments (White) and apicoplast (pink). The red speckles are from the  $\alpha$ -IMC antibody. Scale bar: 10  $\mu$ m. Insert panel shows the apicoplast to wrap around the actin filament. **B)** SR-SIM of chromobody-Halo parasites highlighting the F-actin network (White) and apicoplasts (Pink). Boxes from the main image are zoomed in projections to indicate apicoplast interactions. Scale bar: 10  $\mu$ m. **C)** Schematic representation of *Toxoplasma* tachyzoites within a vacuole, highlighting F-actin and apicoplasts. In this representation, the actin filaments are depicted in red, while the apicoplasts are depicted in pink as per the images in (A and B). Some apicoplasts are drawn to interact with the F-actin where the parasite A represents in image A and parasite B for image B.

## 5.9 Parasites make F-actin connections with neighbouring vacuoles

Immediately after invasion, dense granule proteins are secreted from the parasite where they begin to modulate the parasitophorous vacuole (PV). Key dense granules, namely GRA2, 6, 8 and 12 are exported and initiate the formation of the tubo-vesicular network. This network has been shown to initiate through the residual body of the parasite holding the newly forming parasites (Mercier *et al.*, 2005; Mercier *et al.*, 2002). After observing F-actin connecting individual parasites within the vacuole from the parasites basal complex, we predicted that this might be similar to the tubo-vesicular network (TVN). To test this, dense granule markers were used that make up the TVN (Gra2) and the surrounding PVM (Gra7). While the TVN and PVM formed as expected, a surprising observation arose. On rare occasions, it appeared that the chromobody-Halo signal was observed connecting two distinct vacuoles together (Figure 5-12 A). These connections can be seen both between vacuoles in the same host but more interestingly between vacuoles from different host cells, sometimes over great distances (>50  $\mu\text{m}$ ) (Periz *et al.*, 2017). Moreover, it was observed that dense granule proteins, Gra2 and 7, follow these F-actin extensions (Figure 5-12 A). Upon super resolution of the chromobody-Halo connection with  $\alpha$ -Gra7, it was shown that Gra7 forms a tubule-like structure with an F-actin core (Periz *et al.*, 2017). It was also observed that not all connections were chromobody-Halo positive, indicating that the F-actin connections are very transient and probably depolymerises after the connection is established. This observation was supported with live cell video microscopy of chromobody-Halo parasites, where the chromobody filament touched a neighbouring vacuole then receding (Supp. Movie appendix 12) (Periz *et al.*, 2017). It should be noted that Gra2 positive extensions were also observed in the *act1* KO. However, these extensions were not observed connecting two vacuoles together. Other groups have also described connections between vacuoles with Gra3 and Gra7 (Dunn *et al.*, 2008) and by the group of Dominique Soldati (Abstract BioMalPar XII, 2016). Interestingly, tubular-like connections were also observed in SEM images of the chromobody-Halo and wild-type (RH) parasites (Figure 5-12 B).

Together, it appears that dense granules are pushed out by F-actin and the dense granules make a tubule-like structure around an F-actin core. The exact physiological functions of these protrusions are still unknown. However, the connections could function similar to nanotubes in other systems that are required for intracellular transfer of vesicles (Gerdes & Carvalho, 2008; Zhu *et al.*, 2015) or communication (Marzo *et al.*, 2012; Szempruch *et al.*, 2016).

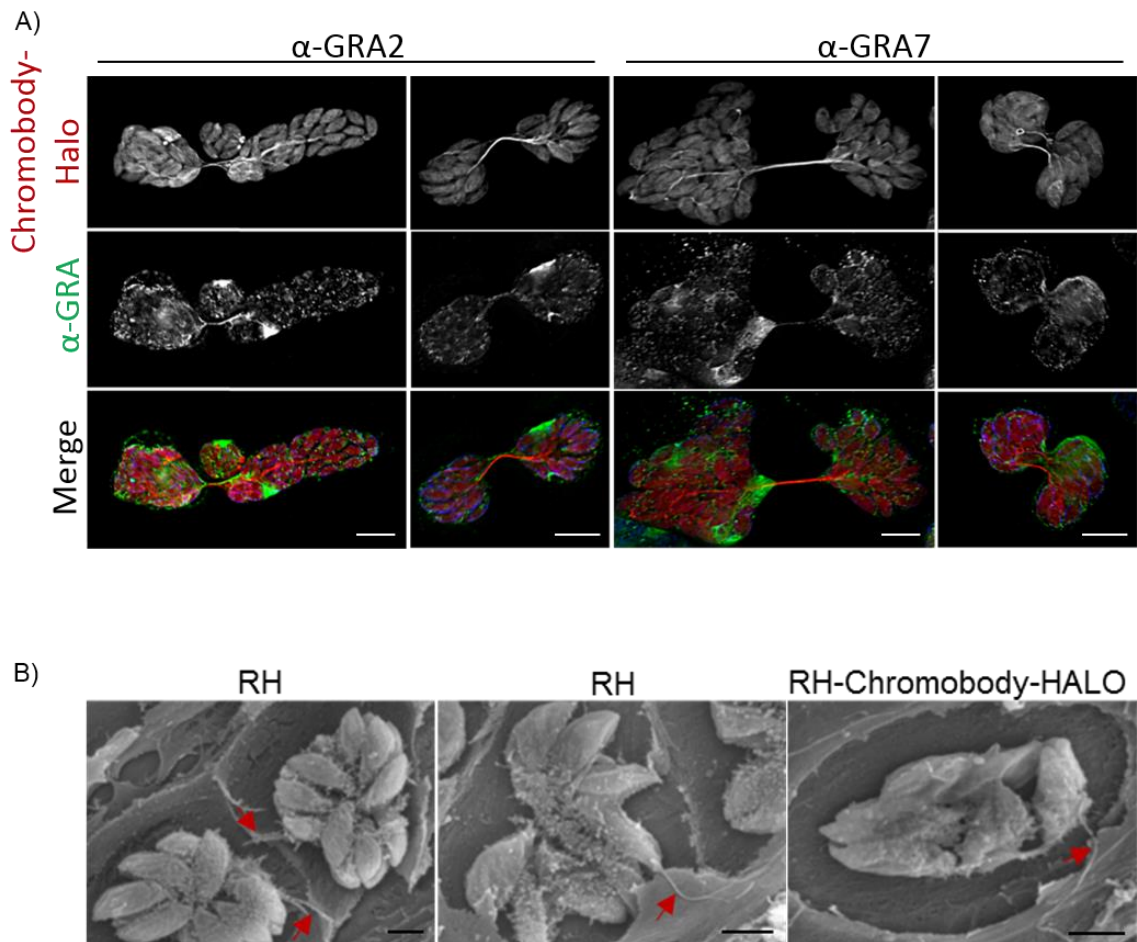


**Figure 5-12: F-actin makes connections between neighbouring vacuoles**

**A)** Connections between vacuoles were observed to be made up of an F-actin core surrounded by a dense granule tubule-like structure. **B)** Tubule-like extensions leaving from one vacuole are also seen in scanning EM of both wild-type (RH) and RH chromobody-Halo vacuoles. Scale bars: IFA: 10  $\mu$ m and SEM: 2  $\mu$ m. EM images provided by Dr. Leandro Lemgruber.

## 5.10 The actin network breaks in a calcium-dependent manner before egress

The mechanism by which parasites escape from the host, termed egress, is thought to be essential to escape the innate immune system *in vivo* or from a dying host cell (Blader *et al.*, 2015). Egress occurs by fluctuations in intracellular calcium levels, either natural or ionophore-induced, a drop in pH or

change in potassium levels (Blader *et al.*, 2015). It is understood that the parasites actomyosin system is necessary for egress to initiate gliding motility in a similar function as invasion (Hoff & Carruthers, 2002; Wirth & Pradel, 2012).

Actin was recently implicated to be essential for egress due to phenotypes observed with the conditional *act1* KO (Egarter *et al.*, 2014) or incubation with high concentrations of CD (Lavine & Arrizabalaga, 2008), indicating that filamentous actin is important during this process. Here, we wished to look at actin filaments during egress through live-cell video microscopy.

Chromobody-Halo parasites were grown in a confluent layer of HFFs in live cell dishes for around 36 hours. Halo-TMR (1:10,000) was incubated in the live cell dish for 10 minutes at 37 °C. The dish was then transferred to the DeltaVision Core with an incubator set for standard culturing conditions. Vacuoles containing an extensive filamentous network were focused on, and images were taken every second for DIC and A<sub>594</sub> with the adjusted exposure for each channel. The image sequence was initiated, after which time, 10 μM Ca<sup>2+</sup> ionophore was added to the media. These filaments appear to break up after addition of calcium to the media (Figure 5-13 A, Supp. Movie appendix 13). Although, it would seem that F-actin disassembly is a downstream result of calcium signalling cascade required for egress, at this time we still do not have the evidence for causation. Once the network breaks, many punctate dots are observed throughout the vacuole along with either one or two large actin dense areas (Figure 5-13). Then the vacuole membrane shrinks and the parasites initiate motility to escape (Figure 5-13 B, C, Supp. Movie appendix 14, 15). Upon closer inspection of the parasites expressing chromobody-Halo, a distinct signal was detected at the rear of the parasites, suggesting that actin may accumulate at the rear similar to the basal signal observed during invasion (Figure 5-8 C, Supp. Movie appendix 15).

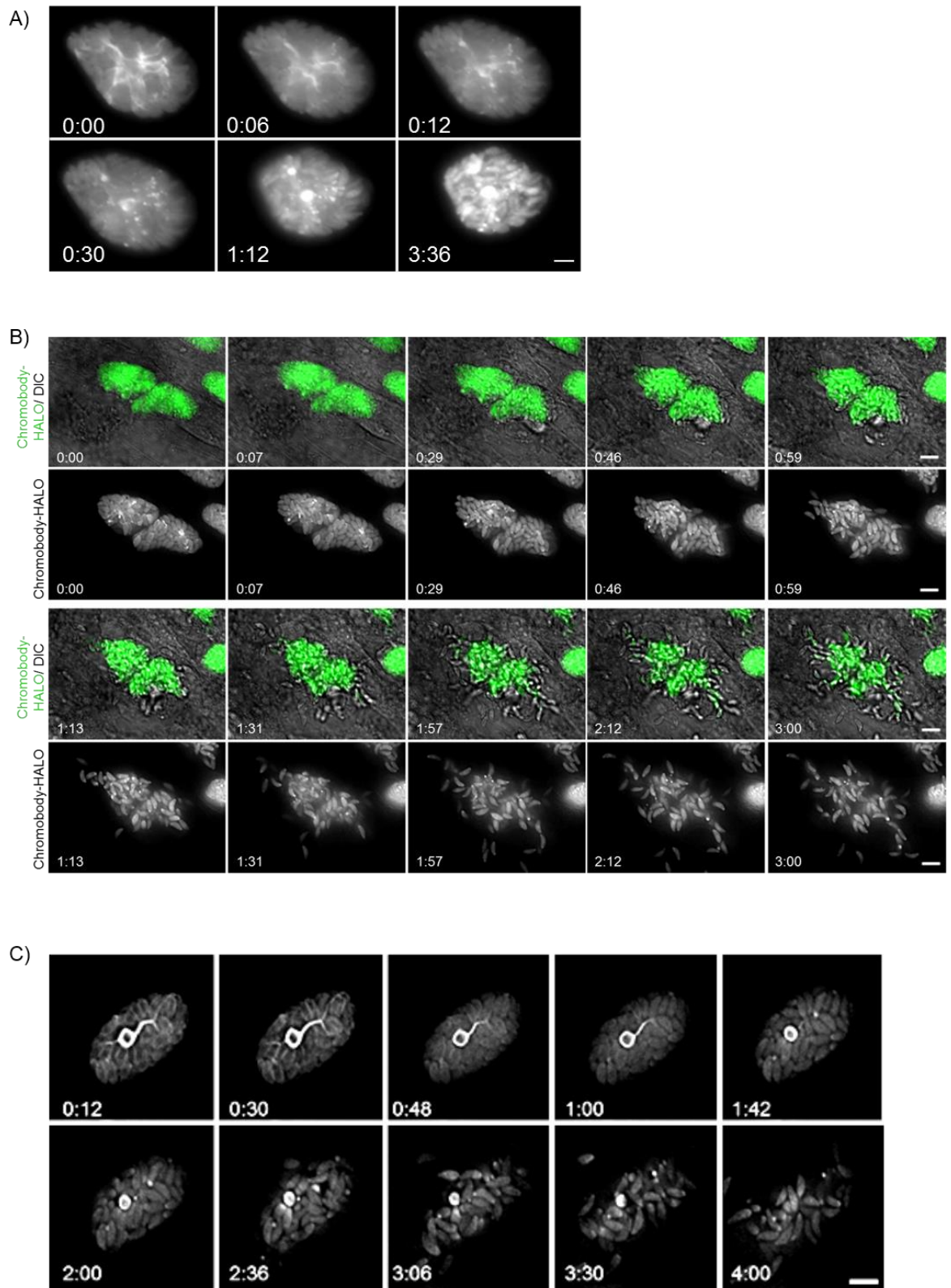


**Figure 5-13: The actin network breaks in a calcium-dependent manner before egress**

Parasite escape was artificially induced with a calcium ionophore. **A)** The filamentous network breaks up in a calcium-dependent manner, and the vacuole shrinks even if the parasites do not escape. **B and C)** Parasites need to break up this network before they initiate motility out of the cell. It appears the signal for membrane rupture is after the filaments break up. Scale bars: 10  $\mu\text{m}$ . Time stamp: m:ss.

In some cases, after the large filamentous network breaks parasites can still be seen connected to other parasites (Figure 5-14 A, Blue arrows). These can stretch while the parasites that are connected move in opposite directions (Supp. Movie appendix 16). Moreover, some escaping parasites were retracted back towards the PV, like being held by an elastic band (Figure 5-14 B, Supp. Movie appendix 17). Upon overexposure of the image, an extremely thin filament was observed holding this parasite (Figure 5-14 C). This may suggest that small microfilaments, possibly containing an F-actin core hold the parasites, and these, in turn, are also required to break to escape the host successfully.

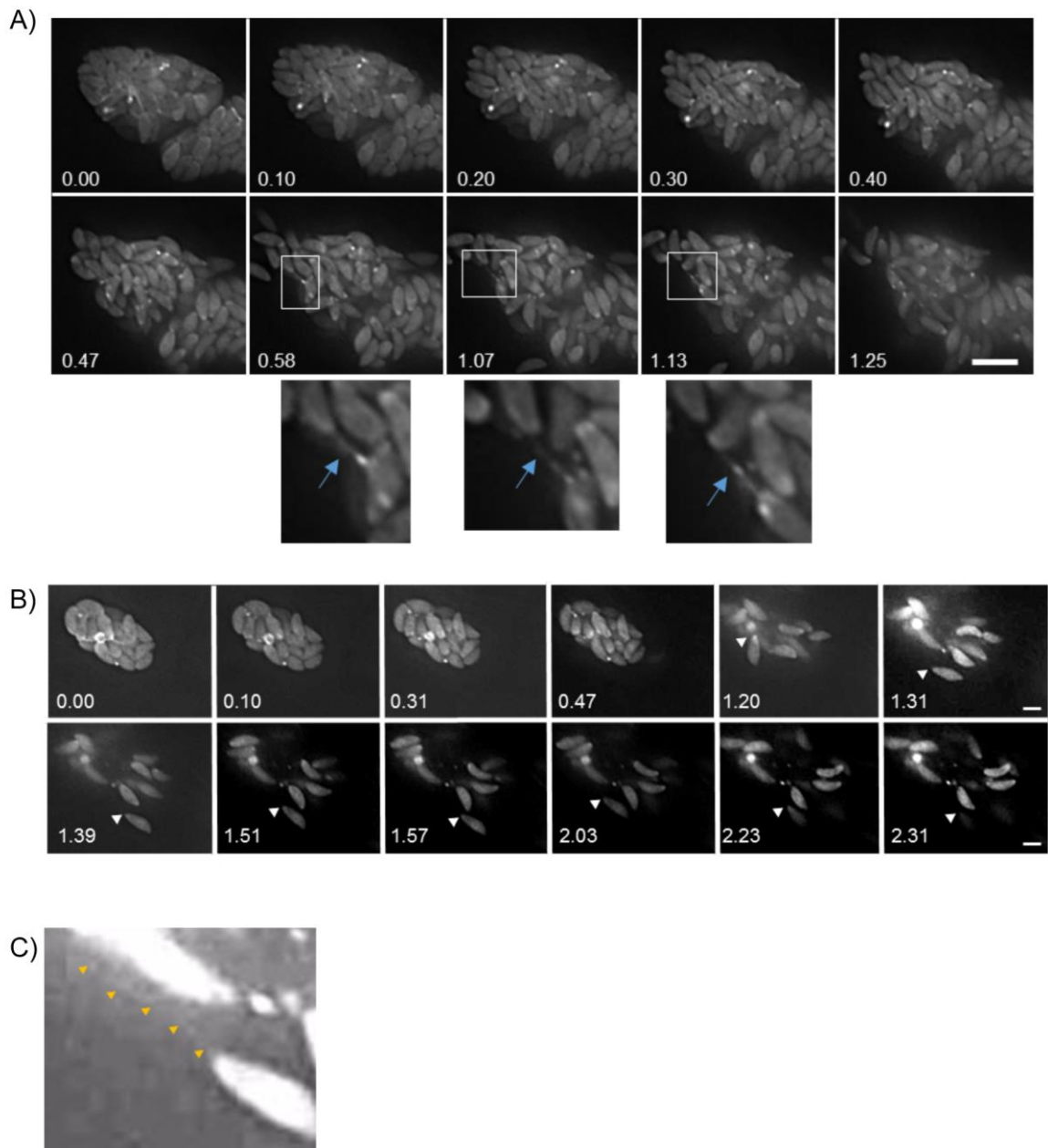


**Figure 5-14: Short filamentous-like structures hold the parasites together even after the vast network has been fragmented.**

After calcium ionophore triggered egress has occurred, parasites initiate motility out of the vacuole. **A)** Some remain held together with filamentous-like structures. **B)** These structures are rather flexible, and the parasites are sprung back towards the vacuole, similar to an elastic band. This must break before the parasite can successfully re-invade a new host cell. **C)** Overexposure of the rebounding parasite from (B). Yellow arrowheads indicate a potential connection. Scale bars: 10  $\mu\text{m}$ . Time stamp; m:ss.

In summary, F-actin is required for parasites to egress and that these filaments may have an essential role in calcium signal transduction. It has previously been shown that CDPK1 and 3 are required for egress (Lourido *et al.*, 2010; McCoy *et al.*, 2012; Nagamune *et al.*, 2008). Moreover, CDPK3 phosphorylates the MyoA motor during egress (McCoy *et al.*, 2012), and is possible that this signal is translocated along F-actin synchronising the parasites to initiate motility.

## 5.11 Summary and conclusions

This chapter has provided evidence that *Toxoplasma* parasites do indeed form actin filaments that appear to depend on a critical concentration of G-actin. F-actin has multiple functions during the intracellular stages of the lifecycle; from parasite replication during endodyogeny, organising the PV, apicoplast division and egress. Parasites replicating by endodyogeny, are held together with tubules containing actin filaments. Upon triggering egress with an increase in intracellular  $\text{Ca}^{2+}$  levels, the filaments depolymerise rapidly which must occur before motility can be initiated. So far, there has been no observed evidence of actin at the parasite pellicle where the motor complex should be situated during gliding and invasion, but this study has provided preliminary observational signs of actin accumulating at the rear of motile and invading parasites. Future experiments controlling the signal to noise ratio of the chromobody may reveal more about this basal localisation or even F-actin at the pellicle.

## Chapter 6 A new outlook on parasite motility

Cell motility of non-flagellated organisms depends on the coupling of intracellular forces to a substrate (Keren, 2011; Mogilner & Oster, 1996). Motility of apicomplexan parasites is predicted to occur through a linear motor complex, once known as the ‘glideosome’ (Keeley & Soldati, 2004). This model predicts that the actin-myosin motor complex produces forces through interactions with transmembrane proteins to propel parasites across the substrate (Meissner, 2013; Soldati & Meissner, 2004). Throughout this thesis, evidence has been shown that actin, at the core of the complex, is important but not essential for motility. Moreover, components of the motor complex once thought to be essential are no longer critical to motility, in particular the myosinA motor (Andenmatten *et al.*, 2012; Egarter *et al.*, 2014). These discoveries lead our group to suggest a novel model of motility based on gelation/solation (Egarter *et al.*, 2014). This model predicts that actin and other cations generate osmotic pressures within the cytoplasm of the parasite. In turn, if adequate adhesion sites exist ahead of the parasite, this pressure pushes the leading edge forward. Subsequently, the parasite detaches from its substrate at the rear and the cytoplasmic flow of macromolecules generates an osmotic gradient that traverses to the apical end in a ‘continual loop’ (Egarter *et al.*, 2014). Here, evidence has been provided in support of this model.

### 6.1 Blocking microneme secretion/recycling abolishes motility

In crawling cells, such as *Dictyostelium* and human leukocytes, it has been shown that these cells not only crawl across a substrate, but can swim efficiently when suspended in a viscous medium consisting of Ficoll 400 (Barry & Bretscher, 2010; Howe *et al.*, 2013). By observing cells swimming, it became apparent that adhesion to a solid surface is not necessary for cell movement, although the rate at which these cells move is decreased compared to adherent cells (Bretscher, 2014). This suggests that motility could be driven purely by surface membrane flow. This ‘swimming’ would result primarily from a secretory-endocytic cycle acting as a fluid drive from the anterior to the posterior end of the cell (Bretscher, 1976; Bretscher, 1996a; Bretscher, 2014). In support of this, *Toxoplasma* tachyzoites move well through a 3D matrix without well-defined

attachment sites (Leung *et al.*, 2014a). Therefore, the possibility of a secretory/endocytic cycle occurring during gliding motility of tachyzoites was investigated. Here we predict that secretion of micronemal proteins at the apical end of the parasite could serve to drive the membrane in a retrograde manner towards the basal end.

The importance of microneme secretion in motility has been shown in many studies over the years. Extracellular parasites incubated in a high potassium buffer (Endo Buffer) are unable to secrete micronemes (Endo & Yagita, 1990) and consequently cannot move (Figure 6-1 A, C). In contrast, all known enhancers of gliding motility are associated with increased levels of microneme secretion (Carey *et al.*, 2004b; Child *et al.*, 2013). While in the past, enhanced gliding motility was attributed to the deposition of micronemal proteins on the parasite membrane, it could be hypothesised that enhanced motility is instead due to the generation of a rapid membrane flow which generates the force for motility. By this model, membrane shedding at the posterior pole would lead to increased lipid disposition at the apical pole to act as a balance, as previously shown (Hakansson *et al.*, 1999). In addition, endocytosis, which is known primarily for nutrient uptake, could also mediate the recycling of lipids. However, no clathrin-mediated endocytosis has been observed in *T. gondii* (Pieperhoff *et al.*, 2013). To determine if clathrin is involved in lipid reuptake, PitStop2 was used as an inhibitor of clathrin independent endocytosis (CIE) and looked for defects in gliding motility. Pitstop2 blocks CIE in mammalian cells by interacting with the amino-terminal domain of clathrin (Dutta *et al.*, 2012). Blocking CIE in extracellular tachyzoites was shown to abolish their ability to glide (Figure 6-1 B, C). It should be noted that studies have shown that PitStop2 can also cause off-target effects (Dutta *et al.*, 2012; Liashkovich *et al.*, 2015). Therefore, other inhibitors of CIE should be tested to validate these observations.

This study presents preliminary data that endocytosis may be important for motility in *Toxoplasma* tachyzoites through an unknown mechanism. Taken together, a secretion and recycling system may be required for motility of the parasites, which would be similar to the retrograde flow observed during amoeboid movement.

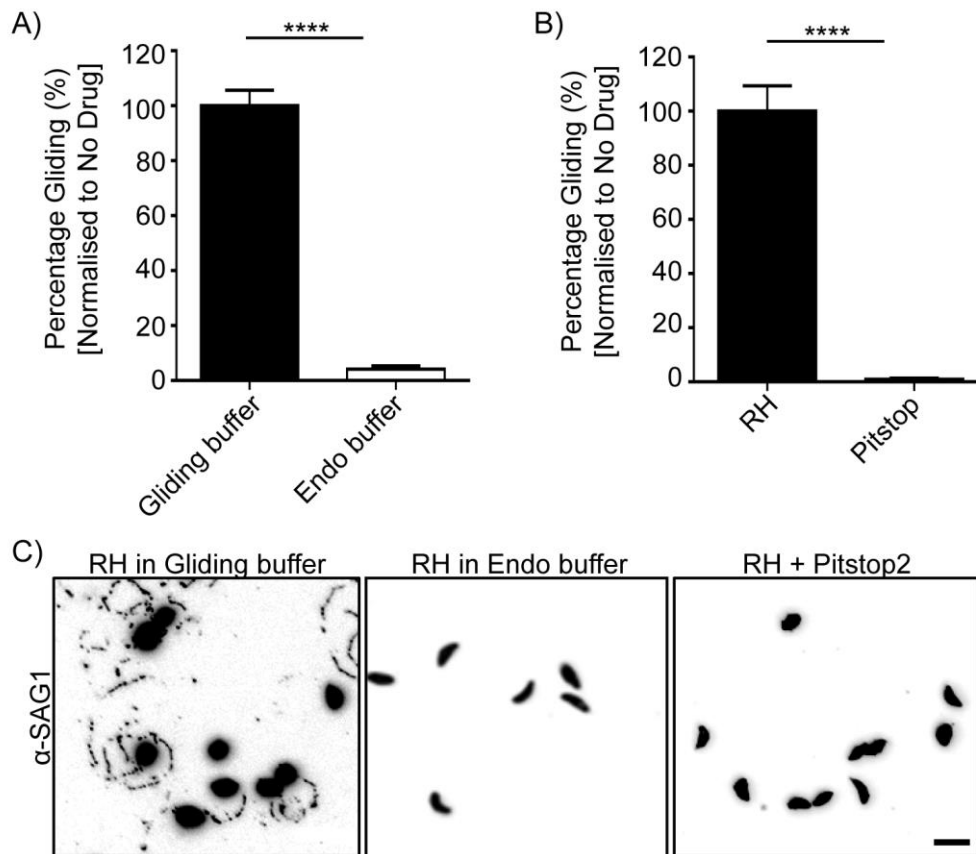


**Figure 6-1: Inhibition of microneme secretion or recycling blocks motility**

Trail deposition assays under conditions that block microneme secretion or membrane recycling. **A)** Wild-type parasites were allowed to glide over FBS-coated coverslips in either gliding or Endo buffer. Endo buffer inhibits microneme secretion and significantly reduces motility. **B)** Wild-type parasites were allowed to glide with or without the endocytic inhibitor; PitStop2 (30  $\mu$ M). Inhibition of membrane recycling abolishes motility. Error bars represent  $\pm$  S.E.M. Datasets were compared with a two-tailed Student's t-test, \*\*\*\*  $p < 0.0001$ . **C)** SAG1 trails deposited during gliding motility of RH in gliding buffer, Endo buffer or with 30  $\mu$ M PitStop2. Scale bar: 10  $\mu$ m.

## 6.2 The ability for parasites to cap their membranes is actin-independent

In motile cells, retrograde membrane flow causes a distinct capping of surface ligands (Bretscher, 1996a; Bretscher, 1996b). In the case of apicomplexan parasites, a recent study demonstrated the importance of a retrograde membrane flow in motile *Plasmodium* sporozoites. This study showed that a bead bound to the parasite surface is translocated to the rear of the parasite through a membrane flow with a rate somewhat faster than motility itself (Quadt *et al.*, 2016). Interestingly, this flow still occurs in the presence of actin disrupting drugs (Quadt *et al.*, 2016). The addition of cytochalasin D (CD) had no significant effect on the speed of bead translocation, while the force generated to move the bead was significantly reduced at high concentrations (Quadt *et al.*, 2016). Previously in this thesis, it was shown that CD and loss of ACT1 have an

effect on parasite attachment under flow conditions (see chapters 3.5 and 4.1.3). Therefore, the reduced force acting on the bead could also result from a failure to transmit, rather than generate, the force. This raises the possibility that apicomplexan motility may be similar to amoeboid-like crawling. We speculate that *Toxoplasma* could generate a retrograde membrane flow in the absence of the acto-myosin system.

To test this hypothesis, an examination was carried out on the parasites ability to translocate fluorescent latex beads (40 nM FluoSpheres® Carboxylate-Modified Microspheres from Invitrogen) to their posterior end in an assay modified from King (1981) (Figure 6-3). This assay was initially designed and performed by Prof. Gary Ward. Parasites were allowed to attach to poly-L-lysine coated dishes on ice. Latex beads were then added and allowed to bind to the parasites before the temperature is raised to facilitate capping. In this experiment, three conditions were scored based on the beads interaction with the parasite. The interaction was defined as ‘bound’ where the beads are attached to the surface of the parasites but had not been translocated to the posterior end of the parasite, ‘capped’ where the associated beads were bound and translocated to the posterior, and finally ‘un-bound’ where no beads were attached to the parasite surface (Figure 6-3 C). Initial experiments by Prof. Gary Ward indicated that latex beads are bound to the surface of the parasite and are actively capped, in the majority of active parasites, to the posterior end of the parasite. This end capping typically occurred within 10 minutes (Whitelaw *et al.*, 2017).

Since the secretion/recycling system appears to be important for gliding motility, we wished to analyse membrane flow under varying conditions including: blocking micronemal protein secretion, constitutive micronemal secretion to the membrane and inhibition of recycling (Figure 6-2) (Whitelaw *et al.*, 2017). Dr. Simon Gras carried out this analysis. It was observed that inhibiting micronemal protein secretion by incubation in Endo buffer causes a significant reduction in bead attachment and thus bead capping (\*\*\*\*  $p < 0.0001$ ) (Figure 6-2). It is predicted that without micronemal proteins present along the surface, the capacity of the beads to interact with the surface of the parasites is reduced (Whitelaw *et al.*, 2017). Moreover, testing of a dynamin-related protein B (DrpB) mutant, termed DrpB<sup>DN</sup> was carried out, which was devoid of secretory organelles and thus unable to secrete micronemal proteins at the apical pole of

the parasite. Instead, the micronemal proteins are secreted to the parasite surface through the constitutive (default) pathway (Breinich *et al.*, 2009). These parasites are unable to glide across a substrate (Breinich *et al.*, 2009). With the micronemes constitutively secreted, it was observed that beads easily bind along the parasites surface, but are almost entirely blocked in translocation to the parasites posterior (Figure 6-2) (Whitelaw *et al.*, 2017). This indicates that polarised secretion of the micronemal proteins is required for efficient capping of the membrane and gliding. Also, we wanted to assess the role of membrane recycling in capping. The addition of PitStop2 allowed parasites to secrete their micronemal proteins at the apical end, but subsequently blocked in endocytosis. Similarly to the DrpB<sup>DN</sup> mutant, we observed beads bound to the surface of the majority of parasites, but noted that capping was significantly blocked by PitStop2 (\*\*\*\*  $p < 0.0001$ ) (Figure 6-2) (unpublished data from Dr. Simon Gras). In summary, these data suggest that a secretory/endocytic pathway is required for efficient translocation of beads by retrograde membrane flow.

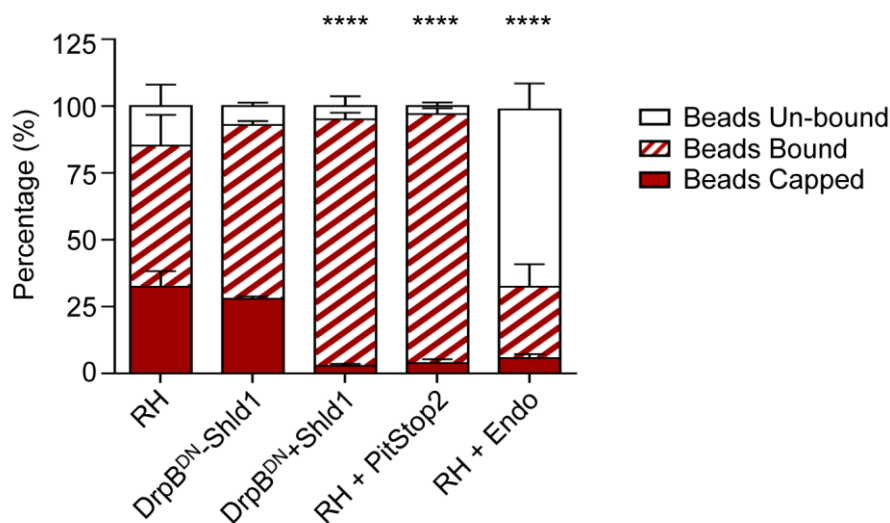


**Figure 6-2: The formation of a retrograde membrane flow with secretion/endocytic inhibitors**

A bead translocation assay was used to evaluate the possibility of a retrograde membrane flow. Quantification of the bead interactions with the parasites after 10 minutes incubation: un-bound (White), bound (Red/white stripes) and capped (red). No significant difference was observed in bead translocation of wild-type parasites (RH and the un-induced DrpB<sup>DN</sup>). Capping is almost blocked when the parasites cannot; secrete their micronemal proteins (Endo), generate a microneme gradient (DrpB<sup>DN</sup> Shld1 induced) or recycle their membranes PitStop2. Parasites incubated in Endo buffer have significantly reduced capacity to bind the beads to their surface. Error bars for represent  $\pm$  S.E.M. from a minimum of 4 independent experiments. Datasets were compared with a two-tailed Student's t-test. \*\*\*\*  $p < 0.001$ .

Next, the role of ACT1 in generating a retrograde membrane flow was assessed (Figure 6-3). Significantly fewer beads bound to the *act1* KO, while the addition of CD to wild-type parasites only had a minor deficiency in attachment (Figure 6-3 A). If we assume that beads must bind before they can be capped, the data could be normalised to the total number of bound parasites and used to determine capping capabilities. Consequently, the *act1* KO has no effect on the ability of the parasites to translocate beads (Figure 6-3 B) as per Quadts *et al.* (2016). However, the addition of 0.5  $\mu$ M CD significantly reduces bead translocation (\*\*  $P < 0.01$ ) (Figure 6-3 B). Since the *act1* KO has no defect in capping, the effect with CD is probably due to the off-target effect of the drug as described in chapter 4.1. Moreover, data from the lab indicates that other critical components of the motor complex (MyoA, MLC1 and MIC2) are not required for bead translocation (Whitelaw *et al.*, 2017). Overall, these results demonstrate that the establishment of a retrograde membrane flow can occur independently of functional ACT1 and more importantly, the whole acto-myosin system (Whitelaw *et al.*, 2017).

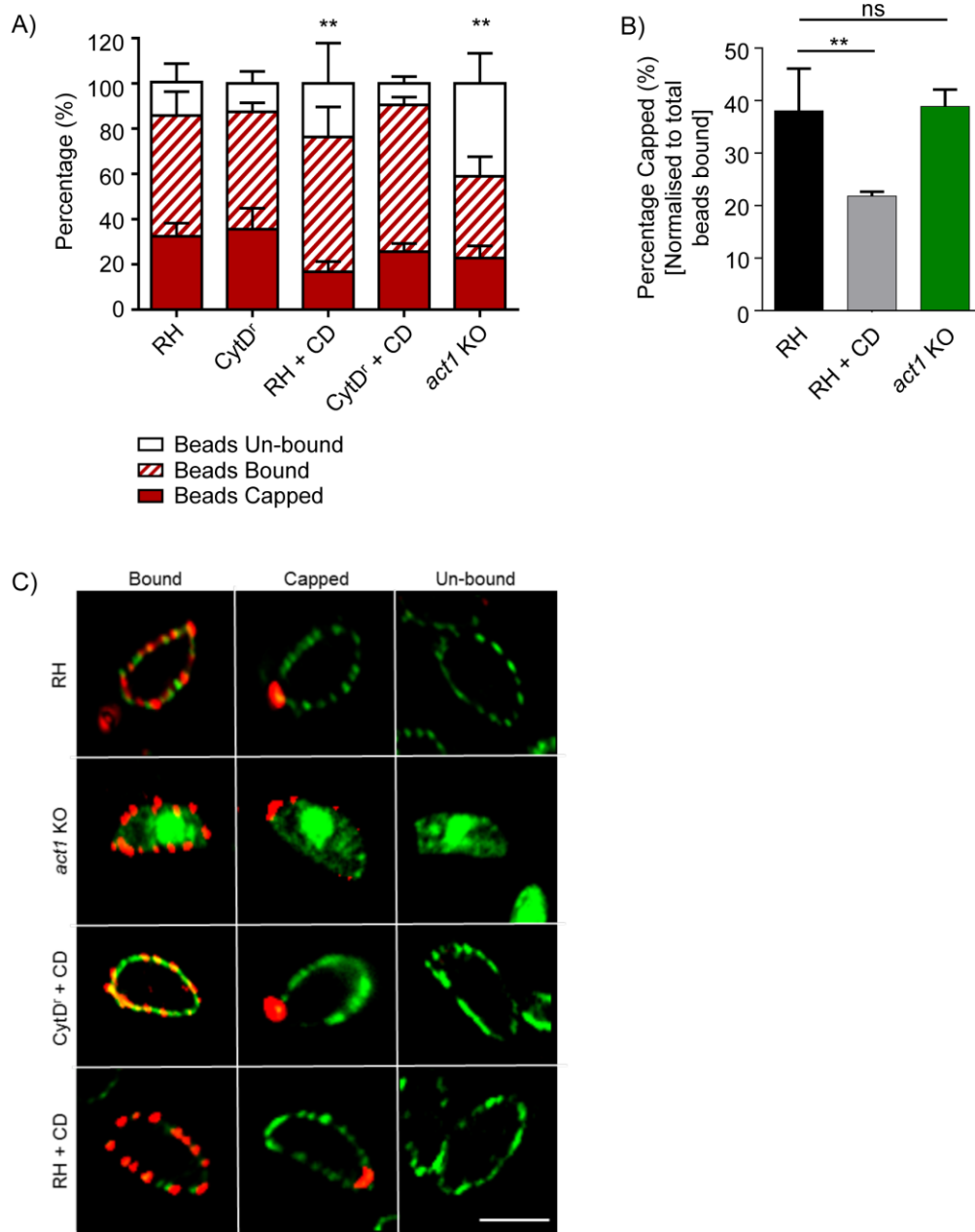


**Figure 6-3: Actin is not required for bead translocation**

A bead translocation assay was used as an indirect measurement of retrograde membrane flow. **A)** Quantification of the bead interactions with the parasites after 10 minutes incubation: un-bound (White), bound (Red/white stripes) and capped (red). Bead translocation of wild-type parasites (RH and CytD') is the same. Beads are significantly impaired in attachment to the *act1* KO, \*\* p < 0.001. The addition of 0.5  $\mu$ M reduces both bead attachment and capping. **B)** Percentage capped normalised to total beads bound. ACT1 has no impact on bead translocation while the addition of 0.5  $\mu$ M CD slightly reduces capping activity, \*\* p < 0.001. Error bars for both (A and B) represent  $\pm$  S.E.M from a minimum of 4 independent experiments. Datasets were compared with a two-tailed Student's t-test. **C)** Representative images of the three conditions observed. Non-fluorescent parasites (RH and CytD') were stained with  $\alpha$ -SAG1 (green) under non-permeabilising conditions to highlight the surface membrane. In all parasites conditions tested, beads were observed to bind and cap at the posterior end. Scale bars: 5  $\mu$ m.

Taken as a whole, these data indicate that bead translocation cannot occur in the absence of polarised micronemes secretion and probably clathrin-mediated

endocytosis, as suggested by inhibition of CIE using Pitstop2. Importantly, this retrograde flow of membranes is actin and myosin-independent.

### 6.3 New model for parasite motility

Here a new hypothetical model for motility based on a retrograde membrane flow is presented, generated by polarised secretion of the micronemes. In this model, a lipid engine could drive motility independent of the acto-myosin system (Figure 6-4). In this scenario, secretion at the apical end and recycling/membrane shedding at the polar end result in a retrograde membrane flow produces the force necessary for motility. In contrast, the acto-myosin system acts primarily by transmitting force through regulation of attachment sites at parasite the surface (Figure 6-4). According to this model, the acto-myosin system would be important for the regulated formation and release of attachment sites, similar to a ‘molecular clutch’ (Case & Waterman, 2015; Elosegui-Artola *et al.*, 2016). Transmembrane micronemal proteins interact with the extracellular matrix (similar to integrins), while the tail domains of these micronemes interact with a yet unknown “connector” within the parasite (Figure 6-4). The interaction of MyoA and short ACT1 filaments engages the clutch to link transmembrane micronemes as described in Elosegui-Artola *et al.* (2016). The forces generated by membrane flow would be physically transmitted to the parasites IMC through this molecular clutch (Figure 6-4), resulting in tension on the membrane. When ACT1 is depolymerised or MyoA disengages from the actin filament, the clutch disengages. This results in disengagement of the attachment site, leading to the parasite project forward. Together, tight regulation of these forces will result in the parasites ability to glide across the substrate and invade the host (Figure 6-4).

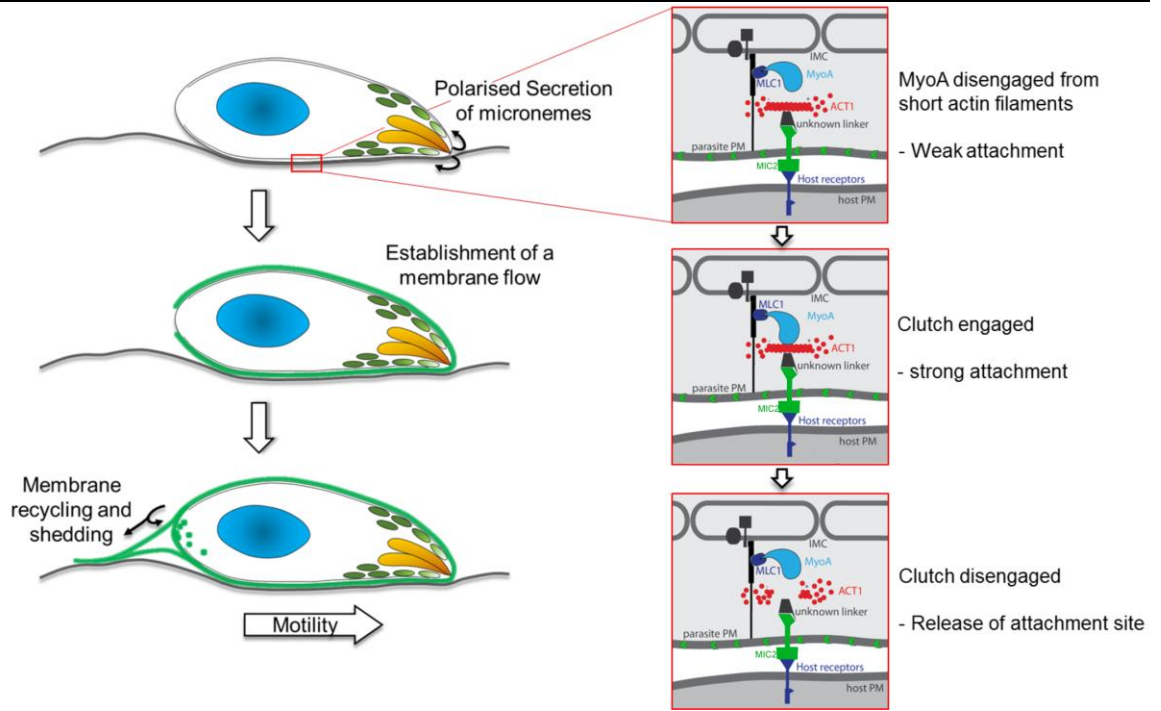


**Figure 6-4: Retrograde membrane flow model for motility**

It is hypothesised that a polarised secretion of micronemes at the apical end creates a retrograde membrane flow. The membrane is translocated to the posterior of the parasites where it is both shed and recycled. Transmembrane microneme proteins bind to host cell receptors and through the membrane flow generates the force. The acto-myosin system is required to transmit the force to the IMC and for the formation and release of attachment sites. Top Right panel: MyoA is disengaged from the short actin filament. Only a weak attachment to the substrate. Middle right panel: MyoA interacts with the actin filament (Clutch engaged). This increases the attachment strength to transmit the force generated by the membrane flow. Bottom right panel: Depolymerisation of F-actin and disengagement of MyoA releases the clutch and weakens the attachment strengths. Together this membrane flow and regulation of attachment sites results in forward translocation of the whole cell.

To conclude, this model consolidates many observations explained in this thesis and work done by others. Important things to note: 1) Filaments between the IMC and PM are still not visualised. Therefore, they may still be either extremely short or have rapid actin dynamics as described in Sahoo *et al.* (2006), 2) The linear motor cannot be the force generator for motility as described in Soldati-Favre (2008), 3) Actin and myosins are important but not essential for motility (Egarter *et al.*, 2014), 4) The acto-myosin motor complex is necessary for regulating surface attachment (Hegge *et al.*, 2010; Munter *et al.*, 2009).

## Chapter 7 General discussion and outlook

### 7.1 Establishment of the chromobody technology in *Toxoplasma*

Filamentous actin has many dynamic processes in eukaryotic cells, such as cell morphogenesis, migration or cell division (Olson & Nordheim, 2010; Pollard & Cooper, 2009). Due to its significance in cellular processes, it is fundamental to understand the basic principles of actin from actin polymerisation to complex processes like motility. Regarding actin dynamics *in vivo* within the cell, many different tools have been developed to visualise actin, such as LifeAct, SiR-Actin and others (Lukinavicius *et al.*, 2014; Riedl *et al.*, 2008). Since the development of tools to visualise the actin dynamics in live-cell conditions, the field of actin dynamics has moved forward rapidly.

The techniques to visualise actin filaments have been around for many years. Phalloidin was successfully used to stain actin filaments back in 1974 (Lengsfeld *et al.*, 1974). Furthermore, phalloidin tagged to fluorescent probes advanced the differentiation and characterisation of F-actin within the cell (Wulf *et al.*, 1979). While phalloidin is highly specific to F-actin and has provided a greater understanding of the actin cytoskeleton, the stabilising properties of the drug become toxic to the cells, where they frequently die or have severe alterations in actin-based functions (Cooper, 1987). The use of actin-tagged approaches such as rhodamine-labelled actin or GFP-actin allowed *in vivo* visualisation of the actin filament. However, these also exhibited several drawbacks: for example, it was demonstrated that they had altered dynamics and reduced functionalities (Feng *et al.*, 2005; Riedl *et al.*, 2008). In 2008, Riedl and colleagues demonstrated that the first 17 N-terminal amino acids of the yeast actin-binding protein Abp140, termed LifeAct, provided a new versatile marker for labelling F-actin (Riedl *et al.*, 2008). Indeed, LifeAct is the smallest actin-binding probe that lies between subdomains 1 and 3 of the actin monomer and its binding site does not have any sequence homology to other actin-binding proteins. Therefore, it does not appear to interfere with actin regulation *in vivo* (Riedl *et al.*, 2008).

While the mammalian system has established a variety of tools to visualise actin in the cell, the area of Apicomplexan actin research is still lagging behind. Filaments in the motile stages of the parasites lifecycle have been elusive leading to the conclusion that the filaments are intrinsically unstable (Sahoo *et al.*, 2006). The use of the above techniques has been rather unsuccessful in Apicomplexa to determine the localisation of actin filaments. Others have previously demonstrated that phalloidin does not label actin filaments in the parasites and reasons such as an actin-binding protein may mask its target site have been proposed (Cintra & De Souza, 1985; Schuler *et al.*, 2005b). Previous attempts to visualise F-actin using GFP-labelled actin in *Toxoplasma gondii* and *Plasmodium berghei* have shown an increased signal at both the apical and basal end of the parasites with the addition of the actin stabilisation drug, jasplakinolide (Jas) (Angrisano *et al.*, 2012a; Wetzel *et al.*, 2003). Detection of filaments with GFP-actin was limited due to the difficulty in differentiating the GFP-actin that is cytosolic from that incorporated in filaments. Furthermore, GFP-actin incorporation into *Toxoplasma gondii* had detrimental effects on parasite viability over time (Personal communication, Prof. David Sibley). The versatile F-actin marker in a mammalian system, LifeAct was also tested in *Plasmodium berghei* but subsequently did not label actin in any form (Personal communication, Prof. Freddy Frischknecht). Additionally, specific antibodies for apicomplexan actin predominantly bind only the monomeric form (see chapter 3.1). Only the antibody employed in Angrisano *et al.* (2012b) appears to preferentially label F-actin, though the signal to noise ratio still made it difficult to clearly identify filaments.

This project set out to use the chromobody technology to try a different approach to visualising actin filaments within the parasite. This technology, based on nanobodies of Camelids, has been used extensively to study actin dynamics in other eukaryotes such as plants (Rocchetti *et al.*, 2014) and animal cells (Panza *et al.*, 2015; Plessner *et al.*, 2015; Rothbauer *et al.*, 2006). Actin chromobodies have several advantages compared to other actin probes in the mammalian system: lower toxicity, no influence on actin dynamics and a high signal to noise ratio (Panza *et al.*, 2015; Plessner *et al.*, 2015). Moreover, it has been suggested that nanobodies might recognise epitopes that are not accessible for conventional antibodies (Muyldermans, 2013). Despite the specificity of

actin-chromobodies for F-actin, the exact epitope that it targets is still unknown (Personal communication, Dr. Tina Romer from Chromotek). This is because nanobodies tend to bind to 3D structures making it difficult to get a direct binding site (Muyldermans, 2013).

In this study, I was able to generate a parasite line stably expressing the chromobody-Halo plasmid in a wild-type RH background. This parasite line was able to complete multiple rounds of the lytic lifecycle with no significant difference compared to the control parasites, as analysed by a plaque assay. Additionally, when testing individual aspects of the lifecycle, it was observed that while no differences were observed in replication, egress or host cell invasion, gliding motility rates were slightly enhanced. From this, I am confident that the expression of actin-chromobodies in *Toxoplasma* has no significant effects on the actin dynamics within the parasite. In support with this finding is that actin chromobodies could be expressed throughout the lifecycle of a live Zebrafish without detrimental side effects (Panza *et al.*, 2015).

By applying the characterised chromobody technology to visualise actin filaments *in vivo*, the first identification of an actin network became apparent in *Toxoplasma gondii* (Periz *et al.*, 2017). This network responds to actin-modulating drugs as expected and is lost over time in the *act1* KO. Using two different correlative-light electron microscopy approaches, it was possible to visualise actin filaments within this network, along with some vesicles being transported. As a result, we now have a robust tool to visualise actin dynamics within the parasite, and can begin to do biochemical characterisation of these filaments, that may reveal novel actin-binding proteins.

## 7.2 Stabilisation of chromobody-RFP

Two different C-terminal fusions of the chromobody were generated, and while the chromobody-Halo had no obvious defects throughout the lifecycle, the chromobody-RFP plasmid appeared deleterious to the parasites. The chromobody-RFP fusion led to strong labelling of a thick filamentous network at the posterior end of the parasites. Furthermore, this network appears to be a collapsed nest of filaments that resulted in both an enlarged residual body and

caused an apicoplast division phenotype. The apicoplast replication defect is consistent with the functional interference of actin (Andenmatten *et al.*, 2012; Egarter *et al.*, 2014). In addition, the chromobody-RFP recapitulates the defects observed with the conditional *act1* KO (Andenmatten *et al.*, 2012; Egarter *et al.*, 2014) and when filaments are artificially stabilised with Jas (Shaw & Tilney, 1999). While analysing the specificity of chromobody-RFP for F-actin, it was noted that the *act1* KO was unaffected by its expression compared to the wild-type parasites. In this study I also show that specific TgACT1 antibodies that typically only stain cytosolic actin in the parasites, co-localised with the filaments, indicating that the chromobody may sequester all available actin monomers for filament formation. Upon depletion of ACT1, no filaments were detected indicating that the chromobody-RFP may artificially stabilise the actin filaments. This could be caused by the capability of RFP to form multimers (Baird *et al.*, 2000). Unlike the chromobody-Halo, attempts to generate stably expressing chromobody-RFP were unsuccessful. Therefore, we predict that by fusing the DD-FKPB domain (Herm-Gotz *et al.*, 2007) to the chromobody-RFP, this overexpression system could be used to conditionally interfere with actin dynamics, resulting in a rapidly functional *act1* KO phenotype.

### 7.3 The phenotypes indicate a cooperative polymerisation process of TgACT1

For actin to fulfil its diverse functions, it must cycle between the monomeric G-actin state and filamentous F-actin state. Conventional actins undergo cooperative assembly to polymerise, where actin monomers are incorporated into the barbed end of growing filaments (Pollard *et al.*, 2000). Polymerisation is a result of nucleation or lag-phase followed by elongation where the critical concentration ( $C_c$ ) is overcome and finally a steady state is reached where there is an equilibrium between monomer association and dissociation (Lodish *et al.*, 2004; Nishida & Sakai, 1983). The slow nucleation step is due to the instability of the dimer, trimer intermediates (Cooper *et al.*, 1983). However, the polymerisation kinetics of *Toxoplasma* ACT1 has been suggested, at least *in vitro*, to lack both a lag-phase and  $C_c$  (Skillman *et al.*, 2013). In an isodesmic polymerisation model, the formation of dimers, trimers and polymers is equally favoured which would lead to formation of many short filaments, independent of actin nucleators. As such, the question arises, what are the role of actin

nucleators, such as formins would be in the parasite, which have been demonstrated to be essential (Daher *et al.*, 2010). This isodesmic polymerisation method would make TgACT1 unique amongst actins, which was predicted to be an evolutionary adaptation to fit with the dynamic lifestyle of the parasites. In comparison, a previous study by Sahoo *et al.* (2006) suggested that TgACT1 has a 3-4 fold lower  $C_c$  required for polymerisation than conventional actins. In this study, they suggest the  $C_c$  of TgACT1 is 0.03  $\mu\text{M}$  (Sahoo *et al.*, 2006) compared to 0.12  $\mu\text{M}$  (Pollard *et al.*, 2000). This is lower than conventional actins but similar to other protozoan actins (Gupta *et al.*, 2015). Herein, I have looked at the phenotypic consequences of the loss of TgACT1 and relate this to either an isodesmic or cooperative polymerisation kinetics as a recent study indicated that heterologously expressed actin is mis-folded due to differences in the chaperonin T-complex (Olshina *et al.*, 2016). This likely makes the previous biochemical analysis of heterologous *Toxoplasma* actin non-functional.

Intriguingly, small decreases in ACT1 levels results in: instability of the apicoplast during division, blocked intracellular dense granule transport and a block in egress even when there are high levels of ACT1 detectable in the parasites. There is further evidence where the *act1* KO parasites are significantly reduced in gliding and invasion rates as early as 24 hours post induction. However, importantly, the phenotype does not change after 48 hours post induction. This indicates that once ACT1 is below a  $C_c$ , the phenotypes remain constant. Overall, these data strongly suggest that TgACT1 polymerises in a cooperative model and that polymerisation kinetics *in vitro* does not match the kinetics *in vivo*. One could assume that both egress and apicoplast maintenance require more F-actin than gliding motility and invasion, therefore these phenotypes are affected more severely. However, while analysing F-actin formation in the *act1* KO, it was noticed that these filaments were reduced in length at early time points after *act1* excision. This indicates that the formation of actin filaments requires a  $C_c$  of TgACT1, strongly supporting a cooperative polymerisation model rather than an isodesmic process.

## 7.4 Off-target effects of actin-modulating drugs

Actin modulating drugs have been used to explore the functions of actin dynamics in cells for many years. Some of the most used actin-modulating drugs are the cytochalasins. Cytochalasin D (CD) has been used as the primary drug to study actin-based dynamics since other cytochalasins have either lower potency or off-target effects such as inhibiting glucose transporters (Copeland, 1974; Foissner & Wasteneys, 2007). The mechanisms by which these drugs interact with canonical actins has been well described (Goddette & Frieden, 1986; MacLean-Fletcher & Pollard, 1980) but how these drugs affect atypical actins may differ significantly. Results described in this thesis provide evidence for an off-target effect of CD. Herein, I have shown that CD affects both the *act1* KO and *act1* KO<sup>CD<sup>r</sup></sup> parasites similarly and also at high concentrations affects the CytD<sup>r</sup> mutant. Nevertheless, while actin is the primary target of CD, its side effects also inhibit motility, possibly through reducing attachment to the substrate. This revelation has direct implications for many studies that have used CD to characterise *Toxoplasma* ACT1 and indicate that TgACT1 is essential for parasite motility and invasion (Dobrowolski & Sibley, 1996; Drewry & Sibley, 2015). Moreover, it was discovered that concentrations above 0.5  $\mu$ M lead to significant, actin-independent effects. In support of a secondary target, a third CD resistant mutant was isolated that did not have a mutation in the actin sequence (Dobrowolski & Sibley, 1996). As a next step, it would be interesting to do whole genome sequencing on this mutant to determine where the CD resistance mutation is. This would enable the secondary mode of action and the effects that drugs has on parasite actin to be quantified and understood.

Furthermore, I have shown that TgACT1 is naturally resistant to latrunculins. This is supported by previous biochemical observations where it was shown that *Plasmodium* actins have a salt bridge present that is only usually observed in latrunculin bound actins (Vahokoski *et al.*, 2014). This is contradictory to a study that showed *Cryptosporidium parvum* sporozoites are sensitive to latB (Wetzel *et al.*, 2005). However, this could be due to the differences in species, where *C. parvum* actin has only 88.1 % amino acid similarity to TgACT1 whereas *Plasmodium* ACT1 is much closer with 93.1 % identity (Dobrowolski *et al.*, 1997). Since there is no structure of *C. parvum* actin, it may not have this structural

alteration. Therefore, latrunculins may have a more significant effect on *C. parvum* actin-based motility.

Together, the phenotypes of the *act1* KO significantly differ from the effects caused by incubating parasites with drugs that affect F-actin dynamics. Therefore, great care should be taken in choosing the correct concentration for each actin-modulating drug, especially CD, where unknown targets also affect parasites motility and possibly many other aspects of the lifecycle. Care should also be taken not to group all Apicomplexan actins as the alterations in amino acid structures may highlight subtle differences in functions. For example, apicomplexan parasites contain the triple membranous structure where the acto-myosin motor complex is located. However, many invade through completely different mechanisms (Meissner *et al.*, 2013).

## 7.5 Cell-cell communication

### 7.5.1 Vesicular transport between parasites

While characterising the chromobody-Halo expression in parasites, it was observed that there were filamentous connections between parasites but surprisingly also between adjacent vacuoles. F-actin connections were observed predominately from the posterior end of the cells, however in some cases they were observed connecting to parasites near their apical ends. In both cases, cytosolic GFP vesicles are transported along actin filaments. This was abrogated with the addition of cytochalasin D (CD) and in the *act1* KO. This suggests that material is transported between parasites while they are within the PV requiring the formation of F-actin connections. Where F-actin localises at the posterior end, the network appears to go through the residual body, making connections to other parasites within the vacuole. The residual body function is relatively undefined but thought to exist as a repository for waste material (Hu *et al.*, 2002a; Shaw *et al.*, 2000) and for remnants released from the posterior end of the parasites during cell division (Muniz-Hernandez *et al.*, 2011). In this thesis, using the GAPM1a and GAPM3 as a marker for the IMC (Harding *et al.*, 2016), a recycling mechanism involving F-actin was seen. At the final stages of endodyogeny, the mother's contents are recycled into the newly forming daughter cells through the F-actin connections. Therefore, the residual body

might not act purely as a disposal item, but function to exchange material between parasites. Muniz-Hernandez *et al.* (2011) also suggest that the residual body may fulfil a role in the organisation of the rosette formation (Muniz-Hernandez *et al.*, 2011). Interestingly, the addition of CD causes the residual body to increase in volume and blocks egress (Shaw *et al.*, 2000). In this thesis, I have shown that the *act1* KO has a flattened basal end (Egarter *et al.*, 2014), which is predicted to be a result of a recycling defect. Furthermore, the loss of actin results in vacuole disorganisation, similar to the *gra2* KO (Mercier *et al.*, 2002). Taken together, this indicates that F-actin has a role during latter stages of endodyogeny by recycling contents through the residual body to the daughter cells. As a future outlook, it would be insightful to look at this actin network in a *gra2* KO and the *myo1* and *myoJ* KO. The *gra2* KO could provide knowledge of the membranous nanotubular network (MNN) and aid in understanding if F-actin is required for the MNN formation. While the *myo1* and *myoJ* KO (Damien Jacot, MPM 2016 abstract) may highlight the role of the myosins in a complementary understanding of F-actin transport.

### 7.5.2 Connections between vacuoles

During this project, F-actin extensions that connect two independent vacuoles were detected. In some cases, these were > 50  $\mu\text{m}$  in length. However, the actual physiological function for this connection is doubtful and may be an *in vitro* artefact. It is of interest that these connections may form with adjacent vacuoles in the same host cell. It is possible that these connections act as a kind of cell-cell communication in the form of membrane nanotubes (Gerdes *et al.*, 2007; Marzo *et al.*, 2012). Membranous nanotubes or cytonemes are protrusions that extend from the plasma membrane of one cell and are able to contact another over relatively large distances. They are quite often visualised in neuronal and immune cells (Onfelt *et al.*, 2004) and used for communication and vesicular transport (Gerdes & Carvalho, 2008). Viruses such as the human immunodeficiency virus (HIV) generate actin-driven protrusions to neighbouring cells for intracellular transmission (Lehmann *et al.*, 2005). In plant cells, it has been shown that plastids can form a nanotubule connection and allow the exchange of material between them (Kohler *et al.*, 1997). It was predicted that this may facilitate the coordination between the plastids (Kohler *et al.*, 1997). This could open up a whole new area of research for the apicoplast during the

intracellular stages, possibly not over large distances but within the vacuole to coordinate replication and nutrient uptake (Lim & McFadden, 2010).

### 7.5.3 Formation and functions of the network

Nanotubes are encompassed by a membranous structure. Therefore, it was difficult to imagine that the F-actin is secreted out of the parasite without being confined in a tubule-like structure. Our CLEM data indicates that these F-actin bundles are inside a membranous structure, however no plasma membrane markers were detected. Nevertheless, F-actin connections surrounded by markers of the MNN were observed, such as GRA2 and GRA7 (Mercier & Cesbron-Delauw, 2015; Mercier *et al.*, 2002). An independent group has also shown connections similar to this with other dense granule proteins GRAs1, 3 and 7 (Dunn *et al.*, 2008). Moreover, *Plasmodium berghei* make tubular extensions of HSP101 within the red blood cell (Matz *et al.*, 2015), which look very similar to the actin network we observed in *Toxoplasma*. Matz and colleagues tested a range of actin inhibitors but never observed a difference, in HSP101 location in the tubule, however both CD and Jasplakinolide delay the development of the tubules (Matz *et al.*, 2015).

From observations so far, F-actin connections appear to control replication and maintain vacuolar organisation. This network might function to hold the parasites during this process. However, the network may have other functions, such as nutrient uptake from the host. *Toxoplasma gondii* is auxotrophic for cholesterol (Coppens *et al.*, 2006; Coppens *et al.*, 2000) and such has been shown to scavenge lipoprotein-derived cholesterol from host endosomal compartments through vesicle transport (Sehgal *et al.*, 2005). As parasite numbers in the PV can exceed 64, it could be envisioned that parasites in direct contact with the PV will uptake cholesterol and other nutrients in a higher abundance than those in the middle of the vacuole.

## 7.6 Localisation of actin filaments at the linear motor complex

*Toxoplasma* parasites actively locate and penetrate a suitable host cell. The prevailing model of *Toxoplasma* motility is through the parasites unique gliding

machinery, known as the glideosome. The glideosome is believed to be located in between the triple membranous structure of the plasma membrane and inner membrane complex that appears to be conserved across the infrakingdom of Alveolata (Gould *et al.*, 2011; Tardieux & Baum, 2016). In this complex, the myosin motor produces the force by actively displacing actin filaments and linked surface adhesions to the rear, creating a traction force that propels the parasites forwards or into a host cell (Soldati & Meissner, 2004). In this system, one would expect to visualise actin filaments beneath the plasma membrane. However, to date, there is little evidence of actin filaments at the motor *in vivo*. This could be explained by the unusual properties of actin in Apicomplexa, such that it forms short filaments that are transient and unstable (Sahoo *et al.*, 2006; Schmitz *et al.*, 2005). Also, it was suggested that the parasites actin is evolutionary altered in its polymerisation kinetics (Skillman *et al.*, 2013). With the applied chromobody technology to detect F-actin in *Toxoplasma gondii*, we were unable to detect filaments at the pellicle of moving parasites. Using 3D super-resolution microscopy, some filamentous-like structures were seen. More recent work to enhance the signal to noise ratio observed that there are long F-actin cables-like structures within the cytoplasm of the parasites but not at the pellicle. These are similar to long F-actin tracks observed in *Plasmodium falciparum* stage IV gametocytes (Hliscs *et al.*, 2015). These possibly act as tracks for myosin motors to transport material such as dense granule proteins (Heaslip *et al.*, 2016). Interestingly, as soon as the parasites lyse out of the host cell during egress, F-actin accumulation was detected at the rear of motile parasites. This is similar to the observations where GFP-actin accumulated at the apical and basal ends of motile *Plasmodium* ookinetes (Angrisano *et al.*, 2012a). A recent study indicated that during *Plasmodium* sporozoite motility, an increase in calcium levels causes the relocation of the F-actin binding protein, coronin, from the pellicle to the basal end of the parasites (Bane *et al.*, 2016). Similarly, *Toxoplasma* coronin relocates from the cytoplasm to the basal pole of motile parasite (Salamun *et al.*, 2014).

A recent review on the mechanisms of gliding motility of apicomplexan highlighted three alternative models of the glideosome architecture and how they have evolved over time (Tardieux & Baum, 2016). This is very interesting, as F-actin in each case is thought to lie between the IMC and plasma membrane.

With the new marker for F-actin indicating that the filaments are located within the cytoplasm, the topology of the myosin motor complex may require to be reevaluated. The reverse topology model suggested by King and colleague has never properly been disproved (King, 1988; Tardieux & Baum, 2016). Therefore, with high-resolution markers for each component of the motor complex, the arrangement of this will need to be re-evaluated. Importantly, this could lead to a new mechanistic model that fits all known data for gliding motility.

### 7.6.1 Alternative models of gliding

During gliding motility, the force is produced by the acto-myosin motor complex and transformed into traction forces through the interactions of adhesive proteins (Soldati & Meissner, 2004). Undeniably, the acto-myosin motor complex as a whole is required for motility. However, exactly how such observations within this thesis and work by others fit a simplified linear motor is questionable. In this thesis, it is shown that the *act1* KO has a severe attachment defect but can still move with similar speeds in both 2D and 3D to wild-type cells. This is somewhat similar to other motility systems. For example, dendritic cells treated with latrunculin A (latA) had no difference in motility speeds (Renkawitz *et al.*, 2009), while the loss of all integrins completely abrogated attachment and 2D migration but not 3D motility (Lammermann *et al.*, 2008). These results and work by others led us to speculate on other mechanisms involved in the force generation for *Toxoplasma* motility. For example, the fundamental mechanism for the gel-solution model predicted in Egarter *et al.* (2014) works in principle and can be consolidated with many (but not all) of the available data. It predicts that the force is generated from changes in hydrodynamic pressures caused by osmotic differences with a poroelastic cytosol, generated either by the acto-myosin activity itself or osmogenic ion transporters located on the plasma membrane, which results in shape changes during motility (Charras *et al.*, 2005; Mitchison *et al.*, 2008). A similar model for an osmotic engine has been demonstrated for tumour cells confined in space (Stroka *et al.*, 2014b).

Results presented in this thesis indicate that the acto-myosin system is not essential for producing the force as once predicted. Interfering with polarised microneme secretion causes a block in motility (Breinich *et al.*, 2009; Endo &

Yagita, 1990). In support of this, enhancers of cell motility target the secretion of microneme proteins (Carey *et al.*, 2004b; Child *et al.*, 2013), while inhibitors of microneme secretion block motility (Endo & Yagita, 1990). Moreover, these micronemes are translocated to the basal end after secretion in a process known as capping (Carruthers *et al.*, 2000b; Dowse & Soldati, 2004; Quadt *et al.*, 2016). It has been suggested that motility can be driven by a surface membrane flow that acts as fluid drive and is generated by a secretory-endocytic cycle from anterior to posterior (Barry & Bretscher, 2010; Bretscher, 2014). To test this, a bead translocation assay was adapted, first described in King (1981), as an indicator of a retrograde membrane flow. Surprisingly, it was found that bead translocation occurs independently of the major components of the glideosome: ACT1, MyoA, MLC1 and MIC2 (Whitelaw *et al.*, 2017). In comparison, bead translocation was completely blocked if we inhibited the polarised secretion of the micronemes using Endo buffer or a dynamin mutant that is devoid of its microneme organelles (Breinich *et al.*, 2009). Akin to other systems it is speculated that polarised secretion is critical for establishing a membrane flow that can generate the force required for motility. In support of this, Quadt and colleagues measured the retrograde membrane flow in *Plasmodium* sporozoites with bead movement. Interestingly, they demonstrate that bead movement was faster than the overall parasite gliding speeds (Quadt *et al.*, 2016). This suggested that the rate of retrograde flow does not directly translate into forward migration, but requires regulation of attachment and detachment in form of a molecular clutch (Tardieux & Baum, 2016). Unfortunately, in our study, we were unable to measure bead translocation speeds and correlate this to parasite motility directly. However, retrograde membrane flow can differ due to the diffusion coefficient of the protein, where non-circulating protein are swept to the rear of the cell quicker (Bretscher, 2014). For example, GPI-linked antigens may be capped sufficiently as a result of reduced diffusion coefficient and hence is more sensitive to the membrane flow (Bretscher, 2014).

It has been shown that parasites leave behind membranous trails during gliding motility (Hakansson *et al.*, 1999). It is hard to imagine how the parasites can cope with the loss of lipids. In other systems, surface proteins are recycled through an endocytic pathway and trafficked back to the leading edge of motile cells (Bretscher, 1976; Bretscher, 1996a; Bretscher, 2014). Since conventional

endocytosis through clathrin-coated pits has not been observed in *Toxoplasma* (Pieperhoff *et al.*, 2013), a clathrin-independent endocytic (CIE) inhibitor on both gliding motility and bead translocation was tested. Here, preliminary evidence is shown that both gliding motility and bead translocation are inhibited with a CIE inhibitor, PitStop2. Therefore, it is suspected that endocytosis is occurring and involved in gliding motility. In support of this, extracellular *Toxoplasma* can uptake molecules through receptor-specific or fluid-phase endocytosis (Botero-Kleiven *et al.*, 2001). The authors demonstrate that glycosaminoglycans (GAG) heparin that bind to tachyzoite surface proteins are internalised in an endocytic manner (Botero-Kleiven *et al.*, 2001). Since microneme proteins bind to surface receptors, it would be exciting to see which sets, if any, of the micronemes are endocytosed. For example, it would be interesting to use photoactivatable proteins tagged to different micronemes and see if different coloured micronemes are internalised. Therefore, more work is necessary to understand endocytosis and a reanalysis of the role of the micropore might be required (Nichols *et al.*, 1994).

The other aspect of this model includes the role of the acto-myosin system in force transmission. In this thesis, it is shown that the acto-myosin system plays an important role in surface attachment. Together these results are consistent with a molecular clutch hypothesis where the myosin engages the clutch, reducing the actin flow and transmitting the force produced by the membrane tension (Bard *et al.*, 2008; Case & Waterman, 2015). Interestingly, a *Plasmodium* coronin mutant failed to attach properly to substrate (Bane *et al.*, 2016), a similar observation to the *Toxoplasma act1* KO. However, the exact role of F-actin and coronin during attachment is still speculative as F-actin visibility in motile cells is lacking (Bane *et al.*, 2016). To shed light on the distribution and turnover of adhesion sites in *Toxoplasma gondii*, one could use reflection interference contrast microscopy (RICM), traction force microscopy (TFM) or optical tweezers to trap the parasites or beads in a laser beam as these have been used successfully to show *Plasmodium* sporozoite motility is dependent on the turnover of adhesion sites (Hegge *et al.*, 2010; Hegge *et al.*, 2012; Munter *et al.*, 2009).

Together, the results presented in this thesis, suggest that a retrograde membrane flow works coordinately with the acto-myosin system for forward propulsion and gliding motility.

### 7.6.2 The role of the host actin during invasion

Actin from the parasite is thought to be essential for parasite invasion, while actin of the host was thought to be rather passive. In this study, it is demonstrated that a conditional *act1* KO can still invade host cells at variable kinetic speeds, supporting data previously published (Andenmatten *et al.*, 2012; Egarter *et al.*, 2014). The finding that *Toxoplasma* tachyzoites are naturally resistant to the actin sequestering drug, latrunculin A (latA) is also shown. This provided a potent inhibitor of actin polymerisation of the host cell without perturbing the actin dynamics of the parasite. From this, it is shown that in non-phagocytic (HeLa) cells, the actin cytoskeleton is required for invasion, as the addition of latA reduced invasion rates compared to the negative control and latA resistant host cells. This observation was also supported in phagocytic macrophages where invasion was significantly reduced upon addition of latA (results from Mario del Rosario).

Overall, this work along with others indicates that the host cell is not passive in invasion as previously suggested (Bichet *et al.*, 2014; Gonzalez *et al.*, 2009; Zuccala *et al.*, 2016). Moreover, this actin reorganisation of the host to wrap around the *Toxoplasma* tachyzoite during invasion may, in fact, represent an alternative invasion mechanism the cell uses when under stress. More work in the future will have to be conducted to elucidate the exact role.

## 7.7 The role of *Toxoplasma* ACT1 during the lytic cycle of actin: Summary

Actin has many functions in eukaryotic cells, including apicomplexan parasites. Here, I have shown that shortly after invasion, during replication of the parasite, F-actin surrounded by membranous dense granules begin to form a dynamic network that is required for the organisation and structural stability of the parasites within the vacuole. Moreover, as vesicles were seen moving along these actin filaments, they could also be involved in cell-cell communication. As

the parasites are dividing, actin along with the class XXII myosin F control apicoplast division (Jacot *et al.*, 2013). Increases in calcium levels causes a signalling cascade required for egress. At this point, the F-actin network depolymerises in a yet unknown manner, allowing the parasites to initiate motility and escape the host cell.

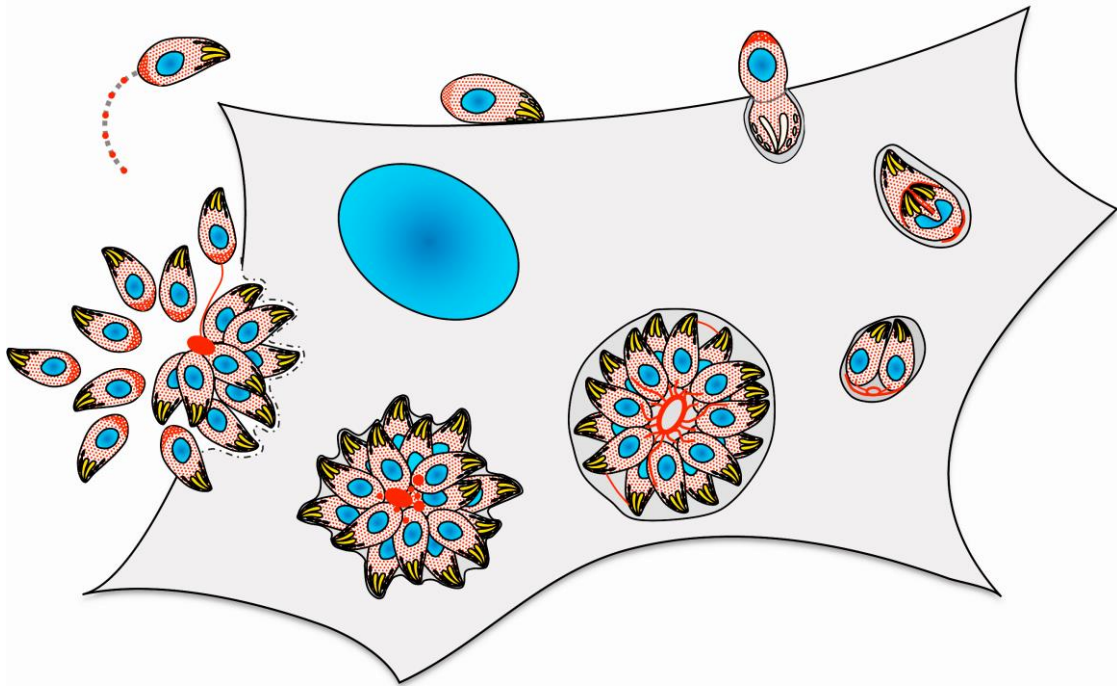


**Figure 7-1: Actin throughout the lifecycle of *Toxoplasma gondii***

*Toxoplasma* actin is dynamic throughout the lytic lifecycle. All parasite stages have a large pool of monomeric G-actin (Dobrowolski *et al.*, 1997) indicated in light red from antibody analysis, while F-actin indicated by the chromobody technology is highlighted in thick red structures. **1)** Gliding parasites have an increased actin signal at the basal end of the cell. Moreover, actin is also found in the trails of gliding parasites. **2)** Actin is important for attachment, although the localisation of F-actin during this process is still unknown. **3)** As the parasites invade a host cell, F-actin accumulates at the basal (extracellular) part of the cell until the closure of the parasitophorous vacuole membrane (PVM). **4)** Once inside the parasitophorous vacuole, F-actin and dense granule proteins begin to form a membranous nanotubular network from the basal end of the parasites. At late stages of endodyogeny, F-actin focuses around the daughter cells and recycles contents of the mother cell. **5)** The daughter cells are held in at the basal end by F-actin network. **6)** As endodyogeny continues, the actin network is continually reorganised to hold the parasites in a conformational rosette. Cell to cell connections are also observed and may transfer material. **7)** The F-actin network collapses and PVM constricts after the parasites sense the increase in calcium levels. **8)** Parasites egress leaving behind parasite actin that is in the residual body. The motile parasites have an increase in actin signal at their basal end, and some have to break microfilaments before they can fully egress. Image adapted from Periz *et al.* (2017) to highlight actins observed role for the whole lytic lifecycle.

## 7.8 Outlook and future studies

Within this thesis, I have provided evidence for the functions of actin within *Toxoplasma gondii*. I have characterised an *act1* KO, shown that actin-modulating drugs are not specific to TgACT1 and demonstrated novel functions

of F-actin during intracellular development of the parasites. Furthermore, I have provided first evidences for a new hypothesis for motility that places the generation of retrograde membrane flow, potentially caused by a secretory-endocytic cycle, into the centre as a force producer for motility. In contrast, this view predicts a function of the acto-myosin system as a molecular clutch for attachment regulation. While such a hypothesis can consolidate many of the (sometimes) conflicting data, more work is required to clarify the exact mechanisms involved in this process.

Firstly, obtaining a chromobody fusion that enhances the signal to noise ratio may indeed highlight more important questions regarding actin dynamics. Would there be a clarification of F-actin within the parasites, such that filaments may be present at the pellicle for motility and could we see filament formation to visualise dense granule migration? Can we determine the polymerisation kinetics and movement of the filaments? Some interesting questions are the roles and functions of actin-binding proteins, which will need to be readdressed in light of the presented data. For example, the actin-binding protein coronin appears to bundle actin filaments to control adhesion and motility (Bane *et al.*, 2016; Salamun *et al.*, 2014). It would be interesting to see the link between the coronin and actin filaments during *Toxoplasma* motility. Moreover, it would be beneficial to see how the loss of the actin-depolymerisation factor (ADF) affects the formation and maintenance of the network. Loss of ADF may enhance and stabilise the F-actin within the network, similar to jasplakinolide treatment. Furthermore, it would be useful to see if the Co-IP and mass-spec identifies any novel actin-binding proteins that may be contributing to controlling F-actin dynamics. Also, the role of actin-like proteins (ALPs) should be clarified in detail, since they might play important roles in organisation of F-actin and F-actin dynamics, for example acting as bundling proteins. Finally, the role of the myosins in *Toxoplasma* is an interesting area of research. Some questions posed include; what would their role be with regard to the filaments? Are they involved in shunting F-actin to the posterior end of the parasites and into the network? Whatever the roles, more work will need to be addressed to understand the nature of this network and how F-actin is involved in motility and invasion.

## Chapter 8 List of References

- Achanta, S. S., Varunan, S. M., Bhattacharyya, S. and Bhattacharyya, M. K. (2012). Characterization of Rad51 from apicomplexan parasite *Toxoplasma gondii*: an implication for inefficient gene targeting. *PLoS One*, **7**, e41925. doi: 10.1371/journal.pone.0041925.
- Adjogble, K. D., Mercier, C., Dubremetz, J. F., Hucke, C., Mackenzie, C. R., Cesbron-Delauw, M. F. and Daubener, W. (2004). GRA9, a new *Toxoplasma gondii* dense granule protein associated with the intravacuolar network of tubular membranes. *Int J Parasitol*, **34**, 1255-1264.
- Adl, S. M., Leander, B. S., Simpson, A. G., Archibald, J. M., Anderson, O. R., Bass, D., Bowser, S. S., Brugerolle, G., Farmer, M. A., Karpov, S., Kolisko, M., Lane, C. E., Lodge, D. J., Mann, D. G., Meisterfeld, R., Mendoza, L., Moestrup, O., Mozley-Standridge, S. E., Smirnov, A. V. and Spiegel, F. (2007). Diversity, nomenclature, and taxonomy of protists. *Syst Biol*, **56**, 684-689. doi: 10.1080/10635150701494127.
- Agop-Nersesian, C., Egarter, S., Langsley, G., Foth, B. J., Ferguson, D. J. and Meissner, M. (2010). Biogenesis of the Inner Membrane Complex Is Dependent on Vesicular Transport by the Alveolate Specific GTPase Rab11B. *PLoS Pathog*, **6**, e1001029.
- Agop-Nersesian, C., Naissant, B., Ben Rached, F., Rauch, M., Kretzschmar, A., Thiberge, S., Menard, R., Ferguson, D. J., Meissner, M. and Langsley, G. (2009). Rab11A-controlled assembly of the inner membrane complex is required for completion of apicomplexan cytokinesis. *PLoS Pathog*, **5**, e1000270. doi: 10.1371/journal.ppat.1000270.
- Alberts, B., Johnson, A., Lewis, J., Morgan, D., Raff, M., Roberts, K., Walter, P., Wilson, J. and Hunt, T. (2014). *Molecular biology of the cell, 6th Edition*, Sixth edition. edn. Garland Pub., New York.
- Altschul, S. F., Gish, W., Miller, W., Myers, E. W. and Lipman, D. J. (1990). Basic local alignment search tool. *J Mol Biol*, **215**, 403-410. doi: 10.1016/S0022-2836(05)80360-2.
- Amino, R., Thiberge, S., Shorte, S., Frischknecht, F. and Menard, R. (2006). Quantitative imaging of Plasmodium sporozoites in the mammalian host. *C R Biol*, **329**, 858-862. doi: 10.1016/j.crv.2006.04.003.
- Ananthakrishnan, R. and Ehrlicher, A. (2007). The forces behind cell movement. *Int J Biol Sci*, **3**, 303-317.
- Andenmatten, N., Egarter, S., Jackson, A. J., Jullien, N., Herman, J. P. and Meissner, M. (2012). Conditional genome engineering in *Toxoplasma gondii* uncovers alternative invasion mechanisms. *Nature Methods*, 1-3. doi: 10.1038/nmeth.2301.
- Angrisano, F., Delves, M. J., Sturm, A., Mollard, V., McFadden, G. I., Sinden, R. E. and Baum, J. (2012a). A GFP-actin reporter line to explore microfilament dynamics across the malaria parasite lifecycle. *Mol Biochem Parasitol*, **182**, 93-96. doi: 10.1016/j.molbiopara.2011.11.008.
- Angrisano, F., Riglar, D. T., Sturm, A., Volz, J. C., Delves, M. J., Zuccala, E. S., Turnbull, L., Dekiwadia, C., Olshina, M. A., Marapana, D. S., Wong, W., Mollard, V., Bradin, C. H., Tonkin, C. J., Gunning, P. W., Ralph, S. A., Whitchurch, C. B., Sinden, R. E., Cowman, A. F., McFadden, G. I. and Baum, J. (2012b). Spatial localisation of actin filaments across developmental stages of the malaria parasite. *PLoS One*, **7**, e32188. doi: 10.1371/journal.pone.0032188.
- Aranda, P. S., LaJoie, D. M. and Jorcyk, C. L. (2012). Bleach gel: a simple agarose gel for analyzing RNA quality. *Electrophoresis*, **33**, 366-369. doi: 10.1002/elps.201100335.
- Arrizabalaga, G. and Boothroyd, J. C. (2004). Role of calcium during *Toxoplasma gondii* invasion and egress. *Int J Parasitol*, **34**, 361-368. doi: 10.1016/j.ijpara.2003.11.017.
- Asakura, S., Taniguchi, M. and Oosawa, F. (1963). Mechano-chemical behaviour of F-actin. *J. Mol. Biol.*, **7**, 55-69.

- Ayscough, K., Stryker, J., Pokala, N., Sanders, M., Crews, P. and Drubin, D. G. (1997). High rates of actin filament turnover in budding yeast and roles for actin in establishment and maintenance of cell polarity using the actin inhibitor latrunculin-A. *J Cell Biol*, **137**, 399-416.
- Azab, M. and Beverley, J. K. (1974). Schizogony of *Toxoplasma gondii* in tissue culture. *Zeitschrift für Parasitenkunde*, **44**, 33-41.
- Baird, G. S., Zacharias, D. A. and Tsien, R. Y. (2000). Biochemistry, mutagenesis, and oligomerization of DsRed, a red fluorescent protein from coral. *Proc Natl Acad Sci U S A*, **97**, 11984-11989. doi: 10.1073/pnas.97.22.11984.
- Ballestrem, C., Wehrle-Haller, B. and Imhof, B. A. (1998). Actin dynamics in living mammalian cells. *Journal of Cell Science*, 1649-1658.
- Balzer, E. M., Tong, Z., Paul, C. D., Hung, W. C., Stroka, K. M., Boggs, A. E., Martin, S. S. and Konstantopoulos, K. (2012). Physical confinement alters tumor cell adhesion and migration phenotypes. *FASEB J*, **26**, 4045-4056. doi: 10.1096/fj.12-211441.
- Bamburg, J. R. and Bernstein, B. W. (2010). Roles of ADF/cofilin in actin polymerization and beyond. *F1000 Biol Rep*, **2**, 62. doi: 10.3410/B2-62.
- Bane, K. S., Lepper, S., Kehrer, J., Sattler, J. M., Singer, M., Reinig, M., Klug, D., Heiss, K., Baum, J., Mueller, A. K. and Frischknecht, F. (2016). The Actin Filament-Binding Protein Coronin Regulates Motility in *Plasmodium* Sporozoites. *PLoS Pathog*, **12**, e1005710. doi: 10.1371/journal.ppat.1005710.
- Bard, L., Boscher, C., Lambert, M., Mege, R. M., Choquet, D. and Thoumine, O. (2008). A molecular clutch between the actin flow and N-cadherin adhesions drives growth cone migration. *J Neurosci*, **28**, 5879-5890. doi: 10.1523/JNEUROSCI.5331-07.2008.
- Barden, J. A., Miki, M., Hambly, B. D. and Dos Remedios, C. G. (1987). Localization of the phalloidin and nucleotide-binding sites on actin. *Eur J Biochem*, **162**, 583-588.
- Bargieri, D. Y., Andenmatten, N., Lagal, V., Thiberge, S., Whitelaw, J. A., Tardieux, I., Meissner, M. and Menard, R. (2013). Apical membrane antigen 1 mediates apicomplexan parasite attachment but is dispensable for host cell invasion. *Nat Commun*, **4**, 2552. doi: 10.1038/ncomms3552.
- Barry, N. P. and Bretscher, M. S. (2010). Dictyostelium amoebae and neutrophils can swim. *PNAS*, **107**, 11376-11380.
- Batchelder, E. L., Hollopeter, G., Campillo, C., Mezanges, X., Jorgensen, E. M., Nassoy, P., Sens, P. and Plastino, J. (2011). Membrane tension regulates motility by controlling lamellipodium organization. *Proc Natl Acad Sci U S A*, **108**, 11429-11434. doi: 10.1073/pnas.1010481108.
- Baum, J. and Frischknecht, F. (2015). Motorizing pathogens. *Semin Cell Dev Biol*, **46**, 78-81. doi: 10.1016/j.semcdb.2015.09.019.
- Baum, J., Gilberger, T. W., Frischknecht, F. and Meissner, M. (2008a). Host-cell invasion by malaria parasites: insights from *Plasmodium* and *Toxoplasma*. *Trends Parasitol*, **24**, 557-563. doi: 10.1016/j.pt.2008.08.006.
- Baum, J., Papenfuss, A. T., Baum, B., Speed, T. P. and Cowman, A. F. (2006). Regulation of apicomplexan actin-based motility. *Nat Rev Microbiol*, **4**, 621-628. doi: 10.1038/nrmicro1465.
- Baum, J., Tonkin, C. J., Paul, A. S., Rug, M., Smith, B. J., Gould, S. B., Richard, D., Pollard, T. D. and Cowman, A. F. (2008b). A malaria parasite formin regulates actin polymerization and localizes to the parasite-erythrocyte moving junction during invasion. *Cell Host Microbe*, **3**, 188-198. doi: 10.1016/j.chom.2008.02.006.
- Bear, J. E. and Gertler, F. B. (2009). Ena/VASP: towards resolving a pointed controversy at the barbed end. *J Cell Sci*, **122**, 1947-1953. doi: 10.1242/jcs.038125.
- Beck, J. R., Chen, A. L., Kim, E. W. and Bradley, P. J. (2014). RON5 is critical for organization and function of the *Toxoplasma* moving junction complex. *PLoS Pathog*, **10**, e1004025. doi: 10.1371/journal.ppat.1004025.
- Behnke, M. S., Fentress, S. J., Mashayekhi, M., Li, L. X., Taylor, G. A. and Sibley, L. D. (2012). The polymorphic pseudokinase ROP5 controls virulence in *Toxoplasma*

- gondii by regulating the active kinase ROP18. *PLoS Pathog*, **8**, e1002992. doi: 10.1371/journal.ppat.1002992.
- Behnke, M. S., Khan, A., Lauron, E. J., Jimah, J. R., Wang, Q., Tolia, N. H. and Sibley, L. D. (2015). Rhoptry Proteins ROP5 and ROP18 Are Major Murine Virulence Factors in Genetically Divergent South American Strains of *Toxoplasma gondii*. *PLoS Genet*, **11**, e1005434. doi: 10.1371/journal.pgen.1005434.
- Beltzner, C. C. and Pollard, T. D. (2008). Pathway of actin filament branch formation by Arp2/3 complex. *J Biol Chem*, **283**, 7135-7144. doi: 10.1074/jbc.M705894200.
- Bergert, M., Chandradoss, S. D., Desai, R. A. and Paluch, E. (2012). Cell mechanics control rapid transitions between blebs and lamellipodia during migration. *Proc Natl Acad Sci U S A*, **109**, 14434-14439. doi: 10.1073/pnas.1207968109.
- Bernstein, B. W. and Bamburg, J. R. (2010). ADF/cofilin: a functional node in cell biology. *Trends Cell Biol*, **20**, 187-195. doi: 10.1016/j.tcb.2010.01.001.
- Besteiro, S., Michelin, A., Poncet, J., Dubremetz, J. F. and Lebrun, M. (2009). Export of a *Toxoplasma gondii* rhoptry neck protein complex at the host cell membrane to form the moving junction during invasion. *PLoS Pathog*, **5**, e1000309. doi: 10.1371/journal.ppat.1000309.
- Bichet, M., Joly, C., Henni, A., Guilbert, T., Xemard, M., Tafani, V., Lagal, V., Charras, G. and Tardieux, I. (2014). The *Toxoplasma*-host cell junction is anchored to the cell cortex to sustain parasite invasive force. *BMC Biol*, **12**, 773. doi: 10.1186/s12915-014-0108-y.
- Bichet, M., Touquet, B., Gonzalez, V., Florent, I., Meissner, M. and Tardieux, I. (2016a). Genetic impairment of parasite myosin motors uncovers the contribution of host cell membrane dynamics to *Toxoplasma* invasion factors. *BMC Biol*, **14**, 1-19.
- Bichet, M., Touquet, B., Gonzalez, V., Florent, I., Meissner, M. and Tardieux, I. (2016b). Genetic impairment of parasite myosin motors uncovers the contribution of host cell membrane dynamics to *Toxoplasma* invasion forces. *BMC Biol*, **14**. doi: 10.1186/s12915-016-0316-8.
- Bisi, S., Disanza, A., Malinverno, C., Frittoli, E., Palamidessi, A. and Scita, G. (2013). Membrane and actin dynamics interplay at lamellipodia leading edge. *Curr Opin Cell Biol*, **25**, 565-573. doi: 10.1016/j.ceb.2013.04.001.
- Black, M., Seeber, F., Soldati, D., Kim, K. and Boothroyd, J. C. (1995). Restriction enzyme-mediated integration elevates transformation frequency and enables co-transfection of *Toxoplasma gondii*. *Mol Biochem Parasitol*, **74**, 55-63.
- Black, M. W., Arrizabalaga, G. and Boothroyd, J. C. (2000). Ionophore-resistant mutants of *Toxoplasma gondii* reveal host cell permeabilization as an early event in egress. *Mol Cell Biol*, **20**, 9399-9408.
- Blackstock, D. and Chen, W. (2014). Halo-tag mediated self-labeling of fluorescent proteins to molecular beacons for nucleic acid detection. *Chem Commun (Camb)*, **50**, 13735-13738. doi: 10.1039/c4cc07118b.
- Blader, I. J., Coleman, B. I., Chen, C. T. and Gubbels, M. J. (2015). Lytic Cycle of *Toxoplasma gondii*: 15 Years Later. *Annu Rev Microbiol*, **69**, 463-485. doi: 10.1146/annurev-micro-091014-104100.
- Blanchoin, L., Boujemaa-Paterski, R., Sykes, C. and Plastino, J. (2014). Actin Dynamics, Architecture, and Mechanics in Cell Motility. *Physiology Reviews*, **94**, 235-263. doi: 10.1152/physrev.00018.2013.-Tight.
- Bonder, E. M., Fishkind, D. J. and Mooseker, M. S. (1983). Direct Measurement of Critical Concentrations and Assembly Rate Constants at the Two Ends of an Actin Filament. *Cell*, **34**, 491-501.
- Bondzie, P. A., Chen, H. A., Cao, M. Z., Tomolonis, J. A., He, F., Pollak, M. R. and Henderson, J. M. (2016). Non-muscle Myosin-IIA is Critical for Podocyte F-actin Organization, Contractility and Attenuation of Cell Motility. *Cytoskeleton (Hoboken)*. doi: 10.1002/cm.21313.
- Boothroyd, J. C. and Dubremetz, J. F. (2008). Kiss and spit: the dual roles of *Toxoplasma* rhoptries. *Nat Rev Microbiol*, **6**, 79-88.
- Borghi, N., Lowndes, M., Maruthamuthu, V., Gardel, M. L. and Nelson, W. J. (2010). Regulation of cell motile behavior by crosstalk between cadherin- and integrin-

- mediated adhesions. *Proc Natl Acad Sci U S A*, **107**, 13324-13329. doi: 10.1073/pnas.1002662107.
- Bosch, J., Paige, M. H., Vaidya, A. B., Bergman, L. W. and Hol, W. G. (2012). Crystal structure of GAP50, the anchor of the invasion machinery in the inner membrane complex of *Plasmodium falciparum*. *J Struct Biol*, **178**, 61-73. doi: 10.1016/j.jsb.2012.02.009.
- Bosch, J., Turley, S., Roach, C. M., Daly, T. M., Bergman, L. W. and Hol, W. G. (2007). The closed MTIP-myosin A-tail complex from the malaria parasite invasion machinery. *J Mol Biol*, **372**, 77-88. doi: 10.1016/j.jmb.2007.06.016.
- Botero-Kleiven, S., Fernandez, V., Lindh, J., Richter-Dahlfors, A., von Euler, A. and Wahlgren, M. (2001). Receptor-mediated endocytosis in an apicomplexan parasite (*Toxoplasma gondii*). *Exp Parasitol*, **98**, 134-144. doi: 10.1006/expr.2001.4624.
- Boucher, L. E. and Bosch, J. (2015). The apicomplexan glideosome and adhesins - Structures and function. *J Struct Biol*, **190**, 93-114. doi: 10.1016/j.jsb.2015.02.008.
- Bougdour, A., Tardieux, I. and Hakimi, M. A. (2014). *Toxoplasma* exports dense granule proteins beyond the vacuole to the host cell nucleus and rewires the host genome expression. *Cell Microbiol*, **16**, 334-343. doi: 10.1111/cmi.12255.
- Bradley, P. J., Ward, C., Cheng, S. J., Alexander, D. L., Collier, S., Coombs, G. H., Dunn, J. D., Ferguson, D. J., Sanderson, S. J., Wastling, J. M. and Boothroyd, J. C. (2005). Proteomic analysis of rhoptry organelles reveals many novel constituents for host-parasite interactions in *Toxoplasma gondii*. *J Biol Chem*, **280**, 34245-34258.
- Breinich, M. S., Ferguson, D. J., Foth, B. J., van Dooren, G. G., Lebrun, M., Quon, D. V., Striepen, B., Bradley, P. J., Frischknecht, F., Carruthers, V. B. and Meissner, M. (2009). A dynamin is required for the biogenesis of secretory organelles in *Toxoplasma gondii*. *Curr Biol*, **19**, 277-286. doi: 10.1016/j.cub.2009.01.039.
- Bretscher, M. S. (1976). Directed lipid flow in cell membranes. *Nature*, **260**, 21-23.
- Bretscher, M. S. (1996a). Getting Membrane Flow and the Cytoskeleton to Cooperate in Moving Cells. *Cell*, **97**, 601-606.
- Bretscher, M. S. (1996b). Moving Membrane up to the Front of Migrating Cells. *Cell*, **95**, 465-467.
- Bretscher, M. S. (2014). Asymmetry of single cells and where that leads. *Annu Rev Biochem*, **83**, 275-289. doi: 10.1146/annurev-biochem-060713-035813.
- Brossier, F., Jewett, T. J., Lovett, J. L. and Sibley, L. D. (2003). C-terminal processing of the toxoplasma protein MIC2 is essential for invasion into host cells. *J Biol Chem*, **278**, 6229-6234.
- Bubb, M. R., Senderowicz, A. M., Sausville, E. A., Duncan, K. L. and Korn, E. D. (1994). Jasplakinolide, a cytotoxic natural product, induces actin polymerization and competitively inhibits the binding of phalloidin to F-actin. *J Biol Chem*, **269**, 14869-14871.
- Bubb, M. R., Spector, I., Beyer, B. B. and Fosen, K. M. (2000). Effects of jasplakinolide on the kinetics of actin polymerization. An explanation for certain in vivo observations. *J Biol Chem*, **275**, 5163-5170.
- Bugyi, B. and Carlier, M. F. (2010). Control of actin filament treadmilling in cell motility. *Annu Rev Biophys*, **39**, 449-470. doi: 10.1146/annurev-biophys-051309-103849.
- Cai, L., Makhov, A. M., Schafer, D. A. and Bear, J. E. (2008). Coronin 1B antagonizes cortactin and remodels Arp2/3-containing actin branches in lamellipodia. *Cell*, **134**, 828-842. doi: 10.1016/j.cell.2008.06.054.
- Caldas, L. A., de Souza, W. and Attias, M. (2010). Microscopic analysis of calcium ionophore activated egress of *Toxoplasma gondii* from the host cell. *Vet Parasitol*, **167**, 8-18. doi: 10.1016/j.vetpar.2009.09.051.
- Calderwood, D. A., Campbell, I. D. and Critchley, D. R. (2013). Talins and kindlins: partners in integrin-mediated adhesion. *Nat Rev Mol Cell Biol*, **14**, 503-517. doi: 10.1038/nrm3624.
- Campbell, R. E., Tour, O., Palmer, A. E., Steinbach, P. A., Baird, G. S., Zacharias, D. A. and Tsien, R. Y. (2002). A monomeric red fluorescent protein. *Proc Natl Acad Sci U S A*, **99**, 7877-7882. doi: 10.1073/pnas.082243699.

- Carballido-Lopez, R. (2006). The bacterial actin-like cytoskeleton. *Microbiol Mol Biol Rev*, **70**, 888-909. doi: 10.1128/MMBR.00014-06.
- Carey, K. L., Jongco, A. M., Kim, K. and Ward, G. E. (2004a). The *Toxoplasma gondii* rhopty protein ROP4 is secreted into the parasitophorous vacuole and becomes phosphorylated in infected cells. *Eukaryot Cell*, **3**, 1320-1330. doi: 10.1128/EC.3.5.1320-1330.2004.
- Carey, K. L., Westwood, N. J., Mitchison, T. J. and Ward, G. E. (2004b). A small-molecule approach to studying invasive mechanisms of *Toxoplasma gondii*. *Proc Natl Acad Sci U S A*, **101**, 7433-7438.
- Carlier, M. F., Pantaloni, D. and Korn, E. D. (1986). The effects of Mg<sup>2+</sup> at the high-affinity and low-affinity sites on the polymerization of actin and associated ATP hydrolysis. *Journal of Biological Chemistry*, **261**, 10785-10792.
- Carruthers, V. and Boothroyd, J. C. (2007). Pulling together: an integrated model of *Toxoplasma* cell invasion. *Curr Opin Microbiol*, **10**, 83-89. doi: 10.1016/j.mib.2006.06.017.
- Carruthers, V. and Tomley, F. M. (2008). Receptor-ligand interaction and invasion-Microneme proteins in apicomplexans. *Subcell Biochem*, **47**, 33-45.
- Carruthers, V. B. (2002). Host cell invasion by the opportunistic pathogen *Toxoplasma gondii*. *Acta Tropica*, **81**, 111-122.
- Carruthers, V. B., Giddings, O. K. and Sibley, L. D. (1999). Secretion of micronemal proteins is associated with *Toxoplasma* invasion of host cells. *Cell Microbiol*, **1**, 225-235.
- Carruthers, V. B., Hakansson, S., Giddings, O. K. and Sibley, L. D. (2000a). *Toxoplasma gondii* uses sulfated proteoglycans for substrate and host cell attachment. *Infect Immun*, **68**, 4005-4011.
- Carruthers, V. B., Sherman, G. D. and Sibley, L. D. (2000b). The *Toxoplasma* adhesive protein MIC2 is proteolytically processed at multiple sites by two parasite-derived proteases. *J Biol Chem*, **275**, 14346-14353.
- Case, L. B. and Waterman, C. M. (2015). Integration of actin dynamics and cell adhesion by a three-dimensional, mechanosensitive molecular clutch. *Nat Cell Biol*, **17**, 955-963. doi: 10.1038/ncb3191.
- Cesbron-Delauw, M. F., Guy, B., Torpier, G., Pierce, R. J., Lenzen, G., Cesbron, J. Y., Charif, H., Lepage, P., Darcy, F., Lecocq, J. P. and et al. (1989). Molecular characterization of a 23-kilodalton major antigen secreted by *Toxoplasma gondii*. *Proc Natl Acad Sci U S A*, **86**, 7537-7541.
- Chan, K. T., Creed, S. J. and Bear, J. E. (2011). Unraveling the enigma: progress towards understanding the coronin family of actin regulators. *Trends Cell Biol*, **21**, 481-488. doi: 10.1016/j.tcb.2011.04.004.
- Charras, G. and Briehner, W. M. (2016). Regulation and integrated functions of the actin cytoskeleton. *Mol Biol Cell*, **27**, 881. doi: 10.1091/mbc.E15-11-0766.
- Charras, G. T., Yarrow, J. C., Horton, M. A., Mahadevan, L. and Mitchison, T. J. (2005). Non-equilibration of hydrostatic pressure in blebbing cells. *Nature*, **435**, 365-369. doi: 10.1038/nature03550.
- Checkley, W., White, A. C., Jr., Jaganath, D., Arrowood, M. J., Chalmers, R. M., Chen, X. M., Fayer, R., Griffiths, J. K., Guerrant, R. L., Hedstrom, L., Huston, C. D., Kotloff, K. L., Kang, G., Mead, J. R., Miller, M., Petri, W. A., Jr., Priest, J. W., Roos, D. S., Striepen, B., Thompson, R. C., Ward, H. D., Van Voorhis, W. A., Xiao, L., Zhu, G. and Houpt, E. R. (2015). A review of the global burden, novel diagnostics, therapeutics, and vaccine targets for cryptosporidium. *Lancet Infect Dis*, **15**, 85-94. doi: 10.1016/S1473-3099(14)70772-8.
- Chen, X. M., Huang, B. Q., Splinter, P. L., Orth, J. D., Billadeau, D. D., McNiven, M. A. and LaRusso, N. F. (2004). Cdc42 and the actin-related protein/neural Wiskott-Aldrich syndrome protein network mediate cellular invasion by *Cryptosporidium parvum*. *Infect Immun*, **72**, 3011-3021.
- Chen, X. M., O'Hara, S. P., Huang, B. Q., Splinter, P. L., Nelson, J. B. and LaRusso, N. F. (2005). Localized glucose and water influx facilitates *Cryptosporidium parvum*

- cellular invasion by means of modulation of host-cell membrane protrusion. *Proc Natl Acad Sci U S A*, **102**, 6338-6343.
- Chen, Y., Rice, W., Gu, Z., Li, J., Huang, J., Brenner, M. B., Van Hoek, A., Xiong, J., Gundersen, G. G., Norman, J. C., Hsu, V. W., Fenton, R. A., Brown, D. and Lu, H. A. (2012). Aquaporin 2 promotes cell migration and epithelial morphogenesis. *J Am Soc Nephrol*, **23**, 1506-1517. doi: 10.1681/ASN.2012010079.
- Chhabra, E. S. and Higgs, H. N. (2007). The many faces of actin: matching assembly factors with cellular structures. *Nat Cell Biol*, **9**, 1110-1121. doi: 10.1038/ncb1007-1110.
- Chi, Q., Yin, T., Gregersen, H., Deng, X., Fan, Y., Zhao, J., Liao, D. and Wang, G. (2014). Rear actomyosin contractility-driven directional cell migration in three-dimensional matrices: a mechano-chemical coupling mechanism. *J R Soc Interface*, **11**, 20131072. doi: 10.1098/rsif.2013.1072.
- Child, M. A., Hall, C. I., Beck, J. R., Ofori, L., Albrow, V. E., Garland, M., Bowyer, P. W., Bradley, J. P., Powers, J. C., Boothroyd, J. C., Weerapana, E. and Bogoy, M. (2013). Small molecule inhibition of a depalmitoylase enhances Toxoplasma host-cell invasion. *Nature Chemical Biology*, **9**, 651-658. doi: 10.1038/nchembio.1315.
- Cintra, W. M. and De Souza, W. (1985). Immunocytochemical localization of cytoskeletal proteins and electron microscopy of detergent extracted tachyzoites of *Toxoplasma gondii*. *J Submicrosc Cytol*, **17**, 503-508.
- Cleveland, D. W. (1982). Treadmilling of tubulin and actin. *Cell*, **28**, 689-691.
- Coleman, B. I. and Gubbels, M. J. (2012). A genetic screen to isolate *Toxoplasma gondii* host-cell egress mutants. *J Vis Exp*. doi: 10.3791/3807.
- Collins, C. R., Das, S., Wong, E. H., Andenmatten, N., Stallmach, R., Hackett, F., Herman, J. P., Muller, S., Meissner, M. and Blackman, M. J. (2013). Robust inducible Cre recombinase activity in the human malaria parasite *Plasmodium falciparum* enables efficient gene deletion within a single asexual erythrocytic growth cycle. *Mol Microbiol*, **88**, 687-701. doi: 10.1111/mmi.12206.
- Cooper, J. A. (1987). Effects of Cytochalasin and Phalloidin on Actin. *J Cell Biol*, **105**, 1473-1178.
- Cooper, J. A., Buhle, E. L., Jr., Walker, S. B., Tsong, T. Y. and Pollard, T. D. (1983). Kinetic evidence for a monomer activation step in actin polymerization. *Biochemistry*, **22**, 2193-2202.
- Copeland, M. (1974). The cellular response to cytochalasin B: a critical overview. *Cytologia (Tokyo)*, **39**, 709-727.
- Coppens, I., Dunn, J. D., Romano, J. D., Pypaert, M., Zhang, H., Boothroyd, J. C. and Joiner, K. A. (2006). *Toxoplasma gondii* sequesters lysosomes from mammalian hosts in the vacuolar space. *Cell*, **125**, 261-274.
- Coppens, I., Sinai, A. P. and Joiner, K. A. (2000). *Toxoplasma gondii* exploits host low-density lipoprotein receptor-mediated endocytosis for cholesterol acquisition. *J Cell Biol*, **149**, 167-180.
- Coue, M., Brenner, S. L., Spector, I. and Korn, E. D. (1987). Inhibition of actin polymerisation by Latrunculin A. *FEBS Lett*, **213**, 316-318.
- Cowen, D. and Wolf, A. (1937). Granulomatous encephalomyelitis due to an encephalitozoon (encephalitozoic encephalomyelitis), a new protozoon disease of man. *Bull. neurol. Inst. N.Y*, **6**, 306-371.
- Cowman, A. F. and Crabb, B. S. (2006). Invasion of red blood cells by malaria parasites. *Cell*, **124**, 755-766. doi: 10.1016/j.cell.2006.02.006.
- Daher, W., Klages, N., Carlier, M. F. and Soldati-Favre, D. (2011). Molecular Characterization of *Toxoplasma gondii* Formin 3, an Actin Nucleator Dispensable for Tachyzoite Growth and Motility. *Eukaryot Cell*, **11**, 343-352. doi: 10.1128/ec.05192-11.
- Daher, W., Plattner, F., Carlier, M. F. and Soldati-Favre, D. (2010). Concerted action of two formins in gliding motility and host cell invasion by *Toxoplasma gondii*. *PLoS Pathog*, **6**, e1001132. doi: 10.1371/journal.ppat.1001132.
- de Greef, T. F. A., Smulders, M. M., Wolfs, M., Schenning, A. P., Sijbesma, R. P. and Meijer, E. W. (2009). Supramolecular Polymerization. *Chem Rev*, **109**, 5687-5754.

- Deeks, M. J. and Hussey, P. J. (2005). Arp2/3 and SCAR: plants move to the fore. *Nature Reviews Molecular Cell Biology*, **6**, 954-964.
- Del Carmen, M. G., Mondragon, M., Gonzalez, S. and Mondragon, R. (2009). Induction and regulation of conoid extrusion in *Toxoplasma gondii*. *Cell Microbiol*, **11**, 967-982. doi: 10.1111/j.1462-5822.2009.01304.x.
- Delbac, F., Sanger, A., Neuhaus, E. M., Stratmann, R., Ajioka, J. W., Toursel, C., Herm-Gotz, A., Tomavo, S., Soldati, T. and Soldati, D. (2001). *Toxoplasma gondii* myosins B/C: one gene, two tails, two localizations, and a role in parasite division. *J Cell Biol*, **155**, 613-623. doi: 10.1083/jcb.200012116.
- Delorme-Walker, V., Abrivard, M., Lagal, V., Anderson, K., Perazzi, A., Gonzalez, V., Page, C., Chauvet, J., Ochoa, W., Volkmann, N., Hanein, D. and Tardieux, I. (2012). Toxofilin upregulates the host cortical actin cytoskeleton dynamics facilitating *Toxoplasma* invasion. *J Cell Sci*.
- Desjardins, P. and Conklin, D. (2010). NanoDrop microvolume quantitation of nucleic acids. *J Vis Exp*. doi: 10.3791/2565.
- Diz-Munoz, A., Krieg, M., Bergert, M., Ibarlucea-Benitez, I., Muller, D. J., Paluch, E. and Heisenberg, C. P. (2010). Control of directed cell migration in vivo by membrane-to-cortex attachment. *PLoS Biol*, **8**, e1000544. doi: 10.1371/journal.pbio.1000544.
- Dobrowolski, J. and Sibley, L. D. (1997). The role of the cytoskeleton in host cell invasion by *Toxoplasma gondii*. *Behring Inst Mitt*, 90-96.
- Dobrowolski, J. M., Niesman, I. R. and Sibley, L. D. (1997). Actin in the parasite *Toxoplasma gondii* is encoded by a single copy gene, ACT1 and exists primarily in a globular form. *Cell Motil Cytoskeleton*, **37**, 253-262.
- Dobrowolski, J. M. and Sibley, L. D. (1996). *Toxoplasma* invasion of mammalian cells is powered by the actin cytoskeleton of the parasite. *Cell*, **84**, 933-939.
- Dokukina, I. V. and Gracheva, M. E. (2010). A model of fibroblast motility on substrates with different rigidities. *Biophys J*, **98**, 2794-2803. doi: 10.1016/j.bpj.2010.03.026.
- Dominguez, R. (2009). Actin filament nucleation and elongation factors--structure-function relationships. *Crit Rev Biochem Mol Biol*, **44**, 351-366. doi: 10.3109/10409230903277340.
- Dominguez, R. and Holmes, K. C. (2011). Actin structure and function. *Annu Rev Biophys*, **40**, 169-186. doi: 10.1146/annurev-biophys-042910-155359.
- Donald, R. G., Carter, D., Ullman, B. and Roos, D. S. (1996). Insertional tagging, cloning, and expression of the *Toxoplasma gondii* hypoxanthine-xanthine-guanine phosphoribosyltransferase gene. Use as a selectable marker for stable transformation. *J Biol Chem*, **271**, 14010-14019.
- Donald, R. G. and Roos, D. S. (1993). Stable molecular transformation of *Toxoplasma gondii*: a selectable dihydrofolate reductase-thymidylate synthase marker based on drug-resistance mutations in malaria. *Proc Natl Acad Sci U S A*, **90**, 11703-11707.
- Dos Remedios, G., Chhabra, D., Kekic, M., Dedova, I. V., Tsubakihara, M., Berry, D. A. and Nosworthy, N. J. (2003). Actin Binding Proteins: Regulation of Cytoskeleton Microfilaments. *Physiol Rev*, **83**, 433-473.
- Dowse, T. and Soldati, D. (2004). Host cell invasion by the apicomplexans: the significance of microneme protein proteolysis. *Curr Opin Microbiol*, **7**, 388-396. doi: 10.1016/j.mib.2004.06.013.
- Drewry, L. L. and Sibley, L. D. (2015). *Toxoplasma* Actin Is Required for Efficient Host Cell Invasion. *MBio*, **6**. doi: 10.1128/mBio.00557-15.
- Drouin, G., Moniz de Sa, M. and Zuker, M. (1995). The *Giardia lamblia* actin gene and the phylogeny of eukaryotes. *J Mol Evol*, **41**, 841-849.
- Drubin, D. G., Jones, H. D. and Wertman, K. F. (1993). Actin structure and function: roles in mitochondrial organization and morphogenesis in budding yeast and identification of the phalloidin-binding site. *Mol Biol Cell*, **4**, 1277-1294.
- Dubey, J. P. (2009). History of the discovery of the life cycle of *Toxoplasma gondii*. *Int J Parasitol*, **39**, 877-882.

- Dubey, J. P., Lindsay, D. S. and Speer, C. A. (1998). Structures of *Toxoplasma gondii* Tachyzoites, Bradyzoites, and Sporozoites and Biology and Development of Tissue Cysts. *Clinical Microbiology Reviews*, **11**, 267-299.
- Dubey, J. P., Miller, N. L. and Frenkel, J. K. (1970a). *Toxoplasma gondii* life cycle in cats. *J Am Vet Med Assoc*, **157**, 1767-1770.
- Dubey, J. P., Miller, N. L. and Frenkel, J. K. (1970b). The *Toxoplasma gondii* oocyst from cat feces. *J Exp Med*, **132**, 636-662.
- Dubremetz, J. F. (2007). Rhoptries are major players in *Toxoplasma gondii* invasion and host cell interaction. *Cell Microbiol*, **9**, 841-848. doi: 10.1111/j.1462-5822.2007.00909.x.
- Dunn, D., Wallon, M., Peyron, F., Petersen, E., Peckham, C. and Gilbert, R. (1999). Mother-to-child transmission of toxoplasmosis: risk estimates for clinical counselling. *Lancet*, **353**, 1829-1833. doi: 10.1016/S0140-6736(98)08220-8.
- Dunn, J. D., Ravindran, S., Kim, S. K. and Boothroyd, J. C. (2008). The *Toxoplasma gondii* dense granule protein GRA7 is phosphorylated upon invasion and forms an unexpected association with the rhoptry proteins ROP2 and ROP4. *Infect Immun*, **76**, 5853-5861. doi: 10.1128/IAI.01667-07.
- Dutta, D., Williamson, C. D., Cole, N. B. and Donaldson, J. G. (2012). Pitstop 2 is a potent inhibitor of clathrin-independent endocytosis. *PLoS One*, **7**, e45799. doi: 10.1371/journal.pone.0045799.
- Egarter, S., Andenmatten, N., Jackson, A. J., Whitelaw, J. A., Pall, G., Black, J. A., Ferguson, D. J., Tardieux, I., Mogilner, A. and Meissner, M. (2014). The *Toxoplasma* Acto-MyoA motor complex is important but not essential for gliding motility and host cell invasion. *PLoS One*, **9**, e91819. doi: 10.1371/journal.pone.0091819.
- Egelman, E. H. (2004). Acrosomal actin: twists and turns of a versatile filament. *Curr Biol*, **14**, R959-961. doi: 10.1016/j.cub.2004.10.042.
- El Hajj, H., Lebrun, M., Fourmaux, M. N., Vial, H. and Dubremetz, J. F. (2007). Inverted topology of the *Toxoplasma gondii* ROP5 rhoptry protein provides new insights into the association of the ROP2 protein family with the parasitophorous vacuole membrane. *Cell Microbiol*, **9**, 54-64. doi: 10.1111/j.1462-5822.2006.00767.x.
- Elliott, D. A. and Clark, D. P. (2000). *Cryptosporidium parvum* induces host cell actin accumulation at the host-parasite interface. *Infect Immun*, **68**, 2315-2322.
- Elosegui-Artola, A., Oria, R., Chen, Y., Kosmalska, A., Perez-Gonzalez, C., Castro, N., Zhu, C., Trepas, X. and Roca-Cusachs, P. (2016). Mechanical regulation of a molecular clutch defines force transmission and transduction in response to matrix rigidity. *Nat Cell Biol*. doi: 10.1038/ncb3336.
- Endo, T. and Yagita, K. (1990). Effect of extracellular ions on motility and cell entry in *Toxoplasma gondii*. *J Protozool*, **37**, 133-138.
- Evangelista, M., Zigmund, S. and Boone, C. (2003). Formins: signaling effectors for assembly and polarization of actin filaments. *J Cell Sci*, **116**, 2603-2611. doi: 10.1242/jcs.00611.
- Feng, Z., Ning Chen, W., Vee Sin Lee, P., Liao, K. and Chan, V. (2005). The influence of GFP-actin expression on the adhesion dynamics of HepG2 cells on a model extracellular matrix. *Biomaterials*, **26**, 5348-5358. doi: 10.1016/j.biomaterials.2005.01.069.
- Fenn, S., Gerhold, C. B. and Hopfner, K. P. (2011). Nuclear actin-related proteins take shape. *Bioarchitecture*, **1**, 192-195. doi: 10.4161/bioa.1.4.17643.
- Ferguson, D. J. (2009). *Toxoplasma gondii*: 1908-2008, homage to Nicolle, Manceaux and Splendore. *Mem Inst Oswaldo Cruz*, **104**, 133-148.
- Fichera, M. E. and Roos, D. S. (1997). A plastid organelle as a drug target in apicomplexan parasites. *Nature*, **390**, 407-409.
- Field, S. J., Rangachari, K., Dluzewski, A. R., Wilson, R. J. and Gratzer, W. B. (1992). Effect of intra-erythrocytic magnesium ions on invasion by *Plasmodium falciparum*. *Parasitology*, **105** ( Pt 1), 15-19.

- Flegr, J., Prandota, J., Sovickova, M. and Israili, Z. H. (2014). Toxoplasmosis--a global threat. Correlation of latent toxoplasmosis with specific disease burden in a set of 88 countries. *PLoS One*, **9**, e90203. doi: 10.1371/journal.pone.0090203.
- Fogelson, B. and Mogilner, A. (2014). Computational estimates of membrane flow and tension gradient in motile cells. *PLoS One*, **9**, e84524. doi: 10.1371/journal.pone.0084524.
- Foissner, I. and Wasteneys, G. O. (2007). Wide-ranging effects of eight cytochalasins and latrunculin A and B on intracellular motility and actin filament reorganization in characean internodal cells. *Plant Cell Physiol*, **48**, 585-597. doi: 10.1093/pcp/pcm030.
- Forscher, P., Lin, C. H. and Thompson, C. (1992). Novel form of growth cone motility involving site-directed actin filament assembly. *Nature*, **357**, 515-518. doi: 10.1038/357515a0.
- Foth, B. J., Goedecke, M. C. and Soldati, D. (2006). New insights into myosin evolution and classification. *Proc Natl Acad Sci U S A*, **103**, 3681-3686. doi: 10.1073/pnas.0506307103.
- Fox, B. A., Ristuccia, J. G., Gigley, J. P. and Bzik, D. J. (2009). Efficient gene replacements in *Toxoplasma gondii* strains deficient for nonhomologous end joining. *Eukaryot Cell*, **8**, 520-529.
- Frankel, S. and Mooseker, M. S. (1996). The actin-related proteins. *Curr Opin Cell Biol*, **8**, 30-37.
- Frenal, K., Marq, J. B., Jacot, D., Polonais, V. and Soldati-Favre, D. (2014). Plasticity between MyoC- and MyoA-glideosomes: an example of functional compensation in *Toxoplasma gondii* invasion. *PLoS Pathog*, **10**, e1004504. doi: 10.1371/journal.ppat.1004504.
- Frenal, K., Polonais, V., Marq, J. B., Stratmann, R., Limenitakis, J. and Soldati-Favre, D. (2010). Functional dissection of the apicomplexan glideosome molecular architecture. *Cell Host Microbe*, **8**, 343-357. doi: 10.1016/j.chom.2010.09.002.
- Frenal, K. and Soldati, D. (2015). Plasticity and Redundancy in Proteins Important for *Toxoplasma* Invasion. *PLoS Pathog*, **11**, 1-6. doi: 10.1371/journal.ppat.1005069.t001.
- Frenkel, J. K. (1973). *Toxoplasma* in and around us. *BioScience*, **23**, 343-352.
- Frenkel, J. K., Dubey, J. P. and Miller, N. L. (1970). *Toxoplasma gondii* in cats: fecal stages identified as coccidian oocysts. *Science*, **167**, 893-896.
- Friedl, P. and Wolf, K. (2010). Plasticity of cell migration: a multiscale tuning model. *J Cell Biol*, **188**, 11-19. doi: 10.1083/jcb.200909003.
- Fuentes, I., Rubio, J. M., Ramirez, C. and Alvar, J. (2001). Genotypic Characterization of *Toxoplasma gondii* Strains Associated with Human Toxoplasmosis in Spain: Direct Analysis from Clinical Samples. *J Clin Microbiol*, **39**, 1566-1570. doi: 10.1128/jcm.39.4.1566-1570.2001.
- Fujita, M., Ichinose, S., Kiyono, T., Tsurumi, T. and Omori, A. (2003). Establishment of latrunculin-A resistance in HeLa cells by expression of R183A D184A mutant beta-actin. *Oncogene*, **22**, 627-631. doi: 10.1038/sj.onc.1206173.
- Gaji, R. Y., Huynh, M. H. and Carruthers, V. B. (2013). A novel high throughput invasion screen identifies host actin regulators required for efficient cell entry by *Toxoplasma gondii*. *PLoS One*, **8**, e64693. doi: 10.1371/journal.pone.0064693.
- Galdal, K. S., Evensen, S. A., Høglund, A. S. and Nilsen, E. (1983). Actin pools and actin microfilament organization in cultured human endothelial cells after exposure to thrombin. *British Journal of Haematology*, **58**, 617-625.
- Galkin, V. E., Orlova, A., Kudryashov, D. S., Solodukhin, A., Reisler, E., Schroder, G. F. and Egelman, E. H. (2011). Remodeling of actin filaments by ADF/cofilin proteins. *Proc Natl Acad Sci U S A*, **108**, 20568-20572. doi: 10.1073/pnas.1110109108.
- Gandhi, M. and Goode, B. L. (2008). Coronin: the double-edged sword of actin dynamics. *Subcell Biochem*, **48**, 72-87. doi: 10.1007/978-0-387-09595-0\_7.
- Garg, S., Sharma, V., Ramu, D. and Singh, S. (2015). In silico analysis of calcium binding pocket of perforin like protein 1: insights into the regulation of pore formation. *Syst Synth Biol*, **9**, 17-21. doi: 10.1007/s11693-015-9166-x.

- Garrels, J. I. and Gibson, W. (1976). Identification and characterization of multiple forms of actin. *Cell*, **9**, 793-805.
- Gaskins, E., Gilk, S., DeVore, N., Mann, T., Ward, G. and Beckers, C. (2004). Identification of the membrane receptor of a class XIV myosin in *Toxoplasma gondii*. *J Cell Biol*, **165**, 383-393.
- Gerdes, H. H., Bukoreshtliev, N. V. and Barroso, J. F. (2007). Tunneling nanotubes: a new route for the exchange of components between animal cells. *FEBS Lett*, **581**, 2194-2201. doi: 10.1016/j.febslet.2007.03.071.
- Gerdes, H. H. and Carvalho, R. N. (2008). Intercellular transfer mediated by tunneling nanotubes. *Curr Opin Cell Biol*, **20**, 470-475. doi: 10.1016/j.ceb.2008.03.005.
- Gilk, S. D., Gaskins, E., Ward, G. E. and Beckers, C. J. (2009). GAP45 phosphorylation controls assembly of the *Toxoplasma* myosin XIV complex. *Eukaryot Cell*, **8**, 190-196.
- Gisselberg, J. E., Dellibovi-Ragheb, T. A., Matthews, K. A., Bosch, G. and Prigge, S. T. (2013). The suf iron-sulfur cluster synthesis pathway is required for apicoplast maintenance in malaria parasites. *PLoS Pathog*, **9**, e1003655. doi: 10.1371/journal.ppat.1003655.
- Goddette, D. W. and Frieden, C. (1985). The binding of cytochalasin D to monomeric actin. *Biochem Biophys Res Commun*, **128**, 1087-1092.
- Goddette, D. W. and Frieden, C. (1986). Actin polymerisation: The mechanism of action of cytochalasin D. *J Biol Chem*, **261**, 15974-15980.
- Gold, D. A., Kaplan, A. D., Lis, A., Bett, G. C., Rosowski, E. E., Cirelli, K. M., Bougdour, A., Sidik, S. M., Beck, J. R., Lourido, S., Egea, P. F., Bradley, P. J., Hakimi, M. A., Rasmusson, R. L. and Saeij, J. P. (2015). The *Toxoplasma* Dense Granule Proteins GRA17 and GRA23 Mediate the Movement of Small Molecules between the Host and the Parasitophorous Vacuole. *Cell Host Microbe*, **17**, 642-652. doi: 10.1016/j.chom.2015.04.003.
- Goley, E. D. and Welch, M. D. (2006). The ARP2/3 complex: an actin nucleator comes of age. *Nat Rev Mol Cell Biol*, **7**, 713-726. doi: 10.1038/nrm2026.
- Gong, X. W. and Jiang, Y. (2004). Structure, function and modulation of actin-related protein 2/3 complex. *Sheng Li Ke Xue Jin Zhan*, **35**, 306-310.
- Gonzalez, V., Combe, A., David, V., Malmquist, N. A., Delorme, V., Leroy, C., Blazquez, S., Menard, R. and Tardieux, I. (2009). Host cell entry by apicomplexa parasites requires actin polymerization in the host cell. *Cell Host Microbe*, **5**, 259-272. doi: 10.1016/j.chom.2009.01.011.
- Goode, B. L. and Eck, M. J. (2007). Mechanism and function of formins in the control of actin assembly. *Annu Rev Biochem*, **76**, 593-627. doi: 10.1146/annurev.biochem.75.103004.142647.
- Gordon, J. L., Beatty, W. L. and Sibley, L. D. (2008). A novel actin-related protein is associated with daughter cell formation in *Toxoplasma gondii*. *Eukaryot Cell*, **7**, 1500-1512. doi: 10.1128/EC.00064-08.
- Gordon, J. L., Buguliskis, J. S., Buske, P. J. and Sibley, L. D. (2010). Actin-like protein 1 (ALP1) is a component of dynamic, high molecular weight complexes in *Toxoplasma gondii*. *Cytoskeleton (Hoboken)*, **67**, 23-31. doi: 10.1002/cm.20414.
- Gordon, J. L. and Sibley, L. D. (2005). Comparative genome analysis reveals a conserved family of actin-like proteins in apicomplexan parasites. *BMC Genomics*, **6**, 179.
- Gould, S. B., Kraft, L. G., van Dooren, G. G., Goodman, C. D., Ford, K. L., Cassin, A. M., Bacic, A., McFadden, G. I. and Waller, R. F. (2011). Ciliate pellicular proteome identifies novel protein families with characteristic repeat motifs that are common to alveolates. *Mol Biol Evol*, **28**, 1319-1331. doi: 10.1093/molbev/msq321.
- Green, R. and Rogers, E. J. (2013). Transformation of chemically competent *E. coli*. *Methods Enzymol*, **529**, 329-336. doi: 10.1016/B978-0-12-418687-3.00028-8.
- Grigg, M. E., Bonnefoy, S., Hehl, A. B., Suzuki, Y. and Boothroyd, J. C. (2001). Success and virulence in *Toxoplasma* as the result of sexual recombination between two distinct ancestries. *Science*, **294**, 161-165. doi: 10.1126/science.1061888.

- Gross, U., Kempf, M. C., Seeber, F., Luder, C. G., Lugert, R. and Bohne, W. (1997). Reactivation of chronic toxoplasmosis: is there a link to strain-specific differences in the parasite? *Behring Inst Mitt*, 97-106.
- Gubbels, M. J. and Striepen, B. (2004). Studying the cell biology of apicomplexan parasites using fluorescent proteins. *Microsc Microanal*, 10, 568-579. doi: 10.1017/S1431927604040899.
- Gubbels, M. J., Vaishnav, S., Boot, N., Dubremetz, J. F. and Striepen, B. (2006). A MORN-repeat protein is a dynamic component of the *Toxoplasma gondii* cell division apparatus. *J Cell Sci*, 119, 2236-2245.
- Gubbels, M. J., White, M. and Szatanek, T. (2008). The cell cycle and *Toxoplasma gondii* cell division: tightly knit or loosely stitched? *Int J Parasitol*, 38, 1343-1358. doi: 10.1016/j.ijpara.2008.06.004.
- Guo, K., Shillcock, J. and Lipowsky, R. (2010). Treadmilling of actin filaments via Brownian dynamics simulations. *J Chem Phys*, 133, 155105. doi: 10.1063/1.3497001.
- Gupta, C. M., Thiyagarajan, S. and Sahasrabudde, A. A. (2015). Unconventional actins and actin-binding proteins in human protozoan parasites. *Int J Parasitol*, 45, 435-447. doi: 10.1016/j.ijpara.2015.01.011.
- Haase, S., Zimmermann, D., Olshina, M. A., Wilkinson, M., Fisher, F., Tan, Y. H., Stewart, R. J., Tonkin, C. J., Wong, W., Kovar, D. R. and Baum, J. (2015). Disassembly activity of actin-depolymerizing factor (ADF) is associated with distinct cellular processes in apicomplexan parasites. *Mol Biol Cell*, 26, 3001-3012. doi: 10.1091/mbc.E14-10-1427.
- Hakansson, S., Charron, A. J. and Sibley, L. D. (2001). *Toxoplasma* evacuoles: a two-step process of secretion and fusion forms the parasitophorous vacuole. *Embo J*, 20, 3132-3144.
- Hakansson, S., Morisaki, H., Heuser, J. and Sibley, L. D. (1999). Time-lapse video microscopy of gliding motility in *Toxoplasma gondii* reveals a novel, biphasic mechanism of cell locomotion. *Mol Biol Cell*, 10, 3539-3547.
- Hall, A. (1998). Rho GTPases and the actin cytoskeleton. *Science*, 279, 509-514.
- Hall, A. and Nobes, C. D. (2000). Rho GTPases: molecular switches that control the organization and dynamics of the actin cytoskeleton. *Philos Trans R Soc Lond B Biol Sci*, 355, 965-970. doi: 10.1098/rstb.2000.0632.
- Harding, C. R., Egarter, S., Gow, M., Jimenez-Ruiz, E., Ferguson, D. J. and Meissner, M. (2016). Gliding Associated Proteins Play Essential Roles during the Formation of the Inner Membrane Complex of *Toxoplasma gondii*. *PLoS Pathog*, 12, e1005403. doi: 10.1371/journal.ppat.1005403.
- Harker, K. S., Jivan, E., McWhorter, F. Y., Liu, W. F. and Lodoen, M. B. (2014). Shear forces enhance *Toxoplasma gondii* tachyzoite motility on vascular endothelium. *MBio*, 5, e01111-01113. doi: 10.1128/mBio.01111-13.
- Hartman, M. A. and Spudich, J. A. (2012). The myosin superfamily at a glance. *J Cell Sci*, 125, 1627-1632. doi: 10.1242/jcs.094300.
- Havrylenko, S., Mezanges, X., Batchelder, E. and Plastino, J. (2014). Extending the molecular clutch beyond actin-based cell motility. *New J Phys*, 16. doi: 10.1088/1367-2630/16/10/105012.
- He, C. Y., Shaw, M. K., Pltcher, C. H., Striepen, B., Tilney, L. G. and Roos, D. S. (2001). A plastid segregation defect in the protozoan parasite *Toxoplasma gondii*. *The EMBO Journal*, 20, 330-339.
- Heaslip, A., Nelson, S. R. and Warshaw, D. M. (2016). Dense granule trafficking in *Toxoplasma gondii* requires a unique class 27 myosin and actin filaments. *Mol Biol Cell*.
- Hegge, S., Munter, S., Steinbuchel, M., Heiss, K., Engel, U., Matuschewski, K. and Frischknecht, F. (2010). Multistep adhesion of *Plasmodium* sporozoites. *FASEB J*, 24, 2222-2234. doi: 10.1096/fj.09-148700.
- Hegge, S., Uhrig, K., Streichfuss, M., Kynast-Wolf, G., Matuschewski, K., Spatz, J. P. and Frischknecht, F. (2012). Direct manipulation of malaria parasites with optical tweezers reveals distinct functions of *Plasmodium* surface proteins. *ASC Nano*, 6, 4648-4662.

- Heintzelman, M. B. (2015). Gliding motility in apicomplexan parasites. *Semin Cell Dev Biol*. doi: 10.1016/j.semcdb.2015.09.020.
- Heintzelman, M. B. and Schwartzman, J. D. (1997). A novel class of unconventional myosins from *Toxoplasma gondii*. *J Mol Biol*, **271**, 139-146. doi: 10.1006/jmbi.1997.1167.
- Herm-Gotz, A., Agop-Nersesian, C., Munter, S., Grimley, J. S., Wandless, T. J., Frischknecht, F. and Meissner, M. (2007). Rapid control of protein level in the apicomplexan *Toxoplasma gondii*. *Nat Methods*, **4**, 1003-1005. doi: 10.1038/nmeth1134.
- Herm-Gotz, A., Weiss, S., Stratmann, R., Fujita-Becker, S., Ruff, C., Meyhofer, E., Soldati, T., Manstein, D. J., Geeves, M. A. and Soldati, D. (2002). *Toxoplasma gondii* myosin A and its light chain: a fast, single-headed, plus-end-directed motor. *EMBO J*, **21**, 2149-2158. doi: 10.1093/emboj/21.9.2149.
- Herman, I. M. (1993). Actin isoforms. *Curr Opin Cell Biol*, **5**, 48-55.
- Hettmann, C., Herm, A., Geiter, A., Frank, B., Schwarz, E., Soldati, T. and Soldati, D. (2000). A dibasic motif in the tail of a class XIV apicomplexan myosin is an essential determinant of plasma membrane localization. *Mol Biol Cell*, **11**, 1385-1400.
- Higgs, H. N. and Peterson, K. J. (2005). Phylogenetic analysis of the formin homology 2 domain. *Mol Biol Cell*, **16**, 1-13. doi: 10.1091/mbc.E04-07-0565.
- Hill, D. E., Chirukandoth, S. and Dubey, J. P. (2005). Biology and epidemiology of *Toxoplasma gondii* in man and animals. *Anim Health Res Rev*, **6**, 41-61.
- Himes, R. H. and Houston, L. L. (1976). The action of cytochalasin A on the in vitro polymerization of brain tubulin and muscle G-actin. *J Supramol Struct*, **5**, 81-90. doi: 10.1002/jss.400050109.
- Himes, R. H., Kersey, R. N., Ruscha, M. and Houston, L. L. (1976). Cytochalasin A inhibits the in vitro polymerization of brain tubulin and muscle actin. *Biochem Biophys Res Commun*, **68**, 1362-1370.
- Hliscs, M., Millet, C., Dixon, M. W., Siden-Kiamos, I., McMillan, P. and Tilley, L. (2015). Organization and function of an actin cytoskeleton in *Plasmodium falciparum* gametocytes. *Cell Microbiol*, **17**, 207-225. doi: 10.1111/cmi.12359.
- Hliscs, M., Sattler, J. M., Tempel, W., Artz, J. D., Dong, A., Hui, R., Matuschewski, K. and Schuler, H. (2010). Structure and function of a G-actin sequestering protein with a vital role in malaria oocyst development inside the mosquito vector. *J Biol Chem*, **285**, 11572-11583. doi: 10.1074/jbc.M109.054916.
- Hoff, E. F. and Carruthers, V. (2002). Is *Toxoplasma* egress the first step in invasion. *Trends Parasitol*, **18**, 251-255.
- Howe, J. D., Barry, N. P. and Bretscher, M. S. (2013). How Do Amoebae Swim and Crawl? *PLoS One*, **8**, 1-5. doi: 10.1371/journal.pone.0074382.g001.
- Hu, K., Mann, T., Striepen, B., Beckers, C. J., Roos, D. S. and Murray, J. M. (2002a). Daughter cell assembly in the protozoan parasite *Toxoplasma gondii*. *Mol Biol Cell*, **13**, 593-606.
- Hu, K., Roos, D. S. and Murray, J. M. (2002b). A novel polymer of tubulin forms the conoid of *Toxoplasma gondii*. *J Cell Biol*, **156**, 1039-1050. doi: 10.1083/jcb.200112086.
- Hughes, H. P., Hudson, L. and Fleck, D. G. (1986). In vitro culture of *Toxoplasma gondii* in primary and established cell lines. *Int J Parasitol*, **16**, 317-322.
- Hunter, C. A. and Sibley, L. D. (2012). Modulation of innate immunity by *Toxoplasma gondii* virulence effectors. *Nat Rev Microbiol*, **10**, 766-778. doi: 10.1038/nrmicro2858.
- Huynh, M. H. and Carruthers, V. B. (2006). *Toxoplasma* MIC2 is a major determinant of invasion and virulence. *PLoS Pathog*, **2**, e84.
- Huynh, M. H. and Carruthers, V. B. (2009). Tagging of endogenous genes in a *Toxoplasma gondii* strain lacking Ku80. *Eukaryot Cell*, **8**, 530-539.
- Huynh, M. H., Rabenau, K. E., Harper, J. M., Beatty, W. L., Sibley, L. D. and Carruthers, V. B. (2003). Rapid invasion of host cells by *Toxoplasma* requires secretion of the MIC2-M2AP adhesive protein complex. *Embo J*, **22**, 2082-2090.

- Ingram, W. M., Goodrich, L. M., Robey, E. A. and Eisen, M. B. (2013). Mice infected with low-virulence strains of *Toxoplasma gondii* lose their innate aversion to cat urine, even after extensive parasite clearance. *PLoS One*, **8**, e75246. doi: 10.1371/journal.pone.0075246.
- Insall, R. H. and Machesky, L. M. (2009). Actin dynamics at the leading edge: from simple machinery to complex networks. *Dev Cell*, **17**, 310-322. doi: 10.1016/j.devcel.2009.08.012.
- Iwamoto, D. V. and Calderwood, D. A. (2015). Regulation of integrin-mediated adhesions. *Curr Opin Cell Biol*, **36**, 41-47. doi: 10.1016/j.ceb.2015.06.009.
- Jacot, D., Daher, W. and Soldati-Favre, D. (2013). *Toxoplasma gondii* myosin F, an essential motor for centrosomes positioning and apicoplast inheritance. *EMBO J*, **32**, 1702-1716. doi: 10.1038/emboj.2013.113.
- Jaeger, M., Carin, M., Medale, M. and Tryggvason, G. (1999). The osmotic migration of cells in a solute gradient. *Biophys J*, **77**, 1257-1267. doi: 10.1016/S0006-3495(99)76977-8.
- Jewett, T. J. and Sibley, L. D. (2003). Aldolase forms a bridge between cell surface adhesins and the actin cytoskeleton in apicomplexan parasites. *Molecular Cell*, **11**, 885-894.
- Jimenez-Ruiz, E., Wong, E. H., Pall, G. S. and Meissner, M. (2014). Advantages and disadvantages of conditional systems for characterization of essential genes in *Toxoplasma gondii*. *Parasitology*, **141**, 1390-1398. doi: 10.1017/S0031182014000559.
- Jones, L. J., Carballido-Lopez, R. and Errington, J. (2001). Control of cell shape in bacteria: helical, actin-like filaments in *Bacillus subtilis*. *Cell*, **104**, 913-922.
- Jones, T. C. and Hirsch, J. G. (1972). The interaction between *Toxoplasma gondii* and mammalian cells. II. The absence of lysosomal fusion with phagocytic vacuoles containing living parasites. *J Exp Med*, **136**, 1173-1194.
- Joyce, J. A. and Pollard, J. W. (2009). Microenvironmental regulation of metastasis. *Nat Rev Cancer*, **9**, 239-252. doi: 10.1038/nrc2618.
- Jullien, N., Goddard, I., Selmi-Ruby, S., Fina, J. L., Cremer, H. and Herman, J. P. (2007). Conditional transgenesis using Dimerizable Cre (DiCre). *PLoS One*, **2**, e1355.
- Jullien, N., Sampieri, F., Enjalbert, A. and Herman, J. P. (2003). Regulation of Cre recombinase by ligand-induced complementation of inactive fragments. *Nucleic Acids Res*, **31**, e131.
- Jung, C. Y. and Rampal, A. L. (1977). Cytochalasin B binding sites and glucose transport carrier in human erythrocyte ghosts. *J Biol Chem*, **252**, 5456-5463.
- Kabsch, W., Mannherz, H. G., Suck, D., Pai, E. F. and Holmes, K. C. (1990). Atomic structure of the actin:DNase I complex. *Nature*, **347**, 37-44. doi: 10.1038/347037a0.
- Kafsack, B. F., Carruthers, V. B. and Pineda, F. J. (2007). Kinetic modeling of *Toxoplasma gondii* invasion. *J Theor Biol*, **249**, 817-825. doi: 10.1016/j.jtbi.2007.09.008.
- Kafsack, B. F. C., Pena, J. D. O., Coppens, I., Ravindran, S., Boothroyd, J. C. and Carruther, V. B. (2009). Rapid Membrane Disruption by a perforin-like protein facilitates parasite exit from host cells. *Science*, **323**, 530-533.
- Kanellos, G. and Frame, M. C. (2016). Cellular functions of the ADF/cofilin family at a glance. *J Cell Sci*. doi: 10.1242/jcs.187849.
- Katris, N. J., van Dooren, G. G., McMillan, P. J., Hanssen, E., Tilley, L. and Waller, R. F. (2014). The apical complex provides a regulated gateway for secretion of invasion factors in *Toxoplasma*. *PLoS Pathog*, **10**, e1004074. doi: 10.1371/journal.ppat.1004074.
- Keeley, A. and Soldati, D. (2004). The glideosome: a molecular machine powering motility and host-cell invasion by Apicomplexa. *Trends Cell Biol*, **14**, 528-532. doi: 10.1016/j.tcb.2004.08.002
- 10.1016/j.tcb.2004.08.001.
- Keren, K. (2011). Cell motility: the integrating role of the plasma membrane. *Eur Biophys J*, **40**, 1013-1027. doi: 10.1007/s00249-011-0741-0.

- Keren, K., Yam, P. T., Kinkhabwala, A., Mogilner, A. and Theriot, J. A. (2009). Intracellular fluid flow in rapidly moving cells. *Nat Cell Biol*, **11**, 1219-1224. doi: 10.1038/ncb1965.
- Kerkhoff, E. (2006). Cellular functions of the Spir actin-nucleation factors. *Trends Cell Biol*, **16**, 477-483. doi: 10.1016/j.tcb.2006.07.005.
- Kessler, H., Herm-Gotz, A., Hegge, S., Rauch, M., Soldati-Favre, D., Frischknecht, F. and Meissner, M. (2008). Microneme protein 8--a new essential invasion factor in *Toxoplasma gondii*. *J Cell Sci*, **121**, 947-956. doi: 10.1242/jcs.022350.
- Khan, A., Behnke, M. S., Dunay, I. R., White, M. W. and Sibley, L. D. (2009a). Phenotypic and gene expression changes among clonal type I strains of *Toxoplasma gondii*. *Eukaryot Cell*, **8**, 1828-1836.
- Khan, A., Taylor, S., Ajioka, J. W., Rosenthal, B. M. and Sibley, L. D. (2009b). Selection at a single locus leads to widespread expansion of *Toxoplasma gondii* lineages that are virulent in mice. *PLoS Genet*, **5**, e1000404.
- Khan, A., Taylor, S., Su, C., Mackey, A. J., Boyle, J., Cole, R., Glover, D., Tang, K., Paulsen, I. T., Berriman, M., Boothroyd, J. C., Pfefferkorn, E. R., Dubey, J. P., Ajioka, J. W., Roos, D. S., Wootton, J. C. and Sibley, L. D. (2005). Composite genome map and recombination parameters derived from three archetypal lineages of *Toxoplasma gondii*. *Nucleic Acids Res*, **33**, 2980-2992. doi: 10.1093/nar/gki604.
- Kim, K., Soldati, D. and Boothroyd, J. C. (1993). Gene replacement in *Toxoplasma gondii* with chloramphenicol acetyltransferase as selectable marker. *Science*, **262**, 911-914.
- Kim, K. and Weiss, L. M. (2004). *Toxoplasma gondii*: the model apicomplexan. *Int J Parasitol*, **34**, 423-432. doi: 10.1016/j.ijpara.2003.12.009.
- Kimata, I. and Tanabe, K. (1982). Invasion by *Toxoplasma gondii* of ATP-depleted and ATP-restored chick embryo erythrocytes. *J Gen Microbiol*, **128**, 2499-2501.
- Kimura, T., Kaneko, Y., Yamada, S., Ishihara, H., Senda, T., Iwamatsu, A. and Niki, I. (2008). The GDP-dependent Rab27a effector coronin 3 controls endocytosis of secretory membrane in insulin-secreting cell lines. *J Cell Sci*, **121**, 3092-3098. doi: 10.1242/jcs.030544.
- King, C. A. (1981). Cell surface interaction of the protozoan *Gregarina* with concanavalin A beads - implications for models of gregarine gliding. *Cell Biol Int Rep*, **5**, 297-305.
- King, C. A. (1988). Cell motility of sporozoan protozoa. *Parasitol Today*, **4**, 315-319.
- Koch, M. and Baum, J. (2016). The mechanics of malaria parasite invasion of the human erythrocyte - towards a reassessment of the host cell contribution. *Cell Microbiol*, **18**, 319-329. doi: 10.1111/cmi.12557.
- Kohler, R. H., Cao, J., Zipfel, W. R., Webb, W. W. and Hanson, M. R. (1997). Exchange of protein molecules through connections between higher plant plastids. *Science*, **276**, 2039-2042.
- Korn, E. D., Carlier, M. F. and Pantaloni, D. (1987). Actin Polymerization and ATP Hydrolysis. *Science*, **238**, 638-644.
- Kovar, D. R., Harris, E. S., Mahaffy, R., Higgs, H. N. and Pollard, T. D. (2006). Control of the assembly of ATP- and ADP-actin by formins and profilin. *Cell*, **124**, 423-435. doi: 10.1016/j.cell.2005.11.038.
- Kramer, W. (1966). Frontiers of neurological diagnosis in acquired toxoplasmosis. *Psychiatr Neurol Neurochir*, **69**, 43-64.
- Kreidenweiss, A., Hopkins, A. V. and Mordmuller, B. (2013). 2A and the auxin-based degron system facilitate control of protein levels in *Plasmodium falciparum*. *PLoS One*, **8**, e78661. doi: 10.1371/journal.pone.0078661.
- Kremer, K., Kamin, D., Rittweger, E., Wilkes, J., Flammer, H., Mahler, S., Heng, J., Tonkin, C. J., Langsley, G., Hell, S. W., Carruthers, V. B., Ferguson, D. J. and Meissner, M. (2013). An overexpression screen of *Toxoplasma gondii* Rab-GTPases reveals distinct transport routes to the micronemes. *PLoS Pathog*, **9**, e1003213. doi: 10.1371/journal.ppat.1003213.
- Kucera, K., Koblansky, A. A., Saunders, L. P., Frederick, K. B., De La Cruz, E. M., Ghosh, S. and Modis, Y. (2010). Structure-based analysis of *Toxoplasma gondii*

- profilin: a parasite-specific motif is required for recognition by Toll-like receptor 11. *J Mol Biol*, **403**, 616-629. doi: 10.1016/j.jmb.2010.09.022.
- Kudryashev, M., Lepper, S., Baumeister, W., Cyrklaff, M. and Frischknecht, F. (2010). Geometric constrains for detecting short actin filaments by cryogenic electron tomography. *PMC Biophysics*, **3**, 1-14.
- Kuhni-Boghenbor, K., Ma, M., Lemgruber, L., Cyrklaff, M., Frischknecht, F., Gaschen, V., Stoffel, M. and Baumgartner, M. (2012). Actin-mediated plasma membrane plasticity of the intracellular parasite *Theileria annulata*. *Cell Microbiol*, **14**, 1867-1879. doi: 10.1111/cmi.12006.
- Kursula, I., Kursula, P., Ganter, M., Panjekar, S., Matuschewski, K. and Schuler, H. (2008). Structural basis for parasite-specific functions of the divergent profilin of *Plasmodium falciparum*. *Structure*, **16**, 1638-1648. doi: 10.1016/j.str.2008.09.008.
- Kustermans, G., Piette, J. and Legrand-Poels, S. (2008). Actin-targeting natural compounds as tools to study the role of actin cytoskeleton in signal transduction. *Biochem Pharmacol*, **76**, 1310-1322. doi: 10.1016/j.bcp.2008.05.028.
- Laemmli, U. K. (1970). Cleavage of structural proteins during the assembly of the head of bacteriophage T4. *Nature*, **227**, 680-685.
- Lamarque, M., Besteiro, S., Papoin, J., Roques, M., Vulliez-Le Normand, B., Morlon-Guyot, J., Dubremetz, J. F., Fauquenoy, S., Tomavo, S., Faber, B. W., Kocken, C. H., Thomas, A. W., Boulanger, M. J., Bentley, G. A. and Lebrun, M. (2011). The RON2-AMA1 interaction is a critical step in moving junction-dependent invasion by apicomplexan parasites. *PLoS Pathog*, **7**, e1001276. doi: 10.1371/journal.ppat.1001276.
- Lamarque, M. H., Roques, M., Kong-Hap, M., Tonkin, M. L., Rugarabamu, G., Marq, J. B., Penarete-Vargas, D. M., Boulanger, M. J., Soldati-Favre, D. and Lebrun, M. (2014). Plasticity and redundancy among AMA-RON pairs ensure host cell entry of *Toxoplasma* parasites. *Nat Commun*, **5**, 4098. doi: 10.1038/ncomms5098.
- Lammermann, T., Bader, B. L., Monkley, S. J., Worbs, T., Wedlich-Soldner, R., Hirsch, K., Keller, M., Forster, R., Critchley, D. R., Fassler, R. and Sixt, M. (2008). Rapid leukocyte migration by integrin-independent flowing and squeezing. *Nature*, **453**, 51-55. doi: 10.1038/nature06887.
- Lavine, M. D. and Arrizabalaga, G. (2008). Exit from host cells by the pathogenic parasite *Toxoplasma gondii* does not require motility. *Eukaryot Cell*, **7**, 131-140. doi: 10.1128/EC.00301-07.
- Lehmann, M. J., Sherer, N. M., Marks, C. B., Pypaert, M. and Mothes, W. (2005). Actin- and myosin-driven movement of viruses along filopodia precedes their entry into cells. *J Cell Biol*, **170**, 317-325. doi: 10.1083/jcb.200503059.
- Lengsfeld, A. M., Low, I., Wieland, T., Dancker, P. and Hasselbach, W. (1974). Interaction of phalloidin with actin. *Proc Natl Acad Sci U S A*, **71**, 2803-2807.
- Leung, J. M., Rould, M. A., Konradt, C., Hunter, C. A. and Ward, G. E. (2014a). Disruption of TgPHIL1 alters specific parameters of *Toxoplasma gondii* motility measured in a quantitative, three-dimensional live motility assay. *PLoS One*, **9**, e85763. doi: 10.1371/journal.pone.0085763.
- Leung, J. M., Tran, F., Pathak, R. B., Poupart, S., Heaslip, A. T., Ballif, B. A., Westwood, N. J. and Ward, G. E. (2014b). Identification of *T. gondii* Myosin Light Chain-1 as a Direct Target of TachypleglinA-2, a Small-Molecule Inhibitor of Parasite Motility and Invasion. *PLoS One*, **9**, e98056. doi: 10.1371/journal.pone.0098056.
- Levine, N. D. (1988). Progress in Taxonomy of the Apicomplexan Protozoa. *The Journal of Protozoology*, **35**, 518-520.
- Li, A., Dawson, J. C., Forero-Vargas, M., Spence, H. J., Yu, X., Konig, I., Anderson, K. and Machesky, L. M. (2010). The actin-bundling protein fascin stabilizes actin in invadopodia and potentiates protrusive invasion. *Curr Biol*, **20**, 339-345. doi: 10.1016/j.cub.2009.12.035.
- Liazhkovich, I., Pasrednik, D., Prystopiuk, V., Rosso, G., Oberleithner, H. and Shahin, V. (2015). Clathrin inhibitor Pitstop-2 disrupts the nuclear pore complex permeability barrier. *Sci Rep*, **5**, 9994. doi: 10.1038/srep09994.

- Lim, L. and McFadden, G. I. (2010). The evolution, metabolism and functions of the apicoplast. *Philos Trans R Soc Lond B Biol Sci*, **365**, 749-763. doi: 10.1098/rstb.2009.0273.
- Lin, S. and Spudich, J. A. (1974). Biochemical studies on the mode of action of cytochalasin B. Cytochalasin B binding to red cell membrane in relation to glucose transport. *J Biol Chem*, **249**, 5778-5783.
- Lodish, H., Berk, A., Matsudaira, P., Kaiser, C. A., Krieger, M., Scott, M. P., Zipursky, S. L. and Darnell, J. (2004). *Molecular Cell Biology*, 5th edn. W. H. Freeman and Co., New York.
- Lorestani, A., Ivey, F. D., Thirugnanam, S., Busby, M. A., Marth, G. T., Cheeseman, I. M. and Gubbels, M. J. (2012). Targeted proteomic dissection of *Toxoplasma* cytoskeleton sub-compartments using MORN1. *Cytoskeleton (Hoboken)*, **69**, 1069-1085. doi: 10.1002/cm.21077.
- Los, G. V., Encell, L. P., McDougall, M. G., Hartzell, D. D., Karassina, N., Zimprich, C., Wood, M. G., Learish, R., Ohana, R. F., Urh, M., Simpson, D., Mendez, J., Zimmerman, K., Otto, P., Vidugiris, G., Zhu, J., Darzins, A., Klaubert, D. H., Bulleit, R. F. and Wood, K. V. (2008). HaloTag: A Novel Protein Labeling Technology for Cell Imaging and Protein Analysis. *ACS Chemical Biology*, **3**, 373-382.
- Lourido, S., Shuman, J., Zhang, C., Shokat, K. M., Hui, R. and Sibley, L. D. (2010). Calcium-dependent protein kinase 1 is an essential regulator of exocytosis in *Toxoplasma*. *Nature*, **465**, 359-362.
- Lourido, S., Tang, K. and Sibley, L. D. (2012). Distinct signalling pathways control *Toxoplasma* egress and host-cell invasion. *EMBO J*, **31**, 4524-4534. doi: 10.1038/emboj.2012.299.
- Loussert, C., Forestier, C. L. and Humbel, B. M. (2012). Correlative light and electron microscopy in parasite research. *Methods Cell Biol*, **111**, 59-73. doi: 10.1016/B978-0-12-416026-2.00004-2.
- Lovett, J. L., Marchesini, N., Moreno, S. N. and Sibley, L. D. (2002). *Toxoplasma gondii* microneme secretion involves intracellular Ca<sup>2+</sup> release from inositol 1,4,5-triphosphate (IP<sub>3</sub>)/ryanodine-sensitive stores. *J Biol Chem*, **277**, 25870-25876.
- Lukinavicius, G., Reymond, L., D'Este, E., Masharina, A., Gottfert, F., Ta, H., Guthier, A., Fournier, M., Rizzo, S., Waldmann, H., Blaukopf, C., Sommer, C., Gerlich, D. W., Arndt, H. D., Hell, S. W. and Johnsson, K. (2014). Fluorogenic probes for live-cell imaging of the cytoskeleton. *Nat Methods*, **11**, 731-733. doi: 10.1038/nmeth.2972.
- Lyons, R. E., McLeod, R. and Roberts, C. W. (2002). *Toxoplasma gondii* tachyzoite-bradyzoite interconversion. *Trends Parasitol*, **18**, 198-201.
- Machesky, L. and Gould, K. L. (1999). The Arp2/3 complex: a multifunctional actin organizer. *Curr Opin Cell Biol*, **11**, 117-121.
- Machesky, L. M. (2008). Lamellipodia and filopodia in metastasis and invasion. *FEBS Lett*, **582**, 2102-2111. doi: 10.1016/j.febslet.2008.03.039.
- MacLean-Fletcher, S. and Pollard, T. D. (1980). Mechanism of Action of Cytochalasin B on Actin. *Cell*, **20**, 329-341.
- Maenz, M., Schluter, D., Liesenfeld, O., Schares, G., Gross, U. and Pleyer, U. (2014). Ocular toxoplasmosis past, present and new aspects of an old disease. *Prog Retin Eye Res*, **39**, 77-106. doi: 10.1016/j.preteyeres.2013.12.005.
- Magalhaes, M. A., Larson, D. R., Mader, C. C., Bravo-Cordero, J. J., Gil-Henn, H., Oser, M., Chen, X., Koleske, A. J. and Condeelis, J. (2011). Cortactin phosphorylation regulates cell invasion through a pH-dependent pathway. *J Cell Biol*, **195**, 903-920. doi: 10.1083/jcb.201103045.
- Magno, R. C., Lemgruber, L., Vommaro, R. C., De Souza, W. and Attias, M. (2005). Intravacuolar network may act as a mechanical support for *Toxoplasma gondii* inside the parasitophorous vacuole. *Microscopy Research and Technique*, **67**, 45-52. doi: 10.1002/jemt.20182.
- Manivasakam, P., Aubrecht, J., Sidhom, S. and Schiestl, R. H. (2001). Restriction enzymes increase efficiencies of illegitimate DNA integration but decrease homologous integration in mammalian cells. *Nucleic Acids Research*, **29**, 4826-4833.

- Mann, T. and Beckers, C. (2001). Characterization of the subpellicular network, a filamentous membrane skeletal component in the parasite *Toxoplasma gondii*. *Mol Biochem Parasitol*, **115**, 257-268.
- Maritzen, T., Schachtner, H. and Legler, D. F. (2015). On the move: endocytic trafficking in cell migration. *Cell Mol Life Sci*, **72**, 2119-2134. doi: 10.1007/s00018-015-1855-9.
- Marzo, L., Gousset, K. and Zurzolo, C. (2012). Multifaceted roles of tunneling nanotubes in intercellular communication. *Front Physiol*, **3**, 72. doi: 10.3389/fphys.2012.00072.
- Matz, J. M., Goosmann, C., Brinkmann, V., Grutzke, J., Ingmundson, A., Matuschewski, K. and Kooij, T. W. (2015). The *Plasmodium berghei* translocon of exported proteins reveals spatiotemporal dynamics of tubular extensions. *Sci Rep*, **5**, 12532. doi: 10.1038/srep12532.
- McCoy, J. M., Whitehead, L., van Dooren, G. G. and Tonkin, C. J. (2012). TgCDPK3 regulates calcium-dependent egress of *Toxoplasma gondii* from host cells. *PLoS Pathog*, **8**, e1003066. doi: 10.1371/journal.ppat.1003066.
- McFadden, G. I., Reith, M. E., Munholland, J. and Lang-Unnasch, N. (1996). Plastid in human parasites. *Nature*, **381**, 482. doi: 10.1038/381482a0.
- Mehta, S. and Sibley, L. D. (2010). *Toxoplasma gondii* actin depolymerizing factor acts primarily to sequester G-actin. *J Biol Chem*, **285**, 6835-6847. doi: 10.1074/jbc.M109.068155.
- Mehta, S. and Sibley, L. D. (2011). Actin depolymerizing factor controls actin turnover and gliding motility in *Toxoplasma gondii*. *Mol Biol Cell*, **22**, 1290-1299. doi: 10.1091/mbc.E10-12-0939.
- Meissner, M. (2013). The asexual cycle of apicomplexan parasites: new findings that raise new questions. *Curr Opin Microbiol*, **16**, 421-423. doi: 10.1016/j.mib.2013.07.017.
- Meissner, M., Brecht, S., Bujard, H. and Soldati, D. (2001). Modulation of myosin A expression by a newly established tetracycline repressor-based inducible system in *Toxoplasma gondii*. *Nucleic Acids Res*, **29**, E115.
- Meissner, M., Ferguson, D. J. and Frischknecht, F. (2013). Invasion factors of apicomplexan parasites: essential or redundant? *Curr Opin Microbiol*, **16**, 438-444. doi: 10.1016/j.mib.2013.05.002.
- Meissner, M., Krejany, E., Gilson, P. R., de Koning-Ward, T. F., Soldati, D. and Crabb, B. S. (2005). Tetracycline analogue-regulated transgene expression in *Plasmodium falciparum* blood stages using *Toxoplasma gondii* transactivators. *Proc Natl Acad Sci U S A*, **102**, 2980-2985. doi: 10.1073/pnas.0500112102.
- Meissner, M., Schluter, D. and Soldati, D. (2002). Role of *Toxoplasma gondii* myosin A in powering parasite gliding and host cell invasion. *Science*, **298**, 837-840.
- Mercier, C., Adjogble, K. D., Daubener, W. and Delauw, M. F. (2005). Dense granules: are they key organelles to help understand the parasitophorous vacuole of all apicomplexa parasites? *Int J Parasitol*, **35**, 829-849. doi: 10.1016/j.ijpara.2005.03.011.
- Mercier, C. and Cesbron-Delauw, M. F. (2015). *Toxoplasma* secretory granules: one population or more? *Trends Parasitol*, **31**, 60-71. doi: 10.1016/j.pt.2014.12.002.
- Mercier, C., Dubremetz, J. F., Rauscher, B., Lecordier, L., Sibley, L. D. and Cesbron-Delauw, M. F. (2002). Biogenesis of nanotubular network in *Toxoplasma* parasitophorous vacuole induced by parasite proteins. *Mol Biol Cell*, **13**, 2397-2409.
- Michelin, A., Bittame, A., Bordat, Y., Travier, L., Mercier, C., Dubremetz, J. F. and Lebrun, M. (2009). GRA12, a *Toxoplasma* dense granule protein associated with the intravacuolar membranous nanotubular network. *Int J Parasitol*, **39**, 299-306. doi: 10.1016/j.ijpara.2008.07.011.
- Mih, J. D., Marinkovic, A., Liu, F., Sharif, A. S. and Tschumperlin, D. J. (2012). Matrix stiffness reverses the effect of actomyosin tension on cell proliferation. *J Cell Sci*, **125**, 5974-5983. doi: 10.1242/jcs.108886.

- Mineo, J. R. and Kasper, L. H. (1994). Attachment of *Toxoplasma gondii* to host cells involves major surface protein, SAG-1 (P30). *Exp Parasitol*, **79**, 11-20. doi: 10.1006/expr.1994.1054.
- Miraldi, E. R., Thomas, P. J. and Romberg, L. (2008). Allosteric Models for Cooperative Polymerization of Linear Polymers. *Biophys J*, **95**, 2470-2486. doi: 10.1529/biophysj.107.126219.
- Mital, J., Meissner, M., Soldati, D. and Ward, G. E. (2005). Conditional expression of *Toxoplasma gondii* apical membrane antigen-1 (TgAMA1) demonstrates that TgAMA1 plays a critical role in host cell invasion. *Mol Biol Cell*, **16**, 4341-4349. doi: 10.1091/mbc.E05-04-0281.
- Mitchison, T. J., Charras, G. T. and Mahadevan, L. (2008). Implications of a poroelastic cytoplasm for the dynamics of animal cell shape. *Semin Cell Dev Biol*, **19**, 215-223. doi: 10.1016/j.semcdb.2008.01.008.
- Mitchison, T. J. and Cramer, L. P. (1996). Actin-Based Cell Motility and Cell Locomotion. *Cell*, **84**, 371-379.
- Mizuno, Y., Makioka, A., Kawazu, S., Kano, S., Kawai, S., Akaki, M., Aikawa, M. and Ohtomo, H. (2002). Effect of jasplakinolide on the growth, invasion, and actin cytoskeleton of *Plasmodium falciparum*. *Parasitol Res*, **88**, 844-848. doi: 10.1007/s00436-002-0666-8.
- Mogilner, A. (2006). On the edge: modeling protrusion. *Curr Opin Cell Biol*, **18**, 32-39. doi: 10.1016/j.ceb.2005.11.001.
- Mogilner, A. and Oster, G. (1996). Cell Motility Driven by Actin Polymerization. *Biophys J*, **71**, 330-3045.
- Moncada, P. A. and Montoya, J. G. (2012). Toxoplasmosis in the fetus and newborn: an update on prevalence, diagnosis and treatment. *Expert Rev Anti Infect Ther*, **10**, 815-828. doi: 10.1586/eri.12.58.
- Montagna, G. N., Matuschewski, K. and Buscaglia, C. A. (2012). Plasmodium sporozoite motility: an update. *Front Biosci*, **17**, 726-744.
- Mordue, D. G. and Sibley, L. D. (1997). Intracellular fate of vacuoles containing *Toxoplasma gondii* is determined at the time of formation and depends on the mechanism of entry. *J Immunol*, **159**, 4452-4459.
- Morisaki, J. H., Heuser, J. E. and Sibley, L. D. (1995). Invasion of *Toxoplasma gondii* occurs by active penetration of the host cell. *Journal of Cell Science*, **108**, 2457-2464.
- Morrisette, N. S., Murray, J. M. and Roos, D. S. (1997). Subpellicular microtubules associate with an intramembranous particle lattice in the protozoan parasite *Toxoplasma gondii*. *J Cell Sci*, **110** ( Pt 1), 35-42.
- Morrisette, N. S. and Sibley, L. D. (2002). Cytoskeleton of Apicomplexan Parasites. *Microbiology and Molecular Biology Reviews*, **66**, 21-38. doi: 10.1128/mubr.66.1.21-38.2002.
- Morton, W. M., Ayscough, K. R. and McLaughlin, P. L. (2000). Latrunculin alters the actin-monomer subunit interface to prevent polymerization. *Nature Cell Biology*, **2**, 376-378.
- Moudy, R., Manning, T. J. and Beckers, C. J. (2001). The loss of cytoplasmic potassium upon host cell breakdown triggers egress of *Toxoplasma gondii*. *J Biol Chem*, **276**, 41492-41501. doi: 10.1074/jbc.M106154200.
- Mueller, C., Klages, N., Jacot, D., Santos, J. M., Cabrera, A., Gilberger, T. W., Dubremetz, J. F. and Soldati-Favre, D. (2013). The *Toxoplasma* protein ARO mediates the apical positioning of rhoptry organelles, a prerequisite for host cell invasion. *Cell Host Microbe*, **13**, 289-301. doi: 10.1016/j.chom.2013.02.001.
- Muller, J., Oma, Y., Vallar, L., Friederich, E., Poch, O. and Winsor, B. (2005). Sequence and comparative genomic analysis of actin-related proteins. *Mol Biol Cell*, **16**, 5736-5748. doi: 10.1091/mbc.E05-06-0508.
- Mullins, R. D., Kelleher, J. F., Xu, J. and Pollard, T. D. (1998). Arp2/3 Complex from *Acanthamoeba* Binds Profilin and cross-links actin filaments. *Mol Biol Cell*, **9**, 841-852.

- Muniz-Hernandez, S., Carmen, M. G., Mondragon, M., Mercier, C., Cesbron, M. F., Mondragon-Gonzalez, S. L., Gonzalez, S. and Mondragon, R. (2011). Contribution of the residual body in the spatial organization of *Toxoplasma gondii* tachyzoites within the parasitophorous vacuole. *J Biomed Biotechnol*, **2011**, 473983. doi: 10.1155/2011/473983.
- Munter, S., Sabass, B., Selhuber-Unkel, C., Kudryashev, M., Hegge, S., Engel, U., Spatz, J. P., Matuschewski, K., Schwarz, U. S. and Frischknecht, F. (2009). Plasmodium sporozoite motility is modulated by the turnover of discrete adhesion sites. *Cell Host Microbe*, **6**, 551-562. doi: 10.1016/j.chom.2009.11.007.
- Murakami, K., Yasunaga, T., Noguchi, T. Q., Gomibuchi, Y., Ngo, K. X., Uyeda, T. Q. and Wakabayashi, T. (2010). Structural basis for actin assembly, activation of ATP hydrolysis, and delayed phosphate release. *Cell*, **143**, 275-287. doi: 10.1016/j.cell.2010.09.034.
- Muyldermans, S. (2013). Nanobodies: natural single-domain antibodies. *Annu Rev Biochem*, **82**, 775-797. doi: 10.1146/annurev-biochem-063011-092449.
- Nagamune, K., Moreno, S. N., Chini, E. N. and Sibley, L. D. (2008). Calcium regulation and signaling in apicomplexan parasites. *Subcell Biochem*, **47**, 70-81.
- Nair, S. C., Brooks, C. F., Goodman, C. D., Sturm, A., McFadden, G. I., Sundriyal, S., Anglin, J. L., Song, Y., Moreno, S. N. and Striepen, B. (2011). Apicoplast isoprenoid precursor synthesis and the molecular basis of fosmidomycin resistance in *Toxoplasma gondii*. *J Exp Med*, **208**, 1547-1559. doi: 10.1084/jem.20110039.
- Nair, U. B., Joel, P. B., Wan, Q., Lowey, S., Rould, M. A. and Trybus, K. M. (2008). Crystal structures of monomeric actin bound to cytochalasin D. *J Mol Biol*, **384**, 848-864. doi: 10.1016/j.jmb.2008.09.082.
- Neuhaus, J. M., Wanger, M., Keiser, T. and Wegner, A. (1983). Treadmilling of actin. *J Muscle Res Cell Motil*, **4**, 507-527.
- Nichols, B. A., Chiappino, M. L. and Pavesio, C. E. (1994). Endocytosis at the micropore of *Toxoplasma gondii*. *Parasitol Res*, **80**, 91-98.
- Nicolle, C. and Manceaux, L. (1908). Sur une infection à corps de Leishman (ou organismes voisins) du gondi. *C. R. Seances Acad. Sci.*, **147**, 763-766.
- Nicolle, C. and Manceaux, L. (1909). Sur un protozoaire nouveau du gondi. *C. R. Seances Acad. Sci.*, **148**, 369-372.
- Niculescu, I., Textor, J. and de Boer, R. J. (2015). Crawling and Gliding: A Computational Model for Shape-Driven Cell Migration. *PLoS Comput Biol*, **11**, e1004280. doi: 10.1371/journal.pcbi.1004280.
- Niedelman, W., Gold, D. A., Rosowski, E. E., Sprokholt, J. K., Lim, D., Farid Arenas, A., Melo, M. B., Spooner, E., Yaffe, M. B. and Saeij, J. P. (2012). The rhoGTPase proteins ROP18 and ROP5 mediate *Toxoplasma gondii* evasion of the murine, but not the human, interferon-gamma response. *PLoS Pathog*, **8**, e1002784. doi: 10.1371/journal.ppat.1002784.
- Nishi, M., Hu, K., Murray, J. M. and Roos, D. S. (2008). Organellar dynamics during the cell cycle of *Toxoplasma gondii*. *J Cell Sci*, **121**, 1559-1568.
- Nishida, E. and Sakai, H. (1983). Kinetic analysis of actin polymerization. *J Biochem*, **93**, 1011-1020.
- O'Hara, S. P., Small, A. J., Chen, X. M. and LaRusso, N. F. (2008). Host cell actin remodeling in response to *Cryptosporidium*. *Subcell Biochem*, **47**, 92-100.
- Oelz, D. B., Rubinstein, B. Y. and Mogilner, A. (2015). A Combination of Actin Treadmilling and Cross-Linking Drives Contraction of Random Actomyosin Arrays. *Biophys J*, **109**, 1818-1829. doi: 10.1016/j.bpj.2015.09.013.
- Olshina, M. A., Angrisano, F., Marapana, D. S., Riglar, D. T., Bane, K., Wong, W., Catimel, B., Yin, M. X., Holmes, A. B., Frischknecht, F., Kovar, D. R. and Baum, J. (2015). Plasmodium falciparum coronin organizes arrays of parallel actin filaments potentially guiding directional motility in invasive malaria parasites. *Malar J*, **14**, 280. doi: 10.1186/s12936-015-0801-5.
- Olshina, M. A., Baumann, H., Willison, K. R. and Baum, J. (2016). Plasmodium actin is incompletely folded by heterologous protein-folding machinery and likely requires

- the native Plasmodium chaperonin complex to enter a mature functional state. *FASEB J*, **30**, 405-416. doi: 10.1096/fj.15-276618.
- Olson, E. N. and Nordheim, A. (2010). Linking actin dynamics and gene transcription to drive cellular motile functions. *Nat Rev Mol Cell Biol*, **11**, 353-365. doi: 10.1038/nrm2890.
- Onfelt, B., Nedvetzki, S., Yanagi, K. and Davis, D. M. (2004). Cutting edge: Membrane nanotubes connect immune cells. *J Immunol*, **173**, 1511-1513.
- Opitz, C. and Soldati, D. (2002). 'The glideosome': a dynamic complex powering gliding motion and host cell invasion by *Toxoplasma gondii*. *Mol Microbiol*, **45**, 597-604.
- Otterbein, L. R., Graceffa, P. and Dominguez, R. (2001). The crystal structure of uncomplexed actin in the ADP state. *Science*, **293**, 708-711. doi: 10.1126/science.1059700.
- Pantaloni, D. and Carlier, M. F. (1993). How profilin promotes actin filament assembly in the presence of thymosin beta 4. *Cell*, **75**, 1007-1014.
- Pantaloni, D., Carlier, M. F., Coue, M., Lal, A. A., Brenner, S. L. and Korn, E. D. (1984). The critical concentration of actin in the presence of ATP increases with the number concentration of filaments and approaches the critical concentration of actin-ADP. *J Biol Chem*, **259**, 6274-6283.
- Panza, P., Maier, J., Schmees, C., Rothbauer, U. and Sollner, C. (2015). Live imaging of endogenous protein dynamics in zebrafish using chromobodies. *Development*, **142**, 1879-1884. doi: 10.1242/dev.118943.
- Papaioannou, T. G. and Stefanadi, C. (2005). Vascular Wall Shear Stress: Basic Principles and Methods. *Hellenic J Cardiol*, **46**, 9-15.
- Pappas, G., Roussos, N. and Falagas, M. E. (2009). Toxoplasmosis snapshots: global status of *Toxoplasma gondii* seroprevalence and implications for pregnancy and congenital toxoplasmosis. *Int J Parasitol*, **39**, 1385-1394. doi: 10.1016/j.ijpara.2009.04.003.
- Paredes, A. R., Assaf, Z. J., Sept, D., Timofejeva, L., Dawson, S. C., Wang, C. J. and Cande, W. Z. (2011). An actin cytoskeleton with evolutionarily conserved functions in the absence of canonical actin-binding proteins. *Proc Natl Acad Sci U S A*, **108**, 6151-6156. doi: 10.1073/pnas.1018593108.
- Paul, A. S. and Pollard, T. D. (2008). The role of the FH1 domain and profilin in formin-mediated actin-filament elongation and nucleation. *Curr Biol*, **18**, 9-19. doi: 10.1016/j.cub.2007.11.062.
- Pelletier, L., Stern, C. A., Pypaert, M., Sheff, D., Ngo, H. M., Roper, N., He, C. Y., Hu, K., Toomre, D., Coppens, I., Roos, D. S., Joiner, K. A. and Warren, G. (2002). Golgi biogenesis in *Toxoplasma gondii*. *Nature*, **418**, 548-552.
- Periz, J., Whitelaw, J., Harding, C., Gras, S., Del Rosario Minina, M. I., Latorre-Barragan, F., Lemgruber, L., Reimer, M. A., Insall, R., Heaslip, A. and Meissner, M. (2017). *Toxoplasma gondii* F-actin forms an extensive filamentous network required for material exchange and parasite maturation. *eLife*, **10**.7554/eLife.24119. doi: doi.org/10.7554/eLife.24119.
- Peterson, J. R. and Mitchison, T. J. (2002). Small Molecules, Big Impact: A History of Chemical Inhibitors and the Cytoskeleton. *Chem Biol*, **9**, 1275-1285.
- Pfefferkorn, E. R. and Borotz, S. E. (1994). *Toxoplasma gondii*: Characterization of a mutant resistant to 6-thioxanthine. *Exp Parasitol*, **79**, 374-382.
- Pfefferkorn, E. R., Bzik, D. J. and Honsinger, C. P. (2001). *Toxoplasma gondii*: mechanism of the parasitostatic action of 6-thioxanthine. *Exp Parasitol*, **99**, 235-243. doi: 10.1006/expr.2001.4673.
- Pfefferkorn, E. R. and Pfefferkorn, L. C. (1977a). Specific labeling of intracellular *Toxoplasma gondii* with uracil. *J Protozool*, **24**, 449-453.
- Pfefferkorn, E. R. and Pfefferkorn, L. C. (1977b). *Toxoplasma gondii*: characterization of a mutant resistant to 5-fluorodeoxyuridine. *Exp Parasitol*, **42**, 44-55.
- Pfefferkorn, L. C. and Pfefferkorn, E. R. (1980). *Toxoplasma gondii*: genetic recombination between drug resistant mutants. *Exp Parasitol*, **50**, 305-316.

- Philip, N. and Waters, A. P. (2015). Conditional Degradation of Plasmodium Calcineurin Reveals Functions in Parasite Colonization of both Host and Vector. *Cell Host Microbe*, **18**, 122-131. doi: 10.1016/j.chom.2015.05.018.
- Pieperhoff, M. S., Pall, G. S., Jimenez-Ruiz, E., Das, S., Melatti, C., Gow, M., Wong, E. H., Heng, J., Muller, S., Blackman, M. J. and Meissner, M. (2015). Conditional U1 Gene Silencing in *Toxoplasma gondii*. *PLoS One*, **10**, e0130356. doi: 10.1371/journal.pone.0130356.
- Pieperhoff, M. S., Schmitt, M., Ferguson, D. J. and Meissner, M. (2013). The role of clathrin in post-Golgi trafficking in *Toxoplasma gondii*. *PLoS One*, **8**, e77620. doi: 10.1371/journal.pone.0077620.
- Pinkerton, H. and Weinman, D. (1940). *Toxoplasma* infection in man. *Arch Pathol*, **30**, 374-392.
- Plattner, F., Yarovinsky, F., Romero, S., Didry, D., Carlier, M. F., Sher, A. and Soldati-Favre, D. (2008). *Toxoplasma* profilin is essential for host cell invasion and TLR11-dependent induction of an interleukin-12 response. *Cell Host Microbe*, **3**, 77-87.
- Plessner, M., Melak, M., Chinchilla, P., Baarlink, C. and Grosse, R. (2015). Nuclear F-actin formation and reorganization upon cell spreading. *J Biol Chem*, **290**, 11209-11216. doi: 10.1074/jbc.M114.627166.
- Poglazov, B. F. (1983). [Regulatory functions of actin in the cell]. *Izv Akad Nauk SSSR Biol*, 667-677.
- Pollard, T. D. (1984). Polymerization of ADP-Actin. *J Cell Biol*, **99**, 769-777.
- Pollard, T. D. (1986). Rate Constants for the Reactions of ATP- and ADP-Actin with the Ends of Actin Filaments. *J Cell Biol*, **103**, 2747-2754.
- Pollard, T. D. (2003). The cytoskeleton, cellular motility and the reductionist agenda. *Nature*, **422**, 741-745. doi: 10.1038/nature01598.
- Pollard, T. D. (2007). Regulation of actin filament assembly by Arp2/3 complex and formins. *Annu Rev Biophys Biomol Struct*, **36**, 451-477. doi: 10.1146/annurev.biophys.35.040405.101936.
- Pollard, T. D., Blanchoin, L. and Mullins, R. D. (2000). Molecular mechanisms controlling actin filament dynamics in nonmuscle cells. *Annu Rev Biophys Biomol Struct*, **29**, 545-576. doi: 10.1146/annurev.biophys.29.1.545.
- Pollard, T. D. and Borisy, G. G. (2003). Cellular motility driven by assembly and disassembly of actin filaments. *Cell*, **112**, 453-465.
- Pollard, T. D. and Cooper, J. A. (2009). Actin, a central player in cell shape and movement. *Science*, **326**, 1208-1212. doi: 10.1126/science.1175862.
- Poupel, O., Boleti, H., Axisa, S., Couture-Tosi, E. and Tardieux, I. (2000). Toxofilin, a Novel Actin-binding Protein from *Toxoplasma gondii*, sequesters actin monomers and caps actin filaments. *Mol Biol Cell*, **11**, 355-368.
- Poupel, O. and Tardieux, I. (1999). *Toxoplasma gondii* motility and host cell invasiveness are drastically impaired by jasplakinolide, a cyclic peptide stabilizing F-actin. *Microbes and Infection*, **1**, 653-662.
- Pring, M., Evangelista, M., Boone, C., Yang, C. and Zigmond, S. H. (2003). Mechanism of formin-induced nucleation of actin filaments. *Biochemistry*, **42**, 486-496. doi: 10.1021/bi026520j.
- Pruyne, D., Evangelista, M., Yang, C., Bi, E., Zigmond, S., Bretscher, A. and Boone, C. (2002). Role of formins in actin assembly: nucleation and barbed-end association. *Science*, **297**, 612-615. doi: 10.1126/science.1072309.
- Quadt, K. A., Streichfuss, M., Moreau, C. A., Spatz, J. P. and Frischknecht, F. (2016). Coupling of Retrograde Flow to Force Production During Malaria Parasite Migration. *ACS Nano*, **10**, 2091-2102. doi: 10.1021/acsnano.5b06417.
- Rabenau, K. E., Sohrabi, A., Tripathy, A., Reitter, C. P., Ajioka, J. W., Tomley, F. M. and Carruthers, V. (2001). TgM2AP participates in *Toxoplasma gondii* invasion of host cells and is tightly associated with the adhesive protein TgMIC2. *Molecular Microbiology*, **41**, 537-547.

- Radke, J. R., Striepen, B., Guerini, M. N., Jerome, M. E., Roos, D. S. and White, M. W. (2001). Defining the cell cycle for the tachyzoite stage of *Toxoplasma gondii*. *Molecular & Biochemical Parasitology*, **115**, 165-175.
- Ramakrishnan, S., Docampo, M. D., Macrae, J. I., Pujol, F. M., Brooks, C. F., van Dooren, G. G., Hiltunen, J. K., Kastaniotis, A. J., McConville, M. J. and Striepen, B. (2012). Apicoplast and endoplasmic reticulum cooperate in fatty acid biosynthesis in apicomplexan parasite *Toxoplasma gondii*. *J Biol Chem*, **287**, 4957-4971. doi: 10.1074/jbc.M111.310144.
- Rangachari, K., Dluzewski, A. R., Wilson, R. J. and Gratzer, W. B. (1987). Cytoplasmic factor required for entry of malaria parasites into RBCs. *Blood*, **70**, 77-82.
- Regen, C. M. and Horwitz, A. F. (1992). Dynamics of B1 Integrin-mediated Adhesive contacts in motile fibroblasts. *J Cell Biol*, **119**, 1347-1359.
- Remington, J. S. (1974). Toxoplasmosis in the adult. *Bull N Y Acad Med*, **50**, 211-227.
- Renkawitz, J., Schumann, K., Weber, M., Lammermann, T., Pflücke, H., Piel, M., Polleux, J., Spatz, J. P. and Sixt, M. (2009). Adaptive force transmission in amoeboid cell migration. *Nat Cell Biol*, **11**, 1438-1443. doi: 10.1038/ncb1992.
- Ridley, A. J. (2006). Rho GTPases and actin dynamics in membrane protrusions and vesicle trafficking. *Trends Cell Biol*, **16**, 522-529. doi: 10.1016/j.tcb.2006.08.006.
- Ridley, A. J. (2011). Life at the leading edge. *Cell*, **145**, 1012-1022. doi: 10.1016/j.cell.2011.06.010.
- Ridley, A. J., Schwartz, M. A., Burridge, K., Firtel, R. A., Ginsberg, M. H., Borisy, G., Parsons, J. T. and Horwitz, A. R. (2003). Cell migration: integrating signals from front to back. *Science*, **302**, 1704-1709. doi: 10.1126/science.1092053.
- Riedl, J., Crevenna, A. H., Kessenbrock, K., Yu, J. H., Neukirchen, D., Bista, M., Bradke, F., Jenne, D., Holak, T. A., Werb, Z., Sixt, M. and Wedlich-Soldner, R. (2008). Lifeact: a versatile marker to visualize F-actin. *Nature Methods*, **5**, 605-607. doi: 10.1038/nmeth.1220.
- Roberts, T. M. and Ward, S. (1982). Membrane flow during nematode spermiogenesis. *J Cell Biol*, **92**, 113-120.
- Rocchetti, A., Hawes, C. and Kriechbaumer, V. (2014). Fluorescent labelling of the actin cytoskeleton in plants using a cameloid antibody. *Plant Methods*, **10**, 1-8.
- Roos, D. S., Donald, R. G., Morrisette, N. S. and Moulton, A. L. (1994). Molecular tools for genetic dissection of the protozoan parasite *Toxoplasma gondii*. *Methods Cell Biol*, **45**, 27-63.
- Rothbauer, U., Zolghadr, K., Tillib, S., Nowak, D., Schermelleh, L., Gahl, A., Backmann, N., Conrath, K., Muyltermans, S., Cardoso, M. C. and Leonhardt, H. (2006). Targeting and tracing antigens in live cells with fluorescent nanobodies. *Nat Methods*, **3**, 887-889. doi: 10.1038/nmeth953.
- Rueckschloss, U. and Isenberg, G. (2001). Cytochalasin D reduces Ca<sup>2+</sup> currents via cofilin-activated depolymerization of F-actin in guinea-pig cardiomyocytes. *J Physiol*, **537**, 363-370.
- Rugarabamu, G., Marq, J. B., Guerin, A., Lebrun, M. and Soldati-Favre, D. (2015). Distinct contribution of *Toxoplasma gondii* rhomboid proteases 4 and 5 to micronemal protein protease 1 activity during invasion. *Mol Microbiol*, **97**, 244-262. doi: 10.1111/mmi.13021.
- Ryan, G. L., Petroccia, H. M., Watanabe, N. and Vavylonis, D. (2012). Excitable actin dynamics in lamellipodial protrusion and retraction. *Biophys J*, **102**, 1493-1502. doi: 10.1016/j.bpj.2012.03.005.
- Ryning, F. W. and Remington, J. S. (1978). Effect of cytochalasin D on *Toxoplasma gondii* cell entry. *Infection and Immunity*, **20**, 739-743.
- Sahoo, N., Beatty, W., Heuser, J., Sept, D. and Sibley, L. D. (2006). Unusual kinetic and structural properties control rapid assembly and turnover of actin in the parasite *Toxoplasma gondii*. *Mol Biol Cell*, **17**, 895-906.
- Salamun, J., Kallio, J. P., Daher, W., Soldati-Favre, D. and Kursula, I. (2014). Structure of *Toxoplasma gondii* coronin, an actin-binding protein that relocalizes to

- the posterior pole of invasive parasites and contributes to invasion and egress. *FASEB J*, **28**, 4729-4747. doi: 10.1096/fj.14-252569.
- Salazar Gonzalez, R. M., Shehata, H., O'Connell, M. J., Yang, Y., Moreno-Fernandez, M. E., Chougnat, C. A. and Aliberti, J. (2014). Toxoplasma gondii-derived profilin triggers human toll-like receptor 5-dependent cytokine production. *J Innate Immun*, **6**, 685-694. doi: 10.1159/000362367.
- Sauer, B. and Henderson, N. (1988). Site-specific DNA recombination in mammalian cells by the Cre recombinase of bacteriophage P1. *Proc Natl Acad Sci U S A*, **85**, 5166-5170.
- Schafer, D. A., Gill, S. R., Cooper, J. A., Heuser, J. E. and Schroer, T. A. (1994). Ultrastructural analysis of the dynactin complex: an actin-related protein is a component of a filament that resembles F-actin. *J Cell Biol*, **126**, 403-412.
- Schafer, D. A. and Schroer, T. A. (1999). Actin Related Proteins. *Annu. Rev. Cell Dev. Biol.*, **15**, 341-363.
- Schatten, H., Sibley, L. D. and Ris, H. (2003). Structural evidence for actin-like filaments in Toxoplasma gondii using high-resolution low-voltage field emission scanning electron microscopy. *Microsc Microanal*, **9**, 330-335.
- Scherer, W. F., Syverton, J. T. and Gey, G. O. (1953). Studies on the propagation in vitro of poliomyelitis viruses. IV. Viral multiplication in a stable strain of human malignant epithelial cells (strain HeLa) derived from an epidermoid carcinoma of the cervix. *J Exp Med*, **97**, 695-710.
- Scherlach, K., Boettger, D., Remme, N. and Hertweck, C. (2010). The chemistry and biology of cytochalasins. *Nat Prod Rep*, **27**, 869-886. doi: 10.1039/b903913a.
- Schindelin, J., Arganda-Carreras, I., Frise, E., Kaynig, V., Longair, M., Pietzsch, T., Preibisch, S., Rueden, C., Saalfeld, S., Schmid, B., Tinevez, J. Y., White, D. J., Hartenstein, V., Eliceiri, K., Tomancak, P. and Cardona, A. (2012). Fiji: an open-source platform for biological-image analysis. *Nat Methods*, **9**, 676-682. doi: 10.1038/nmeth.2019.
- Schmitz, S., Grainger, M., Howell, S., Calder, L. J., Gaeb, M., Pinder, J. C., Holder, A. A. and Veigel, C. (2005). Malaria parasite actin filaments are very short. *J Mol Biol*, **349**, 113-125. doi: 10.1016/j.jmb.2005.03.056.
- Schonichen, A. and Geyer, M. (2010). Fifteen formins for an actin filament: a molecular view on the regulation of human formins. *Biochim Biophys Acta*, **1803**, 152-163. doi: 10.1016/j.bbamcr.2010.01.014.
- Schroer, T. A., Fyrberg, E., Cooper, J. A., Waterston, R. H., Helfman, D., Pollard, T. D. and Meyer, D. I. (1994). Actin-related protein nomenclature and classification. *J Cell Biol*, **127**, 1777-1778.
- Schuler, H., Mueller, A. K. and Matuschewski, K. (2005a). A Plasmodium actin-depolymerizing factor that binds exclusively to actin monomers. *Mol Biol Cell*, **16**, 4013-4023. doi: 10.1091/mbc.E05-02-0086.
- Schuler, H., Mueller, A. K. and Matuschewski, K. (2005b). Unusual properties of Plasmodium falciparum actin: new insights into microfilament dynamics of apicomplexan parasites. *FEBS Lett*, **579**, 655-660. doi: 10.1016/j.febslet.2004.12.037.
- Sebastian, S., Brochet, M., Collins, M. O., Schwach, F., Jones, M. L., Goulding, D., Rayner, J. C., Choudhary, J. S. and Billker, O. (2012). A Plasmodium calcium-dependent protein kinase controls zygote development and transmission by translationally activating repressed mRNAs. *Cell Host Microbe*, **12**, 9-19. doi: 10.1016/j.chom.2012.05.014.
- Seeber, F. and Soldati-Favre, D. (2010). Metabolic pathways in the apicoplast of apicomplexa. *Int Rev Cell Mol Biol*, **281**, 161-228. doi: 10.1016/S1937-6448(10)81005-6.
- Sehgal, A., Bettiol, S., Pypaert, M., Wenk, M. R., Kaasch, A., Blader, I. J., Joiner, K. A. and Coppens, I. (2005). Peculiarities of host cholesterol transport to the unique intracellular vacuole containing Toxoplasma. *Traffic*, **6**, 1125-1141. doi: 10.1111/j.1600-0854.2005.00348.x.
- Sellers, J. R. (2000). Myosins: a diverse superfamily. *Biochim Biophys Acta*, **1496**, 3-22.

- Sept, D. and McCammon, J. A. (2001). Thermodynamics and kinetics of actin filament nucleation. *Biophys J*, **81**, 667-674.
- Sharman, P. A., Smith, N. C., Wallach, M. G. and Katrib, M. (2010). Chasing the golden egg: vaccination against poultry coccidiosis. *Parasite Immunol*, **32**, 590-598. doi: 10.1111/j.1365-3024.2010.01209.x.
- Shaw, M. K. (1999). Theileria parva: sporozoite entry into bovine lymphocytes is not dependent on the parasite cytoskeleton. *Exp Parasitol*, **92**, 24-31.
- Shaw, M. K. (2003). Cell invasion by Theileria sporozoites. *Trends Parasitol*, **19**, 2-6.
- Shaw, M. K., Compton, H. L., Roos, D. S. and Tilney, L. G. (2000). Microtubules, but not actin filaments, drive daughter cell budding and cell division in Toxoplasma gondii. *Journal of Cell Science*, **113**, 1241-1254.
- Shaw, M. K. and Tilney, L. G. (1999). Induction of an acrosomal process in Toxoplasma gondii- Visualisation of actin filaments in a protozoan parasite. *Proc. Natl. Acad. Sci. USA*, **96**, 9095-9099.
- Sheiner, L., Santos, J. M., Klages, N., Parussini, F., Jemmely, N., Friedrich, N., Ward, G. E. and Soldati-Favre, D. (2011). Toxoplasma gondii transmembrane microneme proteins and their modular design. *Mol Microbiol*.
- Shen, B., Brown, K. M., Lee, T. D. and Sibley, L. D. (2014). Efficient gene disruption in diverse strains of Toxoplasma gondii using CRISPR/CAS9. *MBio*, **5**, e01114-01114. doi: 10.1128/mBio.01114-14.
- Shen, B. and Sibley, L. D. (2014). Toxoplasma aldolase is required for metabolism but dispensable for host-cell invasion. *Proc Natl Acad Sci U S A*, **111**, 3567-3572. doi: 10.1073/pnas.1315156111.
- Sibley, L. D. (2003). Toxoplasma gondii: perfecting an intracellular life style. *Traffic*, **4**, 581-586.
- Sibley, L. D. (2004). Intracellular parasite invasion strategies. *Science*, **304**, 248-253.
- Sibley, L. D. and Boothroyd, J. C. (1992). Construction of a molecular karyotype for Toxoplasma gondii. *Mol Biochem Parasitol*, **51**, 291-300.
- Sibley, L. D., Niesman, I. R., Parmley, S. F. and Cesbron-Delauw, M. F. (1995). Regulated secretion of multi-lamellar vesicles leads to formation of a tubulo-vesicular network in host-cell vacuoles occupied by Toxoplasma gondii. *J Cell Sci*, **108** ( Pt 4), 1669-1677.
- Sibley, L. D., Weidner, E. and Krahenbuhl, J. L. (1985). Phagosome acidification blocked by intracellular Toxoplasma gondii. *Nature*, **315**, 416-419.
- Siden-Kiamos, I., Louis, C. and Matuschewski, K. (2012). Evidence for filamentous actin in ookinetes of a malarial parasite. *Mol Biochem Parasitol*, **181**, 186-189. doi: 10.1016/j.molbiopara.2011.11.002.
- Siden-Kiamos, I., Schuler, H., Liakopoulos, D. and Louis, C. (2010). Arp1, an actin-related protein, in Plasmodium berghei. *Mol Biochem Parasitol*, **173**, 88-96. doi: 10.1016/j.molbiopara.2010.05.008.
- Sidik, S. M., Hackett, C. G., Tran, F., Westwood, N. J. and Lourido, S. (2014). Efficient Genome Engineering of Toxoplasma gondii Using CRISPR/Cas9. *PLoS One*, **9**, e100450. doi: 10.1371/journal.pone.0100450.
- Sidik, S. M., Huet, D., Ganesan, S. M., Huynh, M. H., Wang, T., Nasamu, A. S., Thiru, P., Saeij, J. P., Carruthers, V. B., Niles, J. C. and Lourido, S. (2016). A Genome-wide CRISPR Screen in Toxoplasma Identifies Essential Apicomplexan Genes. *Cell*, **166**, 1423-1435 e1412. doi: 10.1016/j.cell.2016.08.019.
- Silva, M. C., Fox, S., Beam, M., Thakkar, H., Amaral, M. D. and Morimoto, R. I. (2011). A genetic screening strategy identifies novel regulators of the proteostasis network. *PLoS Genet*, **7**, e1002438. doi: 10.1371/journal.pgen.1002438.
- Sinai, A. P., Webster, P. and Joiner, K. A. (1997). Association of host cell endoplasmic reticulum and mitochondria with the Toxoplasma gondii parasitophorous vacuole membrane: a high affinity interaction. *J Cell Sci*, **110** ( Pt 17), 2117-2128.
- Skillman, K. M., Daher, W., Ma, C. I., Soldati-Favre, D. and Sibley, L. D. (2012). Toxoplasma gondii profilin acts primarily to sequester G-actin while formins efficiently nucleate actin filament formation in vitro. *Biochemistry*, **51**, 2486-2495. doi: 10.1021/bi201704y.

- Skillman, K. M., Diraviyam, K., Khan, A., Tang, K., Sept, D. and Sibley, L. D. (2011). Evolutionarily divergent, unstable filamentous actin is essential for gliding motility in apicomplexan parasites. *PLoS Pathog*, **7**, e1002280.
- Skillman, K. M., Ma, C. I., Fremont, D. H., Diraviyam, K., Cooper, J. A., Sept, D. and Sibley, L. D. (2013). The unusual dynamics of parasite actin result from isodesmic polymerization. *Nat Commun*, **4**, 2285. doi: 10.1038/ncomms3285.
- Smulders, M. M., Nieuwenhuizen, M. M., de Greef, T. F., van der Schoot, P., Schenning, A. P. and Meijer, E. W. (2010). How to distinguish isodesmic from cooperative supramolecular polymerisation. *Chemistry*, **16**, 362-367. doi: 10.1002/chem.200902415.
- Soldati, D. and Boothroyd, J. C. (1993). Transient transfection and expression in the obligate intracellular parasite *Toxoplasma gondii*. *Science*, **260**, 349-352.
- Soldati, D. and Boothroyd, J. C. (1995). A selector of transcription initiation in the protozoan parasite *Toxoplasma gondii*. *Mol Cell Biol*, **15**, 87-93.
- Soldati, D. and Meissner, M. (2004). *Toxoplasma* as a novel system for motility. *Curr Opin Cell Biol*, **16**, 32-40. doi: 10.1016/j.ceb.2003.11.013.
- Soldati-Favre, D. (2008). Molecular dissection of host cell invasion by the apicomplexans: the glideosome. *Parasite*, **15**, 197-205.
- Spector, I., Shochet, N. R., Blasberger, D. and Kashman, Y. (1989). Latrunculins-novel marine macrolides that disrupt microfilament organization and affect cell growth: I. Comparison with Cytochalasin D. *Cell Motil Cytoskeleton*, **13**, 127-144.
- Speer, C. A. and Dubey, J. P. (1998). Ultrastructure of early stages of infections in mice fed *Toxoplasma gondii* oocysts. *Parasitology*, **116** ( Pt 1), 35-42.
- Splendore, A. (1908). Un nuovo protozoa parassita de' conigli. incontrato nelle lesioni anatomiche d'une malattia che ricorda in molti punti il Kala-azar dell' uomo. *Nota preliminare pel. Rev. Soc. Scient. Sao Paulo*, **3**, 109-112.
- Srinivasan, P., Beatty, W. L., Diouf, A., Herrera, R., Ambroggio, X., Moch, J. K., Tyler, J. S., Narum, D. L., Pierce, S. K., Boothroyd, J. C., Haynes, J. D. and Miller, L. H. (2011). Binding of Plasmodium merozoite proteins RON2 and AMA1 triggers commitment to invasion. *Proc Natl Acad Sci U S A*, **108**, 13275-13280. doi: 10.1073/pnas.1110303108.
- Stagge, F., Mitronova, G. Y., Belov, V. N., Wurm, C. A. and Jakobs, S. (2013). SNAP-, CLIP- and Halo-tag labelling of budding yeast cells. *PLoS One*, **8**, e78745. doi: 10.1371/journal.pone.0078745.
- Starnes, G. L., Coincon, M., Sygusch, J. and Sibley, L. D. (2009). Aldolase is essential for energy production and bridging adhesin-actin cytoskeletal interactions during parasite invasion of host cells. *Cell Host Microbe*, **5**, 353-364.
- Stevenson, R. P., Veltman, D. and Machesky, L. M. (2012). Actin-bundling proteins in cancer progression at a glance. *J Cell Sci*, **125**, 1073-1079. doi: 10.1242/jcs.093799.
- Straub, F. B. (1942). Actin. *Stud. Inst. Med. Chem. Univ. Szeged*, **2**, 3-15.
- Straub, F. B. (1943). Actin II. *Stud. Inst. Med. Chem. Univ. Szeged*, **2**, 23-37.
- Straub, F. B. and Feuer, G. (1989). Adenosinetriphosphate. The functional group of actin. 1950. *Biochim Biophys Acta*, **1000**, 180-195.
- Stroka, K. M., Gu, Z., Sun, S. X. and Konstantopoulos, K. (2014a). Bioengineering paradigms for cell migration in confined microenvironments. *Curr Opin Cell Biol*, **30**, 41-50. doi: 10.1016/j.ceb.2014.06.001.
- Stroka, K. M., Jiang, H., Chen, S. H., Tong, Z., Wirtz, D., Sun, S. X. and Konstantopoulos, K. (2014b). Water permeation drives tumor cell migration in confined microenvironments. *Cell*, **157**, 611-623. doi: 10.1016/j.cell.2014.02.052.
- Su, C., Evans, D., Cole, R. H., Kissinger, J. C., Ajioka, J. W. and Sibley, L. D. (2003). Recent expansion of *Toxoplasma* through enhanced oral transmission. *Science*, **299**, 414-416.
- Suss-Toby, E., Zimmerberg, J. and Ward, G. E. (1996). *Toxoplasma* invasion: The parasitophorous vacuole is formed from host cell plasma membrane and pinches off via fission pore. *Proc Natl Acad Sci U S A*, **93**, 8413-8418.

- Suvorova, E. S., Lehmann, M. M., Kratzer, S. and White, M. W. (2012). Nuclear actin-related protein is required for chromosome segregation in *Toxoplasma gondii*. *Mol Biochem Parasitol*, **181**, 7-16. doi: 10.1016/j.molbiopara.2011.09.006.
- Svitkina, T. M. and Borisy, G. G. (1999). Arp2/3 complex and actin depolymerizing factor/cofilin in dendritic organization and treadmilling of actin filament array in lamellipodia. *J Cell Biol*, **145**, 1009-1026.
- Sweeney, K. R., Morrissette, N. S., LaChapelle, S. and Blader, I. J. (2010). Host cell invasion by *Toxoplasma gondii* is temporally regulated by the host microtubule cytoskeleton. *Eukaryot Cell*, **9**, 1680-1689.
- Szempruch, A. J., Sykes, S. E., Kieft, R., Dennison, L., Becker, A. C., Gartrell, A., Martin, W. J., Nakayasu, E. S., Almeida, I. C., Hajduk, S. L. and Harrington, J. M. (2016). Extracellular Vesicles from *Trypanosoma brucei* Mediate Virulence Factor Transfer and Cause Host Anemia. *Cell*, **164**, 246-257. doi: 10.1016/j.cell.2015.11.051.
- Szent-Gyorgyi, A. G. (2004). The early history of the biochemistry of muscle contraction. *J Gen Physiol*, **123**, 631-641. doi: 10.1085/jgp.200409091.
- Tambara, K., Olsen, J. C., Hansen, D. E. and Pantos, G. D. (2014). The thermodynamics of the self-assembly of covalently linked oligomeric naphthalendiimides into helical organic nanotubes. *Org Biomol Chem*, **12**, 607-614.
- Tapon, N. and Hall, A. (1997). Rho, Rac and Cdc42 GTPases regulate the organization of the actin cytoskeleton. *Curr Opin Cell Biol*, **9**, 86-92.
- Tardieux, I. and Baum, J. (2016). Reassessing the mechanics of parasite motility and host-cell invasion. *J Cell Biol*, **214**, 507-515. doi: 10.1083/jcb.201605100.
- Tardieux, I., Liu, X., Poupel, O., Parzy, D., Dehoux, P. and Langsley, G. (1998). A *Plasmodium falciparum* novel gene encoding a coronin-like protein which associates with actin filaments. *FEBS Lett*, **441**, 251-256.
- Tenter, A. M., Heckeroth, A. R. and Weiss, L. M. (2000). *Toxoplasma gondii*: from animals to humans. *Int J Parasitol*, **30**, 1217-1258.
- Theriot, J. A. and Mitchison, T. J. (1991). Actin microfilament dynamics in locomoting cells. *Nature*, **352**, 126-132.
- Tonkin, M. L., Roques, M., Lamarque, M. H., Pugniere, M., Douguet, D., Crawford, J., Lebrun, M. and Boulanger, M. J. (2011). Host cell invasion by apicomplexan parasites: insights from the co-structure of AMA1 with a RON2 peptide. *Science*, **333**, 463-467. doi: 10.1126/science.1204988.
- Trees, A. J., Davison, H. C., Innes, E. A. and Wastling, J. M. (1999). Towards evaluating the economic impact of bovine neosporosis. *Int J Parasitol*, **29**, 1195-1200.
- Vahokoski, J., Bhargava, S. P., Desfosses, A., Andreadaki, M., Kumpula, E. P., Martinez, S. M., Ignatev, A., Lepper, S., Frischknecht, F., Siden-Kiamos, I., Sachse, C. and Kursula, I. (2014). Structural differences explain diverse functions of *Plasmodium* actins. *PLoS Pathog*, **10**, e1004091. doi: 10.1371/journal.ppat.1004091.
- Vaishnav, S. and Striepen, B. (2006). The cell biology of secondary endosymbiosis-how parasites build, divide and segregate the apicoplast. *Mol Microbiol*, **61**, 1380-1387.
- van den Hoff, M. J. B., Moorman, A. F. M. and Lamers, W. H. (1992). Electroporation in 'intracellular' buffer increases cell survival. *Nucleic Acids Research*, **20**, 2982.
- van Dooren, G. G., Kennedy, A. T. and McFadden, G. I. (2012). The use and abuse of heme in apicomplexan parasites. *Antioxid Redox Signal*, **17**, 634-656. doi: 10.1089/ars.2012.4539.
- van Dooren, G. G., Reiff, S. B., Tomova, C., Meissner, M., Humbel, B. M. and Striepen, B. (2009). A novel dynamin-related protein has been recruited for apicoplast fission in *Toxoplasma gondii*. *Curr Biol*, **19**, 267-276. doi: 10.1016/j.cub.2008.12.048.
- van Poppel, N. F., Welagen, J., Duisters, R. F., Vermeulen, A. N. and Schaap, D. (2006). Tight control of transcription in *Toxoplasma gondii* using an alternative tet repressor. *Int J Parasitol*, **36**, 443-452. doi: 10.1016/j.ijpara.2006.01.005.

- Visegrady, B., Lorinczy, D., Hild, G., Somogyi, B. and Nyitrai, M. (2004). The effect of phalloidin and jasplakinolide on the flexibility and thermal stability of actin filaments. *FEBS Lett*, **565**, 163-166. doi: 10.1016/j.febslet.2004.03.096.
- Visegrady, B., Lorinczy, D., Hild, G., Somogyi, B. and Nyitrai, M. (2005). A simple model for the cooperative stabilisation of actin filaments by phalloidin and jasplakinolide. *FEBS Lett*, **579**, 6-10. doi: 10.1016/j.febslet.2004.11.023.
- Vitriol, E. A., McMillen, L. M., Kapustina, M., Gomez, S. M., Vavylonis, D. and Zheng, J. Q. (2015). Two functionally distinct sources of actin monomers supply the leading edge of lamellipodia. *Cell Rep*, **11**, 433-445. doi: 10.1016/j.celrep.2015.03.033.
- Vyas, A. (2015). Mechanisms of Host Behavioral Change in *Toxoplasma gondii* Rodent Association. *PLoS Pathog*, **11**, e1004935. doi: 10.1371/journal.ppat.1004935.
- Waller, R. F., Keeling, P. J., Donald, R. G., Striepen, B., Handman, E., Lang-Unnasch, N., Cowman, A. F., Besra, G. S., Roos, D. S. and McFadden, G. I. (1998). Nuclear-encoded proteins target to the plastid in *Toxoplasma gondii* and *Plasmodium falciparum*. *Proc Natl Acad Sci U S A*, **95**, 12352-12357.
- Waller, R. F. and McFadden, G. I. (2005). The Apicoplast: A Review of the Derived Plastid of Apicomplexan Parasites. *Curr. Issues Mol. Biol.*, **7**, 57-80.
- Wang, J. L., Huang, S. Y., Behnke, M. S., Chen, K., Shen, B. and Zhu, X. Q. (2016). The Past, Present, and Future of Genetic Manipulation in *Toxoplasma gondii*. *Trends Parasitol*. doi: 10.1016/j.pt.2016.04.013.
- Waters, J. C. (2009). Accuracy and precision in quantitative fluorescence microscopy. *J Cell Biol*, **185**, 1135-1148. doi: 10.1083/jcb.200903097.
- Wear, M. A., Schafer, D. A. and Cooper, J. A. (2000). Actin dynamics: Assembly and disassembly of actin networks. *Curr Biol*, **10**, 891-895.
- Webster, J. P. (2001). Rats, cats, people and parasites: the impact of latent toxoplasmosis on behaviour. *Microbes Infect*, **3**, 1037-1045.
- Wegner, A. (1976). Head to tail polymerization of actin. *J Mol Biol*, **108**, 139-150.
- Welch, M. D., DePace, A. H., Verma, S., Iwamatsu, A. and Mitchison, T. J. (1997a). The human Arp2/3 complex is composed of evolutionarily conserved subunits and is localized to cellular regions of dynamic actin filament assembly. *J Cell Biol*, **138**, 375-384.
- Welch, M. D., Mallavarapu, A., Rosenblatt, J. and Mitchison, T. J. (1997b). Actin dynamics in vivo. *Curr Opin Cell Biol*, **9**, 54-61.
- Welch, M. D. and Mullins, R. D. (2002). Cellular control of actin nucleation. *Annu Rev Cell Dev Biol*, **18**, 247-288. doi: 10.1146/annurev.cellbio.18.040202.112133.
- Wertman, K. F., Drubin, D. G. and Botstein, D. (1992). Systematic mutational analysis of the yeast ACT1 gene. *Genetics*, **132**, 337-350.
- Wesseling, J. G., de Ree, J. M., Ponnudurai, T., Smits, M. A. and Schoenmakers, J. G. (1988a). Nucleotide sequence and deduced amino acid sequence of a *Plasmodium falciparum* actin gene. *Mol Biochem Parasitol*, **27**, 313-320.
- Wesseling, J. G., Smits, M. A. and Schoenmakers, J. G. (1988b). Extremely diverged actin proteins in *Plasmodium falciparum*. *Mol Biochem Parasitol*, **30**, 143-153.
- Wetzel, D. M., Hakansson, S., Hu, K., Roos, D. and Sibley, L. D. (2003). Actin filament polymerization regulates gliding motility by apicomplexan parasites. *Mol Biol Cell*, **14**, 396-406.
- Wetzel, D. M., Schmidt, J., Kuhlenschmidt, M. S., Dubey, J. P. and Sibley, L. D. (2005). Gliding motility leads to active cellular invasion by *Cryptosporidium parvum* sporozoites. *Infect Immun*, **73**, 5379-5387.
- Whitelaw, J. A., Latorre-Barragan, F., Gras, S., Pall, G. S., Leung, J. M., Heaslip, A., Egarter, S., Andenmatten, N., Nelson, S. R., Warshaw, D. M., Ward, G. E. and Meissner, M. (2017). Surface attachment, promoted by the actomyosin system of *Toxoplasma gondii* is important for efficient gliding motility and invasion. *BMC Biol*, **15**. doi: 10.1186/s12915-016-0343-5.
- Williams, M. J., Alonso, H., Enciso, M., Egarter, S., Sheiner, L., Meissner, M., Striepen, B., Smith, B. J. and Tonkin, C. J. (2015). Two Essential Light Chains Regulate the MyoA Lever Arm To Promote *Toxoplasma* Gliding Motility. *MBio*, **6**, e00845-00815. doi: 10.1128/mBio.00845-15.

- Wilson, C. A., Tsuchida, M. A., Allen, G. M., Barnhart, E. L., Applegate, K. T., Yam, P. T., Ji, L., Keren, K., Danuser, G. and Theriot, J. A. (2010). Myosin II contributes to cell-scale actin network treadmill through network disassembly. *Nature*, **465**, 373-377. doi: 10.1038/nature08994.
- Wilson, R. J., Denny, P. W., Preiser, P. R., Rangachari, K., Roberts, K., Roy, A., Whyte, A., Strath, M., Moore, D. J., Moore, P. W. and Williamson, D. H. (1996). Complete gene map of the plastid-like DNA of the malaria parasite *Plasmodium falciparum*. *J Mol Biol*, **261**, 155-172.
- Winder, S. J. and Ayscough, K. R. (2005). Actin-binding proteins. *J Cell Sci*, **118**, 651-654. doi: 10.1242/jcs.01670.
- Wirth, C. C. and Pradel, G. (2012). Molecular mechanisms of host cell egress by malaria parasites. *Int J Med Microbiol*, **302**, 172-178. doi: 10.1016/j.ijmm.2012.07.003.
- Withers-Martinez, C., Strath, M., Hackett, F., Haire, L. F., Howell, S. A., Walker, P. A., Christodoulou, E., Dodson, G. G. and Blackman, M. J. (2014). The malaria parasite egress protease SUB1 is a calcium-dependent redox switch subtilisin. *Nat Commun*, **5**, 3726. doi: 10.1038/ncomms4726.
- Woods, L. C., Berbusse, G. W. and Naylor, K. (2016). Microtubules Are Essential for Mitochondrial Dynamics-Fission, Fusion, and Motility-in *Dictyostelium discoideum*. *Frontiers in Cell and Developmental Biology*, **4**. doi: 10.3389/fcell.2016.00019.
- Wulf, E., Deboben, A., Bautz, F. A., Faulstich, H. and Wieland, T. (1979). Fluorescent phallotoxin, a tool for the visualization of cellular actin. *Proc Natl Acad Sci U S A*, **76**, 4498-4502.
- Yadav, R., Pathak, P. P., Shukla, V. K., Jain, A., Srivastava, S., Tripathi, S., Krishna Pulavarti, S. V., Mehta, S., Sibley, L. D. and Arora, A. (2011). Solution structure and dynamics of ADF from *Toxoplasma gondii*. *J Struct Biol*, **176**, 97-111. doi: 10.1016/j.jsb.2011.07.011.
- Yang, C. and Svitkina, T. (2011). Visualizing branched actin filaments in lamellipodia by electron tomography. *Nat Cell Biol*, **13**, 1012-1013; author reply 1013-1014. doi: 10.1038/ncb2321.
- Yang, N., Farrell, A., Niedelman, W., Melo, M., Lu, D., Julien, L., Marth, G. T., Gubbels, M. J. and Saeij, J. P. (2013). Genetic basis for phenotypic differences between different *Toxoplasma gondii* type I strains. *BMC Genomics*, **14**, 467. doi: 10.1186/1471-2164-14-467.
- Yarmola, E. G., Somasundaram, T., Boring, T. A., Spector, I. and Bubb, M. R. (2000). Actin-latrunculin A structure and function. Differential modulation of actin-binding protein function by latrunculin A. *J Biol Chem*, **275**, 28120-28127. doi: 10.1074/jbc.M004253200.
- Yarovinsky, F. (2014). Innate immunity to *Toxoplasma gondii* infection. *Nat Rev Immunol*, **14**, 109-121. doi: 10.1038/nri3598.
- Yarovinsky, F., Zhang, D., Andersen, J. F., Bannenberg, G. L., Serhan, C. N., Hayden, M. S., Hieny, S., Sutterwala, F. S., Flavell, R. A., Ghosh, S. and Sher, A. (2005). TLR11 activation of dendritic cells by a protozoan profilin-like protein. *Science*, **308**, 1626-1629. doi: 10.1126/science.1109893.
- Yeh, E. and DeRisi, J. L. (2011). Chemical rescue of malaria parasites lacking an apicoplast defines organelle function in blood-stage *Plasmodium falciparum*. *PLoS Biol*, **9**, e1001138. doi: 10.1371/journal.pbio.1001138.
- Yeoh, S., Pope, B., Mannherz, H. G. and Weeds, A. (2002). Determining the differences in actin binding by human ADF and cofilin. *J Mol Biol*, **315**, 911-925. doi: 10.1006/jmbi.2001.5280.
- Yuan, F., Liu, Z. Z., Zhang, B., Cao, J. P., Zheng, K. Y. and Wang, D. G. (2015). [Prokaryotic Expression and Immunoreactivity Analysis on Profilin of *Toxoplasma gondii*]. *Zhongguo Ji Sheng Chong Xue Yu Ji Sheng Chong Bing Za Zhi*, **33**, 21-24.
- Zech, T., Calaminus, S. D., Caswell, P., Spence, H. J., Carnell, M., Insall, R. H., Norman, J. and Machesky, L. M. (2011). The Arp2/3 activator WASH regulates alpha5beta1-integrin-mediated invasive migration. *J Cell Sci*, **124**, 3753-3759. doi: 10.1242/jcs.080986.

- 
- Zhao, Y., Marple, A. H., Ferguson, D. J., Bzik, D. J. and Yap, G. S. (2014). Avirulent strains of *Toxoplasma gondii* infect macrophages by active invasion from the phagosome. *Proc Natl Acad Sci U S A*, **111**, 6437-6442. doi: 10.1073/pnas.1316841111.
- Zhu, G., Marchewka, M. J. and Keithly, J. S. (2000). *Cryptosporidium parvum* appears to lack a plastid genome. *Microbiology*, **146**, 315-321.
- Zhu, S., Victoria, G. S., Marzo, L., Ghosh, R. and Zurzolo, C. (2015). Prion aggregates transfer through tunneling nanotubes in endocytic vesicles. *Prion*, **9**, 125-135. doi: 10.1080/19336896.2015.1025189.
- Zuccala, E. S., Satchwell, T. J., Angrisano, F., Tan, Y. H., Wilson, M. C., Heesom, K. J. and Baum, J. (2016). Quantitative phospho-proteomics reveals the *Plasmodium* merozoite triggers pre-invasion host kinase modification of the red cell cytoskeleton. *Sci Rep*, **6**, 19766. doi: 10.1038/srep19766.

## Chapter 9 Appendices

### 9.1 List of supplementary movies

**Supplementary Movie 1: Example of helical gliding motility of RH KillerRed.**

Time-lapse video microscopy of a RH KillerRed parasite gliding in a helical motion over an FBS-coated Ibidi glass bottom dish. Images were taken at 1 frame per second in A<sub>594</sub> channel, DV Core. Movie supports Figure 3-6 D.

**Supplementary Movie 2: Example of circular gliding motility of RH KillerRed.**

Same conditions as supplementary movie 1 where a wild-type parasite moves in a circular motion. Movie supports Figure 3-6 D.

**Supplementary Movie 3: Example of helical gliding motility of the *act1* KO.**

Time-lapse video microscopy of an *act1* KO parasite gliding in a helical motion over a FBS-coated Ibidi glass bottom dish. Images were taken at 1 frame per second in FITC channel to represent YFP+ *act1* KO parasites, DV Core. Movie supports Figure 3-6 D.

**Supplementary Movie 4: Example of circular gliding motility of the *act1* KO.**

Same conditions as supplementary movie 3 where an *act1* KO parasite moves in a circular motion. Movie supports Figure 3-6 D.

**Supplementary Movie 5: Penetration of a RH parasite.**

Time-lapse video microscopy of RH invading an HFF cell. Images were taken at 1 frame per second in DIC channel, DV Core. Movie supports Figure 3-8.

**Supplementary Movie 6: Penetration of a LoxPAct1 parasite.**

Same conditions as supplementary movie 5 where a LoxPAct1 parasite invades an HFF cell. Movie supports Figure 3-8.

**Supplementary Movie 7: Penetration of an *act1* KO parasite with speeds similar to wild-type.**

Same conditions as supplementary movie 5 with a final image in FITC (not shown) to distinguish YFP+ *act1* KO parasites from the un-induced LoxPAct1 parasites, DV Core. This parasite invades at a similar speed to wild-type cells. Movie supports Figure 3-8.

**Supplementary Movie 8: Penetration of a slowly invading *act1* KO parasite.**

Same conditions as supplementary movie 7, DV Core. This *act1* KO parasite invades significantly slower than wild-type parasites. Movie supports Figure 3-8.

**Supplementary Movie 9: Penetration of Chromobody-Halo parasites.**

Time-lapse video microscopy of a chromobody-Halo parasite invading an HFF cell. Images were taken at 1 frame per second in DIC and A<sub>594</sub> channel, DV Core. Movie supports Figure 5-8 D.

**Supplementary Movie 10: Penetration of Chromobody-RFP parasites.**

Same conditions as supplementary movie 9. F-actin can only be seen at the basal end of the parasite and isn't dynamic during invasion. Movie supports Figure 5-8 E.

**Supplementary Movie 11: F-actin during replication.**

Time-lapse video microscopy of a chromobody-Halo parasite expressing GAPM1a as a marker for the IMC replicating within an HFF cell. F-actin accumulates at the residual body during replication and appears to recycle contents to the new daughter cells. Images were taken at 1 frame per second in FITC (GAPM1a) and A<sub>594</sub> (chromobody-Halo) channels, DV Core. Movie supports Figure 5-9.

**Supplementary Movie 12: Chromobody-Halo parasites making an F-actin connection to a neighbouring vacuole during replication.**

Time-lapse video microscopy of a GAPM1a parasite transiently expressing chromobody-Halo replicating within an HFF cell. The chromobody-Halo vacuole makes a dynamic connection with a neighbouring non-transfected vacuole and retracts. Images were taken at 1 frame per second in DIC and A<sub>594</sub> channel, DV Core. Movie supports Figure 5-12.

**Supplementary Movie 13: The F-actin connections break up prior to egress.**

Time-lapse video microscopy of a chromobody-Halo parasite egressing an HFF cell. This network breaks up after addition of Ca<sup>2+</sup> ionophore even if the parasites do not escape. Images were taken at 1 frame per second in a Z-stack of 15 slices of 0.2 μm (total time per stack was around 6 seconds) in A<sub>594</sub> channel, DV Core. Movie supports Figure 5-13 A.

**Supplementary Movie 14: F-actin dynamics during egress 1.**

Time-lapse video microscopy of chromobody-Halo parasites escaping after calcium induced egress. Images were taken at 1 frame per second in DIC and A<sub>594</sub> channel, DV Core. This movie shows that many of the vacuoles egress at similar times after an increase in calcium levels. Movie supports Figure 5-13 B.

**Supplementary Movie 15: F-actin dynamics during egress 2.**

Same conditions for supplementary movie 13. Focused vacuole indicating the network breaks prior to parasites escaping. F-actin can be seen to be left behind in the residual body after egress. Movie supports Figure 5-13 C.

**Supplementary Movie 16: Parasites are held together by tubule structures stained with Halo.**

Time-lapse video microscopy of a chromobody-Halo parasite during induced egress. Some parasites within the vacuole can be seen moving in opposite directions while being held together by tubule-like structures. Images were taken at 1 frame per second in A<sub>594</sub> channel, DV Core. Movie supports Figure 5-14 A.

**Supplementary Movie 17: Parasite is recoiled after egress.**

Same conditions as supplementary movie 17. A single parasite is recoiled to the vacuole by an F-actin connection before it breaks and the parasite invades a new cell. Movie supports Figure 5-14 B, C.

## 9.2 Figure copyright permissions

Table 9-1: Copyright permissions obtained for figures reproduced from journal publications

Publisher	Journal	Reference journal title	Author (Year)	Figure No. in paper	Figure No. in this thesis	Copyright permission code
NPG	<i>Nature Reviews Microbiology</i>	Modulation of innate immunity by <i>Toxoplasma gondii</i> virulence effectors	Hunter and Sibley (2012)	Figure 1	Figure 1-1	<a href="https://doi.org/10.1038/3931340226607">3931340226607</a>
American Society for Microbiology	<i>Clinical Reviews Microbiology</i>	Structures of <i>Toxoplasma gondii</i> Tachyzoites, Bradyzoites, and Sporozoites and Biology and Development of Tissue Cysts	(Dubey <i>et al.</i> , 1998)	Figure 6	Figure 1-4B	*
NPG	<i>Nature</i>	The cytoskeleton, cellular motility and the reductionist agenda	Pollard (2003)	Figure 1	Figure 1-10A	<a href="https://doi.org/10.1038/3936070623227">3936070623227</a>
Ivyspring Int.	<i>International Journal of Biological Sciences</i>	The forces behind cell movement	Ananthakrishnan and Ehrlicher (2007)	Figure 1	Figure 1-10B	**
Elsevier	<i>Cell</i>	Water Permeation Drives Tumor Cell Migration in Confined Microenvironments	Stroka <i>et al.</i> (2014b)	Graphical Abstract	Figure 1-11	<a href="https://doi.org/10.1016/j.cell.2014.11.054">3935331457584</a>

\* Permission granted by email from *Clinical Reviews Microbiology*

\*\* Permission granted by email from *International Journal of Biological Sciences*

